OPTIMIZATION OF HIGHWAY BRIDGE GIRDERS FOR USE WITH ULTRA HIGH PERFORMANCE CONCRETE (UHPC)

Michael Allen Woodworth

Thesis submitted to the faculty of the Virginia Polytechnic Institute and State University in partial fulfillment of the requirements for the degree of

Master of Science
In
Civil Engineering

Carin Roberts-Wollmann

Elisa D. Sotelino

Thomas E. Cousins

October 22nd 2008
Blacksburg, Virginia

Keywords: UHPC, Optimization, Girder

OPTIMIZATION OF HIGHWAY BRIDGE GIRDERS FOR USE WITH ULTRA HIGH PERFORMANCE CONCRETE (UHPC)

Michael Allen Woodworth

ABSTRACT

Ultra High Performance Concrete (UHPC) is a class of cementitious materials that share similar characteristics including very large compressive strengths, tensile strength greater than conventional concrete and high durability. The material consists of finely graded cementitious particles and aggregates to develop a durable dense matrix. The addition of steel fibers increases ductility such that the material develops usable tensile strength. The durability and strength of UHPC makes it a desirable material for the production of highway bridge girders. However, UHPC's unique constitutive materials make it more expensive than conventional concrete. The cost and lack of appropriate design guidelines has limited its introduction into bridge products.

The investigation presented in this thesis developed several optimization formulations to determine a suitable bridge girder shape for use with UHPC. The goal of this optimization was to develop a methodology of using UHPC in highway bridge designs that was cost competitive with conventional concrete solutions. Several surveys and field visits were performed to identify the important aspects of girder fabrication. Optimizations were formulated to develop optimized girder cross sections and full bridge design configurations that utilize UHPC. The results showed that for spans greater than 90 ft UHPC used in the proposed girder shape was more economical than conventional girders. The optimizations and surveys resulted in the development of a proposed method to utilize UHPC in highway bridges utilizing existing girder shapes and formwork. The proposed method consists of three simple calculations to transform an initial conventional design to an initial design using modified UHPC girders.

Table of Contents

Figure List

Table List

CHAPTER 1 INTRODUCTION

Introduction

Ultra High Performance Concrete (UHPC) represents the next generation of cementitious structural materials. Signature characteristics of UHPC are very high compressive strengths, ductile tensile capability, superior durability and low permeability. The superior performance of UHPC is due to unique constitutive materials including reactive powder cements, specially graded fine aggregates and distributed fiber reinforcement. The constituents of UHPC give it superior properties that make it an advantageous material for use in structural applications.

The advantages of UHPC over other cementitious concretes have led to its gradual incorporation into the bridge industry. Nine bridge projects have been completed using UHPC. The material lends itself well to prestressed applications and in each of the nine cases prestressing was used to take advantage of UHPC's superior strength and other properties. Wider adoption of UHPC in the national highway bridge industry is a goal of the Federal Highway Administration (FHWA). The strength of UHPC has the potential to reduce material and construction costs by allowing for lighter super structures. The tensile capabilities of UHPC translate to superior shear capacity that can be used to reduce or eliminate the need for shear reinforcement. Most exciting is the prospect of the durability of UHPC prolonging structure life cycles, thereby reducing total infrastructure costs for state and federal agencies.

UHPC has high material costs when compared to conventional concretes such that in order to be competitive with conventional solutions the material's strength must be fully utilized. One way to do this is individualized designs as exemplified by the footbridges created with UHPC to date. Custom and unique bridges are uneconomical for common highway bridges. Most highway bridges are repetitive and prestressed girder bridges have been designed traditionally from available sets of standard girders. To achieve full utilization of UHPC in highway bridges new optimized girder shapes have been developed such as the pi-girder developed at MIT . However, the precast prestressed segment of the bridge industry has yet to adopt UHPC and its optimal girder shapes.

The industry is slow to change because of a desire to avoid increased costs. Formwork represents an investment to a precaster and must be reused as many times as possible to recover initial costs and avoid the cost associated with new forms. Using UHPC with traditional girder shapes would increase the viability of UHPC as an option in the bridge industry. Direct substitution of UHPC for conventional concrete in precast prestressed girders is not economic because of the aforementioned under utilization of the material. In order for UHPC to be adopted these difficulties must be overcome.

Objective

The goal of this research is the development of a modification to existing girder shapes for UHPC. Modification of girder shapes would allow for the use of UHPC in bridge projects without inducing the risks precasters would have to take on in conjunction with the purchase of new formwork. Facilitating the introduction of UHPC into the industry with modified shapes would allow precasters and designers to gain familiarity with UHPC. The advantages of UHPC would then become apparent to many, which would lead to greater interest in and the adoption of UHPC.

Research Procedure

The research was divided into two phases the first being required before delving into the more intensive second phase. The first phase was the investigation of the practices being used in precast prestressed concrete bridge construction. This was conducted with surveys of industry websites, research into State agencies' specifications and surveys of State Departments of transportations officials. After identifying the most prevalent practice as slab on bulb-tee girder bridges, representative girder cross sections were selected. The second phase was the development of an optimization procedure. A system was developed in *Matlab*® to optimize existing girder shapes using feasible modifications to take advantage of UHPC. These optimized shapes were then analyzed for viability against AASHTO code and other requirements.

Organization

This report is divided in to five chapters. Chapter one introduces UHPC and the aspects of the project. Chapter Two presents a literature review of previous UHPC research, bridge projects and background theory. In chapter Three the procedure of the research is detailed. Chapter Four presents the results of the phases of the research and analyzes the data produced. Conclusions and recommendations are presented in Chapter Five. Relevant data generated in the conduct of the research and code generated in the process of optimization is included in the subsequent appendices.

CHAPTER 2 LITERATURE REVIEW AND BACKGROUND

Ultra High Performance Concrete Characteristics and Background

Ultra High Performance Concrete (UHPC) exhibits many desirable properties which make it a logical material for use in bridge systems. These properties have been documented by both manufactures and researchers interested in implementing UHPC in bridges and other structural applications.

UHPC is represented in the market by proprietary concrete products created by three companies. Located primarily in France, these companies are the main proponents of the use of UHPC in a variety of projects. Beton Special Industriel (BSI) markets a UHPC called *Ceracem*®. *Ductal*® is a UHPC developed by Bouygues Lafarge and Rhodia. Finally the Vinci group has developed a UHPC known as *BCV*®. Ductal® is the most readily available in North America and is marketed by Lafarge North America. (Resplendino and Petitjean 2003)

UHPC is different from other high performance concrete products in that it exhibits high compressive strengths and other unique properties. Resplendino defines the three characteristics that differentiate UHPC from other products as;

- High compressive strength in the range of 21.8 ksi to 36.3 ksi
- The use of steel fibers to improve tensile and shear properties
- A controlled constitutive material selection including a large percentage of binder material and the use of fine aggregates. (Resplendino and Petitjean 2003)

The typical mix presented in Table 1 (Graybeal 2005) demonstrate theses material characteristics.

Table 1. Typical Composition of UHPC

Material	Amount (lb/yd3)	Percent by Weight
Portland Cement	1200	28.5%
Fine Sand	1720	40.8%
Silica Fume	390	9.3%
Ground Quartz	355	8.4%
Super Plasticizer	51.8	1.2%
Accelerator	50.5	1.2%
Steel Fibers	263	6.2%
Water	184	4.4%

The fine aggregates are carefully selected to create a gradation of particle sizes that result in a tightly packed matrix of materials minimizing voids. This has the effect of creating a very durable material with low porosity and permeability. The dense microstructure also eliminates shrinkage and limits creep when heat treated during curing. (Ahlborn, Steinberg et al. 2003) The difference between UHPC and other concretes' gradation is illustrated by this image used in promotion of *Ductal*® (Figure 1).

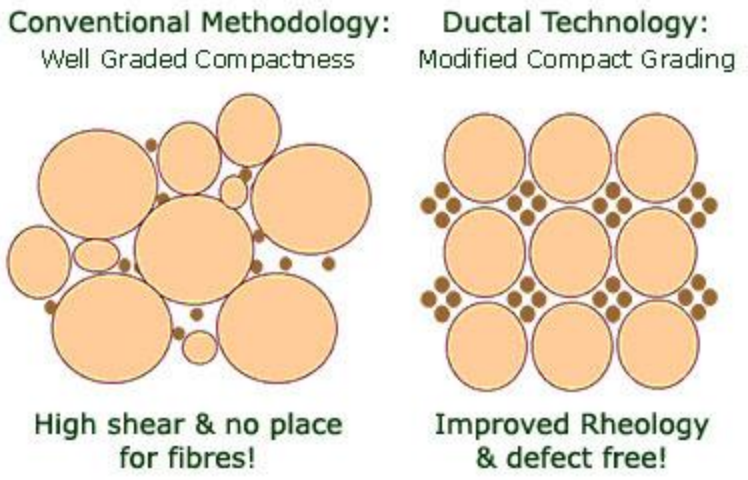

Figure 1. Image. A comparison of the differences in matrix structures between coventional concrete and LaFarge's Ductal © Lafarge North America Inc.

The inclusion of steel or organic fibers imbues UHPC with ductility not inherent in other concrete products. The fibers reinforce the material across micro cracks. The fibers allow UHPC to develop flexural and tensile stresses well after the formation of initial micro cracks.

The fibers used the UHPC investigated exhaustively by Graybeal had a manufacture specified minimum tensile strength of 377 ksi with yield actually occurring at 457 ksi on average. The fibers quickly reach ultimate strength after yield and exhibit a lack of ductility beyond yield. (Graybeal 2005) The unique constituent materials of UHPC lead to its superior performance in a wide range of material characteristics presented in (Table 2) (Graybeal 2005).

Table 2. Manufacturer Supplied Characteristics

Material Characteristics	Range
Compressive Strength (ksi)	26 - 33
Modulus of Elasticity (ksi)	8000 - 8500
Flexural Strength (ksi)	5.8 - 7.2
Chloride Ion Diffusion (ft^2/s)	0.02×10^{-11}
Carbonation Penetration Depth (in)	< 0.02
Freeze-Thaw Resistance (RDM)	1
Salt-Scaling Resitance (lb/ft^2)	< 0.0025
Entrapped Air Content	2-4%
Post-Cure Shrinkage (microstrain)	0
Creep Coefficient ($x10^{-6}$ in/in/°C)	0.2 - 0.5
Density (lb/ft^3)	152 - 159

UHPC is well suited for prestressed applications because of these superior properties. High strengths allow for the use of more prestressing force and shallower depths. The tensile strength allows for the elimination of passive and shear reinforcement. Specifically in bridges, lighter superstructure elements can reduce the total project cost by reducing substructure requirements as well as secondary costs such as construction costs. Life cycle costs are also reduced because of improved durability and impermeability of bridge components extending their life. (Perry and Zakariasen 2003) The producers of UHPC contend that the savings garnered by the reduction of construction cost due to lighter weight components and the reduction of life cycle costs can offset the initial expense associated with the specialty materials required for UHPC construction as presented in Figure 2.

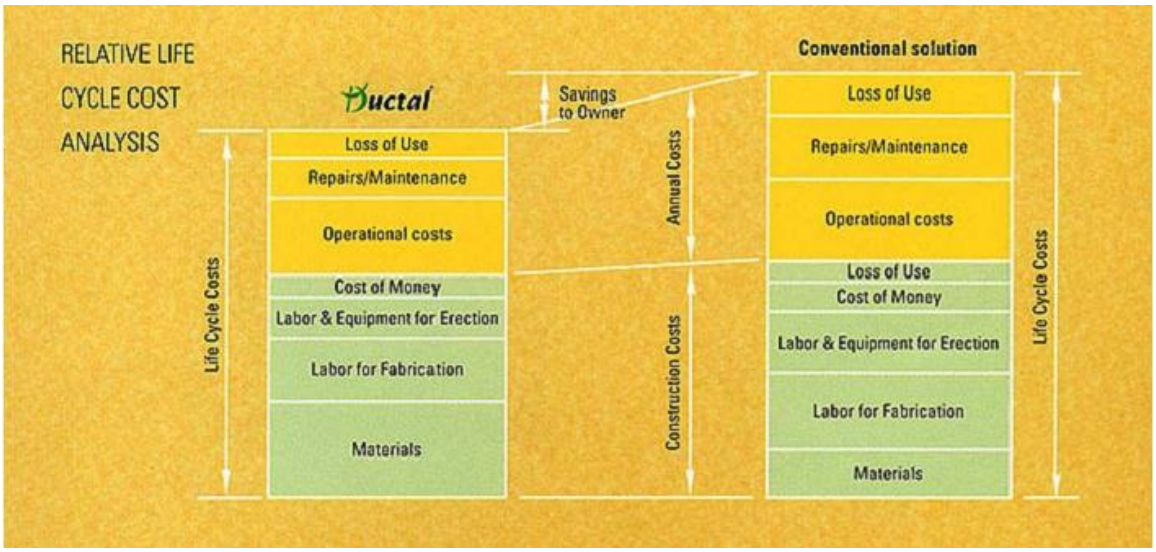

Figure 2. Image. A comparison of the total costs between Lafarge's Ductal and a conventional solution. © Lafarge North America Inc.

As the comparison indicates, the increased initial material costs of UHPC must be offset in order for it to compete against traditional bridge systems. Other difficulties must be overcome in order for UHPC to be adopted in North American bridges. One is education of precasters in the handling and preparation of UHPC. Care is required in following batching procedures recommended by UHPC producers to create a material with the desired characteristics. Another is the adoption of testing and quality control methods consistent with ASTM methods but suited for UHPC. One example is that standard cylinder sizes, when used with UHPC, result in specimens too strong to test in many precaster's quality control facilities. Precasters may also need to acquire high shear capacity mixers to properly batch UHPC. (Ahlborn, Steinberg et al. 2003)

The main focus of this research was to overcome another set of disadvantages to UHPC. The best practice for using UHPC in bridges is the development of cross sections that take full advantage of its superior qualities. One such shape is the Pi girder presented in (Park, Ulm et al. 2003) but it requires the creation of entire new formwork and procedures. However, precasters are already equipped and have years of experience with existing standard girder shapes. Direct substitution of UHPC into these girder shapes would not take advantage of the material and would offer little cost savings. To facilitate transition to UHPC, research was conducted into the

best way to use UHPC with existing girder standards in ways that take advantage of its properties and provide the necessary cost savings to make UHPC the more economic solution.

Bridge Projects Utilizing UHPC

The use of UHPC in various projects around the world demonstrates its unique capabilities. UHPC has been utilized in many unique footbridges. All such examples have used the high compressive capacity of UHPC effectively by incorporating prestressing elements. UHPC is able to withstand high prestressing forces because of its high compressive strength and inherent confinement provided by the steel fiber reinforcement. These bridges demonstrate some of the approaches used by designers to incorporate UHPC into bridges effectively and economically.

The Sherbrooke Bridge is a foot bridge supported by a three chord triangular space truss arrangement. All the components of the truss use UHPC. The top chord consist of the deck and two bulbs where the diagonals connect, the bottom chord consists of two 12.5 in. wide x 15 in. deep rectangular sections that contain prestressing tendons. The diagonals are 6 in. diameter stainless steel tubes filled with UHPC and are strengthened by prestressing strand which is also used in the connection to the chord elements by the use of small steel anchorages. This bridge is significant because it was the first to use UHPC in a bridge structure and demonstrated UHPC's ability to be used in conjunction with high prestressing forces. (Blais and Couture 1999)

The Papatoetoe Rail Station foot bridges are traditional girder bridges. These girders use Ductal® the UHPC product offered by Lafarge. The cross section is a Pi shape consisting of a 2 in. deck with two webs terminating in a prestressing bulb. The prestressing in the bulb consists of ten 0.5 in. strands stressed to 80% of capacity or 32.8 kip each. The cost of the bridge was reduced by forming circular holes in the webs. UHPC made this possible because of its inherent shear and tensile strength making vertical reinforcement unnecessary. The light weight of the prestressed Ductal solution lowered the overall cost of substructure associated with seismic design limit states. (Rebentrost and Cavill 2006)

The Peace Bridge in Seoul South Korea is a 394 ft span bridge using UHPC in its main structural arch. The arch is a 4.25 ft deep Pi section with a scant 1.2 in. thick deck with

transverse ribs spaced at 4 ft. The Pi webs and bottom bulb contain post-tensioning tendons to secure the 72 ft segments together. The Peace Bridge demonstrates UHPC's ability to be used in slender and elegant designs. (Brouwer 2001)

UHPC has also been used in several roadway bridges. The durability and weight savings of UHPC based designs has the potential to lower the overall life-time costs of a bridge associated with bridge maintenance and repair. Lowering a bridge's super structure self weight may reduce the cost of substructure elements and construction costs. Increased bridge durability increases the life span of a bridge and reduces the maintenance costs over that extended life. Two of the first bridges used girder shapes specifically designed for use with UHPC.

The first vehicular traffic bridge made using UHPC was constructed in France in 2001. It is a system of UHPC double stem T-girders that uses the top flange as the bridge deck. The 39.5 ft (12 m) wide bridge is made up of five 7 ft wide girders that were made continuous with closure pours in the transverse direction in situ. The 3 ft deep girders are prestressed by 26 strands, 13 in each bulb. No regular reinforcement longitudinally or as shear stirrups was necessary because of UHPC's high strength and its shear capacity provided by the integrated steel fibers. Development of the bridge design included many verification tests. The anchorage stresses and development lengths of the prestressing strand were verified by constructing a half girder with one leg. The deck of this test girder was then sawn into specimens for prism and slab flexural tests. Finally the continuity joint of the deck was tested in flexure. (Hajar, Simon et al. 2003)

The Federal Highway Administration (FHWA) constructed another bridge using an integrated deck and double tee legs. The cross section was developed using optimization techniques by Park, Ulm et al. (2003) at MIT. The method used to find the optimized Pi section required the development of a 3-D UHPC material model for use with finite element software. This formulation was used to optimize the section against "Service III" load case of AASHTO where cracking was limited and "Strength I" where ultimate capacity is considered (Park, Ulm et al. 2003) The shape developed was scalable and the investigators developed a discrete suggested size for six spans of 70 ft through 120 ft with depths ranging from 33 in. through 63 in. The width of the girders is dependant on the bridge configuration and is meant to be adjusted such

that a traffic lane is supported by a girder and a half or three legs (Figure 3) (Park, Ulm et al. 2003).

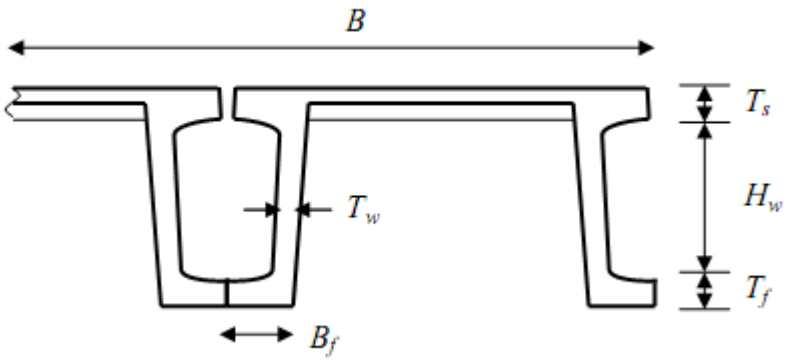

Figure 3. Diagram. The Pi-girder shape has several scalable parameters

The resulting Pi section is 96 in. wide and 33 in. deep when scaled for a 70 ft span as used on the demonstration bridge. The bridge uses two such girders and was load tested to determine the lateral distribution properties of such a design. It was found that the girder legs act independently, resulting in a load distribution behavior similar to a four girder bridge. Duplicate individual girders were also tested for flexural capacity and shear behavior. The flexural capacity test demonstrated the ability of the fibers to minimize crack size and improve the ductility of the girder. Seven and one half in. of mid-span deflection resulted in approximately 1100 cracks with crack widths near 0.001 in. and spacing of about 0.2 in. at mid-span. The shear test showed the fibers' contribution to the ductility of UHPC as the girder exhibited significant reserve load and deflection capacity after initial shear cracking. (Graybeal and Hartman 2005)

The previous two bridges demonstrated how optimized girder shapes using integrated decks could full take advantage of UHPC. Each showed that girder webs of UHPC members are adequate for shear strength without additional shear reinforcement. The research and development employed in creating these bridges lead to a greater understanding of UHPC properties and behavior in flexure.

Another focus of development for UHPC bridges is using UHPC in girders supporting a regular reinforced concrete deck known as slab-on-girder construction. This method of construction is familiar to bridge designers, erectors and transportation authorities. A composite girder system was constructed in Wapello County, Iowa using the method. The Mars Hill Bridge consists of a regular reinforced concrete deck placed on three UHPC girders. These girders were modified Iowa 45 in. Bulb-Tees. In order to reduce the amount of UHPC used, the shape was modified by thinning the web and bottom flanges by 2 in. and the top flange by 1 in. The bridge design development included flexural and shear tests on the proposed cross section as well as additional investigation into the shear strength of UHPC using compact beams with a generalized bulb-tee cross section (Bierwagen and McDonald 2005).

A similar approach to the Mars Hill Bridge is the Shepherd's Creek Road bridge designed by VSL –Australia. This bridge uses sixteen I-shaped precast, pretensioned girders. The girders weigh less than half of an appropriate prestressed girder of regular concrete. A unique feature of this bridge was the use of UHPC panels as stay in place form work for the regular reinforced concrete deck. These slabs are 1 in. thick and span the 7.85 ft clear spacing between the girders. This bridge was load tested to verify its performance relative to design expectations. The observed deflection at midspan corresponding to one and one half times the design load was 0.20 in. and the design methods predicted 0.23 in. (Rebentrost and Cavill 2006).

The use of UHPC panels as formwork was duplicated at the Saint Pierre La Cour bridge in Mayenne, France. As part of this bridge's development three solutions were studied and compared. The double-tee or Pi shape with integrated deck was compared to a regular concrete slab on UHPC girder as well as a design using a UHPC deck and steel girders. It was determined that the first two solutions are suitable for short to medium span bridges and the third may be better for long span bridges. The bridge constructed consisted of the second solution using a regular concrete slab made composite with UHPC girders. It was determined that this solution reduced the superstructure dead load by a factor of 2.2. (Behloul, Bayard et al. 2006)

The Horikoshi C Ramp Bridge is another example of the UHPC girder and regular concrete deck system. Located in the Fukuoka Prefecture of Japan the bridge was the first attempt in using

UHPC for a vehicular bridge in Japan. Like the Iowa Bridge, a customized girder cross section was selected to save on material costs and lighten the structure. The girder has no shear reinforcement which led to the use of a Perfobond Strip to complete the shear connection between the girder and the deck. The strip is a steel plate with holes in it embedded in the girder when its cast. The four girders are 40 in. deep and have a cross section similar to an inverted Tee. The bottom flange is 19 in. wide and the web is 3.5 in. wide. The composite girders were tested in two point flexure to verify their strength. These tests were compared to two finite element models. One had a fully rigid connection between the slab and girder. The second model used springs to model the Perfobond Strip. The results of the analyses bracketed the experimental behavior of the girder (Okuma, Iwasaki et al. 2006).

The construction of these slab on UHPC girder bridges again increased the knowledge base under UHPC. It was shown that modified girder shapes can be used with UHPC to more efficiently use UHPC. The construction of these bridges also showed that girder webs could be left unreinforced. Another advantage shown was that the UHPC systems were lighter than their conventional counterparts.

Material Characterization Studies of UHPC

UHPC has been studied by both its proprietors as well as governmental agencies in conjunction with these projects. The majority of these are investigations of basic material properties that are required for bridge design. Many of the aforementioned projects included flexural and shear tests of the selected girder systems. Additional material characterization studies were performed by various investigators as general inquiries into the behavior of UHPC without association with a particular bridge project. The largest such study was performed as part of a FHWA initiative into the use of UHPC in the United States.

The study entitled *Characterization of the Behavior of Ultra High Performance Concrete* was completed in 2005 and consisted of over 20 material tests as well as a flexural test of an 80 ft beam and three beam shear tests. The study also references four other investigations into the behavior of UHPC. The results of the study included a design philosophy for use with UHPC bridge girders. In flexural design, strain compatibility is suggested as an approach to include the

tensile strength of the material. Shear strength can be predicted using a formulation using web area and predicted diagonal tension angle as variables. (Graybeal 2005)

Another study was performed at Iowa State University entitled *Characterizing an Ultra-High Performance Material for Bridge Applications under Extreme Loads.* In it UHPC cylinders are subjected to four distinct tests. The first was uni-axial unconfined compression testing. The second was a confined uni-axial compression test. The confinement was provided by a 5/8 in. thick steel tube resulting in a confinement pressure of 2 ksi. Cyclic compression testing was also performed in which four load cycles were used. Stress Strain plots showed that large amplitude elastic strain cycles did not diminish the stress-strain behavior of the material. The final test was a flexural prism test. (Sritharan, Bristow et al. 2003)

The extreme performance capabilities of UHPC in compression and tension require alterations to the design procedures used in regular prestressed girder design. Previously it was mentioned that the FHWA initiated research resulted in a design philosophy being developed. Similar design philosophies are outlined in two design guides published overseas. JSCE of Japan and AFGC of France have both published design recommendations for use with UHPC. These both propose stress strain models for use in strain compatibility approach to design ((JSCE), Niwa et al. 2004) and ((AFGC) 2002).

The use of UHPC in varied bridge projects has resulted in many investigations into its material properties, flexural behavior and shear resistance. These properties have been needed to develop the constitutive relationships and material models needed for basic bridge element design. These material models have been implemented in finite element software to model flexural behavior of UHPC girders. The examples and techniques of previous UHPC bridge projects were used in the development of the research methods presented in this report.

Previous Work Concerning Optimization of Concrete Beams, Girders and Bridge Systems

Optimization is the minimization or maximization of a mathematical function. Optimization is useful when the function is a model of some real world phenomena. The most basic optimization is finding the minimum of a single variable continuous function. In this basic example the solution is found by iteratively guessing a solution, evaluating the function and its derivative at that guess and then using that derivative to determine the next guess at the solution. The iterations are repeated until the solution converges, that is to say the next solution is equal to the current solution. When expanded to more complex problems optimization requires complex algorithms to evaluate derivatives and gradients, account for variable constraints and efficiently arrive at correct and global solutions. The development of these algorithms and there application to engineering problems encompasses a large body of research.

The goal of engineered systems such as vehicular bridges is to be as efficient as possible while satisfying basic requirements. In this pursuit many investigations have been made on utilizing optimization techniques to arrive at efficient bridge designs. Some of these efforts have focused on components while others have taken the entire system on as the subject of optimization. Many optimization techniques have been applied in these efforts each suited to the scope of the optimization attempted. Each of these examples was scrutinized for application in the undertaking of optimizing girder shapes for use with UHPC.

Al-Ghatani et al. undertook the optimization of partially prestressed beams. The optimization utilized an existing optimization implementation in the form of a computer program called *IDESIGN*. A custom program was developed to interface with this program called *PCBDOS*. The custom program performed the operations related to the structural analysis of the prestressed beams. The results of these iterative analyses were used by *IDESIGN* to perform the optimization algorithms to arrive at the optimal design solution. The optimization focused on minimizing a cost function that includes concrete and steel material costs. The design variables included beam geometry elements like cross section shape and reinforcement locations as well as area of reinforcement and prestressing tendon profiles. Imposed constraints included logical

geometry constraints, minimum strengths and ACI code limits on allowable stresses and reinforcement ratios. This example provides several formulations of optimizations for prestressed concrete flexural members as well as an approach utilize existing optimization programs in the solution formulation. (Al-Gahtani, Al-Saadoun et al. 1995)

Barakat et al. present in two papers focused on the optimization of prestressed concrete beams. The first of these papers presents the development of an optimization formulation using reliability measures as the objective function. The design variables are geometric considering girder shape and prestressing area. Constraints are dictated by allowable stresses in the ACI code (Barakat, Kallas et al. 2003).

The second paper introduces a competing objective of minimizing cost of the solution. In order to handle the competing objectives the reliability objectives were converted into additional constraints. This publication demonstrates a way to handle multiple competing objectives in the optimization of prestressed concrete beams as well as a unique formulation of such optimizations. (Barakat, Bani-Hani et al. 2004)

Erbatur et al. implemented an optimization of prestressed concrete beams with the purpose of studying the optimization itself without any goals in developing optimum beams for a particular purpose. Beam cross section geometries were optimized with design variables including flange and web widths. The resulting optimum geometries were compared for various girder depths and spans. Two objective functions were utilized in each case, one was minimization on material costs and the other was minimization of total weight. The sensitivities of solutions to changes in span, depth and selection of cost function were observed as well. The results they present include that the optimized shapes are sensitive to changes in depth and span in predictable ways such that increased span length yields a solution including more prestressing area. The solutions were insensitive to selection of cost function minimized. The results presented in this paper are informative when considering the selection of an objective function in formulating an optimization technique for prestressed concrete girders. (Erbatur, Al Zaid et al. 1992)

Hassanain and Loov utilize optimization techniques in designing full bridge superstructures. The focus of the optimization was to demonstrate the applicability of High Performance Concrete; concrete with compressive strength exceeding 14.5 ksi in bridge girders. The girders are selected from standard available shapes. The design variables in this case are prestressing force, tendon eccentricities, deck thickness and girder concrete strength. The objective function is the cost of the super structure. The total cost is a function of the design variables in that girder detail selection influences the allowable sizes and spacing of those girders in the overall super structure. The costs included in the objective function were costs of the girders, the deck, and regular reinforcing steel. The design variables were constrained by AASHTO and OHBDC code requirements related to allowable stresses and girder spacing. The use of optimization in bridge super structure systems is demonstrated by this paper. It also provides an example of the use of a high strength concrete in place of normal strength concrete in bridge girders. (Hassanain and Loov 1999)

Khaleel and Itani present an example of shape optimization for prestressed beams. The objective is to minimize cost of the bridge by reducing the girder's cross sectional area. Design variables include girder flange sizes, steel locations and prestressing force. Their formulation includes shear reinforcement as one of the design variables and shear strength as one of the constraints. Other constraints are based on ACI code provisions. The inclusion of shear in the formulation makes this a unique paper. (Khaleel and Itani 1993)

Leps and Sejnoha set out to optimize rectangular regular reinforced beams. The optimized beams are unremarkable, the interesting aspect of this formulation is the utilization of genetic algorithms as their optimization formulation. The objective is to minimize cost of the beam as a function of the design variables of beam depth, beam width and top and bottom reinforcement amounts. A initial population of solutions are randomly generated and the optimization technique involves selecting the best performing solution candidates and recombining their properties to yield better solution candidates. The focus of the research was the development of the algorithms necessary to create the offspring beam solutions by mixing and recombining the parts of the fittest beams (Leps and Sejnoha 2003) Genetic algorithms are a novel approach to optimization problems.

Lounis and Cohn present another unique optimization technique. They demonstrate a formulation for multi-objective optimization of prestressed structures. Their technique is to transform all but one of the competing objectives into a constraint equation. This technique requires the solution of smaller single objective optimizations to develop the limits used in the additional constraint equations. The results of the technique are several optimal solutions from which a designer could choose the best system (Lounis and Cohn 1993).

Lounis et al. performed an investigation into the optimal girder shape for use in spans made continuous with post tensioned splices. First existing girder shapes were evaluated by optimizing the design of a full bridge super structure. The objective was to maximize girder spacing for various shapes. The girder types were evaluated using a performance indicator of the ratio of area of girder to max feasible spacing. New shapes were then developed in a subsequent optimization using the same optimization techniques but with additional design variables concerning the girder geometry including web width and flange widths and thicknesses. This paper presents a unique use of developing girder section geometry through optimization on the performance of an entire bridge super structure. (Lounis, Mirza et al. 1997)

Rabbat and Russell conducted a study of AASHTO and state sponsored girder shapes in order to compare structural efficiency and cost. The study utilizes three formulations to compare the girders. Guyon developed a factor based on maximum section modulus as presented in Figure 4.

$$\rho = \frac{r^2}{y_t y_b}$$

$r = \sqrt{\frac{I}{A}}$ (Radius of Gyration)
I = Moment of Inertia
A = Area
y_t = Distance from top fiber to centroid
y_b= Distance from bottom fiber to centroid

Figure 4. Equation. Guyon's Efficiency Factor.

Aswad's efficiency factor is also used by Rabbat and Russel. It is focused on bottom fiber section modulus because this usually controls in spans greater than 75ft. It is calculated using the equation presented in Figure 5.

$$\alpha = \frac{3.46\, S_b}{A h}$$

S_b = Section Modulus to bottom fiber
A = Area
h = Depth of section

Figure 5. Equation. Aswad's Efficiency Factor

The third formulation is a cost comparison of the total superstructure utilizing the girders. This paper establishes some techniques for comparison of girder shapes. (Rabbat and Russell 1982)

Sirca and Adeli utilize a neural network approach to the optimization of bridge super structure design. The design variables include continuous variables such as reinforcement areas in the girders and the deck and discrete variables such as number of girders, girder properties and deck thickness. Because of their algorithm's ability to account for a large number of constraints the optimization can include in the design variables for all the components of a superstructure. A

robust cost based objective function is also possible with the detail of the algorithm. The paper identifies and addresses the difficulty of utilizing continuous and discrete variables in an optimization. (Sirca Jr and Adeli 2005)

Park et al. performed an optimization to determine the most efficient girder shape to be used with UHPC. They determined that the unique properties of UHPC were well suited to the development of a girder utilizing an integrated deck which led to the selection of a Pi shaped girder as the starting point. The design variables were the various dimension of this Pi shape. The objective was minimizing area which was constrained by the Strength I and Service III limit states of the AASTHO LRFD code. The limits imposed by the code were applied through limiting crack widths as suggested by the UHPC guidelines published by the French Association of Civil Engineering. The optimization used finite element software to evaluate the objective function and constraints. A large portion of their efforts went into the development of a suitable material model for use with finite element methods. The optimization performed gave examples of constraints to use with UHPC. (Park, Ulm et al. 2003)

The formulations and techniques presented by the previous work on optimization of bridge elements and systems were considered and some selected to be implemented in this research.

Background Concerning Analytical Methods Used

Strain Compatibility and Stress Strain Relationships

In order to optimize girder cross sectional shapes for use with UHPC an analysis technique must be adopted. The unique properties of UHPC have lead to the development of several design recommendations. All of these propose a strain compatibility approach to analyze UHPC flexural members. Strain compatibility is a well known technique used in the analysis of prestressed members. In adapting it for UHPC the additional tension component of the material must be included in the analysis this tension component changes when the section cracks and the fibers are stressed. Several stress strain models have been developed for UHPC to be used in strain compatibility approaches.

The strain compatibility approach is used to analyze flexural members based on an assumed strain distribution. First a limiting strain and location is determined. In concrete members this may be the compression strain in the case of a crushing failure. The strain distribution is assumed to be linear and using the assumption that the strain is zero at the section's neutral axis its equation can be determined. Strain can then be converted to stress using the constitutive relationships of the materials. Stress is then converted to flexural forces by integrating the stress across the cross sectional geometry width. The neutral axis depth may be required to be determined iteratively if, due to complex materials, its location can not easily calculated. In that case, iteration continues until the resulting forces are in equilibrium. This is illustrated in Figure 6.

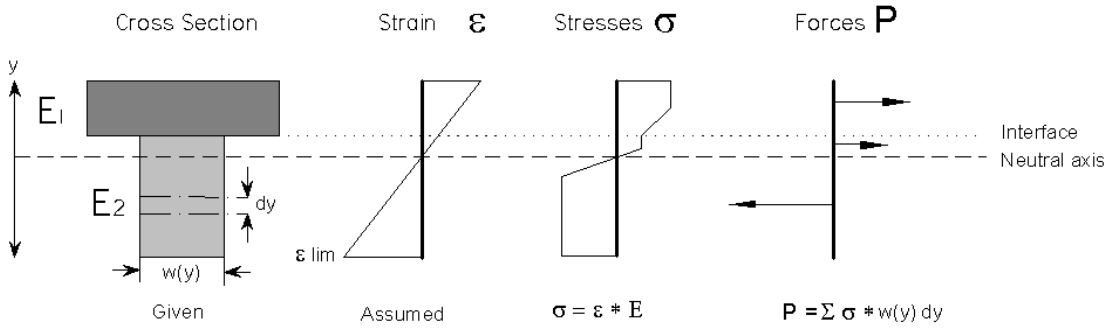

Figure 6. Diagram. The Strain compatibility method of analysis. Note that E1 and E2 are linearly elastic perfectly plastic constitutive models.

In order for strain compatibility to accurately model behavior of flexural systems, accurate stress versus strain relationships are required for each material. In the case of steel prestressing strand and normal concrete these relationships are well known. Steel is a heavily studied material and stress-strain models are available in textbooks as well as from strand suppliers. Concrete has a large number of models that have been developed by investigators. One of the most well known is the model developed by Hognestad. This model was chosen for conventional concrete members in this research.

UHPC has been studied less than conventional materials which limits the number of stress strain models available for use. Three were considered for this research. The first two come from recommendations published by engineering associations in France and Japan. Both utilize a linearly elastic, perfectly plastic model for compressive behavior. Both also have a complex tension behavior consisting of multiple portions. The model produced by the Japanese Society of Engineers (JSCE) uses three linear portions((JSCE), Niwa et al. 2004) (Figure 7).

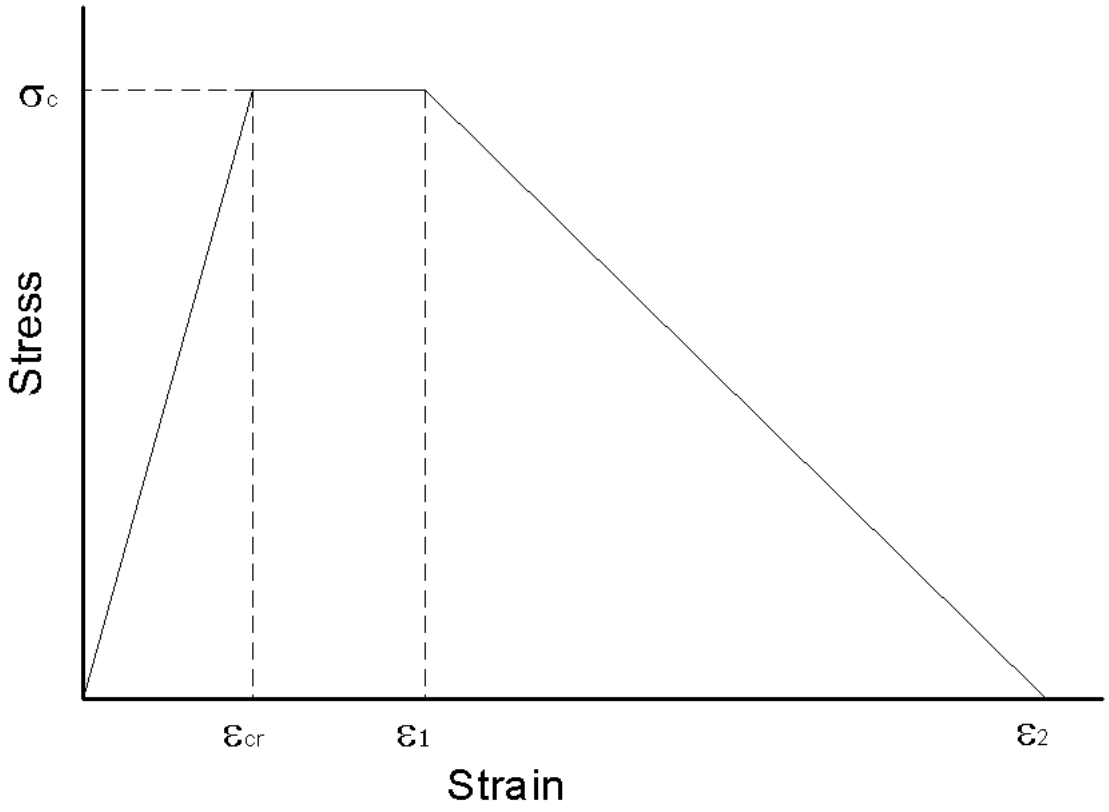

Figure 7. Diagram. Tensile Stress -Strain Diagram for UHPC from JSCE

The model recommended by the French Association of Civil Engineers (AFGC) utilizes 4 linear portions ((AFGC) 2002) as presented in Figure 8.

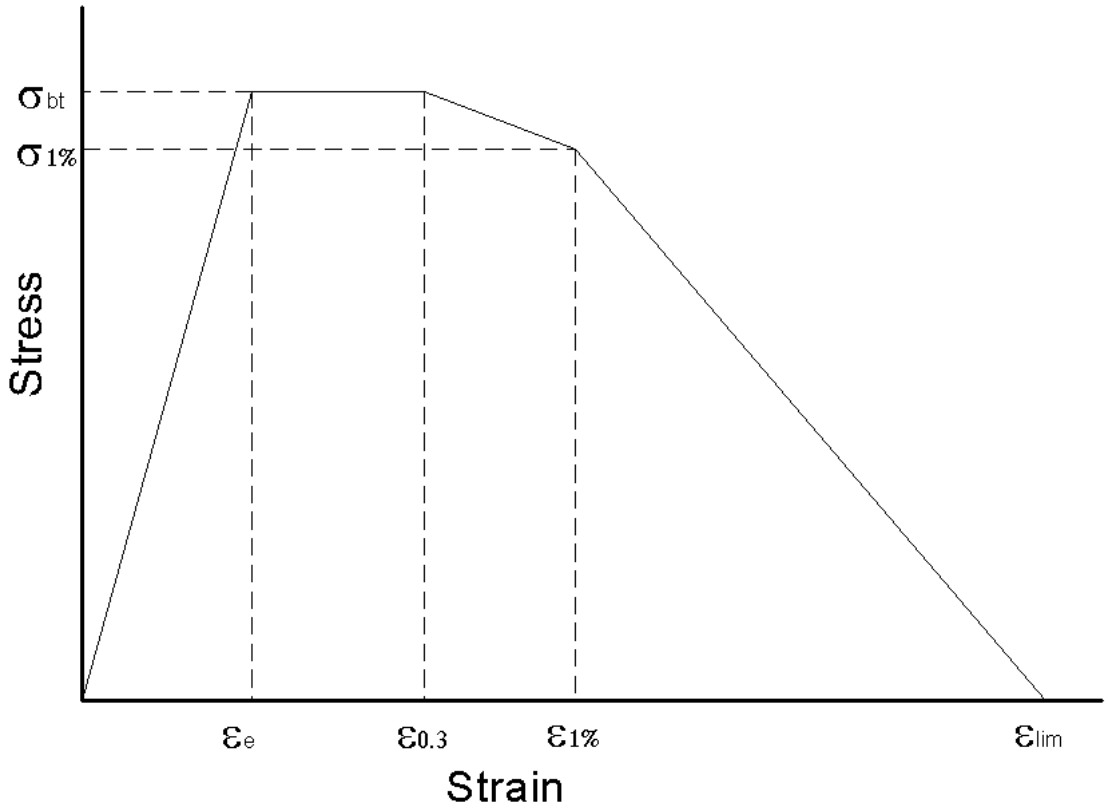

Figure 8. Diagram. Tensile Stress - Strain Diagram for UHPC from AFGC

After full scale girder testing using UHPC, Graybeal recommended a simpler model of UHPC's flexural behavior. It uses an elastic compressive portion up to a usable stress and a simplified tension model depicted (Figure 9).

Figure 9. Diagram. Tensile Stress - Strain Diagram for UHPC recommended by Graybeal for Flexural Design

Steinberg and Ahlborn used strain compatibility methods and a modified version of the AFCG curve to compare analyses techniques to determine the most appropriate method of analyzing UHPC. Their results showed that the tension component of UHPC was required to accurately model the behavior of UHPC flexural members (Steinberg and Ahlborn 2005). Graybeal recommends use of the simpler UHPC constitutive model because it is conservative and reduces computational effort involved in iterating on neutral axis depth until a solution in equilibrium is found (Graybeal 2005). Further discussion of the implementation of the strain compatibility analysis using *Matlab*® is presented in Chapter Two.

The Stability of Prestressed Concrete Girders

Girder stability is becoming an important factor in bridge design and erection. As material strengths rise, longer span lengths are achievable with the same cross section. These increased span lengths lead to stability concerns that were not an issue when common girder shapes were

initially created. Many investigations have been performed corresponding to the manifestation of these stability issues.

Stratford et al. identified the potential hazards of instability of prestressed girders during bridge erection. For each case, they develop and present formulaic methods to calculate the critical distributed load that will cause buckling. The first case occurs at transfer when the beam is simply supported at the ends but rotationally restrained about the beam axis. The second case is during transport when due to the necessary design of the truck, one end of the beam is free to rotate about the beam axis. The controlling case is during erection when the beam is suspended from a crane. In this toppling case, the girder is completely unrestrained from rotation which may result in a rigid body rotation such that a portion of the beam's self weight is causing a flexural condition on the minor axis of the girder. The accompanying figure depicts the support conditions. (Figure 10) (Stratford, Burgoyne et al. 1999)

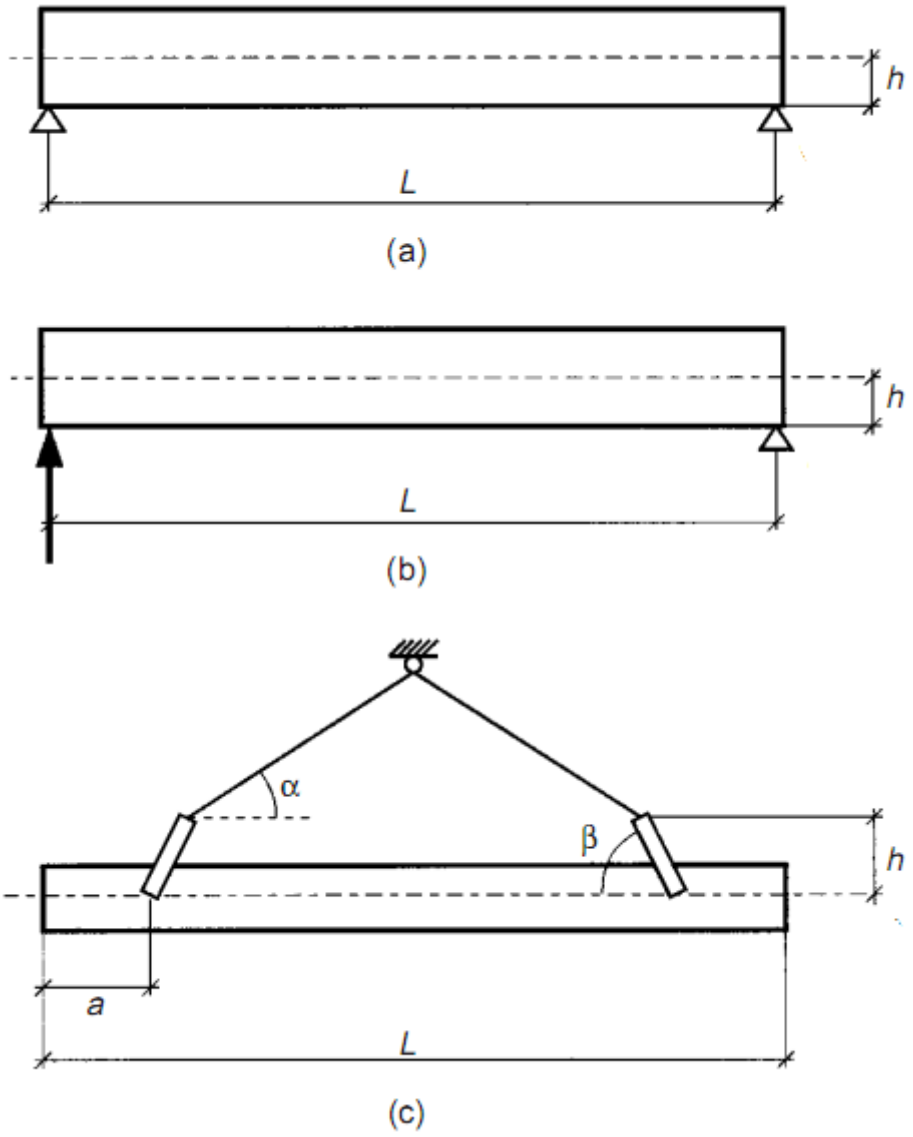

Figure 10. Diagram. The three support conditions for beams considered. (a) simply supported at both ends; (b) supported as for transportation, with the left hand end supported against displacement but not rotation; (c) hanging from cables at an angle alpha, with yokes at angle beta (in practice, beta will be either alpha or 90 degrees)

In the toppling case, the geometry of the crane cables plays an important role because angled cables introduce axial load into the girder. To account for this, Stratford et al. provide some nomagraphs to determine the critical load. In each case, by utilizing a Southwell plot, the expressions for the critical loads are developed which are presented below in Figure 11. In the toppling case, the formula presented results from vertical crane cables. This simplification to the crane geometry avoids the need for nomagraphs.

Simply Supported Case

$$w_{cr} = 28 \cdot 4 \frac{\sqrt{G J E I_y}}{L^3}$$

Transportation Case

$$w_{cr} = 16 \cdot 4 \frac{\sqrt{G J E I_y}}{L^3}$$

Toppling Case with Vertical Crane Cables

$$w_{cr} = \frac{12 E I_y h}{\frac{L^4}{10} - a L^3 + 3 a^2 L^2 - 2 a^3 L - a^4}$$

Where
G = Shear Modulus of Concrete
J = St Venant's Torsion Constant of Girder
E = Youngs Modulus of Concrete
I_y = Moment of Inertia about Minor axis of Girder
L = Length of Girder
h = Height of yoke to cable attachment points above beam centroid
a = Distance from Girder end to yoke attachment point

Figure 11. Equation. Formulas to determine critical distributed loads in three support conditions.

The derivation of the toppling case is presented more in depth in another paper authored by Stratford. This paper presents consideration for imperfections and lateral loads induced by wind. (Stratford and Burgoyne 2000)

A fourth case that also important in bridge erections but does not result directly from girder geometry was investigated more closely in a different paper. Burgoyne and Stratford

investigated the influence flexible bearings have on girder stability at the time of erection. Until a girder is adjoined to its neighbors by diaphragms, the bearing is the only rotational restraint present. The stability of a girder is also influenced by any initial sweep in the girder due to inaccurate placement. Burgoyne and Stratford develop the equations necessary to determine the required rotational stiffness of the bearing to prevent buckling of the girder (Burgoyne and Stratford 2001).

Summary of Literature Review

The literature important to this research is wide and varied. UHPC has been introduced and characterized by various studies. Its presented properties make it evident that its use in bridges will provide many advantages. Examples of UHPC bridge systems provide a direction of research to achieve its further implementation. Previous optimization studies of bridges and correlating investigation into bridge girders yield the tools to accomplish this research.

CHAPTER 3 Investigation Procedure

The goal of this research is the incorporation of UHPC into highway bridges using modified versions of widely available existing girder shapes. In the pursuit of developing a method for doing this several distinct stages of investigation were needed. This chapter describes each stage and the procedures utilized within each one. The stages are divided into an investigation of existing shapes, development of software tools, initial investigations into optimization, a survey to determine feasibility and final optimizations. Each stage is explained subsequently.

Existing Girder Shape Investigation

The first stage was identifying those girder shapes most widely used in the United States. This was accomplished in two surveys. The first survey consisted of conducting a review of state department of transportation and Precast/Prestressed Concrete Institute (PCI) member companies' websites. During the review of manufacturer sites the shapes published as available were documented. In the survey of state departments of transportation (DOT) websites the approved shapes listed were recorded for each site that such information was available. If they were recoverable from the site, the specifications for the shapes were retrieved as well.

The second survey was conducted to supplement the information collected from the websites. This was a traditional survey of practicing engineers working in state DOTs. For each state representatives were selected by searching for contact information on state DOT websites. At least one representative was identified for each state. These representatives were invited by email to complete a small web based survey about the girders used in their state. The language of the email also encouraged the forwarding of the email to other colleagues in order to increase the number of responses to as many as possible. The language of the survey are presented in Appendix 1.

Software Development

The next phase of investigation dealt with the development of the optimization procedure utilized in the course of this research. *Matlab*® was selected as the development platform because of its ease of use and the availability of a multitude of algorithms included with the standard installation as well as available in library extensions known as toolboxes.

Girder Analysis

The first task completed using *Matlab*® was the development and verification of a girder analysis program (GAP). GAP uses a strain compatibility approach to determine the internal forces present in a composite slab and girder section for a given strain condition. This is done by using an included *Matlab*® function for root finding known as *fzero* to determine the solution to the general equation of equilibrium (Figure 12).

$$0 = f_T(y) + f_C(y) + f_S(y)$$

f_T = Sum of the forces in the Steel
f_C = Sum of the forces in the Girder
f_S = Sum of the forces in the Slab
y = Depth of neutral axis

Figure 12. Equation. Girder Equilibrium

The algorithm searches to determine the depth of the neutral axis required to balance the internal forces present in the girder. This required the development of the algorithms to apply strain compatibility to solve for stresses and forces in a girder from a strain distribution. For each iterative guess the solver makes at the neutral axis depth, the solver creates a linear strain distribution from two points. The first point is the limiting strain value. The depth of this point at the location of that value is also required. In most cases this is the crushing strain and its location

is the top of the girder. The second point that defines the line is the zero strain value and the depth of the neutral axis.

Once a strain distribution is determined, the forces in the girder are then calculated. Each component has its own algorithm to determine its forces. The girder forces are calculated by integrating the product of the width and stress as functions of the depth as shown and described in Figure 13.

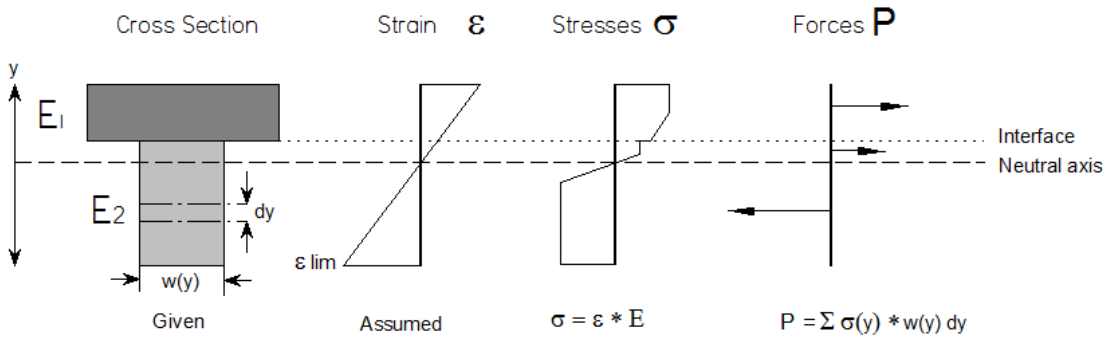

Figure 13. Diagram. Strain compatibility method of analysis. Note that E1 and E2 are linearly elastic perfectly plastic constitutive models.

The stress as a function of depth is determined by a material model function that can be customized. Once a strain is determined at a particular depth it is plugged into a material model to determine the stress at that depth. Hognestad's model is used for conventional concrete; the design model proposed by Graybeal is used for UHPC (Figure 14) (Graybeal 2005).

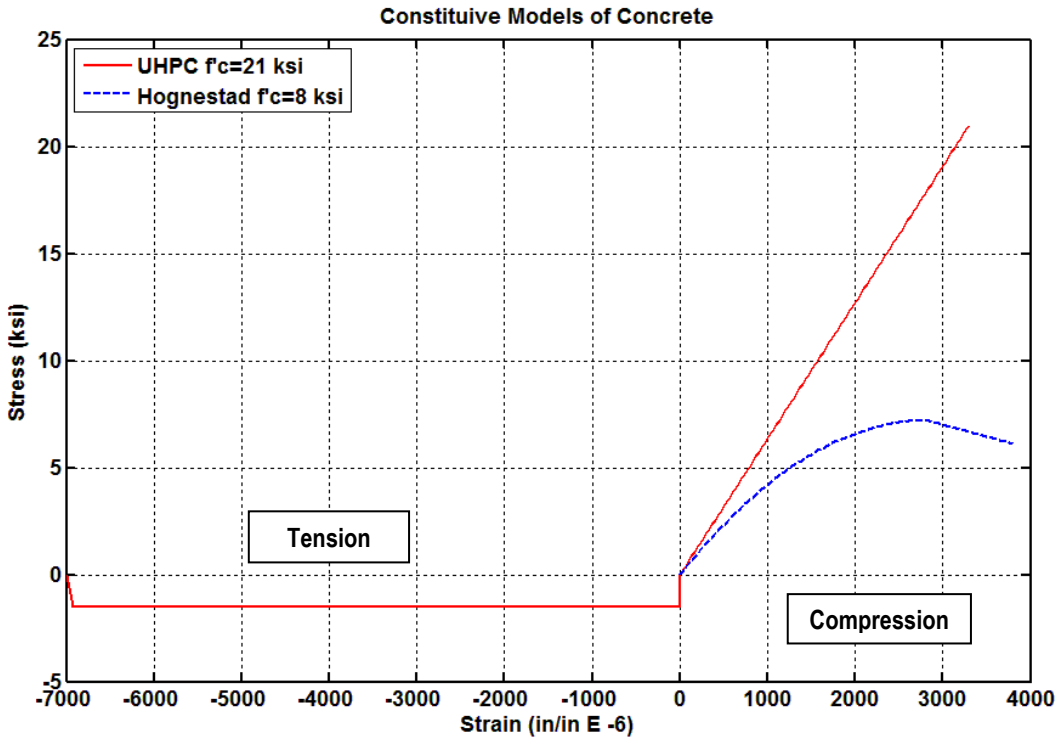

Figure 14. Plot. Constitutive models of conventional and UHPC concrete used in the optimization.

The formulation of each model is done piecewise because of the respective discontinuities and each includes compressive strengths of the material as a parameter. The formulation of Hognestad's model includes a linear and quadratic portion and includes no tensile strength (Figure 15).

$$\sigma(\epsilon) = 0 \qquad \epsilon > 3801$$

$$\sigma(\epsilon) = \frac{-0.15 * fce}{3800 - \epsilon_o}(\epsilon - \epsilon_o) + fce \qquad 3801 \geq \epsilon > \epsilon_o$$

$$\sigma(\epsilon) = \left(\frac{2\epsilon}{\epsilon_o} - \left(\frac{\epsilon}{\epsilon_o}\right)^2\right) * fce \qquad \epsilon_o \geq \epsilon > 0$$

$$\sigma(\epsilon) = 0 \qquad 0 \geq \epsilon$$

Where

σ = Stress in ksi

ϵ = Strain in microstrain

fce = 0.9 *f'c in ksi

$\epsilon_0 = \frac{2000\, fce}{1.8 * 10^6 + 460\,000\, fce} * 10^6$ in microstrain

Figure 15. Equation. Hognestad's Model for Concrete Compressive Stress as a Function of Concrete Strain

The model used for UHPC assumes a tensile strength of -1.5 ksi (10.3 MPa) at tensile strain limit of 7800 microstrain (Figure 16).

$$\sigma(\epsilon) = 0 \qquad \epsilon > 3300$$

$$\sigma(\epsilon) = \frac{f'c}{3300}\epsilon \qquad 3300 \geq \epsilon > 0$$

$$\sigma(\epsilon) = 1.5 \text{ ksi} \qquad 0 \geq \epsilon > -7000$$

$$\sigma(\epsilon) = 0 \qquad -7000 \geq \epsilon$$

Where

σ = Stress in ksi

ϵ = Strain in microstrain

Figure 16. Equation. Graybeal's Simplified UHPC Model fo Concrete Compressive Stress as a Function of Concrete Strain

Each model returns the corresponding stress for a given strain. The integration is completed by a built in *Matlab*® function *quad* that uses adaptive Gaussian quadrature to arrive at a solution. The slab forces are determined in a similar fashion. GAP has the ability to include a differential strain between the slab and girder. Differences in creep and shrinkage strains could cause the slab to have an offset strain profile when compared to a linear continuation of the strain in the

girder. Differential strains are also imposed by the loading stages that occur during construction. In the optimization phases differential strains were ignored because they are difficult to predict.

The steel forces are determined by transforming a strain to a stress and multiplying by the area of the steel to determine the force. When the present steel is prestressed the incompatible strains are accounted for before the steel strain is passed to the constitutive model. The constitutive model for 270 ksi strand was used in the optimization. Other models were developed for mild steel grades but not used in the optimization (Figure 17).

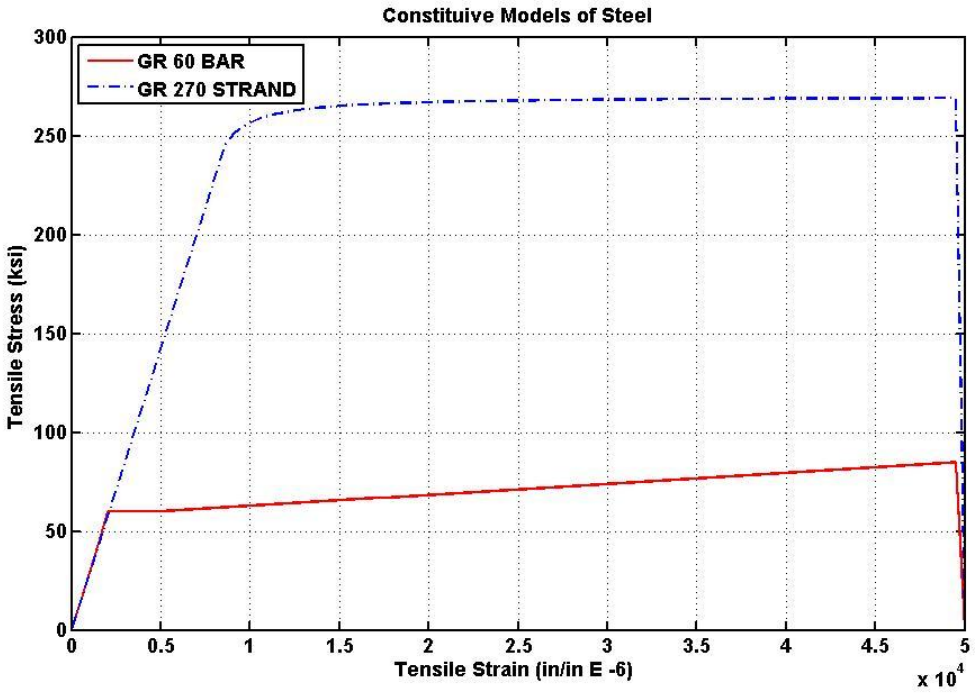

Figure 17. Plot. Constitutive models of mild and strand reinforcement used by the GAP

Steel in the girder is described by three variables, depth, area and prestressing force at jacking. The stress values are reduced by the major losses before forces are calculated. When the steel is prestressed the losses are calculated using the equations taken from AASHTO A5.9.5.3 (Figure 18) for long term losses and C5.9.5.2.3a-1 (Figure 19) for elastic shortening losses.

$$\Delta fp_{LT} = 10 \frac{f_{pi} A_{ps}}{A_g} \gamma_h \gamma_{st} + 12 \gamma_h \gamma_{st} + \Delta f_{pR}$$

$$\gamma_h = 1.7 - 0.01 H$$

$$\gamma_{st} = \frac{5}{1 + f'_{ci}}$$

Where

Δfp_{LT} = Long term losses due to Creep, Shrinkage and Relaxation

f_{pi} = Stress in prestressing prior to transfer

H = Average annual ambient relative humidity (Assumed to be 70 %)

γ_h = Humidty correction factor

γ_{st} = Transfer strength of concrete correction factor

Δf_{pR} = Esitmate of relaxation losess (Assumed to be 2.5 ksi)

Figure 18. Equation. AASHTO Approximate estimate of time-dependant losses (A5.9.5.3)

$$\Delta fp_{ES} = \frac{A_{ps} f_{pi} \left(A_g e_m^2 + I_g\right) - A_g e_m M_g}{\frac{A_g E_{ci} I_g}{E_s} + A_{ps} \left(A_g e_m^2 + I_g\right)}$$

Where

Δfp_{ES} = Elastic Shortening Losses

A_{ps} = Area of Prestressing

f_{pi} = The prestressing force immediatly after transfer ($0.9 * 0.75 * f_{pu}$)

A_g = The area of the girder

I_g = The moment of inertia of the girder

e_m = The strand eccentricity at mid – span

M_g = The self weight moment of the girder at mid – span

E_{ci} = The modulus of elasticity of the concrete at transfer

E_s = The modulus of elasticity of the steel

Figure 19. Equation. AASTHO alternate equation for losses due to elastic shortnening (C5.95.2.3a-1).

The AASHTO equations for creep and shrinkage were developed for conventional concrete girders which undergo creep and shrinkage for many years. UHPC creep and shrinkage is accelerated by the steam heated curing process and afterward the UHPC girder exhibits little to no additional changes in volume or length. This equation remains a good approximation because

the magnitude of creep and shrinkage between UHPC and conventional girders is similar (Graybeal 2005).

Once the forces are balanced, the contributions of each component to the moment are calculated. Steel moments are determined by taking the dot product of the vector containing the steel location depths and steel location forces. Calculation of moments is done in the girder and slab by integration of the product of the force and the vertical distance from the bottom of the girder as depicted (Figure 20).

$$M = \int w(y)\,\sigma(\epsilon(y))\,Y(y)\,dy$$

Where

M = Moment in girder or slab

w(y) = Width of section at depth y

$\sigma(\epsilon)$ = Stress as function of strain defined by relavent constituive model

$\epsilon(y)$ = Strain in section at depth y

Y(y) = Distance from depth y to location of point about which moments are taken

Figure 20. Equation. Calculation of moments in girder or slab by integration of stress.

The culmination of these steps is the calculation of the moment capacity of a girder for a given strain condition. GAP has a graphical front-end to demonstrate the iterations of the solving process (Figure 21).

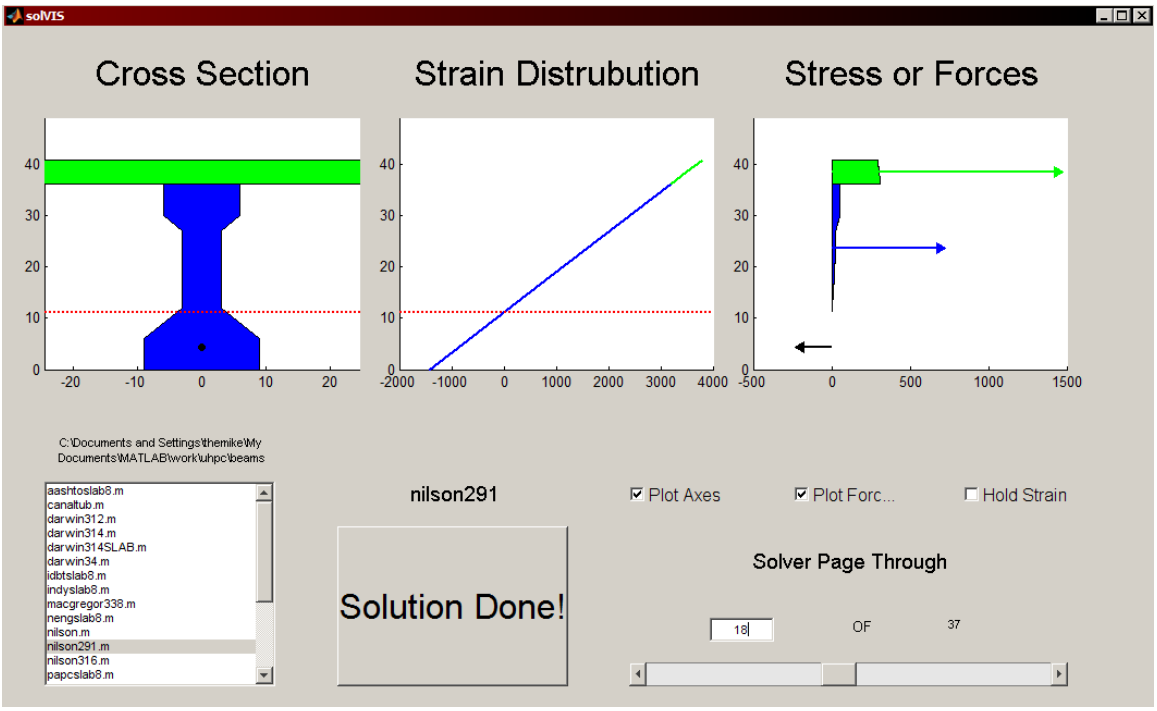

Figure 21. Image. The GUI to display the iterations of the GAP solving program.

In this case the 18th of 37 iterations is shown. The forces window displays both the concrete force as a function of depth as well as the sum of those forces as vectors because the plot forces option is checked. At this iteration the guess at the neutral axis depth is clearly too low in the section resulting in unbalanced forces.

The GAP program includes some assumptions to achieve simplicity and reduce computational time. One is that sections are treated as fully composite when a slab is present. To handle situations where the neutral axis guess made by the *fzero* algorithm is no longer bounded by the dimensions of the girder a conditional catch is implemented. If the solver's gradient leads to a guess wherein the neutral axis depth is negative then the solution will not converge. A neutral axis location below the girder results in all of the concrete and steel in compression and the tension forces are zero making equilibrium impossible. To correct this it is assumed that the system is under-reinforced and the moment capacity for the desired strain location is governed by the tension steel present. In this case the moment capacity is calculated by adjusting the limiting strain to -2070 microstrain for mild reinforcement and -8600 microstrain in the case of strand at the most extreme steel location. The moment capacity is then calculated base on this

imposed tension yielding. Imposing larger strains in the steel resulted in crushing of the concrete. Strains were limited to tension yield because allowing the strand to approach rupture strength resulted in lower moment capacities. The force in a prestressing strand does not increase much as the strain is increased past yield but less and less concrete is in compression resulting in lower moments.

GAP was developed anticipating the shape optimization algorithms and as such was developed to operate on a wide array of variable inputs. The most important is the girder's shape as described by the ordered pairs of shape vertex locations as shown in Figure 22.

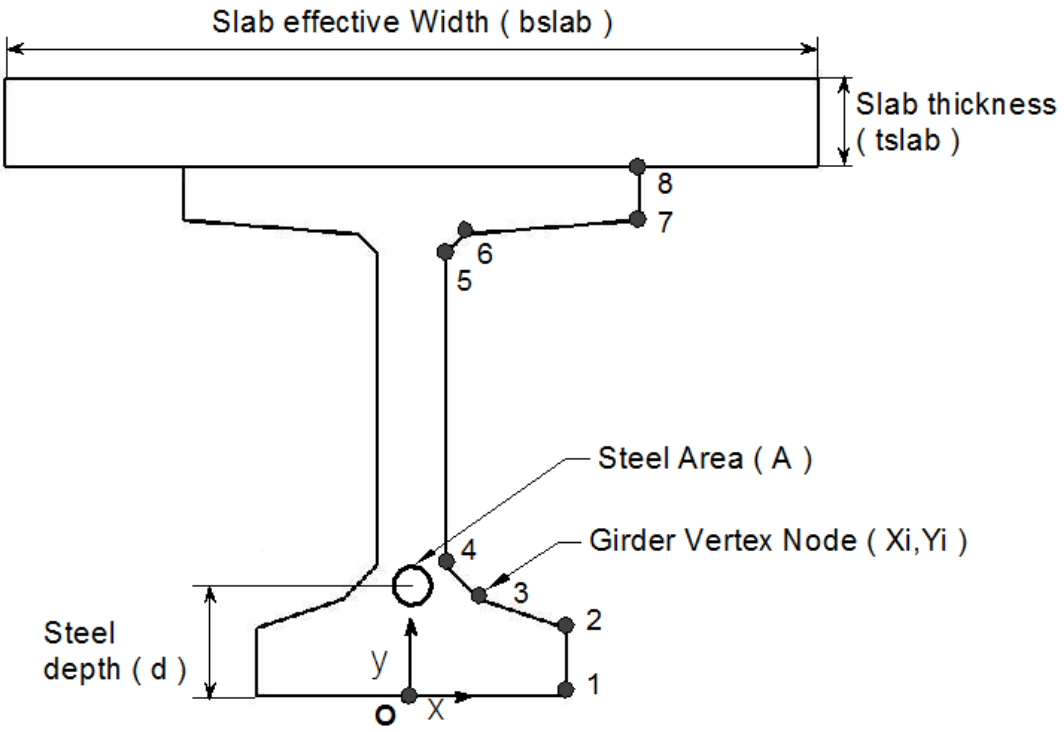

Figure 22. Diagram. Geometric Variables used in the GAP.

The origin is located at the intersection of the centerline of the girder and the bottom fiber. This origin is used consistently through out GAP to describe dimensions and distance. Nodes are numbered from the origin as well with node one at the bottom fiber and node eight at the slab interface.

Other variables considered include steel and concrete properties, steel area and locations, slab thickness and effective width as well as others. Each variable is stored in a single *Matlab*® structure type variable so they all can be passed from function to function easily. Each variable in the girder structure is listed and described in Table 3.

Table 3. Elements of girder structure variable utilized in the GAP

Element	Units	Type	Description	Typical Value
X	in	double	Vector of section node locations	[15,15,8,3,3,20,20]
Y	in	double	Vector of section node locations	[0,8,10,16,36,42,48]
L	in	double	Length of girder	840
UW	lbs/ft^3	double	Unit Weight of girder concrete	150
A	in^2	double	Vector of steel areas	[1.53,1.53,1.53]
d	in	double	Vector of steel depths	[2,4,6]
P	kips	double	Vector of steel jacking force	[372,372,372]
fc	ksi	double	Girder concrete compressive strength	8
conc	NA	char	Girder concrete model	'uhpc2'
elimit	μ strain	double	Limiting strain condition	3300
eloc	in	double	Limiting strain depth	56
steel	NA	char	Steel model	'strand270'
strand	in^2	double	Area of single strand	0.153
tslab	in	double	Thickness of slab	8
bslab	in	double	Effective width of slab	96
CncSlab	NA	char	Slab concrete model	'hognestad'
fcslab	ksi	double	Slab concrete compressive stress	4
ediff	μ strain	double	Differential strain between slab and girder	0
area	in^2	double	Calculated area of girder	850
I	in^4	double	Calculated moment of inertia of girder	2.61E+05
ybar	in	double	Calculated centroid depth of girder	25.413
cy	in	double	Calculated neutral axis of girder	48.882
C	kips	double	Sum of forces present in the girder	0
T	kips	double	Vector of forces in the steel	[-406.81, -406.56, -406.29]
SF	kips	double	Sum of forces present in the slab	1.22E+03
M	in kips	double	Sum of internal moments in the system	6.37E+04

GAP was verified by the solution of various textbook example problems. These problems were selected to verify each feature of the solver and as such each increases in complexity. Regular reinforced beam examples were taken from the textbook *Design of Concrete Structures* (Darwin, Dolan et al. 2003). Prestressed examples were taken from *Design of Prestressed Concrete* (Nilson 1987). The girder tested by Graybeal was used to verify UHPC (Graybeal 2005). The details of each of the verifications are presented in Table 4.

Table 4. Verification of Girder Analysis Program through Example Problems

Standard Reinforced Beams			Source		Solver		Percent Differences	
Beam Name	**Type**	**Depth d (in)**	**c1 (in)**	**M1 (in k)**	**c2 (in)**	**M2 (in k)**	**(c1-c2) / d (%)**	**M1-M2 / M1 (%)**
Darwin 3-2	Simple Rectangular	25	4.92	2976.00	5.39	3142.80	-2%	-5%
Darwin 3-12	Doubly Reinforced	25	8.89	9450.00	8.90	9499.80	0%	-1%
Darwin 3-14	T-Beam	30	8.39	10410.00	8.94	10530.00	-2%	-1%
Darwin 3-14S	T-Beam with top as slab	30	8.39	10410.00	8.94	10530.00	-2%	-1%
Prestressed Beams			**Source**		**Solver**		**Percent Differences**	
Beam Name	**Type**	**Depth d (in)**	**c1 (in)**	**M1 (in k)**	**c2 (in)**	**M2 (in k)**	**(c1-c2) / d (%)**	**M1-M2 / M1 (%)**
Nilson 3-16	Generic Rectilinear I	24	6.10	3089.00	8.07	3228.20	-8%	-4%
Nilson 291	AASHTO II w/ slab	36	3.18	20880.00	4.39	22367.00	-3%	-7%
Graybeal 80F	UHPC AASHTO II	36	5.00	27840.00	6.73	29210.00	-5%	-5%

Larger differences between the textbook solutions and the solver solutions are observed in the more complex the girder systems. The textbook solutions assume values that the solver calculates directly. Prestress losses are calculated in GAP where those in the two text book examples are assumed. The analytical solution presented by Graybeal uses the Whitney stress block to approximate the behavior of UHPC. The analytical solution used by Graybeal also assumed that the UHPC carried no tensile load after cracking where as the UHPC model used by the solver carries 1.5 ksi of strength across cracks straining to -7000 microstrain. This is a conservative design approximation suggested by Graybeal for use in girder design. Both the Graybeal analytical approach anf the strain compatability approach used by GAP were conservative because of the simplified UHPC tension model used.

Sensitivity Analysis

Sensitivity analysis was conducted before proceeding to optimization for two reasons. The first was to determine which girder parameters influence the flexural performance of the girders when paired with a composite slab. The second was to test the robustness of GAP. For each girder parameter listed in Table 5 one hundred analyses were performed with a probabilistic input resulting in a total of 1400 runs.

Table 5. Sensitivity Analysis Variables

Variable	Distribution Type	Distribution Values	Note
Thickness of Bottom Flange (in)	Uniform	[0,12]	Original Edge thickness is 6"
Width of Bottom Flange (in)	Uniform	[10,42]	Original Width is 26"
Limiting Strain (microstrain)	Normal	(3300,40)	Crushing Strain in Hognestad and Graybeal
Slab Concrete Strength (ksi)	Normal	(4,0.5)	Typical Deck Strength
Top Flange Thickness (in)	Uniform	[0,7]	Original edge thickness is 3.5"
Top Flange Width (in)	Uniform	[10,52]	Original Width is 42"
Girder Concrete Strength (ksi)	Normal	(28,0.5)	Graybeal Mean Strength was 28 ksi
Grade 250 Prestressing (ksi)	Normal	(100,50)	188 ksi in between 1 and 2 Deviations
Slab Thickness (in)	Uniform	[4,12]	Typical Decks are 8"
Slab Effective Width (in)	Uniform	[36,128]	Similar to a Spacing Range of 0 - 12 ft
Steel Area (in^2)	Normal	(2.75,1.38)	Max # Strands is 36 Dist. Uses (18,9)*0.153 in^2
Web Width (in)	Uniform	[0,12]	Original Width is 6"
Girder Length (ft)	Normal	(90,20)	2 Deviations yields a range [50,130]
Girder Unit Weight (lbs/ft^3)	Normal	(150,5)	Typical Weight is 150 lbs/ft^3

The initial girder was a PCI BT- 63. Also listed in Table 5 are the random distributions from which the inputs were selected. These distributions were identified by physical constraints such as in the case of girder geometries. Other distributions were taken from literature or typical values. For example the distribution of UHPC strength was taken from results presented in Graybeal. Distributions in square brackets are uniform distributions where the range of the variable is given. Each value in the range has an equal probability of appearance. Parentheses indicate a normal distribution. The first value is the mean and the second the standard deviation. In these distributions the average is more likely to come up. The sensitivity analysis was concluded by comparing the first order sensitivity of the girder moment capacity to changes in the variables.

Optimization of Girder Shapes for Direct Replacement

The optimization scheme designed to develop a methodology for girder modification for use with UHPC. GAP was used as the basis for the development of the optimization objective function. The goal was to create a general list of modifications to standard girder shapes to make them cost effective when used with UHPC. To do this, an optimization formulation was

developed. The general optimization formulation described was carried out on 73 girder shapes drawn from a catalogue of 11 girder shape families presented in Table 6.

Table 6. Girders Included in Optimization

State or Body	Designation	# Of Girders	Depth Range (in)
AASHTO	TYPE I-VI	6	28-72
Idaho	BT-*	10	30-84
Indiana	BT-*	6	54-84
New England PCI	NEBT-*	5	39-71
Pennsylvania	PCEF-*	18	30-96
PCI	BT-*	3	54-72
South Carolinia	Modified BT-*	3	54-72
Virginia	PCBT-*	9	29-93
Washington	WF-*	6	42-95
Washington	BTG-	3	32-62
Washington	DG-	4	35-65
		73	Total

Each family specification was retrieved as part of the surveys conducted of the state DOT websites. Each collection of shapes contained several girder depths. Each girder shape was altered through the course of the optimization such that the optimized UHPC shape would fit inside the original conventional shape and its casting could be executed by adding block outs to the conventional form. It was hypothesized that a commonality across the resulting optimized shapes would emerge leading to a methodology for form modifications to utilize UHPC.

The general formulation of the optimization formulation for the multi objective algorithm used is presented in Figure 23.

Minimize $\gamma \ni F(x) - w\gamma \leq G$

Subject to

$\text{lb} \leq x \leq \text{ub}$

$A\,x <= 0$

Where

$F(x)$ = Objective Function

G = Goals

w = Goal weights

x = Vector of design variables

γ = Feasable Space Coefficent (Indicates size of feasible space at any iteration)

lb = Lower bounds on design variables

ub = Upper bounds on design variables

A = Matrix of linear constraint equation coefficents

Figure 23. Equation. Multi-Objective Optimization Formulation

A vector ***x*** is sought such that the objective function is less than the goals subject to constraints imposed on the design variables. If an objective is to be larger than a goal, then its weighting element is negative. The *Matlab*® function *fgoalattain* was used because of its capability to solve multi-objective problems.

The general steps of the optimization are presented in a flow diagram in Figure 24.

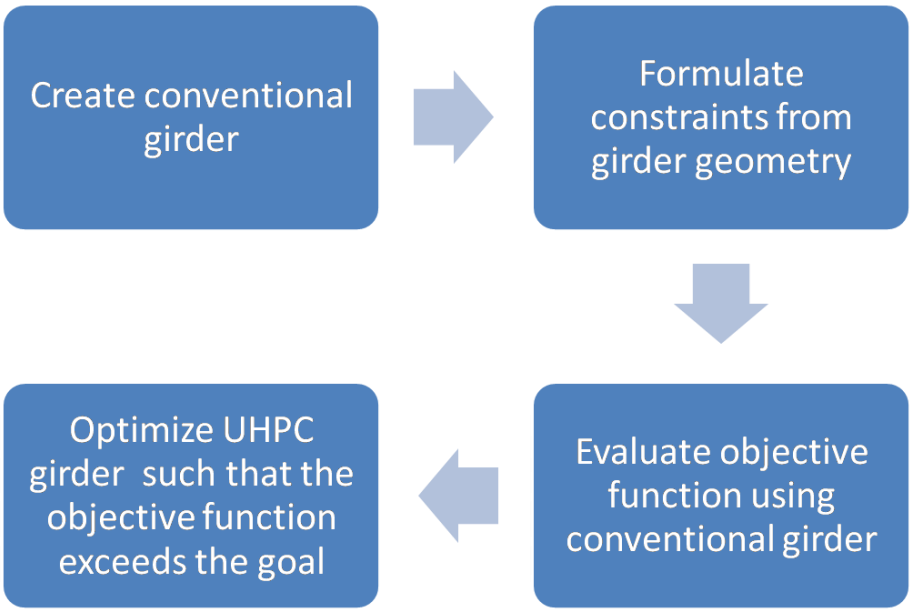

Figure 24. Diagram. The basic organization of the optimization plan for each girder shape.

For each girder shape, a structure-type variable is created to store the girder information. The girder structure was initialized to contain the variables listed in Table 3. The length of the girder, which is required for the calculation of prestress losses, was determined from the max length suggested by the state design guide for that girder using the mean girder spacing listed. Usually that spacing was 6 ft. The girder is matched with a slab with an 8 in. depth and an effective width determined from the portion of AASHTO Equation A4.6.2.6.1 utilizing flange width. The equation result is the minimum of three terms but two of these terms require knowledge of the bridge girder spacing which was omitted in this portion of the investigation.

The objective function is calculated for this composite girder. Then the optimization routine is called to determine the optimized girder that meets or exceeds the objective function value of the conventional girder. Assumed constants used in the conventional stage and the UHPC stage are listed in Table 7.

Table 7. Static Elements of Girder Structure

Element	Units	Description	Value
UW	lbs/ft^3	Unit Weight of girder concrete	150
P	kips	Vector of steel jacking force	Steel Area * 0.75 * 270 ksi
fc	ksi	Girder conventional concrete compressive strength	8
fc	ksi	Girder UHPC compressive strength	21
elimit	μ strain	Limiting strain condition	3300
eloc	in	Limiting strain depth	56
steel	NA	Steel model	'strand270'
strand	in^2	Area of single strand	0.153
tslab	in	Thickness of slab	8
CncSlab	NA	Slab concrete model	'hognestad'
fcslab	ksi	Slab concrete compressive stress	4
ediff	μ strain	Differential strain between slab and girder	0

Design Variables

The design variables for this optimization procedure were elements of the girder geometry. The design variables listed modify the location of the nodes stored as girder structure variables "X" and "Y" shown in Table 8.

Table 8. Design variables used in girder optimization

Variable	Description	Girder Geometry Affected
x1	Top Flange Width	x8,x7
x2	Top Flange Mid-Node X Location	x6
x3	Web Width	x5,x4
x4	Bottom Flange Mid-Node X Location	x3
x5	Bottom Flange Width	x2,x1
x6	Bottom Flange Exterior Egde Thickness	y2
x7	Bottom Flange Mid-Node Y Location	y3
x8	Top Flange Mid-Node Y Location	y6
x9	Top Flange Exterior Edge Thickness	y7

The values are relative to the origin located at the intersection of the centerline and the girder bottom as depicted in Figure 25.

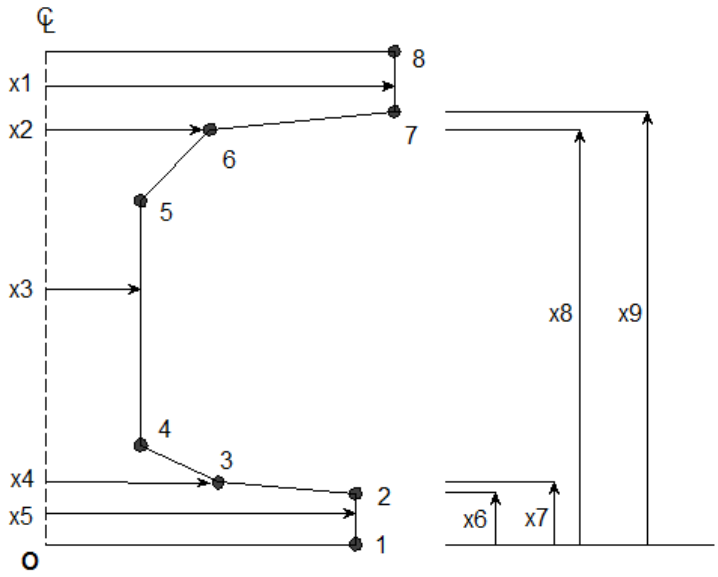

Figure 25. Diagram. Design variables used in the optimization.

Nodes 4 and 5 are fixed in their original vertical position as reference nodes for the constraint equations.

A majority of the shapes require all eight nodes to be described, but in some shapes, girder flanges do not have mid-flange nodes. For these shapes a mid-flange node is inserted so that the formulation of the design variables vector and the constraints remain the same.

The geometric design variables also influence the amount of steel in the girder making it a design variable. The girder bulb is filled to capacity with grid of steel arranged on a 2 in. spacing. Even numbers of strands are always used in each row and a 2 in. clear cover is imposed in the horizontal and vertical directions. The steel patterns were not always the same as those described in the girder specifications. This was because the vertical and horizontal covers are not constant in those girders between rows. The difference manifests itself on rows that are influenced by the sloping part of a flange.

Objective Function

The objective function is divided into two distinct goals. The first is the minimization of the area of the optimized girder. The second is an increase in the moment capacity and ductility at the yield, cracking and the ultimate moment states. The ductility at each of these states is calculated using the results of the girder analysis as shown in Figure 26.

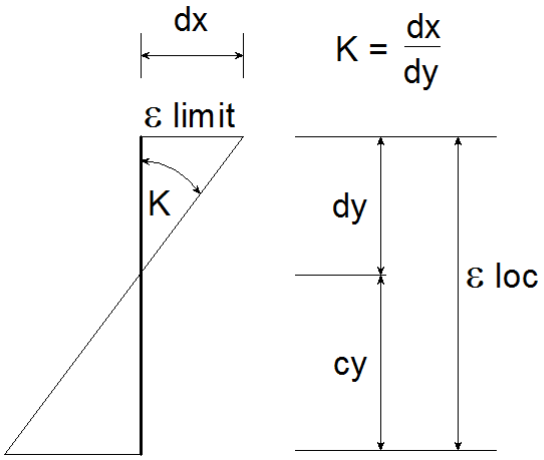

Figure 26. Diagram. Determination of ductility objective variable K from strain distribution in the girder.

To establish goals for the moment and ductility indices, a conventional girder is solved first. The optimization solver selected *fgoalattain* attempts to over achieve these goals. By assigning weights to each goal they can be prioritized over one another. Minimization of area was weighted by a factor of two, ultimate capacity received a weight of three and all other goals were weighted one.

Constraints

The constraints imposed in this optimization were all geometric in nature. First upper and lower bounds were placed on the design variables. The lower bound for each variable of girder dimension in the x direction was 2 in. This bound limited the minimum girder width to 4 in. which was imposed to accommodate harped strands. The upper bound for width related variables was the existing girder shape. The vertical nodes were bounded between zero and the original girder height.

In addition to the bounds, several linear relationships were determined to constrain the location of the nodes. A majority of the constraints were implemented to constrain the nodes to a consecutive order; for example the vertical location of node 6 should be greater than the vertical location of node 5 as shown in Figure 27.

$$
\begin{aligned}
-x_1 + x_2 &\leq 0 \\
-x_2 + x_3 &\leq 0 \\
x_3 - x_4 &\leq 0 \\
x_6 - x_7 &\leq 0 \\
x_8 - x_9 &\leq 0
\end{aligned}
$$

Figure 27. Equation. Linear constraint equations to preserve node sequence

The other type of linear constraint was to impose a limit in the flanges. As the flange's width shrinks the vertical space nodes can occupy within the original girder shape increases. Tjis constraint is illustrated in Figure 28.

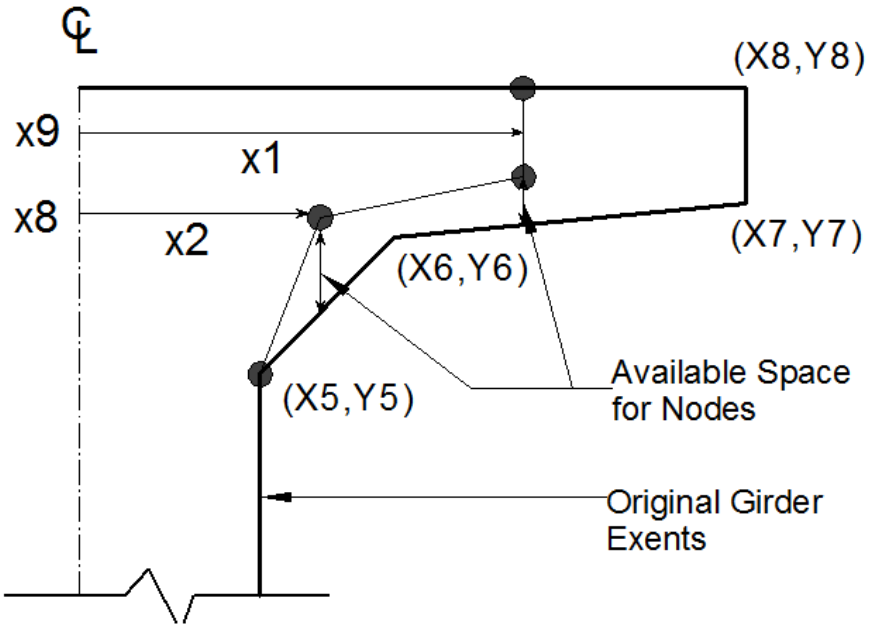

Figure 28. Diagram. The available space in the top flange of a girder for a given configuration of design variables.

This type of constraint calculates the vertical dimension of the original girder flange at the horizontal location of the edge and limits the node at that location to a vertical location within the limits of the original girder. The calculation is presented in Figure 29.

$$-t_1\, x_5 + x_6 \le Y_3 - t_1\, X_3$$
$$-t_2\, x_4 + x_7 \le Y_4 - t_2\, X_4$$
$$-t_3\, x_2 + x_8 \le -Y_5 + t_3\, X_5$$
$$-t_4\, x_1 + x_9 \le -Y_6 + t_4\, X_6$$

Where

X = Original girder geometry definition of X coordinates

Y = Original girder geometry definition of Y coordinates

x = Design variable vector

$$t_1 = \frac{Y_3 - Y_2}{X_3 - X_2},\ t_2 = \frac{Y_4 - Y_3}{X_4 - X_3},\ t_3 = \frac{Y_6 - Y_5}{X_6 - X_5},\ t_4 = \frac{Y_7 - Y_6}{X_7 - X_6}$$

Figure 29. Equation. Linear constraint equations for flange nodes

Secondary Calculations

Each optimized girder was compared to its respective original shape by various means. Girder geometry was divided into three elements; top flange width, web width and bottom flange width. The percent reduction of each of these elements from the conventional girder to the UHPC girder was calculated. The change in section properties was also calculated. The reduction in area, moment of inertia and weak axis moment of inertia were calculated. Guyon's and Aswad's efficiency factors were calculated for each girder pair to evaluate the section properties.

The shear strength capacity was compared between the sections as well. The shear capacities compared were the concrete capacities of the web ignoring the contribution of stirrups. Graybeal suggested an equation for the shear strength of UHPC based on the web dimensions. This was compared to the AASHTO web shear strength equation. The equations are presented in (Figure 30).

Conventional

$$V_C = \left(\frac{3.5\sqrt{1000\, f_c'}}{1000} + 0.3\, f_{CC} \right) b_w \, \mathrm{d}$$

UHPC

$$V_W = 0.24\sqrt{f_c'}\; b_w \, \mathrm{d}$$

$$V_F = \frac{S\,\sigma}{\tan\beta}$$

$$V_C = V_W + V_F$$

Where

V_C = Shear strength of section without stirrups
f_c' = Concrete strength in ksi
f_{CC} = Prestressing stress
b_w = Web width
d = Web depth
V_W = Contribution of web UHPC
V_F = Contribution of fibers present in web
S = $0.9\, b_w$ d
σ = Fiber tensile stress (assumed to be 1 ksi)
β = Crack angle (assumed to be 40°)

Figure 30. Equation. Determiniation of section shear capacity for conventional concrete and UHPC.

Stable lengths of each girder were calculated using the methodology in (Stratford, Burgoyne et al. 1999). The UHPC girders could then be compared to the conventional girders to determine if stability would be a limit on the implementation of the optimized UHPC girders.

Finally transfer and service stresses were calculated in the girder pairs. Transfer stresses were calculated at mid-span and at the girder ends. Long term stresses due to permanent loads were also calculated at mid-span. The method of calculation is presented in Figure 31.

Top-fiber Midspan Transfer Stress

$$f_{\text{mti}} = -\frac{P_i}{A_g} + \frac{P_i e_m}{S_t} - \frac{M_{\text{SW}}}{S_t}$$

Bottom-fiber Midspan Transfer Stress

$$f_{\text{mbi}} = -\frac{P_i}{A_g} - \frac{P_i e_m}{S_b} + \frac{M_{\text{SW}}}{S_b}$$

Top-fiber End Transfer Stress

$$f_{\text{eti}} = -\frac{P_i}{A_g} + \frac{P_i e_e}{S_t}$$

Bottom-fiber End Transfer Stress

$$f_{\text{ebi}} = -\frac{P_i}{A_g} - \frac{P_i e_e}{S_b}$$

Top-fiber Midspan Long Term Stress

$$f_{\text{mte}} = -\frac{P_e}{A_g} + \frac{P_e e_m}{S_t} - \frac{M_{\text{SB}}+M_{\text{SW}}}{S_t} - \frac{M_{\text{DL}}}{S_{\text{tc}}}$$

Bottom-fiber Midspan Long Term Stress

$$f_{\text{mbe}} = -\frac{P_e}{A_g} - \frac{P_e e_m}{S_b} + \frac{M_{\text{SB}}+M_{\text{SW}}}{S_b} + \frac{M_{\text{DL}}}{S_{\text{bc}}}$$

Where

P_i = Prestressing force at transfer

P_e = Prestressing force after long term losses

e_m = Eccentricity at mid-span

e_e = Ecentricity at end

S_t = Section modulus relative to top fiber of girder

S_b = Section modulus relative to bottom fiber of girder

S_{tc} = Composite section modulus relative to top fiber of girder

S_{bc} = Composite section modulus relative to bottom fiber of girder

M_{SW} = Moment at mid-span due to self weight of girder

M_{SB} = Moment at mid-span due to self weight of slab

M_{DL} = Moment due to assumed form, barrier, and wearing surface dead loads

Figure 31. Equation. Calculation of stresses in girder at top and bottom fiber for transfer and long term states.

Several simplifying assumptions were made in these calculations. The self weight of the girder was calculated from the girder area and an assumed unit weight of 150 lbs/ft^3. The slab self weight assumed the effective width of the slab as the influence width for loads. The permanent dead loads assumed are summarized in Table 9.

Table 9. Assumed Permanent Dead Loads

Load	Value	Units
Stay in Place Forms	20	lbs/ft2
Construction Excesses	20	lbs/ft2
Wearing Surface	15	lbs/ft2
Single Parapet	0.3	kips/ft

The service stresses required an estimation of service moment. Moments were calculated using the self weight of the girder, self weight of the slab and an assumed construction and excess dead load. Reductions in stress at the end zones due to development lengths were ignored. For each girder that could accommodate the harping of strands as many strands as possible were harped.

These stresses were compared with the limits imposed by AASHTO A5.9.4.1-2 presented in Figure 32.

Compression at Transfer $f_{tc} = -0.75\ f_{ci}$

Tension at Transfer $f_{tt} = \text{Min}(0.0948\ \sqrt{f_{ci}}\ , 0.2)$

Long Term Compression for Service I $f_{ec} = -0.45\ f'c$

Long Term Tension $f_{et} = 0.19\ \sqrt{f'c}$ for Conventional
$f_{et} = 1.5$ for UHPC

Where for

Conventional Concrete $f_{ci} = 0.75\ f'c$

UHPC $f_{ci} = f'c\ (1 - e^{-\left(\frac{t+3\ln(2)\frac{1}{0.63}-2.5}{3}\right)^{0.63}})$ t = days of cure

t = 2 days was used

Figure 32. Equation. Stress limits as defined by AASHTO A5.9.4.1-2 with modifications for UHPC based on Graybeal

These limits are modified for UHPC. Alterations made because of the material properties of UHPC as reported by the material characterization performed by Graybeal (2005). The modifications were necessary because of UHPC's improved tension capability and its unique cure. UHPC cures slowly for the first day but then undergoes a rapid strength gain. This behavior was modeled by Graybeal using an exponential equation. It was assumed that a two day cure would be used with UHPC.

Field Visits and Interviews

Several field visits were made to discuss the feasibility of utilizing UHPC for bridge girder production. Multiple facets of the girder manufacturing process were investigated. The feasibility of form modifications was documented. Another feature of girder detailing investigated was strand patterns. Manufacturers also offered insight into the potential difficulties of storage and handling of UHPC. The ability of the plants curing systems to produce the temperatures required for UHPC were also investigated.

An extended visit to a facility producing UHPC products was arranged as well. The production of UHPC panels was witnessed. In the course of assisting with the production of the panels the characteristics of UHPC were observed during mixing, casting and curing.

Optimization of Full Bridge System

Based on the results of the direct girder replacement optimization and the feasibility studies conducted in on site interviews a second optimization phase was implemented. This phase sought to optimize a full bridge system in order to include more details. The optimization of the girders showed the cost savings in area reduction to be insufficient to offset the material costs. The feasibility interviews led to the conclusion that some modifications to girder forms would be too costly. Another concern of those interviewed was that vertical shrinkage during curing would present a problem. The full bridge optimization addressed the discrepancies of the girder replacement optimization and the concerns arising from the field visits.

The results of the two previous phases led to a total cost optimization of a full bridge. This total cost included material, transportation and erection costs. The optimization was completed using conventional means and an adapted UHPC solution in order to compare the two. For each family of shapes presented in Table 6 bridges of various lengths and width were optimized using standard girder shapes and UHPC shapes. The bridges were simple spans loaded with an HL-93 design truck. The AASHTO and Washington deck flange shapes were excluded from this phase because the focus was on bulb tee girders. The five lengths investigated ranged from 50 to 130 ft by 20 ft increments. The UHPC shapes consisted of using the standard girder cross section's bottom bulb and web width but removing the top flange entirely. The general optimization formulation was a cost minimization using a penalty function to include nonlinear constraints as shown in Figure 33.

$$\text{Minimize } C(x) + \lambda P(x)$$
$$\text{Subject to } lb \leq x \leq ub$$
Where
$C(x)$ = Cost Function
$P(x)$ = Penalty Function
x = Vector of design variables
λ = Penalty scaling coefficent
lb = Lower bounds on design variables
ub = Upper bounds on design variables

Figure 33. Equation. Formulation of full system optimization

This formulation was selected because attempting to include all the constraints explicitly resulted in an over constrained problem that was too computationally intensive. By incorporating the constraints into the cost function, the optimization is driven towards a solution with the smallest constraint violations. The penalty scaling coefficient is used so that the penalty amount is a larger magnitude than the cost function. The larger the scaling coefficient the more tightly the constraints are met. Each of the elements of the optimization formulation is discussed below.

Design Variables

The optimization was designed to be run for many bridge length and width combinations using each of the girder families in the first optimization phase. For each of these combinations the lowest total cost solution was sought for both the conventional solution and the UHPC solution.

Three variable elements of a bridge design were selected as required in order to effectively develop the cost and constraint equations. Selecting only three reduced the complexity from a design problem with a multitude of parameters. The first is girder depth. The girder depths were allowed to be continuous rather than discrete in order to maintain continuity of the derivative of the cost function. Girders were constructed by the program using the depth at the iteration and the geometry of the girder shape under consideration. The girder shape families' bulb and top flange dimensions do not vary with height in most cases. In cases where they do vary, the bulb

and flange of the shape closest to the desired depth are selected. The girder is made by adjusting the web so that the resulting shape matches the required depth of the iteration (Figure 34).

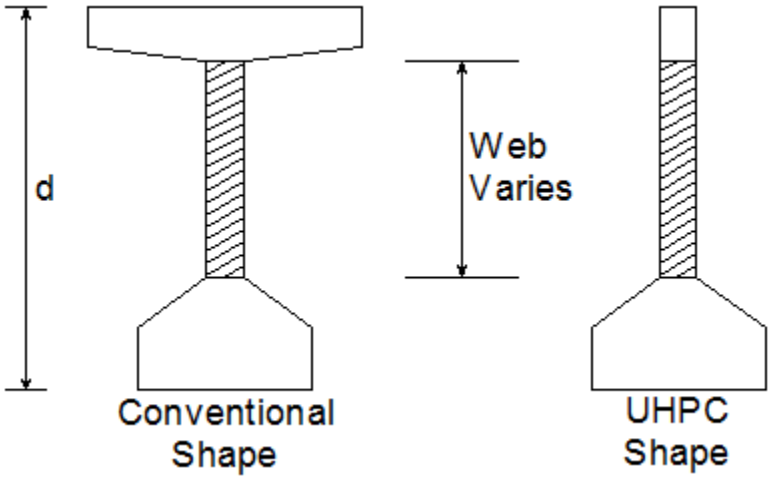

Figure 34. Diagram. Construction of girder shapes from desired depth d by varying the web depth.

The second variable was the number of girders utilized in the bridge. The continuity of this variable was also maintained. In reality there is no such thing as a fractional girder. This variable was rounded to the nearest whole number of girders when it would not impact cost function derivatives. This is further explained in the descriptions of the cost and constraint functions.

The third variable was the area of steel utilized in the girder. As many steel strands as possible were harped. Including this variable allowed for the inclusion of stress limits as a constraint. In the previous optimization it was assumed that each girder contained the maximum amount of steel that would fit in the bulb. Repeating this assumption would require the girder depth to be altered to adjust the stresses. The selection of steel area independent of the depth more accurately represents actual bridge design decisions made in practice.

Other details of the bridge remained constant over the various optimization runs. All the bridges were simply supported and loaded with an HL-93 design truck. For the purpose of calculating AASHTO Strength I demands and Service III stresses, the truck was assumed to have the minimum axle spacing of 14 ft. This axle spacing was selected to create the largest mid-span

moments. The strength demands required the calculation of the girder distribution factors using the methods of AASHTO A4.6.2.2.2. Other elements of the bridge design remained static during the course of an optimization (Table 10).

Table 10. Static Elements of Bridge Design

Element	Units	Description	Values Used
L	ft	Length of Bridge	[50,70,90,110,130]
Nl	NA	Number of 12 ft lanes	[2,3,4]
sc	in	Length of cantilever over exterior girder	36
wp	in	Width of parapet	24
width	in	Width of bridge	[336,480,624]
tslab	in	Thickness of slab	8
fcslab	ksi	Compressive strength of slab concrete	4

Objective Function

The objective function was developed to include the total cost of the bridge superstructure. It was adapted from the cost function developed by Hassanain and Loov (1999) as presented in Figure 35.

Total Cost=Cg+Cs+Cte

Girder Cost Cg:

Girder = ρ \$C A_g L

Cure = t \$T A_g L

Cc = Nb (Girder + Cure)

Where

ρ = Cost ratio of UHPC to conventional concrete

\$C = Cost of concrete per cubic yard (\$47 was used)

\$T = Cost curing process

t = Cure time in Days

A_g = Area of girder

L = Length of girder

Nb = Number of girders

Strand Cost Cs:

Cs = Nb \$S Ns L

Where

\$S = Cost of strand per foot (\$0.35 was used)

Ns = Number of strands in girder

Transportation and Erection Costs Cte:

Cte = 5160 + Nb (Erection+Transportation)

Erection = $40 + \frac{7}{8}$W

$W = A_g$ L γ

Transportation = $5 + \frac{9}{31}$L

Where

Erection = Cost as function of weight

W = Weight of girder in tons

γ = Unit Weight of Concrete

Transportation = Cost as function length in feet

Figure 35. Equation. Cost function developed for the optimization of a full bridge system

The costs of materials and the erection and transportation costs were taken directly from the cited paper. The transportation and erection cost functions were reverse engineered by interpolation of cost curves included therein. Updating the material costs to current levels would have required a similar update to the erection costs and transportation costs as compiled by the original investigators through interviews and surveys. The completion of the research required to effectively do this was outside the scope of the research and was accounted for other ways. The cost ratio of UHPC to conventional concrete allowed for flexibility in the optimization routine. The relative relationships between material and erection cost were maintained and the cost ratio could be used to investigate the differences in material costs of UHPC and conventional concrete.

The goal was to compare the cost of a UHPC solution to a conventional concrete solution and therefore inflation adjustments would be rendered moot because they would apply to both. In order to estimate the cost of UHPC in relative terms to the costs presented in the paper the cost ratio of UHPC to High performance concrete was estimated by comparing the amount of cementitious materials in a typical mix of each. The cost ratio used in the optimization was 1.85 and was calculated from the typical UHPC mix presented by Graybeal and the typical mix presented in AASHTO C5.4.2.1.1. A secondary investigation was performed without repeating the optimization to determine the impacts of larger cost ratios.

Constraints

The design variables are constrained by physical realities and elements of the AASHTO code. The first set of constraints is determined by physical bounds of the bridge. The depths of the girders are bracketed by the largest available girder shape depth and the bulb depth of the girder (Figure 36).

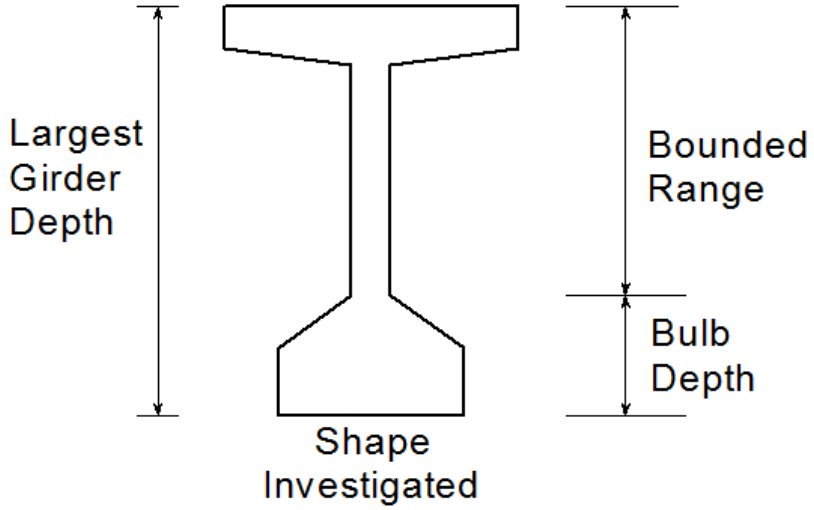

Figure 36. Diagram. Boundary extents for the design variable girder depth

The number of girders is bound by the minimum required to utilize the AASTHO equations for the distribution factors (four girders) and the largest number that will fit within the bridge width. The area of steel is limited to the largest amount that can fit in the girder bulb on a two in. grid and a minimum of two strands.

The other constraints are far more complex. There are the nonlinear constraints associated with girder stability, strength and stresses. The girders must be stable for the length required by the bridge design. The girders must also have adequate strength for the Strength I limit state of the AASHTO code. Finally the girder must have adequate section properties and steel parameters to satisfy the AASHTO requirements for stress limitations at transfer and at the long-term service state as described in Figure 32. The stress checks were modified to include Service III long term stresses because with the full bridge analysis, it was possible to calculate stresses due to live loading (Figure 37).

Top-fiber Midspan Service 1 Stress without Live Load

$$f_{\text{mte}} = -\frac{P_e}{A_g} + \frac{P_e e_m}{S_t} - \frac{M_{\text{SB}}+M_{\text{SW}}}{S_t} - \frac{M_{\text{DL}}}{S_{\text{tc}}} < \text{-0.45 f'c}$$

Top-fiber Midspan Service 1 Stress with Live Load

$$f_{\text{mte}} = 0.5 * \left(-\frac{P_e}{A_g} + \frac{P_e e_m}{S_t} - \frac{M_{\text{SB}}+M_{\text{SW}}}{S_t}\right) - \frac{0.5*M_{\text{DL}}+M_{\text{LL}}}{S_{\text{tc}}} < \text{-0.40 f'c}$$

Bottom-fiber Midspan Long Term Service 3 Stress

$$f_{\text{mbe}} = -\frac{P_e}{A_g} - \frac{P_e e_m}{S_b} + \frac{M_{\text{SB}}+M_{\text{SW}}}{S_b} + \frac{M_{\text{DL}}+0.8\,M_{\text{LL}}}{S_{\text{bc}}} < \text{Same Tensile Limits}$$

Where

P_e = Prestressing force after long term losses

e_m = Eccentricity at mid-span

S_t = Section modulus relative to top fiber of girder

S_b = Section modulus relative to bottom fiber of girder

S_{tc} = Composite section modulus relative to top fiber of girder

S_{bc} = Composite section modulus relative to bottom fiber of girder

M_{SW} = Moment at mid-span due to self weight of girder

M_{SB} = Moment at mid-span due to self weight of slab

M_{DL} = Moment due to assumed dead loads of forms, excess, wearing surface and paparpets

M_{LL} = Moment due to HL-93 Truck and distrubuted Lane loads with appropiate factors

Figure 37. Equation. Additional stress checks possible with the analyses of a full bridge system and their respective limits

The constraints are divided into two portions. The simple constraints of the upper and lower bounds were passed to the optimization software and are handled as boundaries by the algorithm. The *Matlab*® solver selected was *fmincon* because it solves single objective functions subject to linear and nonlinear constraints.

The other constraints behave in a nonlinear way due to equations involved in their calculation. It was attempted to utilize the solver algorithm's features that could handle these nonlinear constraints. The feasible space was far too constricted for the algorithm to successfully terminate. Calculation of the constraint equations was also very computationally expensive. To

overcome the over constrained design space, the nonlinear constraints were instead implemented in a penalty function (Figure 38).

$$P(x) = \text{Max}[\ 0,\ C(x)\ ]^2$$

Where

C(x) = Vector containg the values of the constraint equations evaluated at iteration

Figure 38. Equation. Penalty function utilized to implement non-linear constraints

The penalty function is added to the cost function when a constraint is violated thus driving the solution away from those solutions that are infeasible. The constraint violation is squared so that penalty is magnified for large constraint violations. The constraint vector contains the values of the constraint equations developed for stability strength and stress (Figure 39).

$$C(x) = [C_L(x)\ ,\ C_S(\mathrm{x})\ ,\ C_f(\mathrm{x})]$$

Stability Constraint

$$C_L(\mathrm{x}) = \frac{L_D - L_S(x)}{L_D}$$

Strength Constraint

$$C_S(\mathrm{x}) = \frac{M_D - M_U(x)}{M_D}$$

Stress Constraints for i = 1 : Number of stress checks

$$C_f(x)_i = f_i(\mathrm{x}) - l_i$$

Where

C(x) = Vector of constraint viloations

L_D = Design length of bridge

L_S = Stable length of girder

M_D = Factored demand moment for Strength I distrubuted to girder

M_U = Ultimate moment capacity of composite girder

f_i = Stress at investigation point i

l_i = Stress limit at investigation point i

Figure 39. Equation. Calculation of constraints for use with penalty function

Summary of Procedure

The optimization formulations were carried out to develop a cost effective way to utilize UHPC in highway bridge structures. In order to do this a girder analysis program was developed in *Matlab*® so that its build in optimization algorithms could be used. In the course of developing the optimization many other algorithms were implemented to analyze full bridge systems and apply elements of the AASHTO code. The next chapter contains the results of the investigation.

CHAPTER 4 Results

The results of the investigations into using UHPC in highway bridge girders successively built upon each other with the conclusions of each phase influencing the direction of the next phase. The survey phase indentified the most popular shapes used across the industry. The sensitivity analysis phase identified the elements of those girders most likely to affect moment capacity if modified for use with UHPC. Representative shapes were selected from the survey and those elements identified as important were used in the optimization of girder shapes. The goal of the optimization phase was to develop guidelines for modifications to best utilize UHPC. The results of the girder optimization were scrutinized for feasibility by surveying precasters with on-site visitations. The girder optimization results and the feasibility investigation influenced the formulation of the full bridge optimization phase. The full bridge optimization identified the methodology for using UHPC in typical highway bridge construction.

Survey Results

The survey phase consisted of three attempts to ascertain what girders were being used across the country. First manufactures listed as members of the Precast Concrete Institute were surveyed through their websites. Second the websites of state departments of transportation (DOT) were surveyed for information. Finally a direct e-mail solicitation was sent to representatives of each state's DOT to garner details.

The initial portion of the survey was conducted by visiting the websites of manufactures. Only 20 of those manufactures listed had product descriptions on their website concerning which shapes were produced for bridges. Figure 40 presents the percentage of the 20 manufactures who produce AASHTO and PCI standard girder shapes.

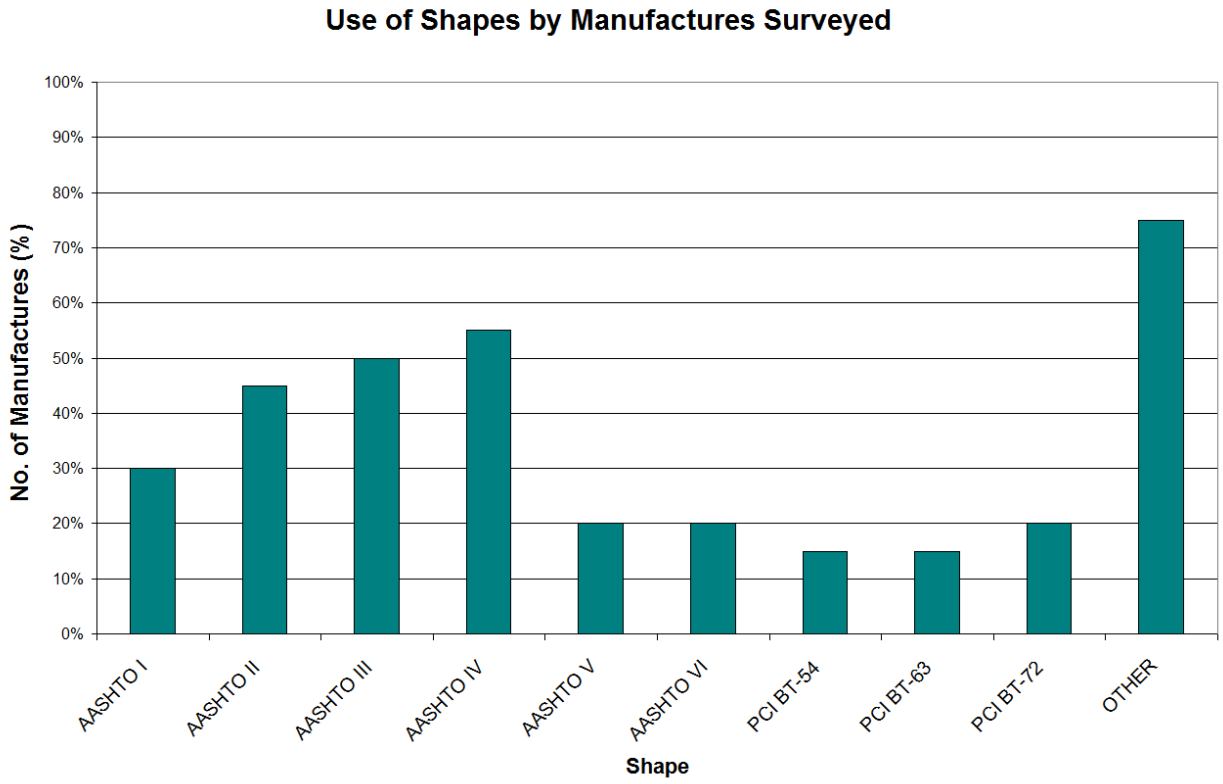

Figure 40. Chart. Percentage of manufactures surveyed who have the named shape available for production

Seventy-five percent of websites listed bulb-tee shapes other than PCI or AASHTO standard shapes. Of the AASHTO shapes types V and VI were the least represented at 20 percent. PCI shapes were nearly evenly represented.

The web survey of state DOT sites retrieved information from 34 of the 51 States. This data was combined with the 34 responses to the email survey to determine more information about the use of various girder shapes. There was large overlap in the reporting resulting in information on a total of 36 states. Figure 41 shows the number of states responding as using a particular shape.

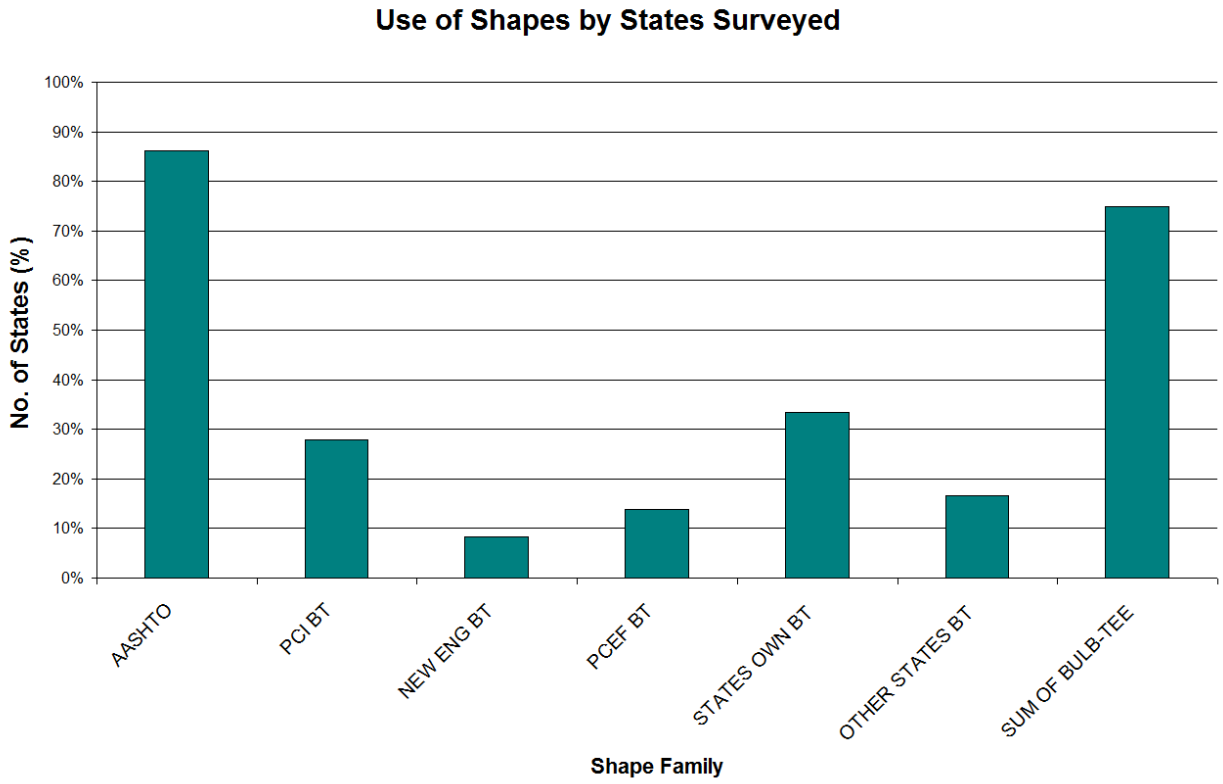

Figure 41. Chart. Percentages of States Using Each Shape Family

Of the states for which information was available, the most widely available shapes are the AASHTO girders at 86 percent of states where information was available. When combined, the bulb tee shapes are used in 27 of 36 states or 75 percent. The response to the question "In your opinion which girder type is used most prevalently in your state?" the responses were 13 for AASHTO shapes followed by 14 for the combined bulb tee shapes (Figure 42).

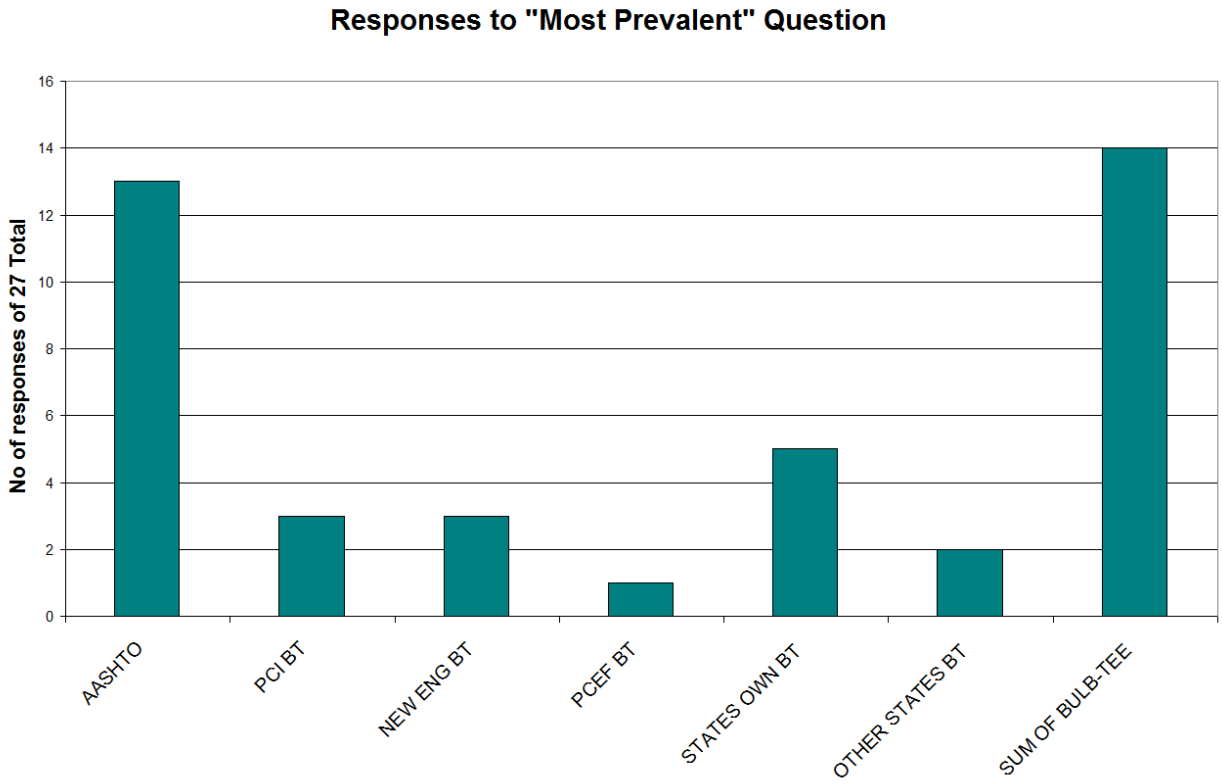

Figure 42. Chart. Number of responses to "Most Prevalent Shape" question.

The bulb tee shape is a widely used shape but varies from state to state. The combined use of bulb tee shapes constitutes a majority. Most states use a customized state shape with 33 percent using their own shape and 17 percent borrowing a shape of another state. Bulb Tee's were identified as the shape most used in bridge construction.

Examples of state shapes were documented and their geometries collected. The shape families were similar in shapes when compared by similar depth. The differences between shapes are most evident in the bottom bulb as shown in Figure 43.

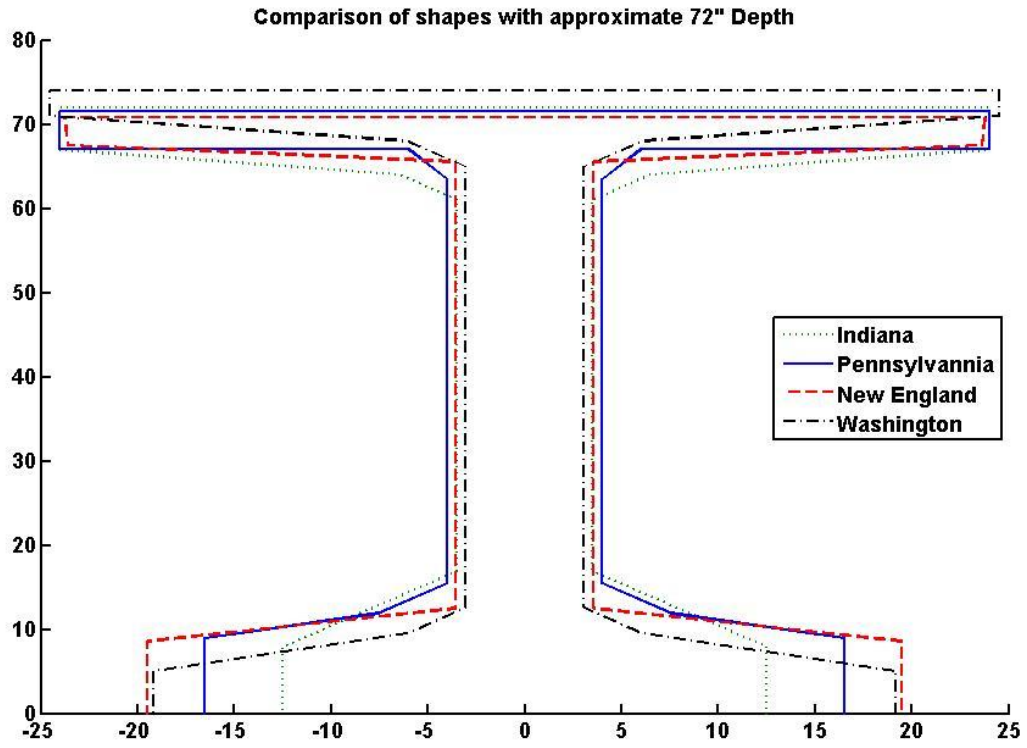

Figure 43. Diagram. Shapes of similar depths have similar profiles varying chiefly in bottom bulb dimensions.

It was evident that optimizing the AASHTO or PCI shapes for UHPC would be insufficient. The variety of shapes made the possibility of adoption of a single optimized shape unlikely. The focus was turned to developing a procedure to apply to a generic bulb tee shape in order to make it efficient with UHPC.

Sensitivity Analysis

A prestressed girder has several elements that have the potential to be altered for use with UHPC. Sets of trials with a large area of prestressing steel were performed to force a crushing of the concrete. When crushing is forced the variables of girder and slab geometry are easily investigated because of the direct relationship between geometry and performance. A simple sensitivity analysis identified those elements with the largest impact on girder strength and area. High impact variables were indentified by the sensitivity coefficients. These coefficients were calculated from the slopes of the regression lines fitted to data plotting the variable value versus

the moment capacity. The slopes were scaled by the average magnitude of the variable so that comparisons between variables could be made (Figure 44).

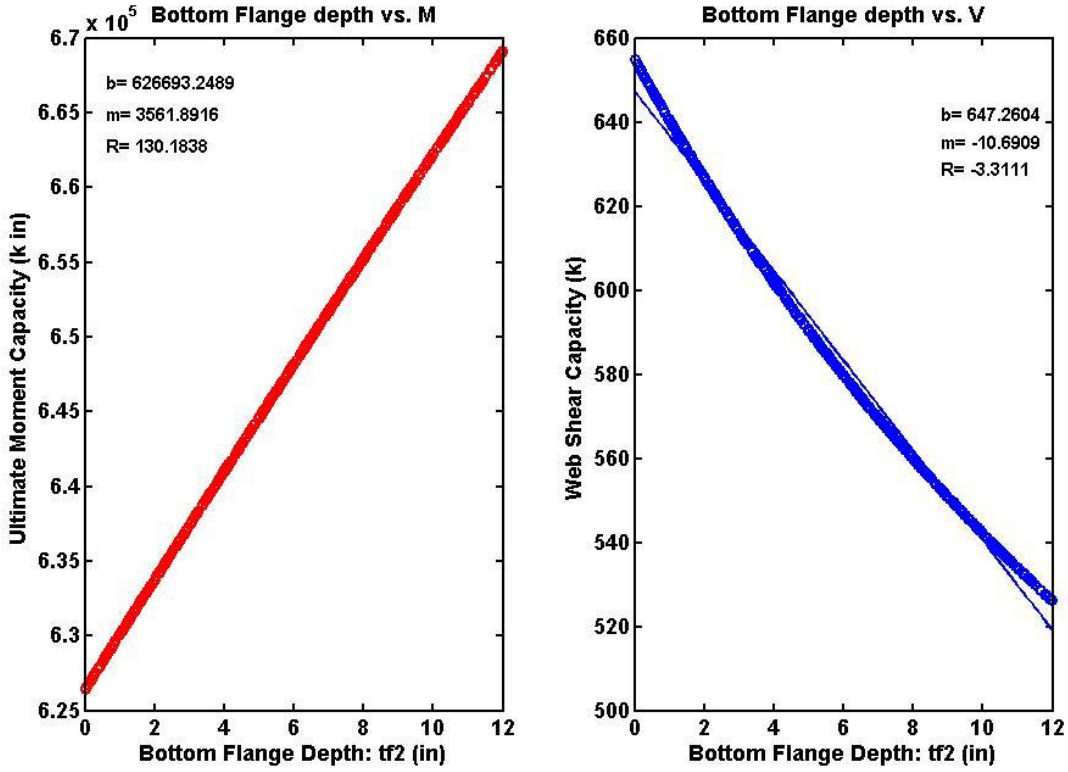

Figure 44. Graph. Moment and shear capacity responses to variation in bottom flange depth.

Shear capacity was also calculated but not investigated further. It was evident from the methods of shear capacity calculation and the subsequent trial results that web width was the driving variable that influenced shear capacity.

Variables dealing with material properties responded non-linearly because of the models utilized for steel and concrete. The simple nature of this initial investigation did not warrant more elaborate description of their behavior. The goal of the sensitivity analysis was the investigation of girder geometry variables which had linear responses. The sensitivity of theses variables was described by their normalized first order derivatives (Table 11).

Table 11. Range and Response of Sensitivity Analysis Variables

Variable	Distribution Values	Response Type	Sensitivity Coeff.
Thickness of Bottom Flange (in)	[0,12]	LINEAR	0.00550
Width of Bottom Flange (in)	[10,42]	LINEAR	0.00468
Limiting Strain (microstrain)	(3300,40)	LINEAR	0.00002
Slab Concrete Strength (ksi)	(4,0.5)	NON-LIN	--
Top Flange Thickness (in)	[0,7]	LINEAR	0.04406
Top Flange Width (in)	[10,52]	LINEAR	0.00541
Girder Concrete Strength (ksi)	(28,0.5)	NON-LIN	--
Grade 250 Prestressing (ksi)	(100,50)	NON-LIN	--
Slab Thickness (in)	[4,12]	LINEAR	0.08358
Slab Effective Width (in)	[36,128]	LINEAR	0.00784
Steel Area (in^2)	(25,7.5)	NON-LIN	--
Web Width (in)	[0,12]	NON-LIN	0.00090

The derivatives of the regression lines fitted to data plotting the variable value versus the moment capacity were used to calculate the sensitivity coefficients. The average magnitude of the variable was used to normalize the coefficients to a similar magnitude.

Girder geometry variables produced linear responses to the random changes in the variables. The exception was web width. The response in moment capacity due to variations in the web width was quadratic but the magnitude of variation was very small compared to other variables (Figure 45).

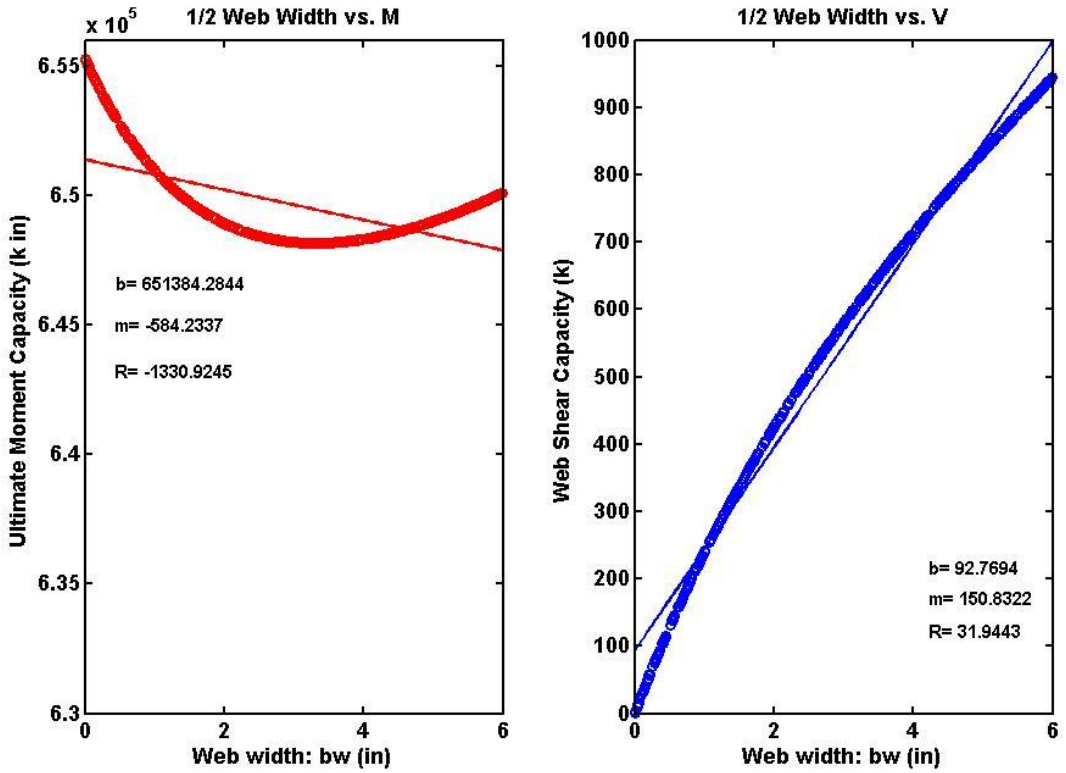

Figure 45. Graph. Moment and shear capacity response to variation in web width.

A secant line was used to approximate a sensitivity coefficient for the response to web width adjustments resulting in a value of 0.0009.

It was also shown that the slab and top flange thickness were the most sensitive with coefficients of 0.0836 and 0.0441 respectively. The responses of the moment capacity to other girder geometry elements were less sensitive by an order of magnitude.

The sensitivity analysis identified variables that were utilized in the direct optimization phase. Elements with low sensitivity coefficients were selected to be altered to reduce girder area without reducing strength. Elements that would produce nonlinearities were identified and relegated to constants for use in the optimization. The sensitivity analysis trials also tested the algorithm for robustness over the range of possible variable values that had a potential of being used in the optimization.

Direct Optimization

The results of the sensitivity analysis led to the identification of the variables used in the direct optimization. The goal of the optimization was development of guidelines in the modification of bulb-tee shapes to use UHPC with the smallest cross-sectional area possible without detriment to strength performance. Several other categories of girder performance were investigated.

Optimization Goals

The goals of the optimization were exceeding the performance of the standard shape at three points of a moment curvature response, cracking, yield and ultimate moment while reducing the area by altering facets of the girder geometry (Figure 46)

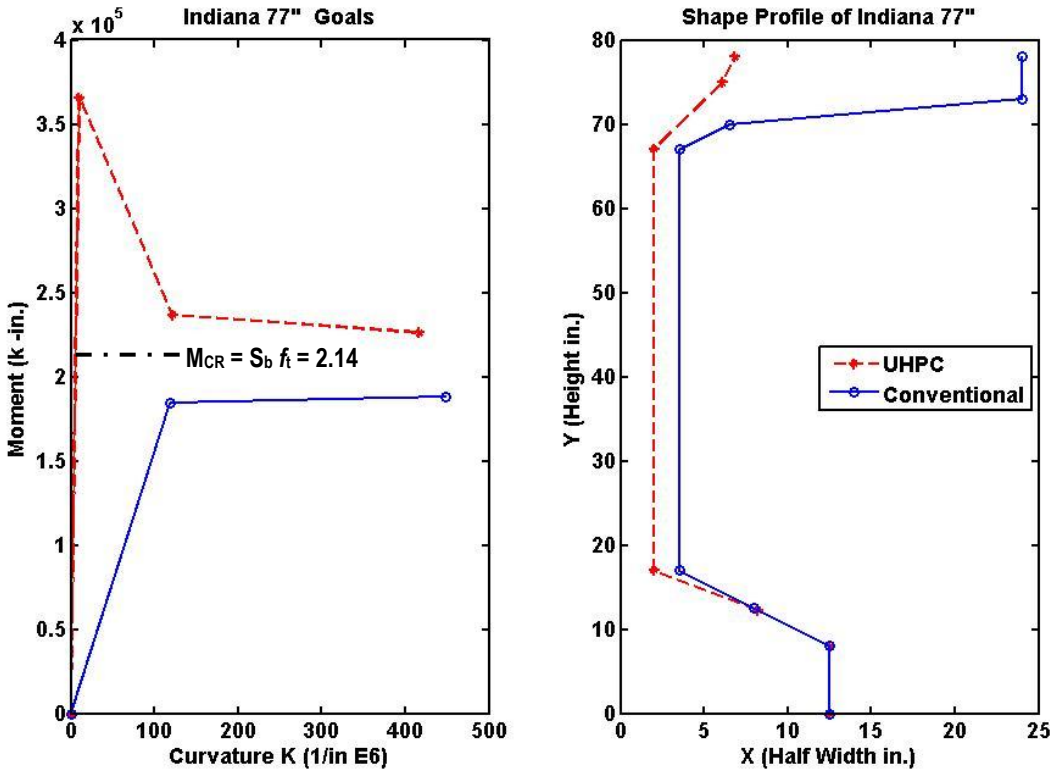

Figure 46. Graph. Optimization results for the Indiana 77 in bulb tee.

The moment curvature responses are presented as performance ratios of UHPC shape to standard shape. The first goal was exceeding the cracking strength. In the example we can see this was easily achieved. This was the case across all of the shapes save a few. The optimization was completed on forty-nine shapes with the ratios shown in Figure 47.

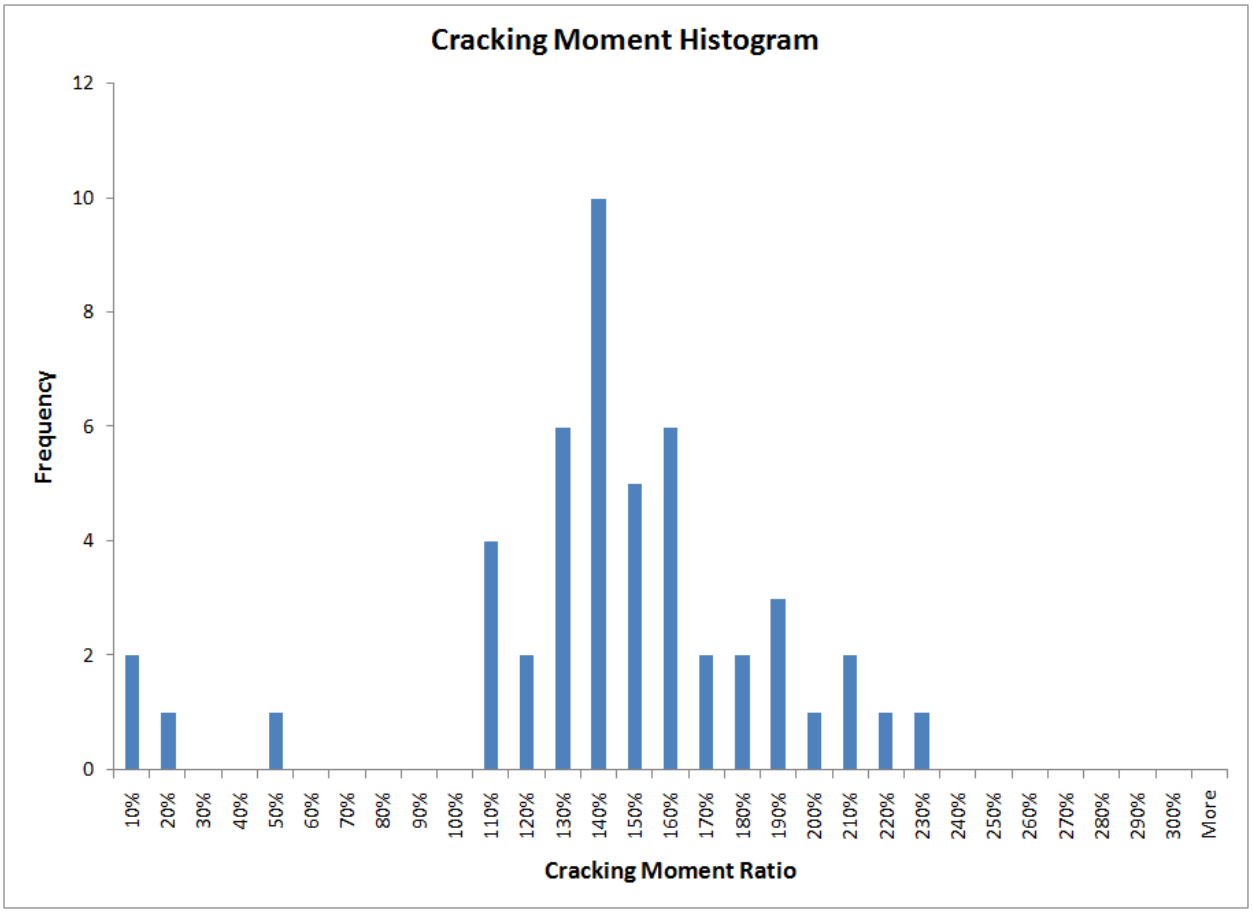

Figure 47. Chart. Observed frequency of ratio of UHPC cracking moment to Conventional Cracking Moment.

The cracking moment calculated by the solver was higher in all cases than the cracking moment derived through the method of transformed sections. This was because the model for UHPC contained some assumptions that affected the calculation of the cracking moment. The cracking moment was approximated by determining the internal moments in the section when the extreme tensile strain was -150 microstrain. The limiting tensile strength for use with Graybeal's model was chosen to be on the conservative side of the strains found by dividing the limiting stress by

the modulus of elasticity which yielded about -200 microstrain. The model used constant stress in the material for a range of tensile strains from zero to -7000 microstrain compared to a more detail model that would assume a linaer response to the tensile limit of the material (Figure 48).

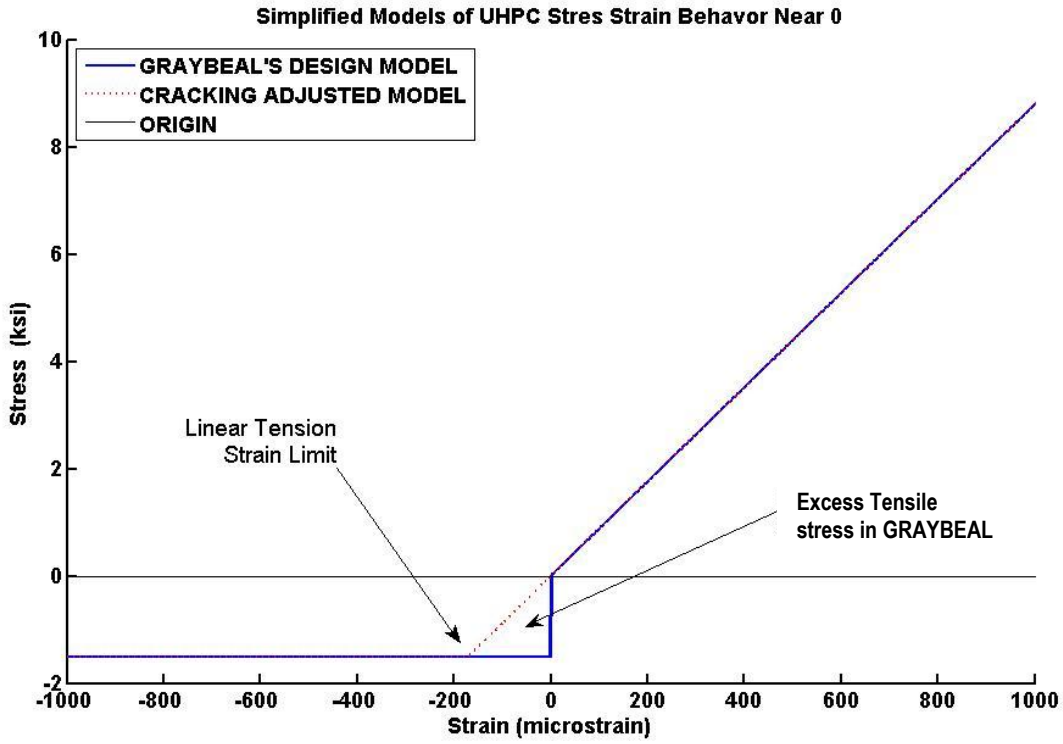

Figure 48. Graph. The excess tensile stress present in Graybeal is amplified in the calculations of forces and moments.

The additional stress in the section is magnified by two factors. The bottom flange of the section carries this excess stress, because of the larger width in the flange this magnifies the additional stress's impact on the internal equilibrium. The resulting additional force alters the location of the neutral axis again magnifying the moment. In an investigation into this disparity it was shown that this can effect the calculated cracking moment. A simple unreinforced rectangular section was analyzed using the two models (Table 12).

Table 12. Cracking Moment of UHPC 6 x 48 inch Rectangular Test Beam

Model	GRAYBEAL	CRACKING ADJUSTED	Difference
Compressive Strength (ksi)	29*	29*	
Limiting Strain (e E -6)	-150	-170.689	12%
Neutral Axis Depth (in)	28.866	24.000	20%
Cracking Moment (k in)	9923	6912	44%
Ultimate NA Depth (in)	7.313	7.276	0.5%
Ultimate Moment (k in)	12777	12746	0.2%
			* Indicates User Defined Value

At each stage in the calculation the differences in the model compound to create more and more error. The assumed cracking limit in the Graybeal model is different than the linear extrapolated cracking strain by 12 percent. The excess stress and this limiting strain difference result in different internal forces when multiplied by the width and integrated over the depth. The difference in the forces affects the location of the neutral axis by 20 percent. The forces multiplied by their lever arms are then integrated again to determine the moments present in the cross section. The assumption in the model used in the optimization increased the cracking moment by 44 percent. The ultimate moment capacity of the section was not impacted because the strains present in the UHPC exceed the tensile linear limit strain where the difference in model behavior occurs.

The simplified model recommended by Graybeal can not be used for the calculation of cracking moments of UHPC. Modifying the model to behave linearly in tension to a tensile stress plateau corrects the cracking moment calculation to match the traditional method of calculating the cracking moment by sectional analysis.

The error in the cracking moments did not radically affect the optimization because of its formulation. The multi-objective goal algorithm in *Matlab*® focuses on only the most under achieved goal at each iteration. The other goals: ultimate moment capacity, yield moment and reduction of area drove the optimization.

Yield moments in the UHPC sections also exceed those in the conventional sections (Figure 49).

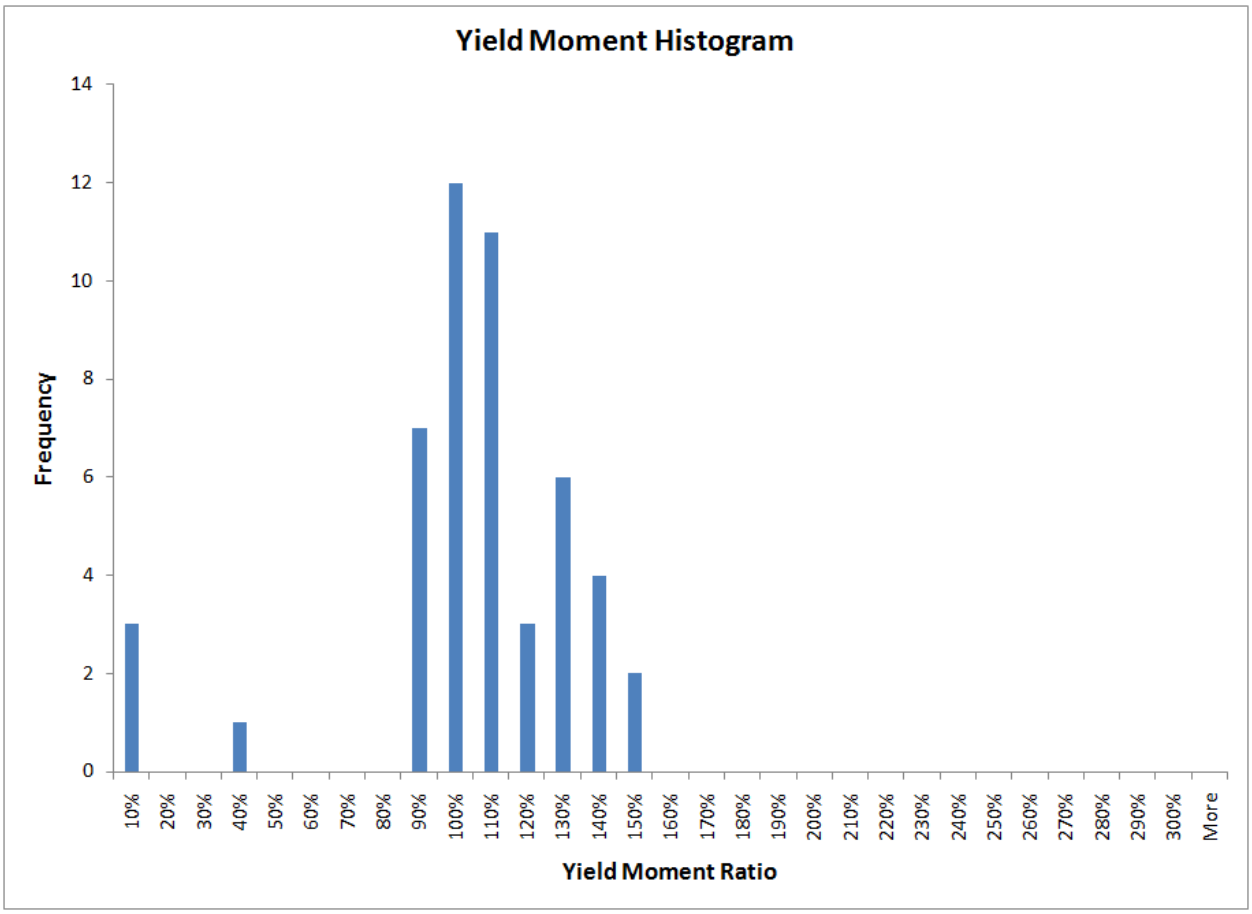

Figure 49. Chart. Observed frequencies of performance ratios of UHPC yield moment to Conventional yield moment.

The third optimization goal was also achieved with the UHPC ultimate moment capacities exceeding those of the source conventional shapes (Figure 50).

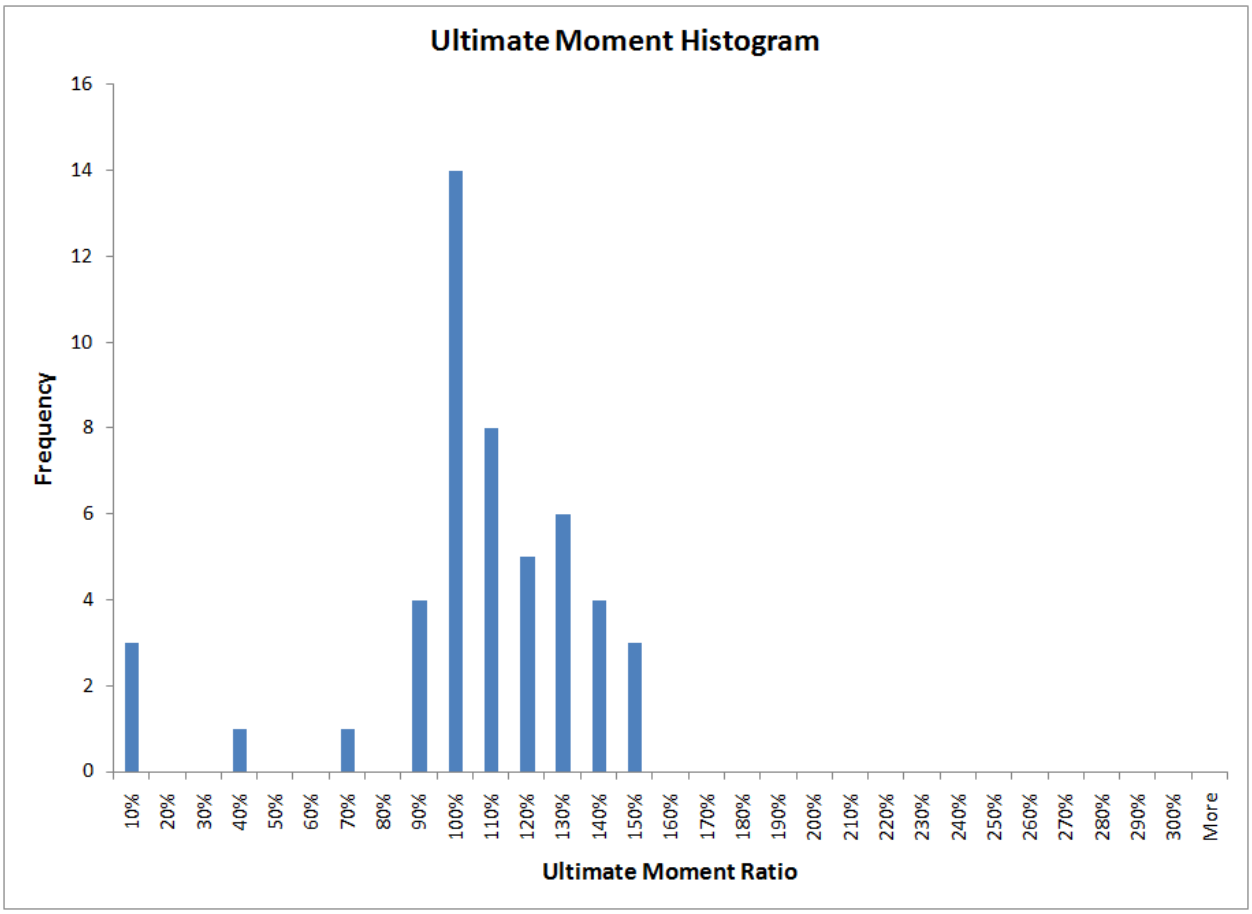

Figure 50. Chart. Observed frequencies of performance ratios of UHPC ultimate moment capacity to conventional ultimate moment capacity.

The observed frequencies presented in Figure 50 show that the ultimate moment was the active goal constraint in the optimizations. The previous two goals have a less condensed grouping of observations which range to much larger over achievement ratios. The dense grouping of the ultimate moment capacity around 100 percent indicates that is was more difficult to achieve. The fact that the ultimate moment was the driving goal constraint combined with magnitude of the cracking moments observed leads to the conclusion that a reduction in the calculated cracking moment would not alter the results of the optimization.

The competing goal to girder performance was the reduction in area over the original shape. The average reduction was 75 percent of the original area and ranged from 42 percent to 98 percent seen in Figure 51.

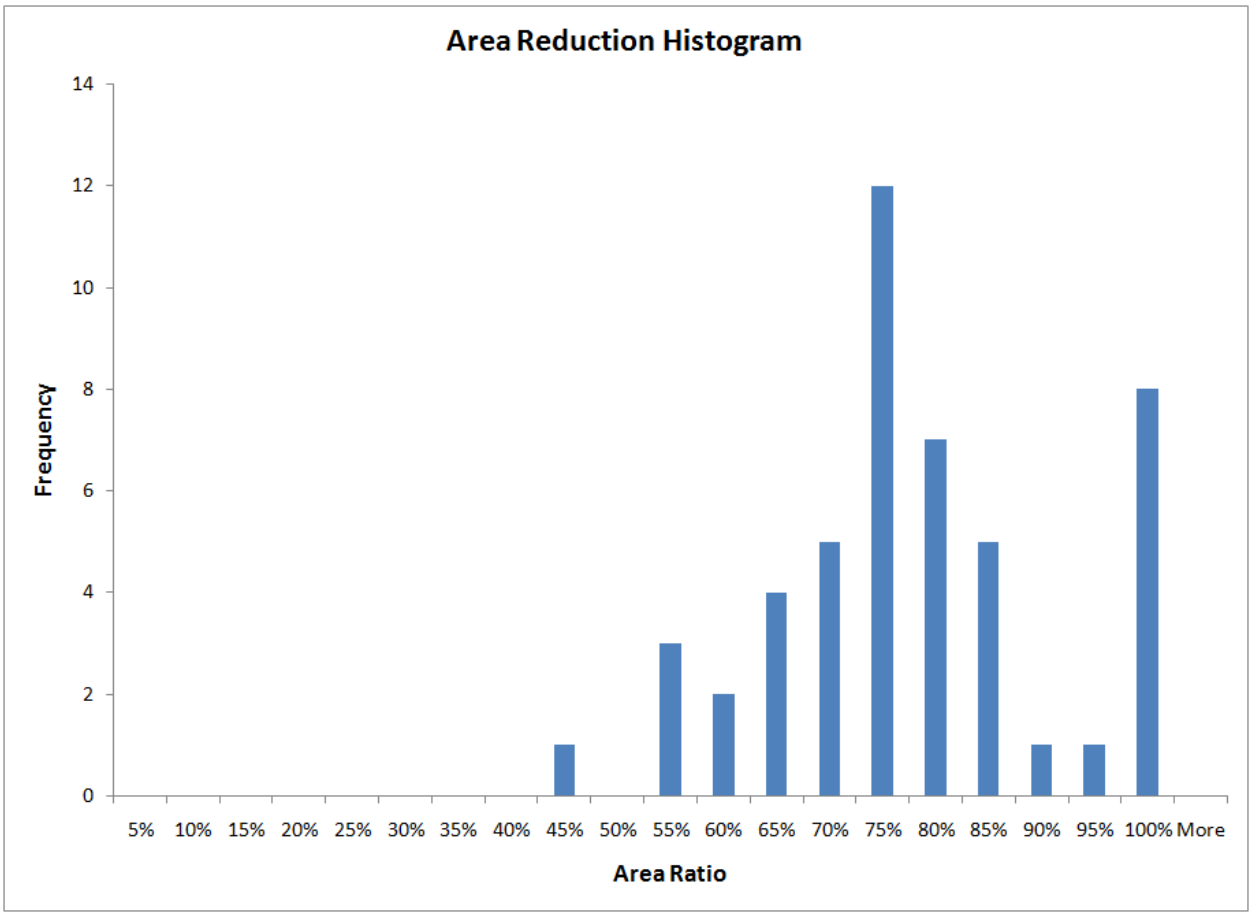

Figure 51. Chart. Observed frequencies of the ratio of UHPC shape cross sectional area to conventional shape area.

Design Variables

The optimization goals were achieved by altering the girder geometry. The alterations reduced flange and web dimensions to minimize area while maintaining moment capacities. Reducing the size of girder elements also impacted several other characteristics of the girders performance.

The reductions can be summarized using the mean and standard deviation (Table 13)

Table 13. Section Element Reductions as Percent of Original Size

Statistic	Top Width (%)	Web Width (%)	Bottom Width (%)	Top Thickness (%)	Bottom Thickness (%)
Mean	56%	85%	77%	78%	101%
Minimum	8%	50%	12%	0%	100%
Maximum	100%	100%	100%	200%	110%
Variance	13%	4%	3%	24%	0%
Standard Deviation	36%	20%	17%	49%	2%

The most volatile element of the girder was the top flange. The width of the top flange was reduced to 56 percent of its original width on average. The top flange thickness changed with the width to an average value of 78 percent of the original thickness. The thickness was measured at the flange edge. Web widths reduced to an average of 85 percent of the original value. This is indicative of the reduction of the webs from the 6 in. nominal width of most sections to the 4 in. lower bound imposed on the optimization. The bottom flange width and depth was altered less because any reduction there would impact the amount of steel present which would reduce moment capacities.

The standard deviation values for the top flange width and depth were 36 percent and 49 percent respectively. These are indicative of a wide distribution, again showing the variance in the optimized sections' top flanges. The other sections had relatively tighter distributions with standard deviations of 20 percent, 17 percent and 2 percent for the web width bottom flange width and bottom flange depth respectively.

Secondary Investigations

The reductions impacted other performance indicators of the girders. Alterations to the girder geometries impacted shear, stability and stress performance. These impacts were investigated by manipulating the results of the optimization without re-optimizing the solutions.

Shear

Shear was directly impacted by the web width. The web width reductions did not result in shear capacity deficiency in the optimized shapes when compared back to the conventional shapes (Figure 52).

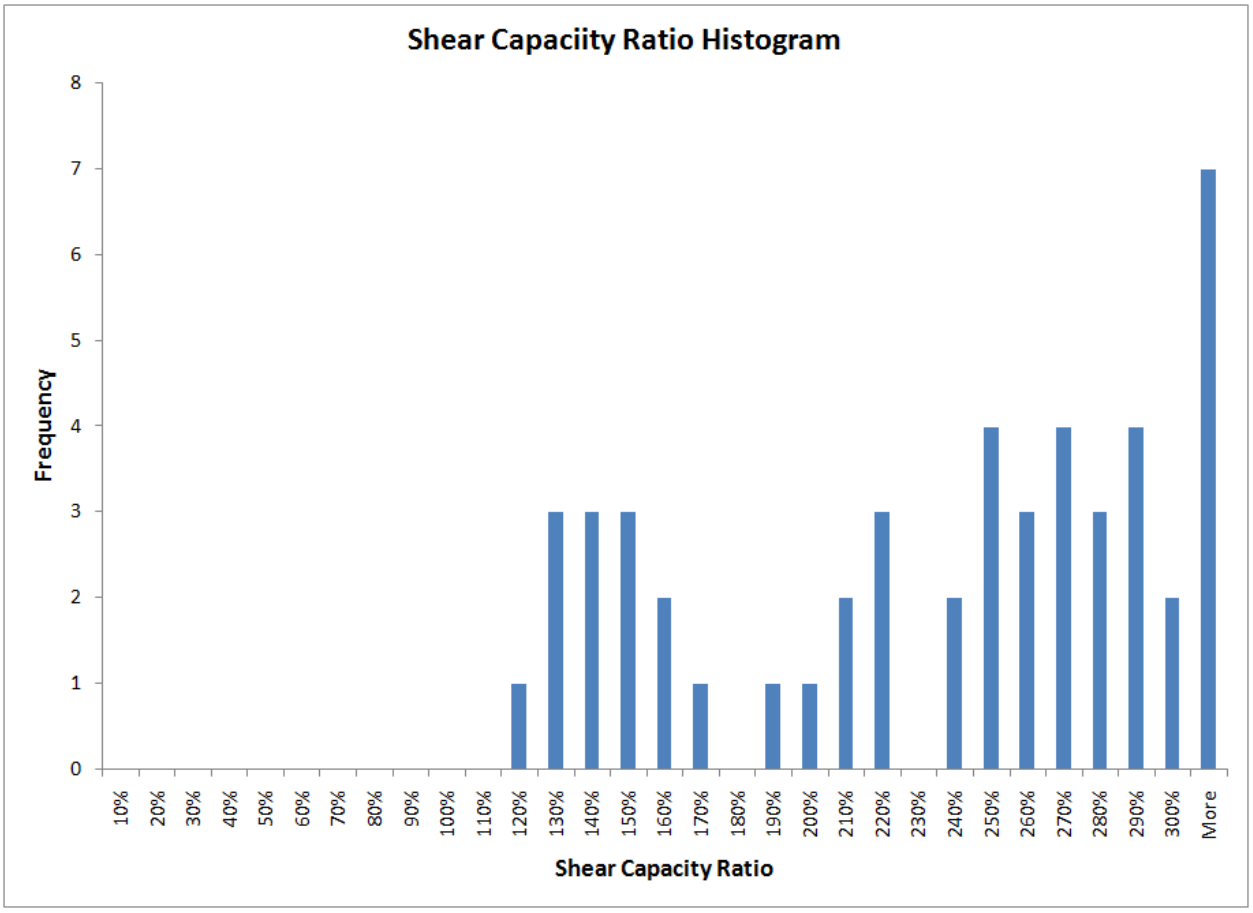

Figure 52. Chart. Observed frequencies of the ratio between UHPC section shear capacity to convetional section capacity

In every optimization run the shear capacity of the section resulting from the optimization had a larger capacity than the conventional shape it was meant to replace.

Stability

Stability is a function of the moments of inertia of the section and is therefore directly impacted by changes in flange geometry. The reductions of flange element sizes reduced both major and minor axis moments of inertia as shown in Figure 53 and Figure 54 respectively.

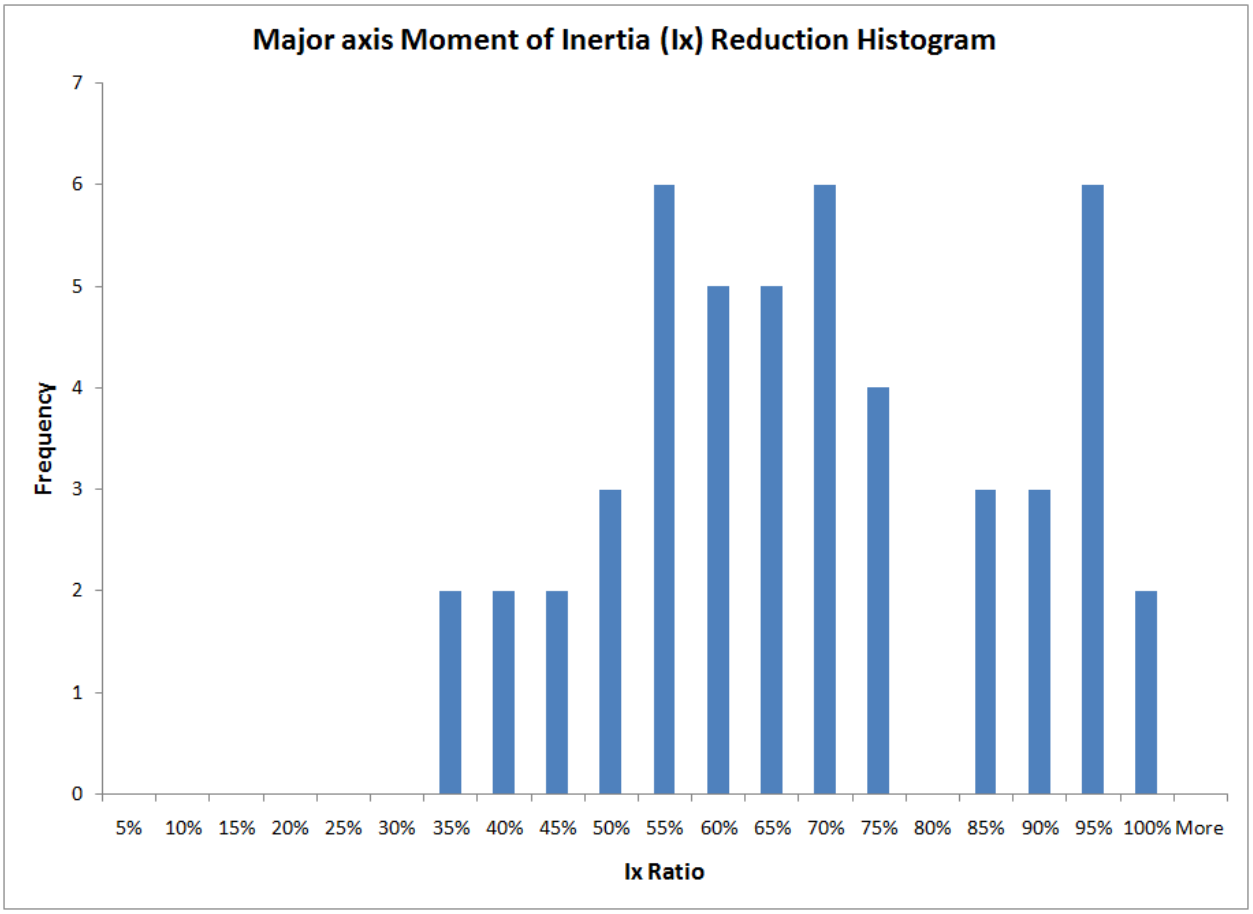

Figure 53. Chart. Observed Frequency major axis moment of inertia reduction ratio.

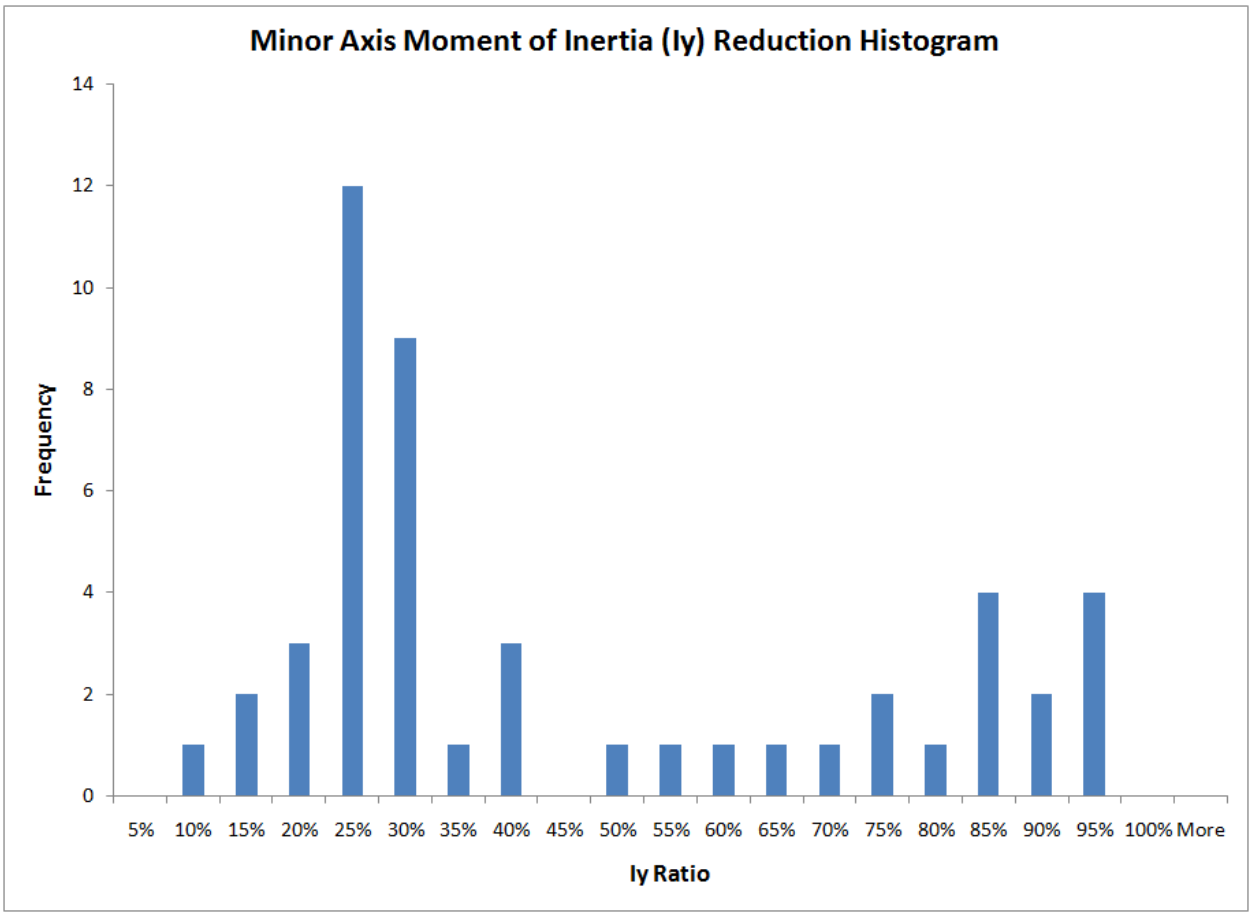

Figure 54. Chart. Observed Frequency major axis moment of inertia reduction ratio.

The governing stability equation is for the case when the beam is suspended from a crane with vertical cables and is calculated using only the minor axis moment of inertia (Figure 11). The stable length of the beam is reduced because of the reduction in the minor axis moment of inertia (Figure 55).

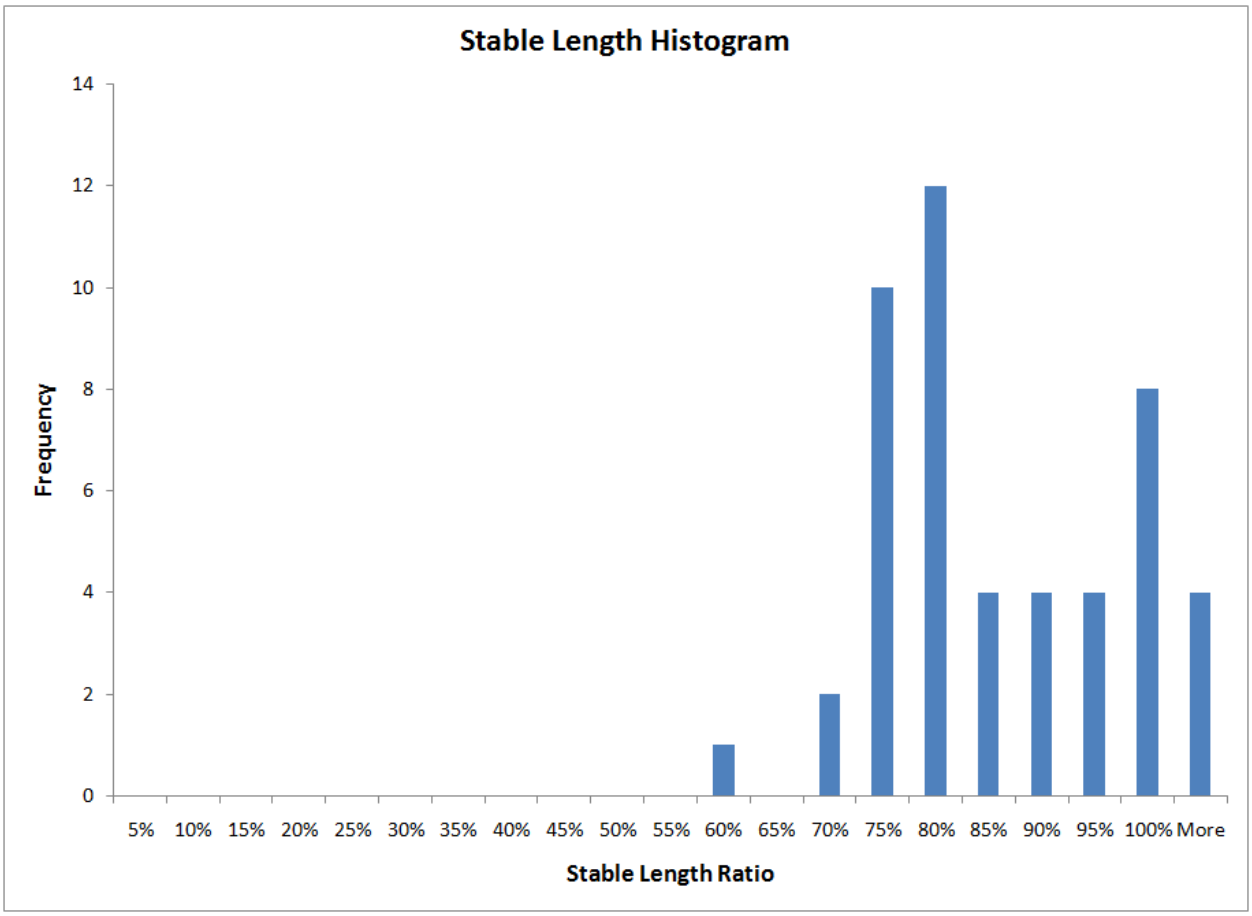

Figure 55. Chart. Observed Frequency of Stable length reduction ratio.

The increase in the modulus of elasticity from conventional concrete to UHPC lessens the severity of the loss in stable length. The average reduction was 83 percent with a corresponding standard of deviation of 11 percent.

Stresses

The estimations of stresses were calculated using assumed loading for the transfer and long term loading cases. The optimization was simplified by using the maximum amount of steel that would fit in the bottom bulb and then harping as many strands as possible through the web. When webs were reduced to a width less than 5 in. harped strands were not used. This simplification resulted in both the conventional and UHPC cross sections being extremely overstressed. There were six stress calculations performed on 49 cross sections resulting in 294 stress checks. The limits for UHPC were adjusted as shown in the equations of Figure 32. The conventional cross sections exhibited 85 stress checks that were within limits and 209 instances

of an over stress. The UHPC cross sections exhibited 116 stress checks within limits and 178 instances of an over stress. In both cases the most extreme over stresses occurred in the long term sections (Table 14).

Table 14. Average Overstress in Optimization Cross Sections

Type	Conventional	UHPC
Transfer Mid Top	426%	1073%
Transfer Mid Bot	133%	93%
Transfer Ends Top	37%	741%
Transfer Ends Bot	107%	83%
Longterm Mid Top	265%	139%
Longterm Mid Bot	1016%	509%

The over stress is a result of several factors. The assumption to force girders to carry a maximum amount of steel rather than as a optimization parameter allowed for easy comparison between the original shapes and the optimized shapes in moment capacity but increased the stresses so much that the stress data is non-informative. The ambiguity of assumed loading detracts from the validity of stress calculations as well. More accurate loading involves the calculation of distribution factors which requires bridge geometry.

Correlation

An investigation of correlation between changes in girder geometry and performance factors was performed to identify those changes in girder geometry that most heavily influenced the results. Identification of these factors furthered the subsequent optimization in the selection of the optimization procedure including design variables and constraint selection. The correlation coefficient is a measure of the closeness between change in the design variable and change in the girder property or performance.

The affect of the changes in girder geometry on section properties is expected. Correlation coefficients quantify the relative effect of each design variable on those properties (Table 15).

Table 15. Section Properties Correlation Coefficients

Properties	Area (%)	Ix (%)	Iy (%)
Top Flange Width Reduction (%)	0.506	0.771	0.833
Web Width Reduction (%)	0.612	0.294	-0.133
Bottom Flange Width Reduction (%)	0.064	0.003	-0.121
Top Flange Thickness Reduction (%)	0.392	0.418	0.238
Bottom Flange Thickness Reduction (%)	0.169	0.040	-0.049

The reduction of cross section area correlates most with web width reduction at 0.612 and the top flange width at 0.506. Modifying the top flange correlates most highly to reducing the major axis moment of inertia. The alteration of the top flange thickness also impacts the major axis moment of inertia. The weak axis moment of inertia is also most closely related to the changes in the top flange width.

The controlling length for stability was always the hanging beam case. The calculation of this length involves the weak axis moment of inertia and thus its correlation is similar (Table 16).

Table 16. Stable Length Ratio Correlation Coefficients

Properties	Simple %	Transport %	Hanging%
Top Flange Width Reduction (%)	0.924	0.924	0.689
Web Width Reduction (%)	-0.051	-0.051	-0.127
Bottom Flange Width Reduction (%)	-0.311	-0.311	0.144
Top Flange Thickness Reduction (%)	0.367	0.367	0.111
Bottom Flange Thickness Reduction (%)	-0.037	-0.037	0.001

The simple and transportation stability condition equations differ by a constant and therefore their correlations to the design variables are identical.

In order to quantify the effects of changes in the design variables on the over stress conditions present in both the conventional girders and the UHPC girders a ratio of UHPC stress over conventional stress was calculated for each shape pair. The stress ratio was then correlated to the design variables in the same way the section properties and stability conditions were (Table 17).

Table 17. Stress Correlation Coefficients

	Transfer				Long Term	
Property	**Mid Top**	**Mid Bot**	**Ends Top**	**Ends Bot**	**Mid Top**	**Mid Bot**
Top Flange Width Reduction (%)	-0.574	0.410	-0.074	0.411	-0.766	-0.197
Web Width Reduction (%)	-0.287	-0.303	-0.423	-0.452	-0.174	-0.195
Bottom Flange Width Reduction (%)	-0.260	-0.871	-0.290	-0.832	0.479	0.091
Top Flange Thickness Reduction (%)	-0.292	0.211	-0.067	0.145	-0.526	-0.098
Bottom Flange Thickness Reduction (%)	-0.065	-0.100	-0.043	-0.135	-0.026	-0.120

Negative correlation coefficients indicate that as design variable trended down, the stresses trended up. Mid-span stresses at transfer were most closely related to changes in the widths of the flanges. Transfer stresses at the girder ends were negatively correlated to the reduction of the web because narrow webs prevented the harping of strands. Long term mid-span stresses at the top and bottom flange correlate to changes in the respective flange widths.

The goal of the optimization of shape geometry was the development of a methodology to alter existing bulb tee shapes to create UHPC girders for direct replacement of conventional girders. The optimization showed that modified shapes using UHPC had the shear and moment capacity to allow for direct replacement. The modified shapes maintained capability while losing 17 percent of their stable length on average.

Several secondary investigations showed direct replacement was not feasible. The reduction in area of the optimized girder sections averaged 75 percent of original area. This reduction equates to a required material cost ratio of 1.33 in order for UHPC girders to be cost comparable to conventional girders. The Portland cement required for a cubic yard of UHPC is approximately 1200 lbs where in a high performance mix it is closer to 650 lbs. A quick comparison shows that cost ratio of the material is 1.85. Actual UHPC material cost ratios may range as high a 6.00 to 8.00 times the cost of conventional materials.

The over stressed conditions of the girders resulting from simplifying assumptions used in the optimization prevented evaluation of the performance of the girder shapes as it relates to AASHTO code limits. In order to fully investigate the stress conditions more detail was required. The implementation of the AASTHO methods required a full bridge simulation instead of investigations into girders alone. The area of steel utilized in a section must be included in the

optimization to control stresses. The correlation investigation showed that web widths should remain large enough to accommodate harped strands to alleviate end stresses.

Field Visit Feasibility Survey

Before the development of the full bridge optimization a feasibility study was conducted through on site surveys of industry practices. Possible modifications to girder geometry suggested by the results of the direct girder replacement were posed to professionals in prestressed concrete manufacturing plants and their comments and concerns were documented. The behavior of UHPC as it is poured and cures combined with the design of existing forms led to the conclusion that a simple modification would be the easiest and most cost effective to be made.

Prestressed girder forms usually consist of a bottom soffit and two side forms that use inserts to modify the web depth to create different depth girders (Figure 56).

Figure 56. Photo. The form pictured uses steam heat pumped through the red tubing to control the cure temperature. ***Woodworth 2008***

The difference lays in the bottom soffit configuration. One style of forms uses a pan to which the form sides are bolted. The second uses a flat soffit block to which the sides are clamped by threaded rods. In both cases the width of the soffit determines both the web and bottom flange widths (Figure 57).

Figure 57. Photo. The bottom soffit pan of this form has bolt holes where the form sides are attached.
Woodworth 2008

The top flange of the girder is formed by the top plates of the form and the pour stops. In some cases these stops are designed to be adjusted for different width as in the Washington deck flange shapes (Figure 58).

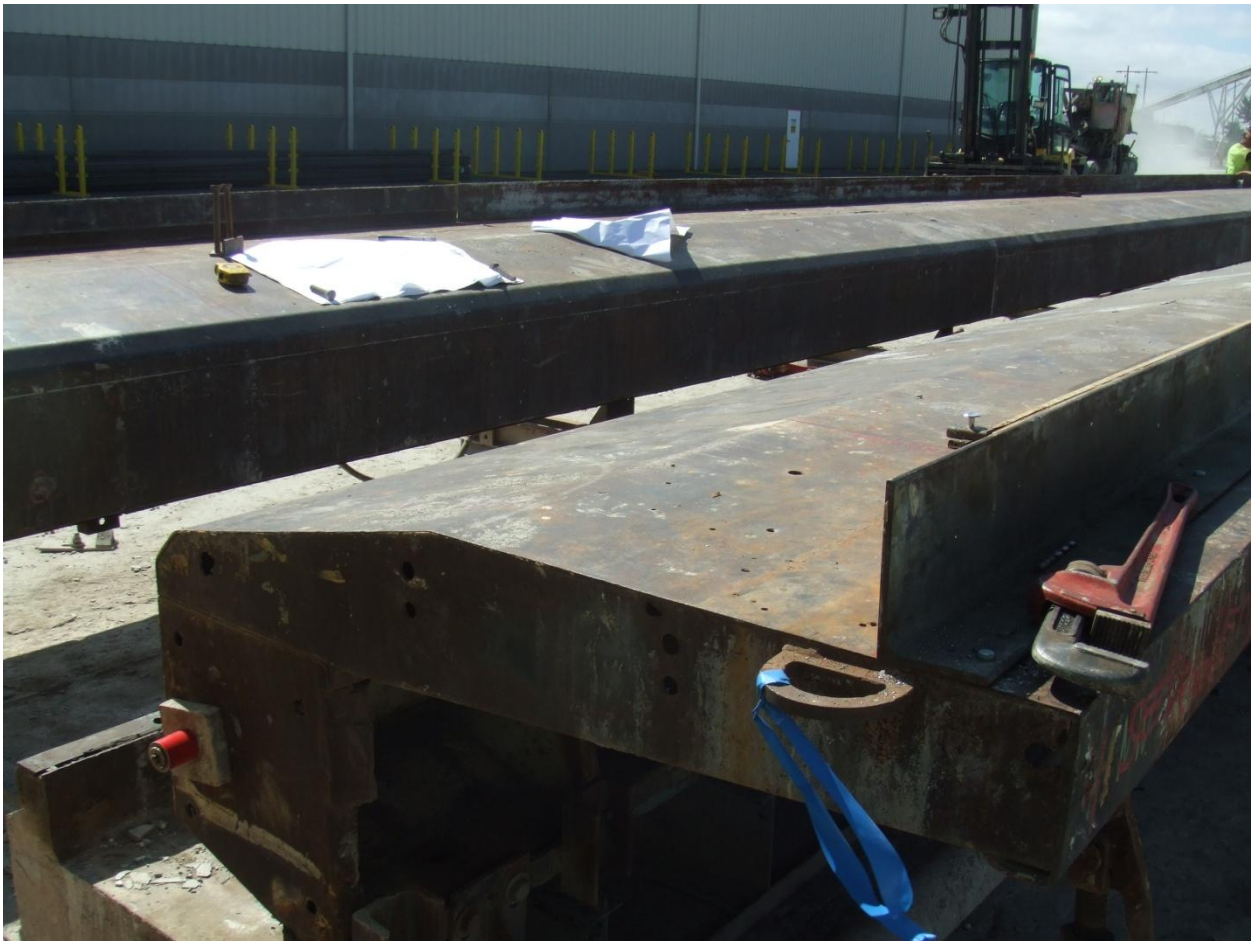

Figure 58. Photo. The bent plate is used to adjust the top flange width of this form. ***Woodworth 2008***

Steel strand patterns are dictated by the perforated endplates against which the strands are jacked. The jacking chucks' diameter requires a typical strand spacing of 2 in. on center. An example of this is the strand couplers used to hasten strand placement which have the same space requirements as chucks. (Figure 59).

Figure 59. Photo. This strand spacing block is used at the end of the form. ***Woodworth 2008***

Alterations to this pattern would require multiple endplates or the use of deviator blocks. All the plants visited as part of the survey harped strands rather than use debonding of strands as it can lead to girder cracking. The release of stress in the strands causes them to expand inside the girder.

Typical girder production process has a one day turn around time. The form is stripped in the morning and the strands cut so that the finished girder can be stored or shipped. The forms are cleaned and reset. The largest portion of a work day is devoted to setting the strand and secondary reinforcement. Finally girders are cast as the final task of the day.

Girders are cured in steam or electrically heated beds to control curing temperatures. Of the beds included in the survey the average temperature of the curing was 170° Fahrenheit. This

temperature is near the maximum capacity of the beds. The temperature is limited by physical capacity of the steam or electrical systems and Occupation Health and Safety Administrations limits on steam temperature to which workers can be exposed.

Another portion of the research survey was conducted with the help of a prestressing and precasting operation that was using UHPC in the production of panels. These panels were 100 mm thick and were 1200 mm by 800 mm in size. Working with the UHPC product led to several observations of its behavior when being poured and cured. UHPC is made of very fine aggregates which allow the very fluid material to squeeze into small openings such gaps in the joints of formwork. Exposed steel fibers were present in panel corners were UHPC had leaked through dragging the fibers into the gap. The UHPC used in the panel production shrunk vertically in the forms requiring excess material to be used to compensate. The exposed UHPC cured quickly forming a skin. The UHPC shrunk away from this external skin creating a small void in the panel. The cured panel had the skin removed to reveal true edge of the panel.

The optimization of girder shapes suggested narrowing the webs of the girders and reducing the widths of the top flanges. Some extreme top flange reductions resulted in shapes with no top flanges at all. Bottom bulbs were reduced by smaller amounts. The feasibility of these changes is circumspect based on the form designs utilized in most operations and the behavior of UHPC. Adjusting the web width would require the purchasing of all new bottom soffits. Narrow webs would also limit harping. The girder optimization showed that this will create unacceptable stress levels. Any insert used to adjust the web width would require additional blocking out in the bottom bulb. Adjustments to the bottom bulb are difficult because of the seal required to prevent UHPC from seeping and leaking. Even small gaps would destroy product finish by exposing steel fibers. Another concern is the use of narrow top flanges. A top flange restrains vertical shrinkage of the UHPC as it cures and may result in cracking in the top flange.

A shape that is both easy to produce from existing forms and represents the trends of the direct replacement optimization results is shown in Figure 60.

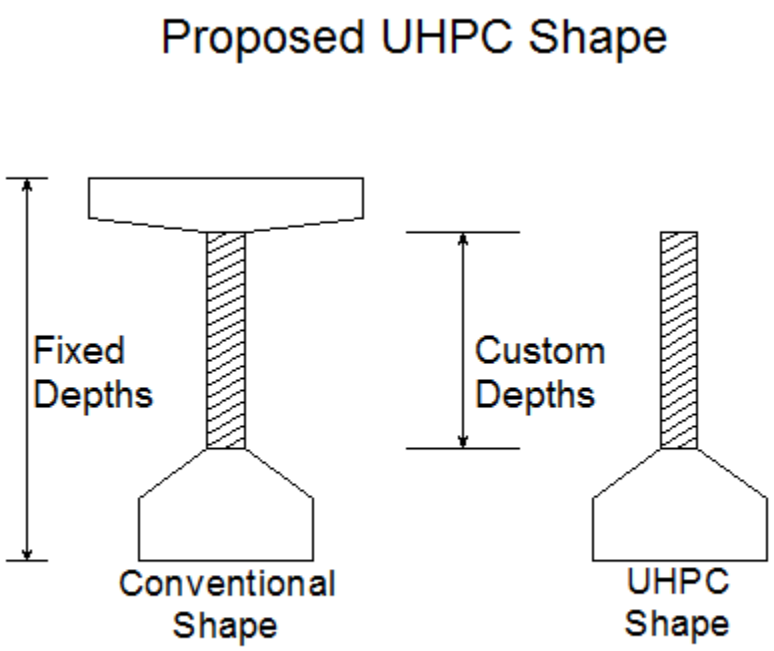

Figure 60. Diagram. The proposed shape is identical to the existing shape with the top flange removed.

Removing the top flange removes the concerns involved with vertical shrinkage. The rest of the form is not adjusted alleviating leaking concerns. The web width is maintained so that harping can take place to alleviate end zone stresses. The shape has the advantage of having a customizable depth without fabricating addition form pieces. The proposed shape was utilized in the full bridge optimization phase of the investigation.

Full Bridge Optimization

In order to overcome the limitations of optimizing single girder cross sections a full bridge optimization procedure was developed. The full bridge procedure included service and strength limit states from the AASHTO code rather than a basic capacity check. It also included stress limits as imposed by the AASHTO code. Considerations for stability were retained from the previous optimization. The greater detail required more computational resources which extended the duration of each optimization. This limited the number of variables that could be investigated. The design variables include the number of girders in the deck, the area of

prestressed reinforcement and the depth of the girders. The investigation was widened by performing the optimization on five bridge lengths, three bridge widths and girder shape families from seven different states. Optimizations were conducted for a conventional solution and a UHPC solution for each combination so that comparisons could be made. The result of the investigation showed that UHPC girders are a viable alternative across all bridge widths for which the length is 90 ft or longer.

Optimization Design Variables

The solution vectors of each bridge are the result of an optimization that altered the design variables to arrive at a minimum solution. On average the vectors were used to analyze the general trends in the optimizations. Each lane and length combination had similar solution vectors (Table 18).

Table 18. Nominal Values of Average Solution Vector of All Shapes

		Conventional				UHPC		
	Length (ft)	No.Girders	Steel Area (in^2)	Depth (in)		No.Girders	Steel Area (in^2)	Depth (in)
2 Lanes	50	6	2.69	40		5	1.67	59
	70	5	2.91	72		5	2.75	69
	90	5	2.91	86		4	3.81	68
	110	5	2.91	86		5	4.79	62
	130	6	3.14	87		5	4.93	64
3 Lanes	50	7	2.59	52		7	1.67	59
	70	5	2.91	84		4	3.34	73
	90	6	2.91	86		4	4.62	65
	110	7	2.91	87		5	4.79	62
	130	8	3.14	87		6	4.93	72
4 Lanes	50	7	2.69	55		8	1.67	59
	70	7	2.91	79		5	3.34	73
	90	6	2.91	86		5	5.00	59
	110	10	2.91	85		6	5.00	62
	130	11	3.14	88		7	4.93	72
NOTE: Number of Girders has been rounded to the ceiling interger and depth to the nearest interger								

The optimization operated on continuous real numbers because the algorithms implemented in *MATLAB*® required continuous functions and derivatives. The results are summarized using the next largest integer and the nearest integer for the number of girders and depth respectively to represent realistic bridge configurations. For all lane widths the number of girders required in

the conventional solutions grows as the bridge lengths increase. The UHPC solution number of girders does not increase by the same amount. This is apparent in the plot of all lanes averaged together (Figure 61).

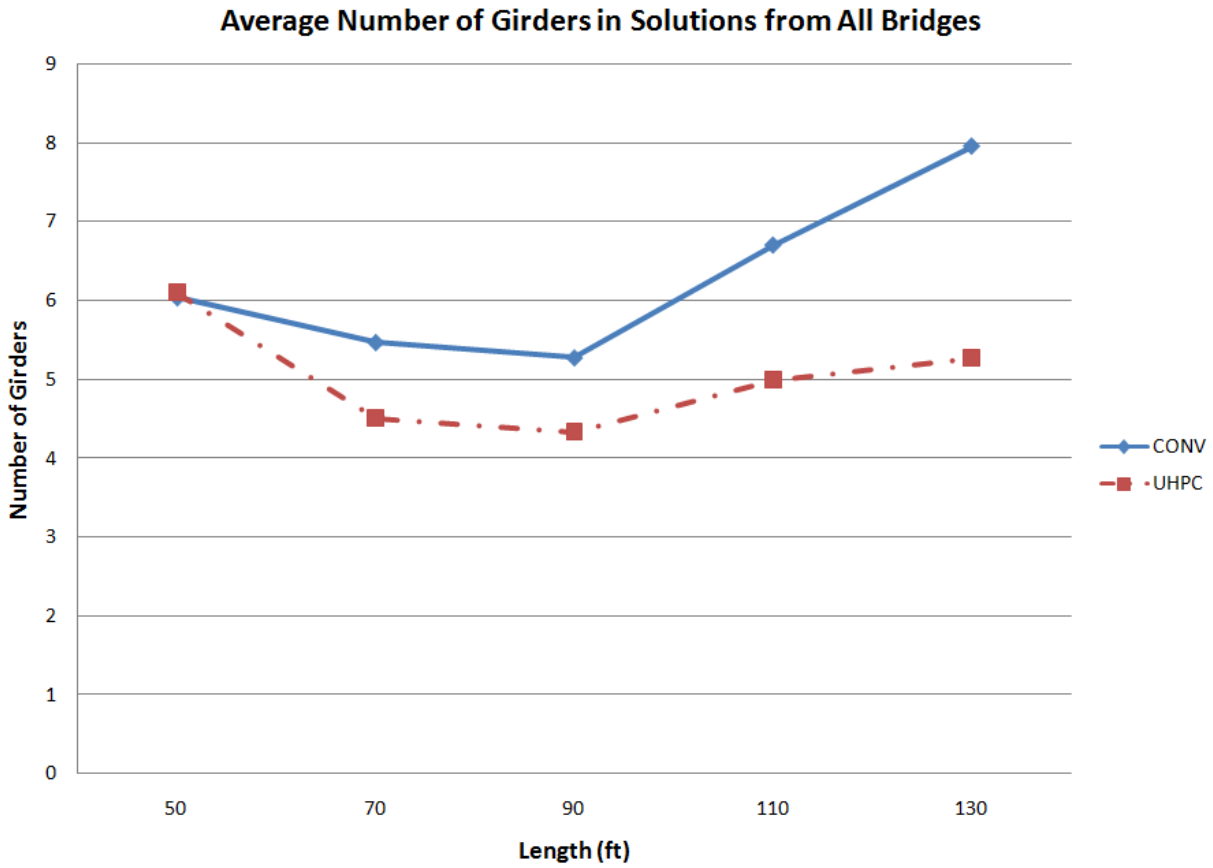

Figure 61. Graph. The conventional solutions require more girders than those of the UHPC.

The repeated values of the prestressing strand area are due to the fact that the area of prestressing is delineated by numbers of 0.5 in. diameter strands that can fit in a girder. The area of prestressing steel does not change much as the conventional bridge lengths increase. As UHPC bridge lengths increase the area of steel in the girders increases. The average across all lanes shows the trend of increasing steel areas (Figure 62).

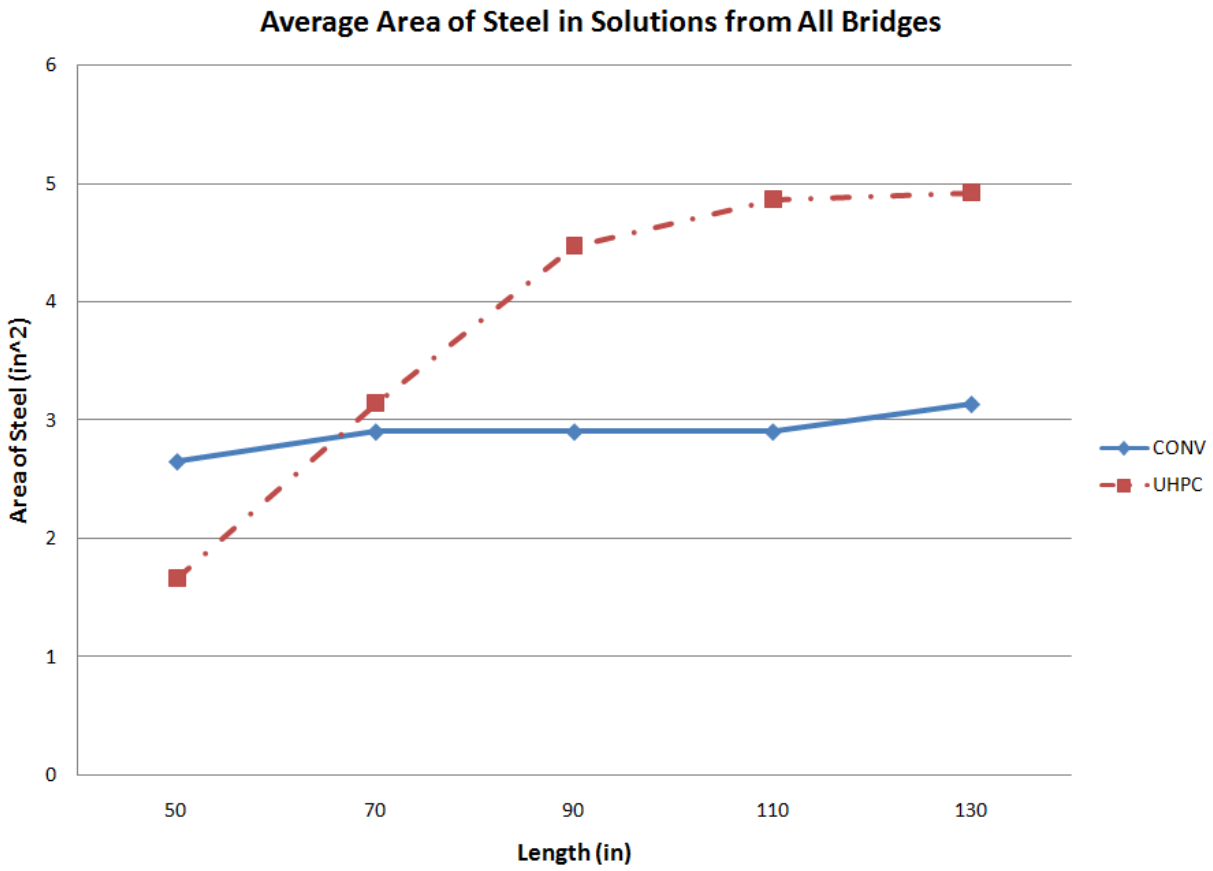

Figure 62. Graph. The area of steel in the conventional girders is less dynamic than the UHPC.

Girder depths of conventional girders are discrete in reality but for the optimization both the conventional and UHPC girders were continuous variables. In the proposed UHPC shape this can be true in reality as well. In general for all lanes both the conventional girders and the UHPC girders maintained a constant depth for the bridge lengths 90 thru 130. The longer spans had depths greater than those required for the 50 and 70 foot spans (Figure 63).

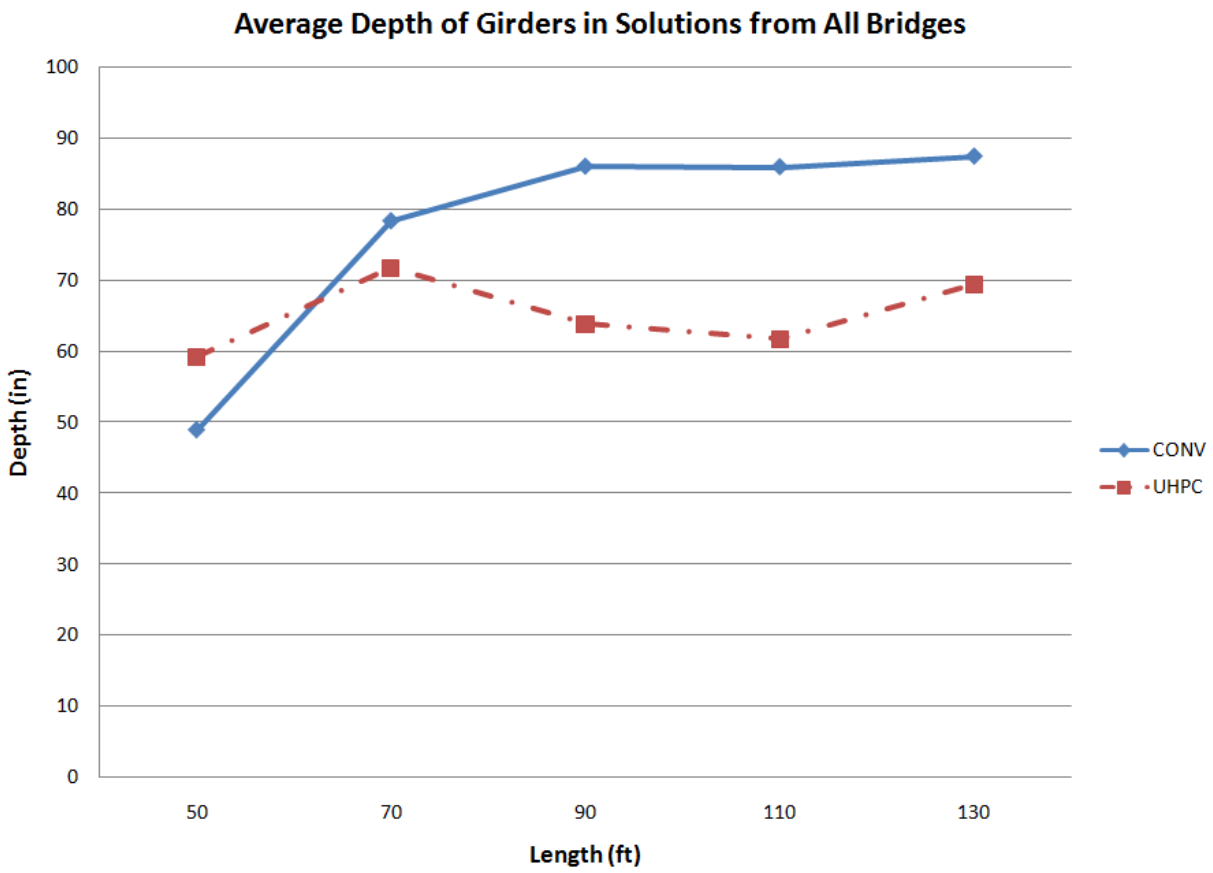

Figure 63. Graph. Girder depths of the solutions tended to stay constant over the longer length spans.

Depth to Steel Ratio

The cost savings of the UHPC bridges correlate to the solution vectors recovered from the optimizations. The ratio between the girder depth and the amount of steel required is the simplest correlation found as plotted in Figure 64.

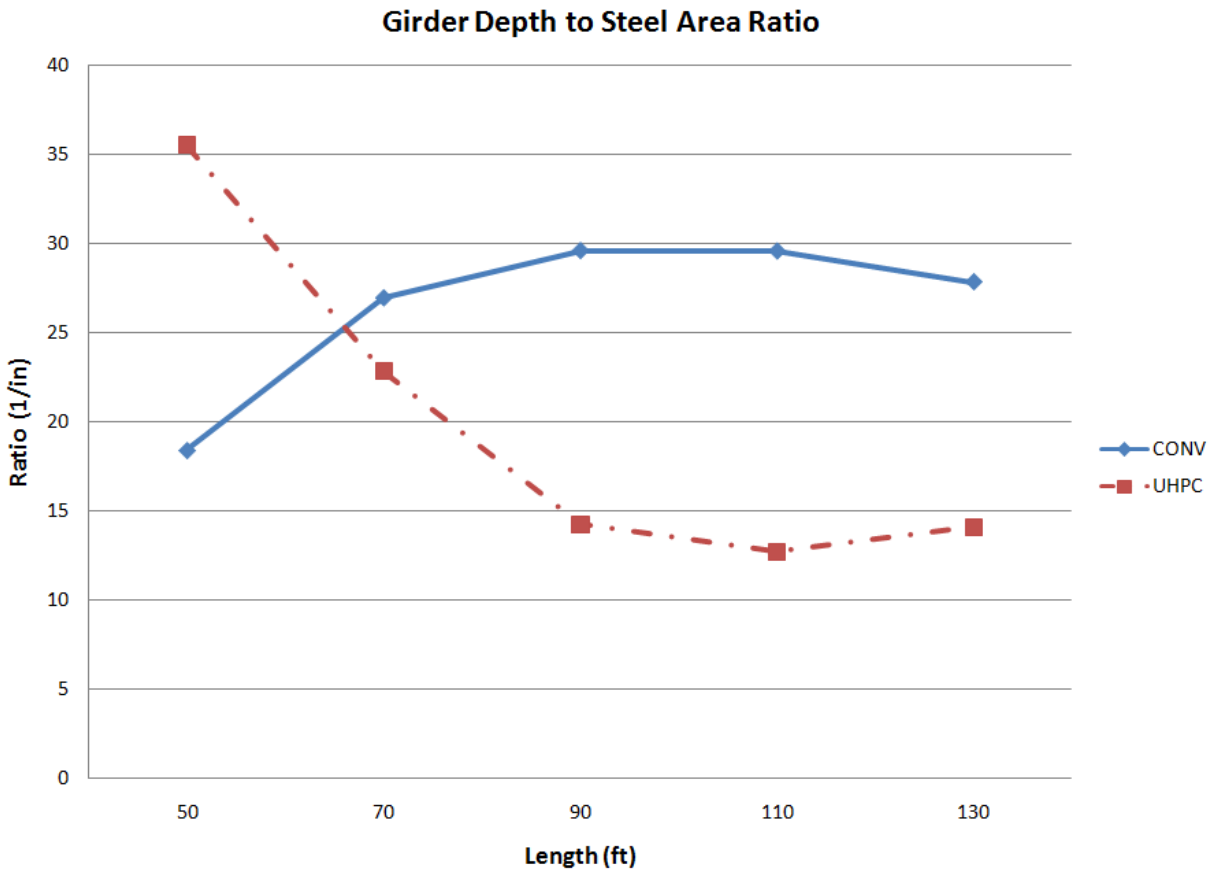

Figure 64. Graph. The ratio of girder depth to area of steel.

The change in performance of the UHPC solutions beyond 70 ft is due to the steel and girder configurations that UHPC can accommodate that the conventional girders cannot. The depth to steel ratio follows an inversely proportional to the cost trends of UHPC bridges. Past 70 ft both UHPC and the conventional solutions had near static values for the ratio.

Objective Function

The objective of the optimization was to minimize the costs of a conventional bridge and a UHPC bridge for each permutation of bridge length, bridge width and shape family. The cost of a bridge system was the sum of the material costs for the girders and the transportation and erection costs for the bridge. The girder cost included concrete and prestressing strand. The total cost of the bridge included constraint costs during the optimization but these were removed

for the comparison of solutions. For each optimization a cost comparison was made between the optimal conventional solution and the UHPC solution at each length (Figure 65).

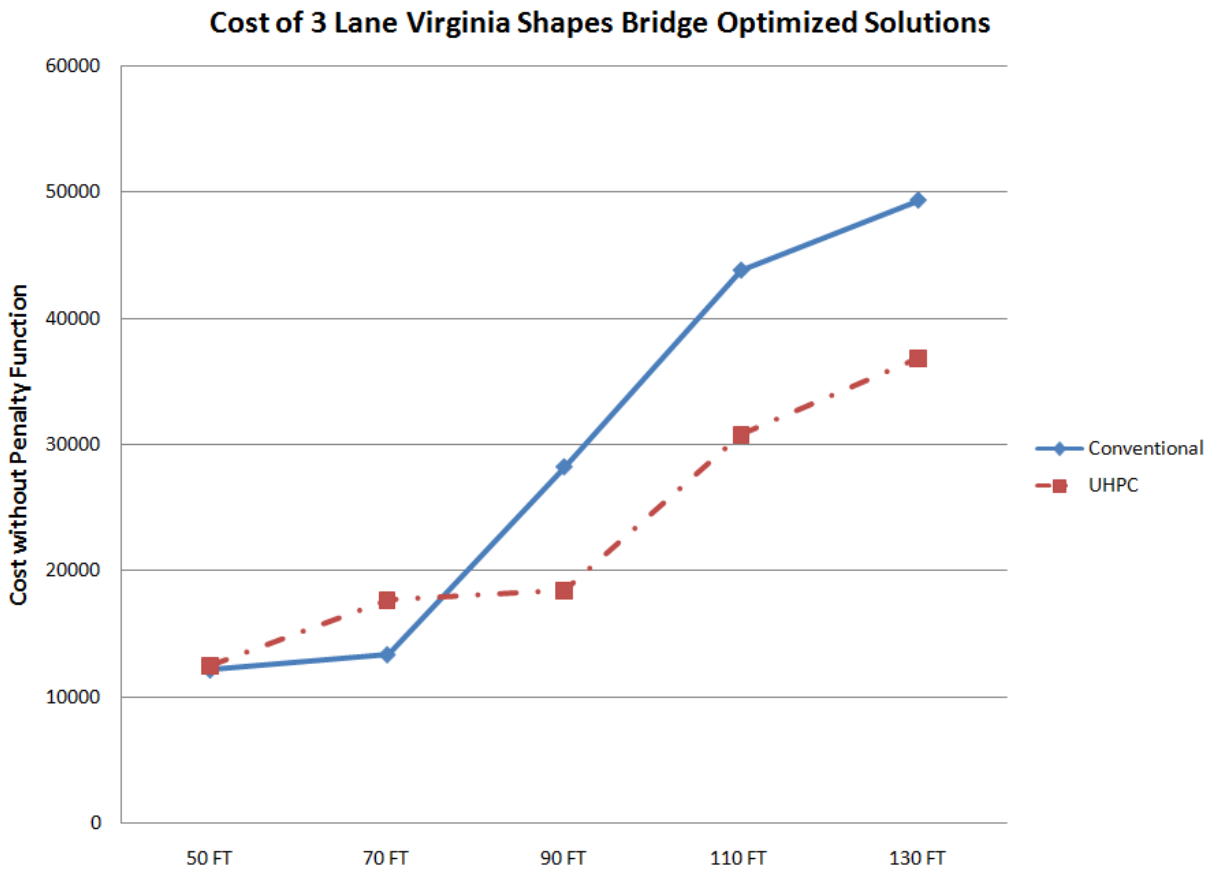

Figure 65. Graph. The typical optimization resulted with UHPC becoming more economical.

The typical performance plots showed that UHPC girder became the more economical choice at a girder length somewhere between 70 and 90 ft. This is evident in each of the lane width's respective average cost performance plots. The first of the three width summaries is from those bridges with two lanes (Figure 66).

Figure 66. Graph. The conventional solution becomes more expensive after 70 ft.

The average two lane cost curve breaks at 70 ft. The percent savings calculated as the cost difference over the conventional costs at 90 ft, 110 ft and 130 ft are 16 percent, 35 percent and 32 percent respectively. The next width considered was three lanes (Figure 67).

Figure 67. Graph. The conventional solution becomes more expensive past 70 ft.

The performance change occurs again at lengths greater than 70 ft. Percent savings of 16 percent, 20 percent and 27 percent at 90 ft, 110 ft and 130 ft respectively were observed. The final and widest bridge considered was 4 lanes (Figure 68).

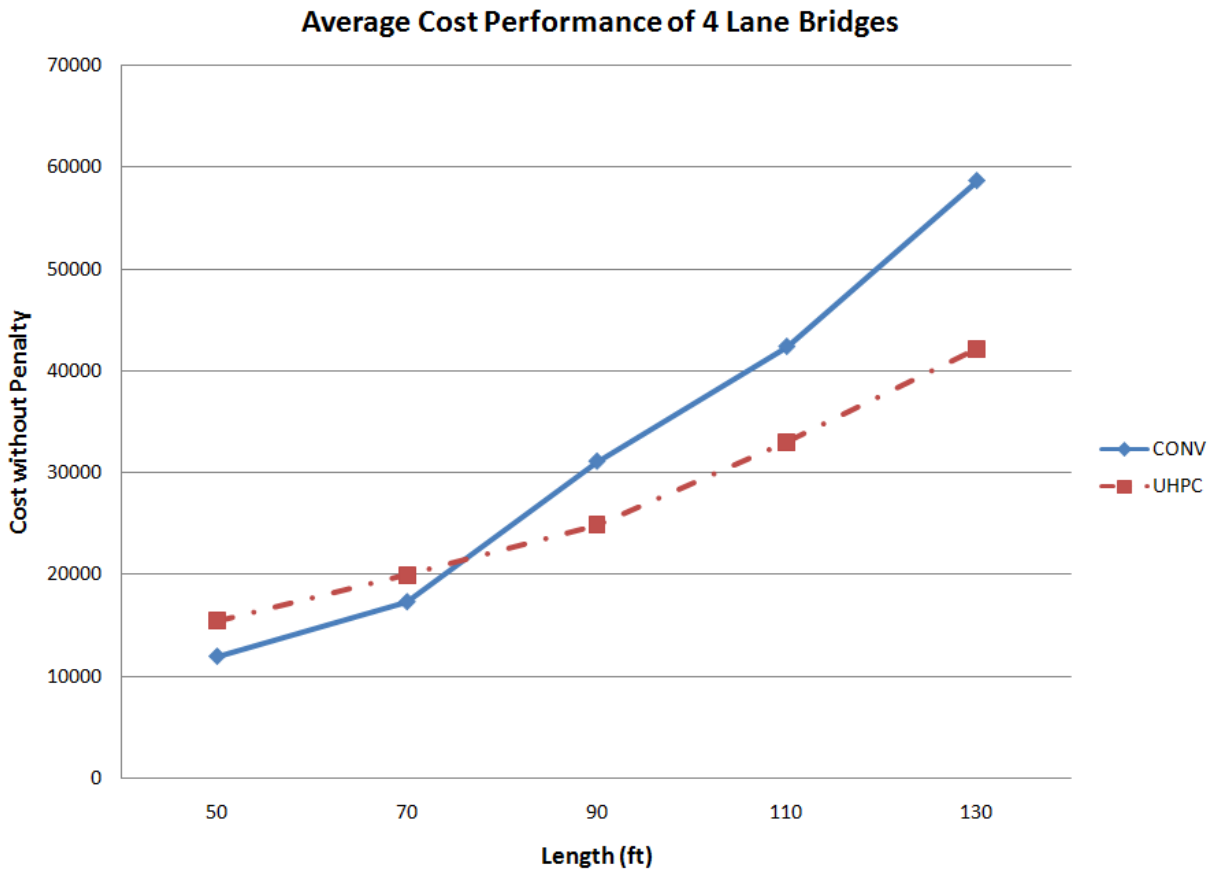

Figure 68. The conventional solution becomes more expensive past 70 ft.

Typical cost savings past 70 ft were observed once again. The four lane bridges had percent savings values of 20 percent 22 percent 28 percent for 90 ft, 110 ft and 130 ft respectively. The four lane bridge required an adjustment to the minimum number of girders constraint to prevent excessively long deck transverse span lengths.

Altering the routine for the four lane bridges was one of several adjustments to the routine to accommodate idiosyncrasies. The Idaho bridge shape was unstable in its conventional configuration at 130 ft and as such the optimization was not performed. The UHPC solution girder would have resulted in a stout girder to overcome the stability constraint making the comparison back to a conventional solution hindered by stability unfair.

Secondary Investigations

The results of the optimizations consisted of two raw data sets, solution vectors and the solution objective function values. The data from these two sources was analyzed in several ways to better explain the reasons behind the results. The data was also extrapolated to investigate changes in variable not explicitly included in the optimization routines. Secondary investigations consider requirements of bridge design practices not included in the optimization procedure.

South Carolina Shape

The average plots in Figure 66 thru Figure 68 exclude the results of the optimizations done with the South Carolina shape family. The South Carolina bridge girders were the only shapes to not exhibit the cost break between a conventional solution and the UHPC solution. The costs of the UHPC solutions were more than the conventional bridges at all five lengths across all bridge widths. The area of prestressing strand is one of the three design variables of the optimization and has direct impact on the cost performance of the optimized solutions. A comparison of the South Carolina solution vectors to the average of the other shape solution vectors shows the variability of the strand area in the solutions (Table 19).

Table 19. South Carolina Solutions vs Other Nominal Values of UHPC Solution Vectors

		South Carolina				Average of All Others		
	Length (ft)	No.Girders	Steel Area (in^2)	Depth (in)		No.Girders	Steel Area (in^2)	Depth (in)
2 Lanes	50	5	1.38	63		5	1.67	59
	70	5	2.31	63		5	2.75	69
	90	9	1.68	68		4	3.81	68
	110	4	14.08	63		5	4.79	62
	130	4	7.20	68		5	4.93	64
3 Lanes	50	6	1.68	68		7	1.67	59
	70	7	2.31	63		4	3.34	73
	90	4	14.08	63		4	4.62	65
	110	4	14.08	63		5	4.79	62
	130	4	7.80	63		6	4.93	72
4 Lanes	50	10	1.23	63		8	1.67	59
	70	10	1.68	68		5	3.34	73
	90	5	14.08	63		5	5.00	59
	110	5	14.08	63		6	5.00	62
	130	5	7.80	63		7	4.93	72
NOTE: Number of Girders has been rounded to the ceiling interger and depth to the nearest interger								

The South Carolina Shapes fluctuate wildly in the number of girders and the area of steel but the depths of the girders remain the same. The product the number of girders and the area of steel per girder is a measure of the approximated the tension capacity of the bridge. The product of the girder depth and the approximate tension capacity is the approximate moment capacity of the bridge. For a given loading the approximate capacities across any configuration should be equivalent. Comparing the South Carolina shapes to the best performing shape family shows the differences that caused its poor performance in the optimization algorithms (Figure 69).

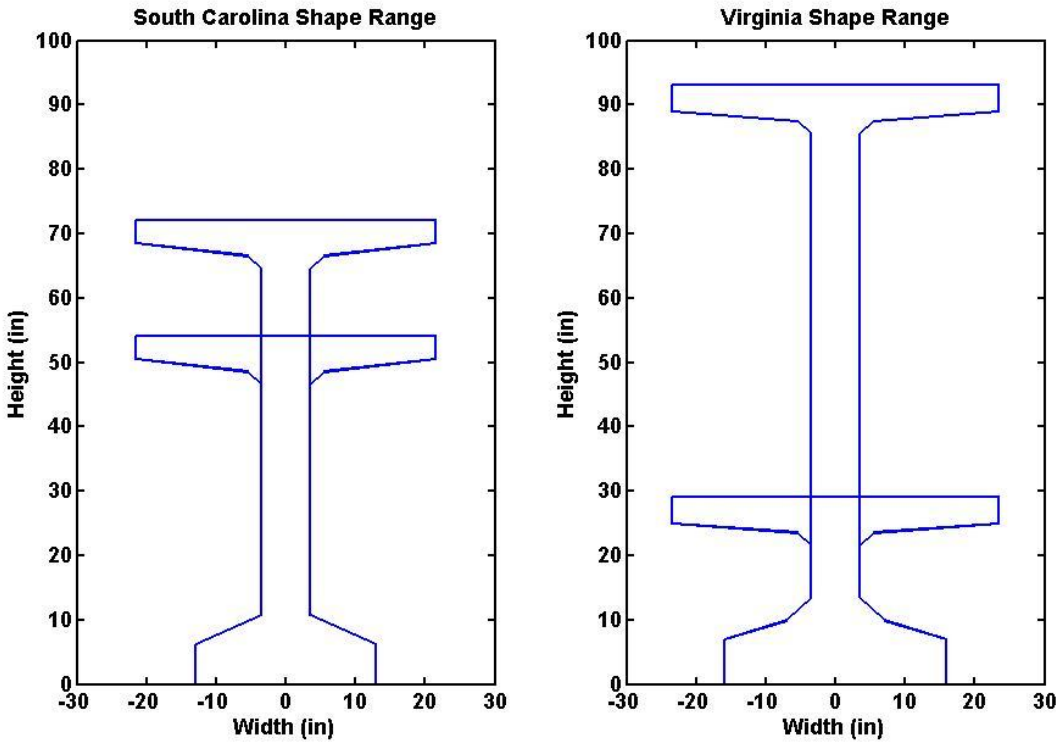

Figure 69. Diagram. The range of the possible South Carolina and Virginia shapes.

The main difference is in the available heights for UHPC girders. The other shape families had existing girder shapes up to 80 in. Without the ability to create deeper the girders with the South Carolina shapes the conventional and UHPC optimization appears to have gotten stuck in local minimums. The other shapes optimized better because of the larger range of configurations that could be tried.

Material Cost Ratio

The cost ratio between UHPC and conventional concrete used in the optimization procedure was 1.85. This represents the lower bound of the cost ratio and was determined by comparing the Portland cement content of a typical UHPC mix and a high performance concrete mix. The actual cost of UHPC materials may be six times as much as conventional concrete. Due to the computationally intensive nature of the optimizations a cost investigation was performed using the objective function. Evaluating only the cost function with Monte Carlo simulations was magnitudes quicker than repeating optimization of the bridge configurations multiple times. The

cost function for a subset of the optimized UHPC bridge solutions was evaluated multiple times to generate data. This data was used to develop a function to determine the cost of a bridge configuration as a function of the cost ratio (Figure 70).

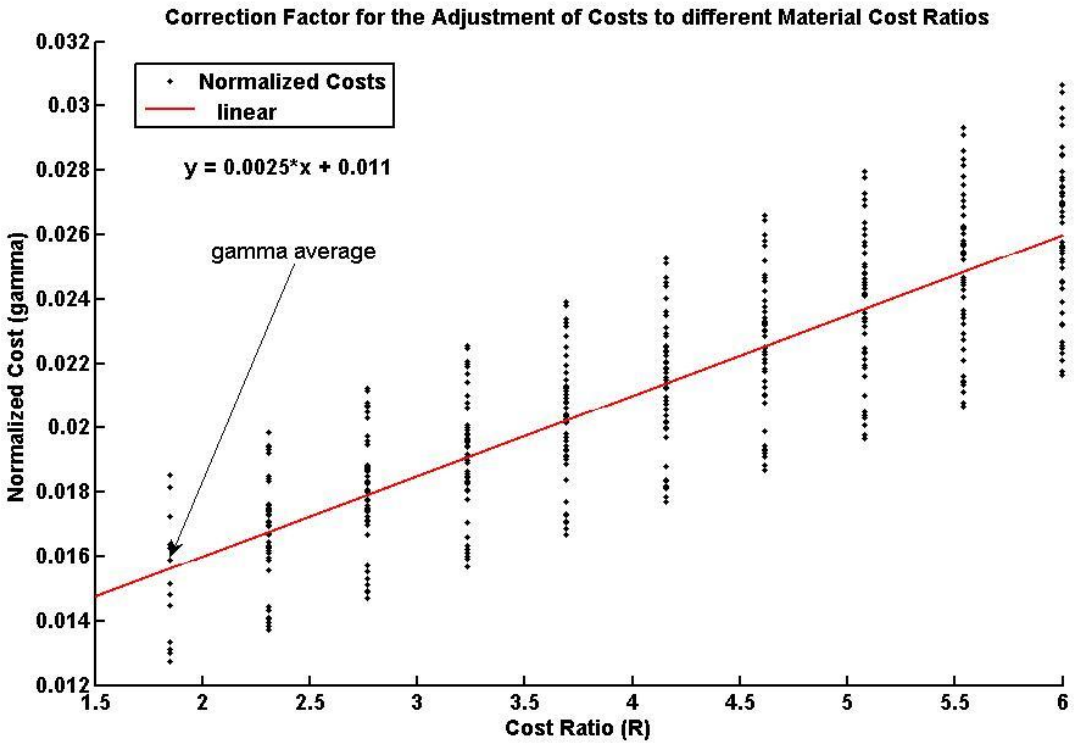

Figure 70. Graph. The costs were normalized to create a correction factor.

The linear regression represents the average normalized cost. The cost functions need to be customized to deal with different initial values in order to be more accurate. The result of the algebraic manipulation of the normalization yielded a function of the cost ratio desired, the initial cost at the ratio 1.85 and the girder depth (Figure 71).

From the Plot:

$$\gamma(R) = 0.0025\ R + 0.0110 + c$$

$$\gamma(R) = \frac{W(R)}{W_o\ d} \qquad \gamma_o = \frac{1}{d} \qquad c = \gamma_o - \gamma_{avg} \qquad \gamma_{avg} = 0.1562$$

Substitute:

$$\frac{W(R)}{W_o\ d} = 0.0025\ R + \frac{1}{d} - 0.0046$$

$$W(R) = W_o\ d\ (\ 0.0025\ R + \frac{1}{d} - 0.0046\ )$$

Where:
W = Bridge Cost
R = Material Cost Ratio
W_o = Bridge Cost at R=1.85
d = Depth of girders in bridge
c = y-intercept adjustment constant

Figure 71. Equation. Bridge cost adjustment equation with derivation.

The function developed was used to determine the maximum cost ratio each optimized UHPC solution would sustain and still be cost effective. The South Carolina shapes were excluded from this investigation. The material cost ratios were uniformly distributed over the range of cost ratios (Figure 72).

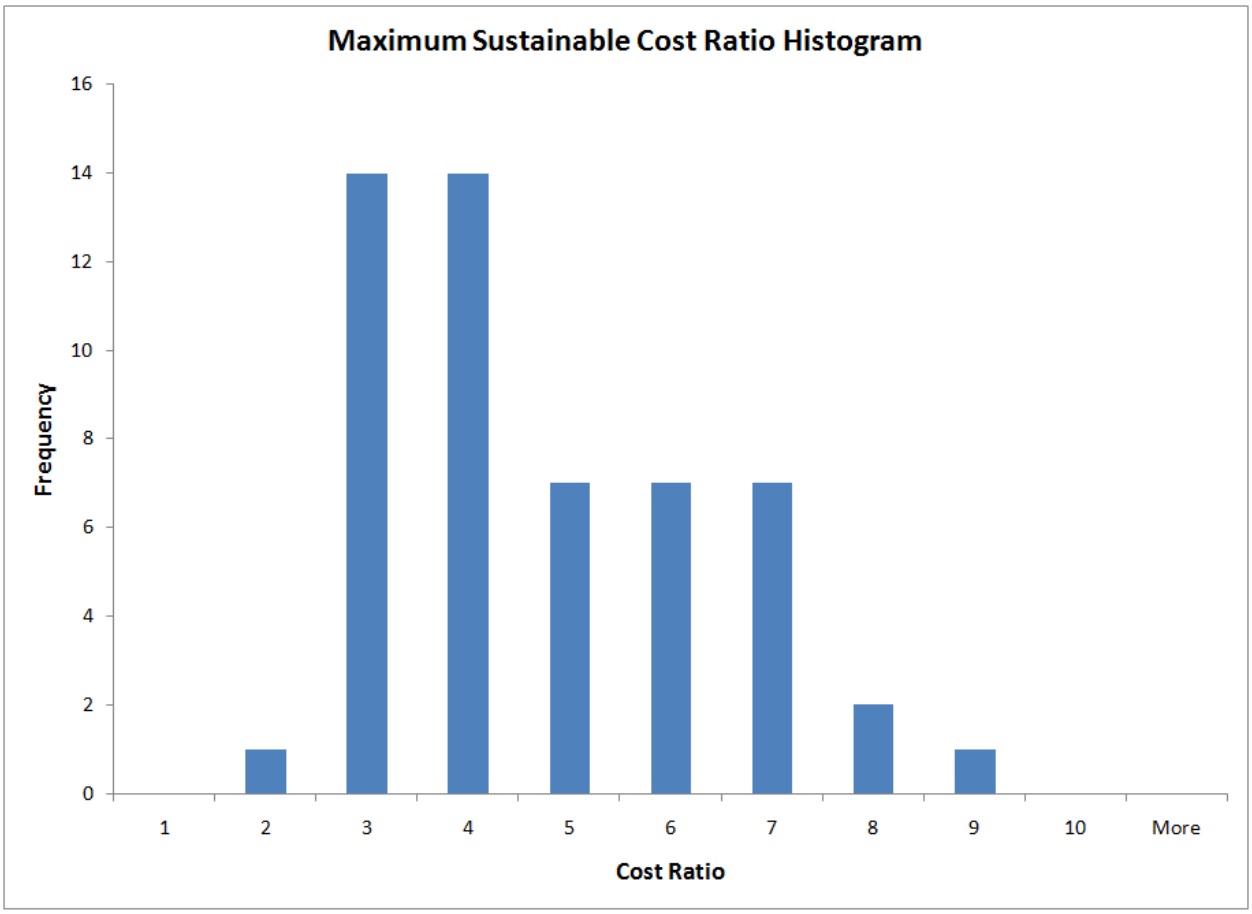

Figure 72. Chart The distribution of sustainable cost ratios descends from a ratio of 3 to 9.

The distribution is not normal with larger frequencies towards the lower values of the range. The mode or median are a better indicator of the distribution than the mean (Table 20).

Table 20. Cost Investigation Results Data Statistics

MEAN	4.2459
MODE*	3
MEDIAN	3.8941
*NOTE: Values Rounded to Intergers	

The cost ratio between UHPC materials and those of conventional of nine was sustained by one solution configuration without the UHPC price tag exceeding the convention bridges. A more reasonable expectation of cost savings exists for cost ratios less than five.

Active Constraints

Including the large number of details associated with the full bridge system led to complex nonlinear behaviors. In order to handle the non-linear functions some of the constraints were moved into the cost function. At the conclusion of the optimization routine the active constraint was recorded. An active constraint is the maximum constraint value which is driving the optimization search. There were nine constraints considered but only five were active at the termination of the optimization runs (Table 21).

Table 21. Full Bridge Optimization Active Constraints

	CONVENTIONAL			UHPC	
Constraint	Count	Average		Count	Average
Stress: End Transfer Top	1	0.08		10	0.25
Stress: Mid Transfer Bot	3	0.33		0	--
Stress: Mid Transfer Top	4	0.04		16	0.16
Stability	0	--		1	-0.05
Strength	94	0.27		75	0.21

In a majority of cases the active constraint was the strength. The strength constraint was the percent difference of strength demand and strength capacity. The average deficiency was 0.27 or 27 percent of the demand for conventional bridges and 0.21 or 21 percent of the demand for UHPC bridges. The only instance of a stability constraint controlling was in one bridge where all the constraints were met.

Strength I Moment Demand Constraint

Because a majority of the bridges were coming up under strength, a secondary investigation was made into the AASHTO Strength I capacity. Each optimized UHPC bridge solution was reevaluated with additional girders to determine if additional girders with the same dimensions would increase strength. The girder depths and steel configurations were unchanged. For each set of configurations the data was sorted to represent the constraint performance improvements (Figure 73).

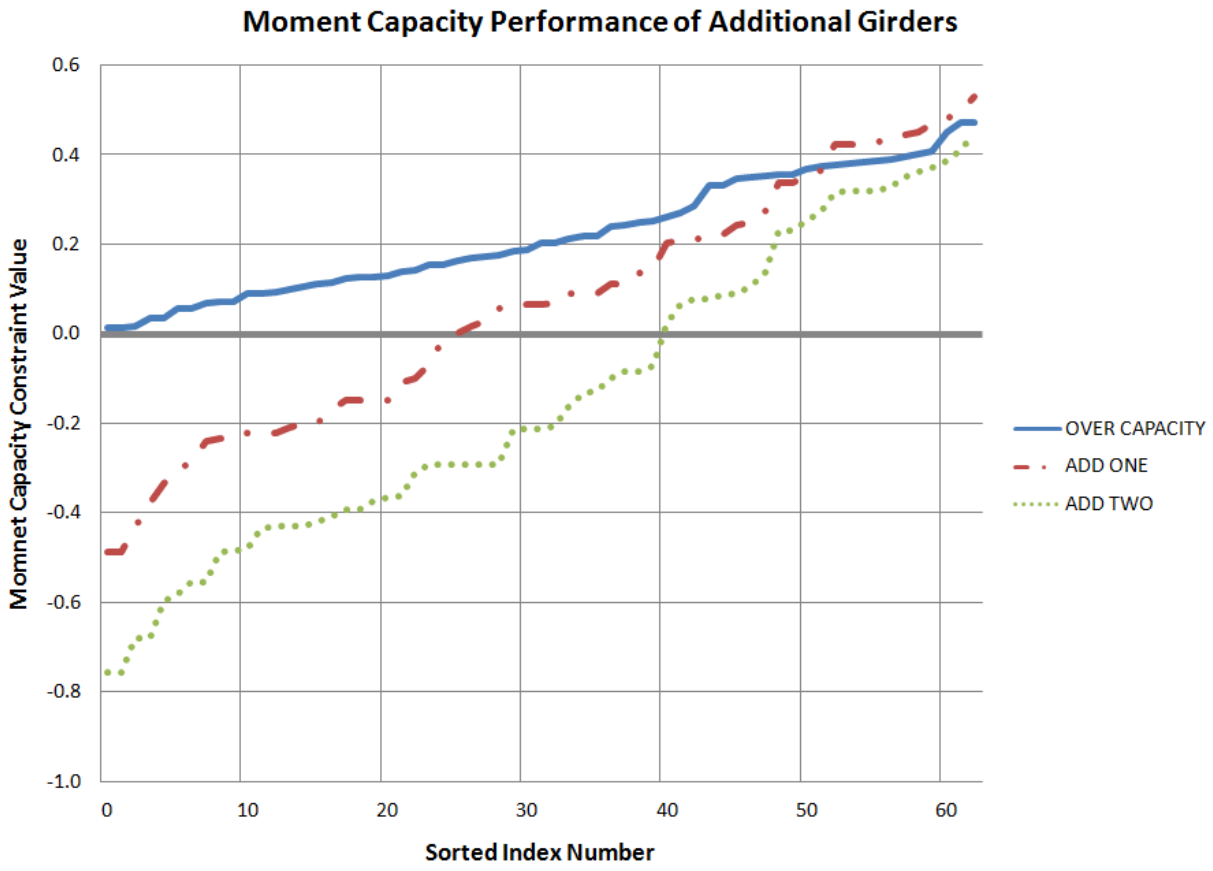

Figure 73. Graph. The data plotted is sorted from high to low in each series. In some bridges adding a girder hurt the performance by increasing the weight.

Not every bridge was improved by adding a girder. The additional weight of the girder resulted in greater demand increasing the constraint value. Almost of all the 63 bridges were improved with a majority having capacity exceeding demand (Table 22).

Table 22. Changes in Moment Capacity with Additional Girders

Additional Girders	One	Two
Number that Exceeded Demand	40%	63%
Number of Improved Bridges	67%	90%
Average Constraint Improvement	-0.29	-0.41

Deflections

The UHPC girders are less stiff than the conventional girders because the absence of a top flange reduces the moment of inertia. The flexibility of the girders could make working with them difficult. Stability and deflection are dependant on the stiffness of the girders. Stability was included explicitly as a constraint in the optimization. Deflections are an optional component of the AASHTO code and were not included in the optimization. Though it is optional, deflection performance of the girders is important to the feasibility of the UHPC solutions.

Three deflection checks were performed on each solution configuration for both the conventional and UHPC systems. Large transfer deflections may topple girders when strands are severed endangering workers. Excessive deflection may cause cracking in the girder even if transfer stress constraints are satisfied. Excessive deflections at the time of erection increase bridge costs because haunches are required to level the girders before the deck. Serviceability concerns such as vibrations and limits the live load deflection of bridge systems. The average deflections of the UHPC bridges were similar to the conventional counter parts (Table 23).

Table 23. Statistics of Conventional and UHPC Bridge Deflections

	Conventional (in)					UHPC (in)			
Deflection	**MAX**	**MIN**	**AVG**	**STDDEV**		**MAX**	**MIN**	**AVG**	**STDDEV**
Camber	1.28	-4.04	-1.50	1.28		6.02	-2.00	0.70	2.28
Self	-0.04	-2.45	-0.68	0.64		-0.08	-5.38	-1.43	1.39
Transfer	0.42	-4.08	-2.17	1.11		1.13	-2.59	-0.73	1.14
ABS(Erecting)	7.33	0.05	3.81	1.94		4.34	0.08	2.49	0.99
Live	-0.05	-2.11	-0.48	0.36		-0.08	-5.31	-1.30	1.20
Limit	-0.75	-1.95	-1.33	0.42		-0.75	-1.95	-1.33	0.42
Relative Live	1.50	-0.16	0.85	0.35		1.04	-3.36	0.04	0.90

The camber deflection is calculated by determining the deformations cause by two loading effects of the prestressing strand. The first is the upward deflection caused by the eccentricity of the strand at midspan. The second is the downward deflection caused by the eccentric axial loads at the girder ends caused by the harped strands. Because of the optimization simplified strand design by harping as many strands as possible the eccentricity of the axial loads was very high. The large difference between eccentricity at midspan and the eccentricity at the girder ends

in both UHPC and conventional shapes caused downward deflections. Downward cambers are not realistic because actual girders would have had more design considerations in the number of strands harped. The important comparison is that the magnitude of the deflections is similar showing that UHPC girders exhibit a similar deflection behavior.

The transfer deflection is the sum of the self weight deflection and the initial camber so the large harping strand eccentricity influences this as well. The UHPC bridges had large magnitudes of self weight deflections and camber deflections than the conventional bridges. Though the magnitudes of the components are larger in UHPC bridges the deflections do not act independently but rather concurrently. Adding the camber and self weight deformations balance their effects resulting in smaller transfer deflection magnitudes over all (Figure 74).

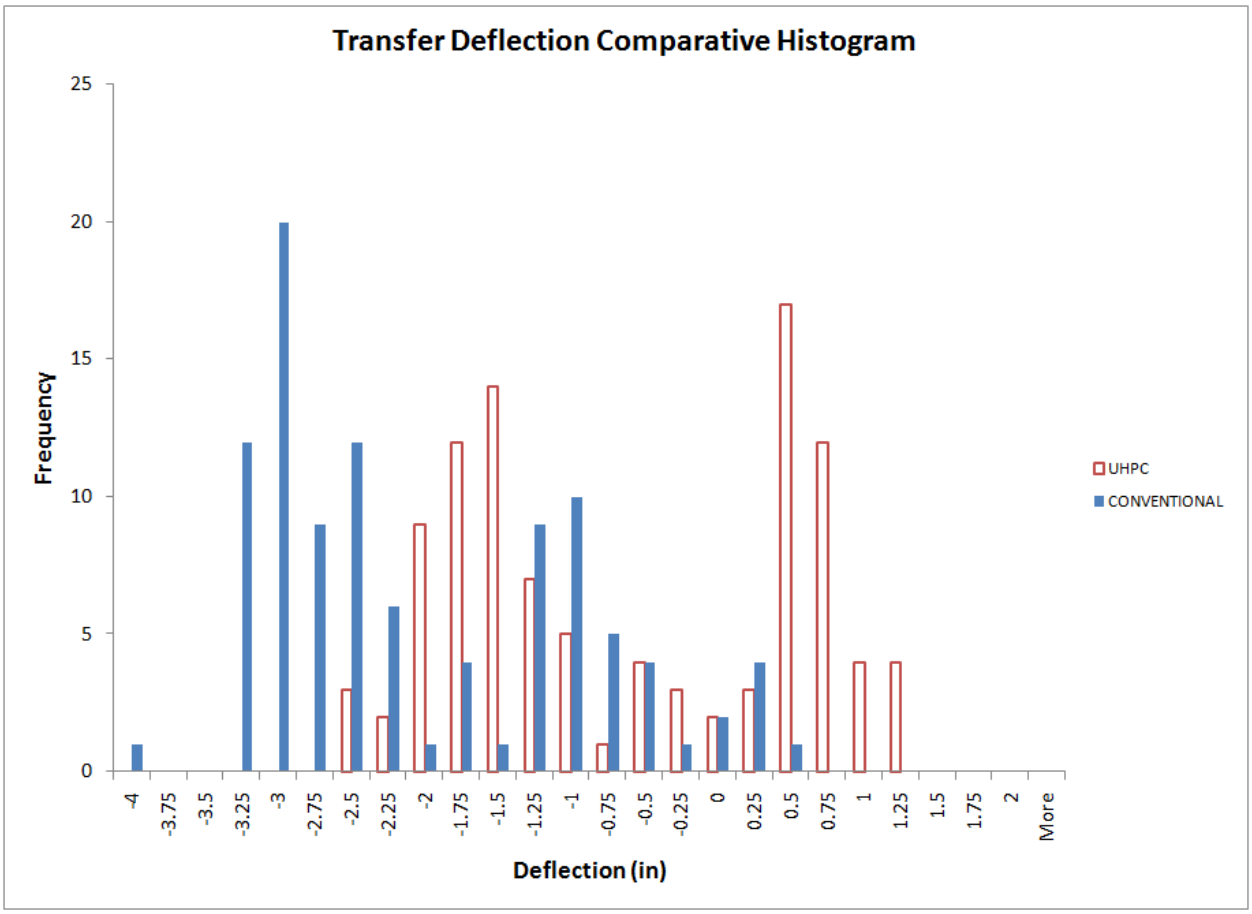

Figure 74. Chart. Transfer deflections are due to the prestressing force and the self weight of the girders.

The erection deflections are similar to the transfer deflections because the erection deflection is the weighted sum of the long term self weight deflection and initial camber. The weighted sum is used to account for additional curing and strand relaxation. The required haunch would be in the middle of the span for negative deflections and at the ends for positive deflections. The largest magnitudes of the erections deflections are a result of the extreme strand harping that influence initial cambers. Absolute value was used to determine the average haunch requirements. On average the UHPC bridges would require 2.49 in. haunches and the conventional bridges 3.81 in. haunches (Figure 75). These values are extremely large but both are extremely large for the same reasons. The simplification of harping strand design used in the optimization caused unrealistic negative cambers. Their relative value to each other is valuable as it shows that the UHPC girders can be expected to behave similarly to conventional girders even though their moments of inertia are reduced. The absence of the top flange is mitigated by the additional stiffness of UHPC.

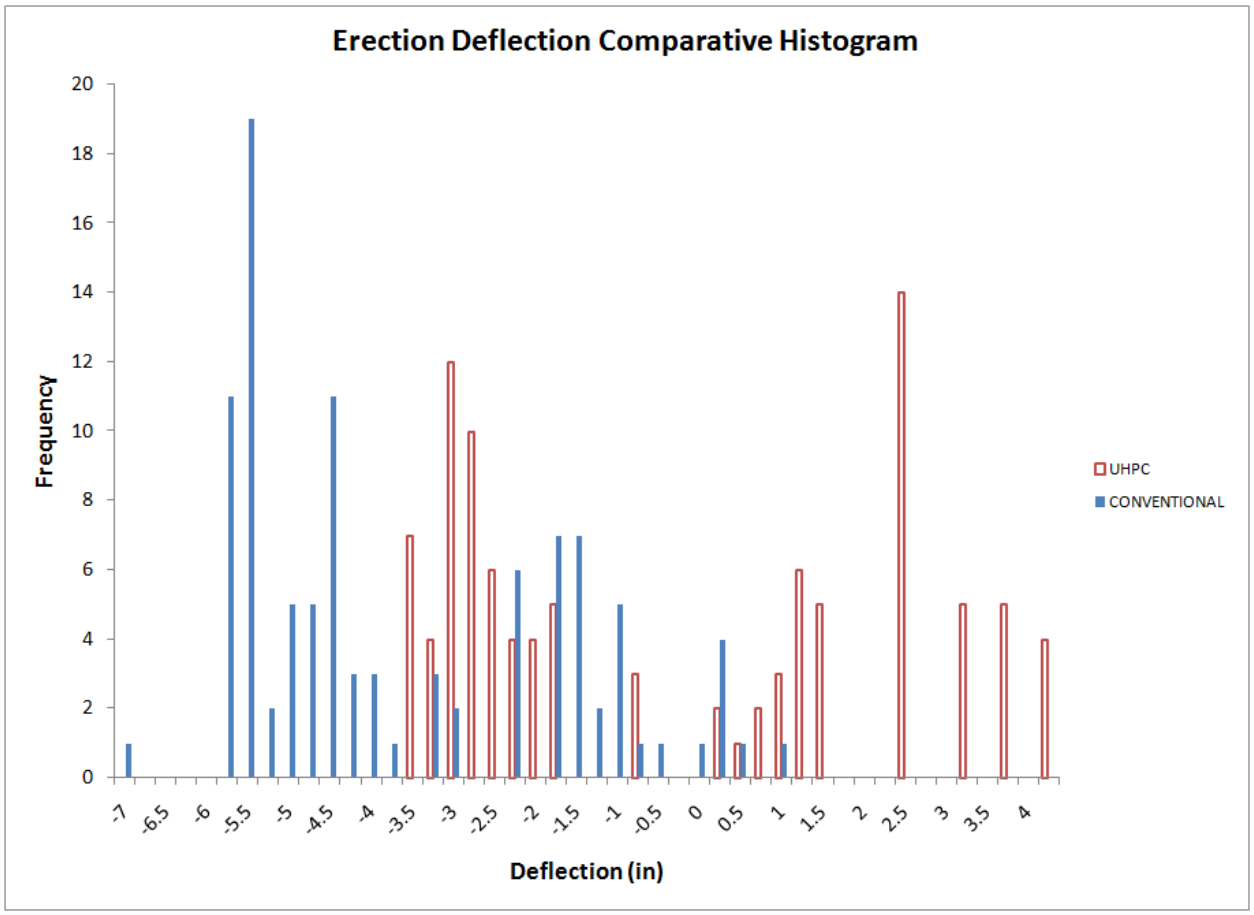

Figure 75. Chart. The deflections at the time of erection are due to prestressing forces and self weight.

The addition of the deck stiffened the bridge structure and increased dead loads. The deck requires the calculation of the transformed section moment of inertia. The additional deck concrete is closer to the conventional girders' concrete and thus has a larger effect on the transformed section. The larger relative deck contribution to the moment of inertia caused the conventional bridges to be more stiff than their UHPC counterparts (Figure 76).

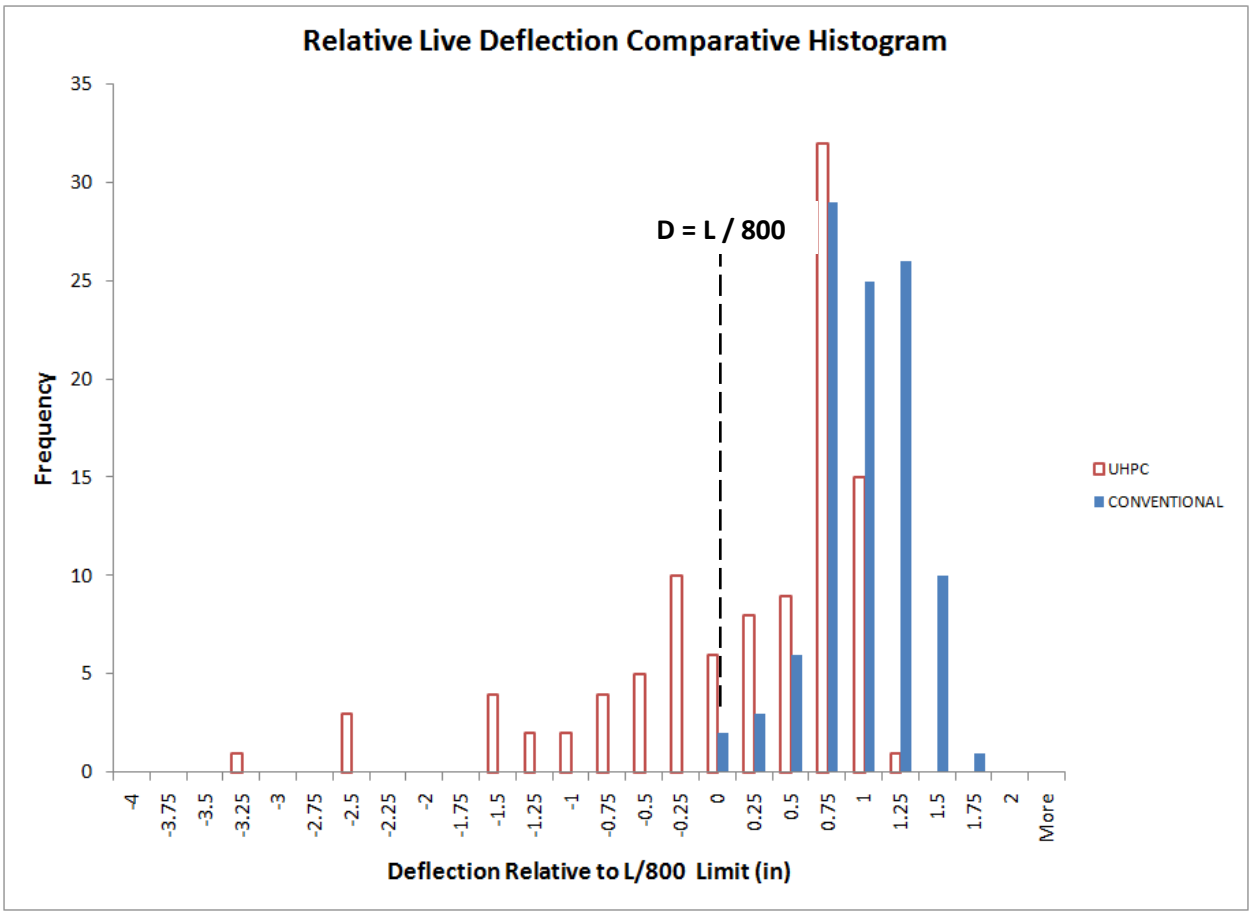

Figure 76. Chart. The comparative histogram shows the conventional bridges are stiffer for live loads.

The deflection plotted in this case is relative to the limit of bridge length divided by 800. Positive values of the difference between the limit and the deflection calculated mean the bridge satisfied the limit. All of the conventional bridges satisfied this requirement with deflections on the conservative side of the limit by 0.85 in. on average. UHPC bridges were only conservative by 0.04 in. on average. Of the 102 bridges 65 of the UHPC solutions satisfied the deflection limit.

Results Summary

The investigations performed started with general girder behavior and ended with full bridge optimizations. Surveys showed general procedures were required instead of a single shape. Sensitivity analysis identified the impacts of altering girder geometry. Optimization og girder section shapes resulted in several trends. Top flange width and web width were the most

dramatic alterations to shapes. The reduction in shape area was not sufficient to offset the material costs preventing the direct replacement of girders. The difficulties presented by changing girder geometries were identified through on site surveys. A general UHPC section proposal was investigated through full bridge optimizations. The proposed section drew on the results of the direct girder optimization and the site visitations. The proposed methodology recommends utilizing a girder shape created from existing formwork but without a top flange. The optimization of the full bridge systems showed that this methodology was cost competitive and more economical for span lengths greater than or equal to 90 feet. Secondary investigations were done into UHPC material models for cracking moment, the effects of UHPC material costs and of discrepancies resulting from the optimization procedures.

CHAPTER 5 Conclusions and Recommendations

The investigation performed had the goal of developing a cost competitive way to utilize UHPC girders in highway bridge designs. The strength and durability of UHPC warrant its use, but its high initial cost has made it an unattractive option even though the predicted total costs over the lifespan of a structure are predicted to be much lower. The solution is to provide a UHPC configuration with lower initial costs than a conventional solution.

Conclusions

Several phases of the investigation were required to develop a lower cost UHPC solution. The first phase attempted to create lower costs bridges through direct girder replacement. One for one replacement of girders did not realize the required cost savings so a second attempt was made to develop a general configuration paradigm using optimizations of full bridges. This investigation showed that UHPC can be used in highway bridges longer than 90 ft. The cost savings of the UHPC configuration is due to a smaller number of shallower girders with more prestressing strands per girder. The relationship between the conventional solutions and the UHPC solutions to the optimization were generalized to develop a formulation as a design guide addendum.

The direct girder replacement phase consisted of several components that resulted in a proposed UHPC girder configuration. A survey of industry members and state officials showed that bulb-tee girders are the most widely used prestressed girder shapes. Bulb-tee girders, however, are not uniform and vary in dimensions from state to state. This array of shapes required the development of a generalized girder alteration procedure that was feasible with existing forms and applicable to the wide array of shapes. The development of this general procedure was attempted through an optimization of shape geometry to create UHPC girders that could directly replace their conventional counterparts in a bridge design.

Sensitivity analysis was used to identify the relationships between elements of girder geometry and the performance of shapes. Moment capacity was most sensitive to slab and top flange width changes. Shear capacity was sensitive only to web width modifications.

The optimized shapes had modified flange and web geometries to reduce cross sectional area without impacting strength. The cost savings through area reduction required a UHPC to conventional concrete cost ratio of 1.61 to make this scheme feasible. This ratio is much lower than actual material cost ratios. Other complications with the stresses in the optimized girders made this scheme infeasible.

The first phase resulted in the identification of the girder geometry elements most highly correlated to the benchmarks of girder performance. Stable length reduction was most heavily correlated to the bottom flange dimension changes. The reduction of the top flange size had the highest correlation to losses in the major axis moment of inertia and section moment capacity.

The field visit survey's of girder production facilities and time spent working with UHPC in the manufacturing of panels presented some obvious deficiencies in the procedures for the reduction of shape area. Alterations to the girder forms would be expensive because new form soffit pans would be required. Using block outs in the forms would create small gaps that the highly fluid UHPC would leak out of, ruining product finishes. Finally the vertical shrinkage of UHPC as it sets would endanger slender flange or web elements that may crack.

The trends identified in the direct girder replacement phase and the caveats of girder production identified by field visits resulted in a simple proposed UHPC girder shape. The proposed shape configuration can be accomplished with any existing bulb-tee girder form. The shape is identical to its parent shape in web and bottom bulb dimensions but the top flange is entirely removed. The shape is not subject to the development of stress as vertical shrinkage occurs during curing. The shape does not require form modification and has a completely customizable depth.

Full bridge optimizations were conducted using conventional concrete and girder shapes. The shapes were modified to the proposed UHPC shape and the configurations optimized again to determine if the UHPC shape could be used in a cost competitive configuration. The optimizations were conducted using seven shape families from representative states. The optimizations were performed for three bridge widths ranging from two to four lanes and five

bridge lengths ranging from 50 to 130 ft. The UHPC bridge configurations were the lower cost solution in those bridges whose length was 90 ft and above. This performance was repeated across all shapes and bridge widths. Forty-five percent of the UHPC configurations would retain the cost savings over the conventional configurations with a material to cost ratio greater than 4, seventy-five percent would for a ratio greater than 3.

The limiting constraint on a majority of the conventional and UHPC optimizations was strength. The UHPC configurations performed better with an average strength deficiency of 0.21 where as conventional solutions had an average deficiency of 0.27. A secondary investigation showed that the addition of girders to the configuration satisfied the strength constraint in a majority of configurations. The strength deficiency could have been caused by several factors. The optimization is a mathematical process involving the minimization of continuous functions. The algorithms involved utilize function derivatives to determine search direction. The solutions found may have been trapped by local minimums.

Secondary investigations also showed that the UHPC configurations satisfied deflection limits. The magnitudes of the camber deflections were quite large with many exhibiting negative deflections which is counter to the expected deflection of prestressed girders. The optimization simplifying decision to harp as many strands as possible amplified the effect of the strands eccentricity at the girder ends. The resulting negative deformations overcame the positive deformations caused by the prestressing force eccentricity at midspan.

The full bridge optimization was successful in the development of a methodology for the use of UHPC in highway bridge systems that have a lower initial cost than conventional solutions. The methodology involves the creation of UHPC girders using a simple cross section modification of removing the top flange. The modified girder was identified through shape optimizations and influenced by practicality of girder production. Larger scale optimizations of full bridge systems showed that the proposed girder shape was effective for spans greater than 90 ft. A series of simple calculations was identified that can be used to determine a initial design using UHPC girders based on the initial design recommended in a conventional design guide.

Recommendations

The results of the full bridge optimization showed several trends in behavior. The cost of the UHPC bridges was lower than the conventional bridges because the UHPC bridges used fewer shallower girders with larger amounts of steel. Past 90 ft, where the cost savings was evident, the differences between the conventional bridge configurations and the UHPC configurations showed a pattern. The number of girders utilized in the UHPC bridges was on average two less than those in the conventional bridges. Further investigation showed this was related to the bridge width (Table 24).

Table 24. Comparison of No. Girders from Raw Solution Vectors

		Conventional	UHPC		
	Length (ft)	No.Girders	No.Girders	Difference	Average
2 Lanes	50	5.25	4.33	0.92	
	70	4.83	4.50	0.33	
	90	4.58	4.00	0.58	*
	110	4.42	4.42	0.00	*
	130	5.72	4.30	1.42	*
					0.67
3 Lanes	50	6.19	6.19	0.00	
	70	4.92	4.00	0.92	
	90	5.33	4.00	1.33	*
	110	6.67	4.92	1.75	*
	130	7.95	5.31	2.64	*
					1.91
4 Lanes	50	6.68	7.79	-1.12	
	70	6.67	5.00	1.67	
	90	5.92	5.00	0.92	*
	110	9.04	5.67	3.37	*
	130	10.21	6.22	3.99	*
NOTE: * = Included in Average					2.76

The UHPC girders were shallower than the girders required by the conventional solution. The UHPC girders were about 75 percent shallower than the conventional girders. The ratio of girder depths was nearly constant across all the bridges (Table 25).

Table 25. Comparison of Depths from Raw Solution Vectors

		Conventional	UHPC		
	Length (ft)	Depth (in)	Depth (in)	Ratio C/U	Average
2 Lanes	50	39.99	59.27	0.67	
	70	72.26	68.95	1.05	
	90	86.07	67.58	1.27	*
	110	86.22	61.77	1.40	*
	130	87.48	63.97	1.37	*
					1.35
3 Lanes	50	52.13	59.27	0.88	
	70	84.18	73.12	1.15	
	90	85.99	64.81	1.33	*
	110	86.56	61.77	1.40	*
	130	87.47	72.15	1.21	*
					1.31
4 Lanes	50	54.67	59.27	0.92	
	70	78.72	73.12	1.08	
	90	86.18	59.27	1.45	*
	110	85.22	61.77	1.38	*
	130	87.54	72.15	1.21	*
NOTE: * = Included in Average					1.35

Finally in both the conventional and the UHPC configurations the ratio between girder depth and the area of prestressing present remained nearly constant across the bridge lengths of 90, 110 and 130 ft. This ratio of ratios was around 2 for all the widths considered (Table 26).

Table 26. Comparison of Depths over Area of Steel Ratio from Raw Solution Vectors

		Conventional	UHPC		
	Length (ft)	Ratio (1/in)	Ratio (1/in)	Ratio C/U	Average
2 Lanes	50	14.88	35.54	0.42	
	70	24.86	25.04	0.99	
	90	29.61	17.72	1.67	*
	110	29.66	12.88	2.30	*
	130	27.86	12.98	2.15	*
					2.04
3 Lanes	50	20.12	35.54	0.57	
	70	28.96	21.92	1.32	
	90	29.58	14.03	2.11	*
	110	29.78	12.88	2.31	*
	130	27.86	14.64	1.90	*
					2.11
4 Lanes	50	20.34	35.54	0.57	
	70	27.08	21.92	1.24	
	90	29.64	11.85	2.50	*
	110	29.32	12.35	2.37	*
	130	27.88	14.64	1.90	*
NOTE: * = Included in Average					2.26

These trends were used to develop a formulaic procedure involving simple calculations to generate an initial design for a UHPC girder bridge from an initial conventional design as suggested by existing preliminary design tables (Figure 77).

1) Use Exisitng Design Aid to Select:

Number of Conventional Girders N_{GC}

Conventional Girder Depth D_C

Conventional Number of Strands S_C

2) Identify Number of 12 foot Lanes N_L

3) Compute Number of UHPC Girders N_{GU}

$$N_{GU} = N_{GC} - (N_L - 1)$$

4) Calculate Conventional Ratio ω_C

$$\omega_c = \frac{D_C}{S_C}$$

5) Calculate UHPC Girder Depth D_U

$$D_U = 0.75 * D_C$$

6) Calculate UHPC Girder Number of Strands S_U

$$S_U = \frac{2 D_U}{\omega_c}$$

Figure 77. Equation. Initial Design Modification Procedure

The procedure outlined was tried on the initial design suggested for a 40 ft wide three lane bridge with a 97 ft span using Virginia shapes. The Virginia design guide suggested a design utilizing six girders whose depth was 53 in.. Thirty-four 0.5 in. diameter strands were suggested resulting in a prestressing area of 5.202 in^2.

Applying the procedure to these initial design variables resulted in a UHPC configuration consisting of four 40 in. deep girders. The area of steel required is 7.956 in^2 or fifty 0.5 in. diameter strands.

These two bridge configurations were used as starting points for a full bridge design by hand. The results are based on a deck compressive strength of 4 ksi and the girder compressive strength of 8 ksi and 21 ksi for the conventional and UHPC girders respectively. The final designs were slightly different from the suggested start points (Table 27).

Table 27. Comparative Results of Detailed Bridge Design

	Conventional		UHPC-43	
	Suggested	Designed	Suggested	Designed
Depth	53	53	40	43
Girders	6	6	4	5
Strands	34	42	48	42
Cost		2.21E+04		1.87E+04

The cost was calculated using the same objective function used in the full bridge optimization procedure. Each design required iterative processes for strand selection to satisfy strength requirements and stress limits. The depth of the UHPC girder was increased slightly to account for the lower of number strands used in the design. The Virginia PCBT-53 has a strand pattern that accommodates only 46 strands in the first four rows. The depth was increased to allow for less than the 48 strands suggested to be used. The number of girders was increased so that similar decks could be used on both designs. The conventional deck had positive and negative reinforcement of No. 6 bars at 6 in. spacing. The UHPC bridge used the same deck thickness and deck concrete strength at eight in. and four ksi respectively. The larger transverse spacing required No. 7 bars at 6 in. for positive moments and No 8 bars at 6 in. for negative reinforcement. Other options would have been putting a thicker or stronger deck on the UHPC bridge but this would make cost comparisons more difficult because deck cost would have to be calculated relative to the values of the established cost function.

Further Research

The focus of this research had to be restricted in scope to the optimization on cost for flexural performance. The proposed shape meets these requirements. The lack of a top flange requires investigation into the behavior of the transverse deck moments over the girder and the behavior of the shear interface of deck and girder. Without a flange transverse negative moments over the

girders will increase. An investigation into shear transfer procedure for flangeless girders is proposed.

By embedding the top of the girder in the deck and transferring the shear through horizontal bars it is hypothesized that the interaction and extra steel will reduce negative moment concerns in the deck. The other advantage of this proposal is that shear connectors can be drilled and secured with epoxy. Placing the shear connectors after curing reduces girder production time by eliminating the placement of steel stirrups. The reduction in time spent placing steel may offset the additional curing time UHPC requires before strands may be released. An investigation is required into the feasibility of placing shear connectors after girder curing and their effects on the composite action and transverse deck moments.

A second proposal is an investigation into the arrangement of steel strand in the proposed section. In the traditional model prestressing steel is placed to balance dead load moments and strands are harped to alleviate stresses at the girder ends. The strength of UHPC allows for the use of much more prestressing force. It may be possible to impose only compressive stresses in the girder at transfer using additional top strands. Strands would not have to be harped reducing labor of construction. An investigation is required into the effect of changing the prestressing and strand conventions on the overall girder and bridge performance.

CHAPTER 6 Appendices

Appendix A: Industry Survey Summary

Figure 78

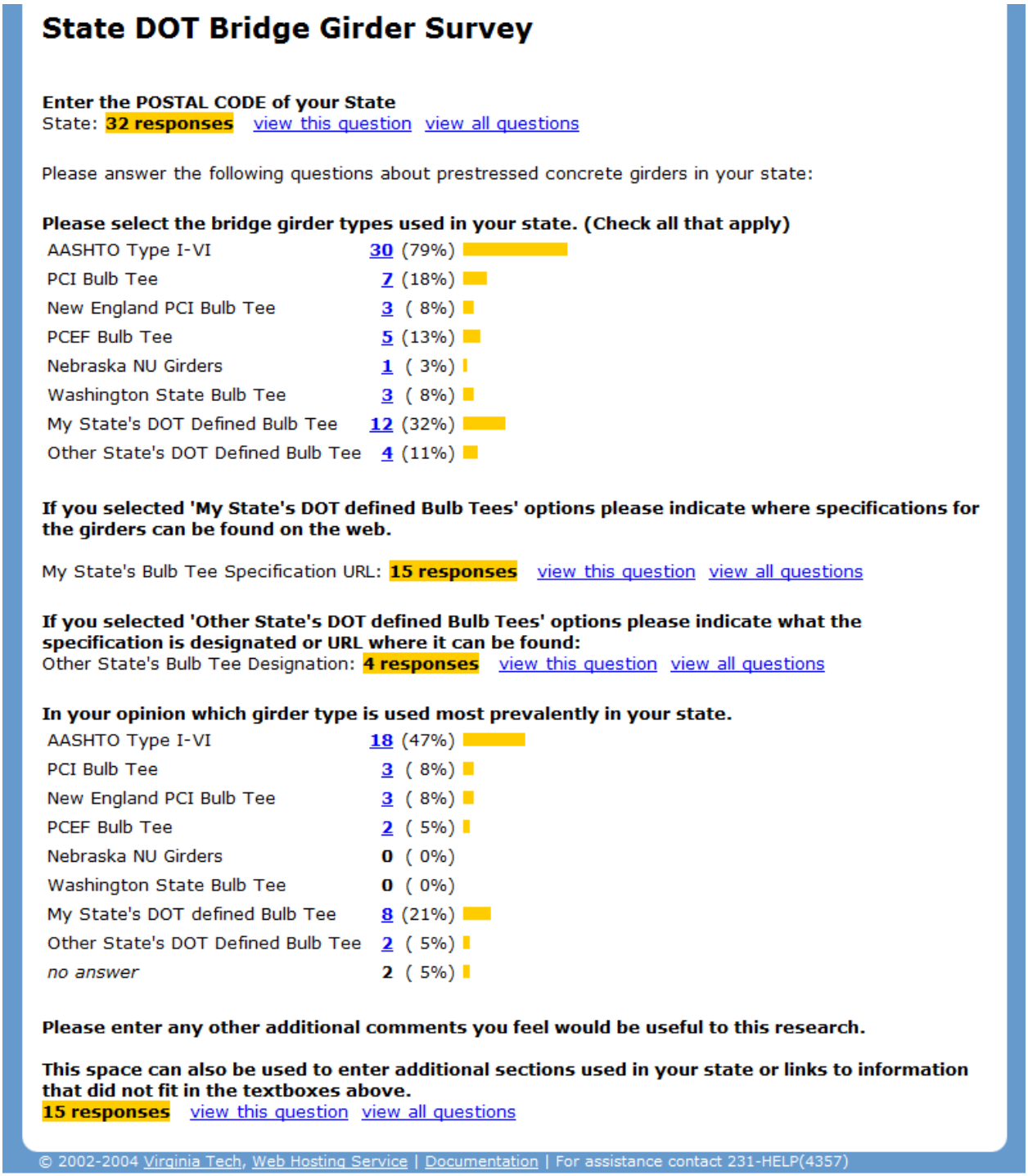

State DOT Bridge Girder Survey

Enter the POSTAL CODE of your State
State: **32 responses** view this question view all questions

Please answer the following questions about prestressed concrete girders in your state:

Please select the bridge girder types used in your state. (Check all that apply)

AASHTO Type I-VI	30 (79%)
PCI Bulb Tee	7 (18%)
New England PCI Bulb Tee	3 (8%)
PCEF Bulb Tee	5 (13%)
Nebraska NU Girders	1 (3%)
Washington State Bulb Tee	3 (8%)
My State's DOT Defined Bulb Tee	12 (32%)
Other State's DOT Defined Bulb Tee	4 (11%)

If you selected 'My State's DOT defined Bulb Tees' options please indicate where specifications for the girders can be found on the web.

My State's Bulb Tee Specification URL: **15 responses** view this question view all questions

If you selected 'Other State's DOT defined Bulb Tees' options please indicate what the specification is designated or URL where it can be found:
Other State's Bulb Tee Designation: **4 responses** view this question view all questions

In your opinion which girder type is used most prevalently in your state.

AASHTO Type I-VI	18 (47%)
PCI Bulb Tee	3 (8%)
New England PCI Bulb Tee	3 (8%)
PCEF Bulb Tee	2 (5%)
Nebraska NU Girders	0 (0%)
Washington State Bulb Tee	0 (0%)
My State's DOT defined Bulb Tee	8 (21%)
Other State's DOT Defined Bulb Tee	2 (5%)
no answer	2 (5%)

Please enter any other additional comments you feel would be useful to this research.

This space can also be used to enter additional sections used in your state or links to information that did not fit in the textboxes above.
15 responses view this question view all questions

Figure 78. Image. Summary of State Officials Survey Results

Appendix B: Direct Girder Replacement Optimization Results

Ten shape families were selected for direct optimization. The following Appendix presents 48 result plots of those optimizations. The shapes were previously listed in Table 6.

AASHTO I Girders

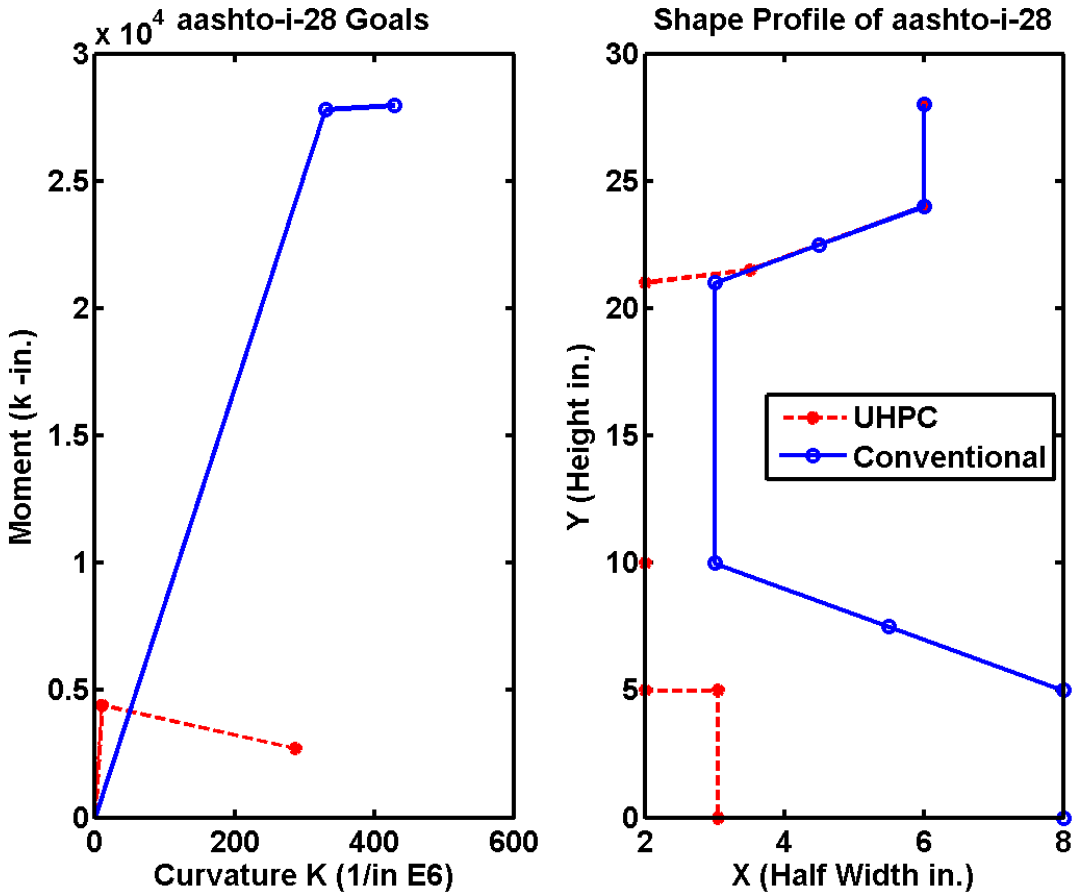

Figure 79. Graph. AASHTO I-28 Direct Replacement Optimization Results

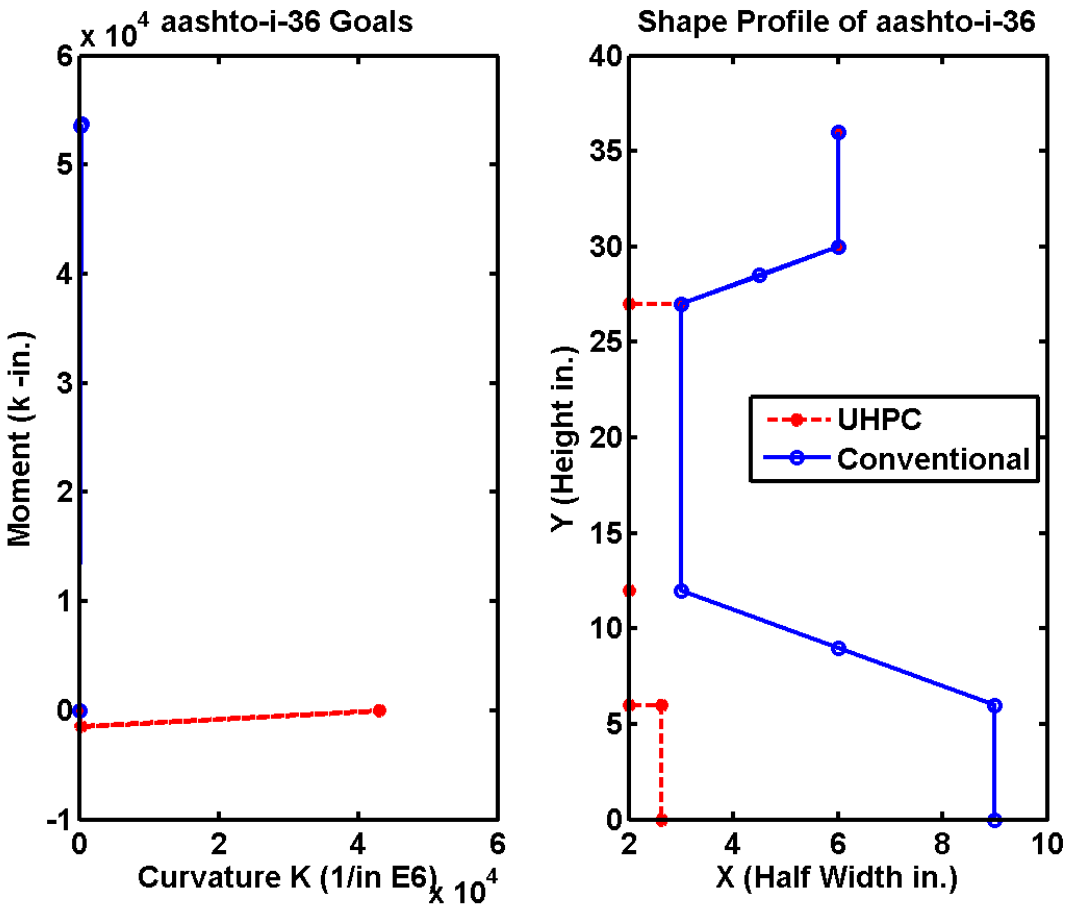

Figure 80. Graph. AASHTO I-36 Direct Replacement Optimization Results

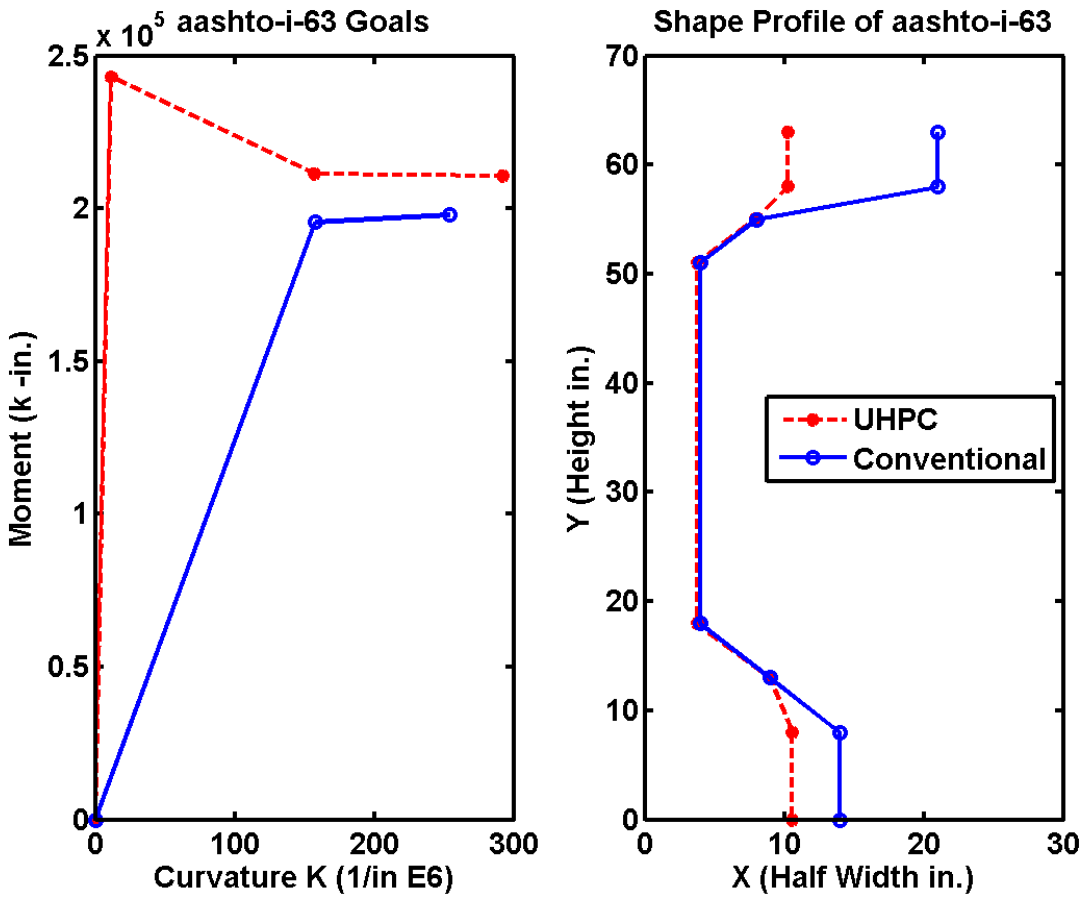

Figure 81. Graph. AASHTO I-63 Direct Replacement Optimization Results

Figure

82

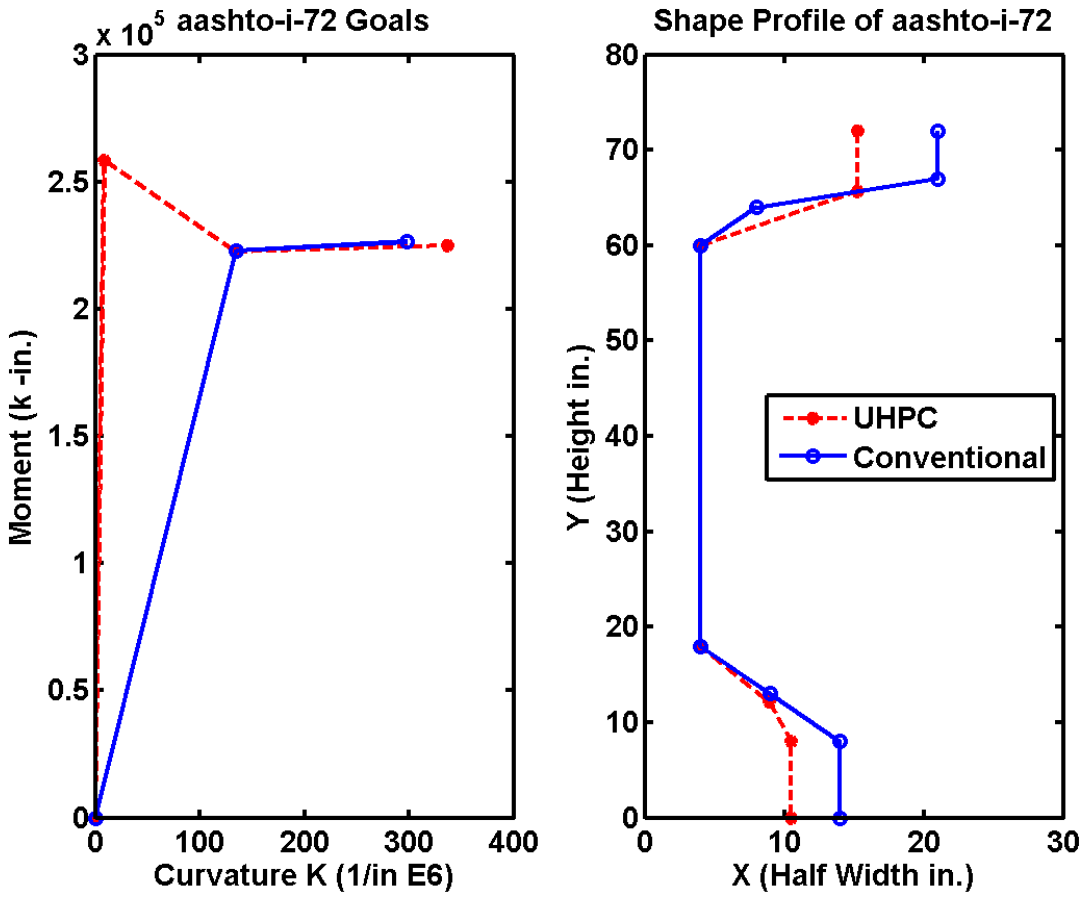

Figure 82. Graph. AASHTO I-72 Direct Replacement Optimization Results

Idaho Bulb Tee Girders

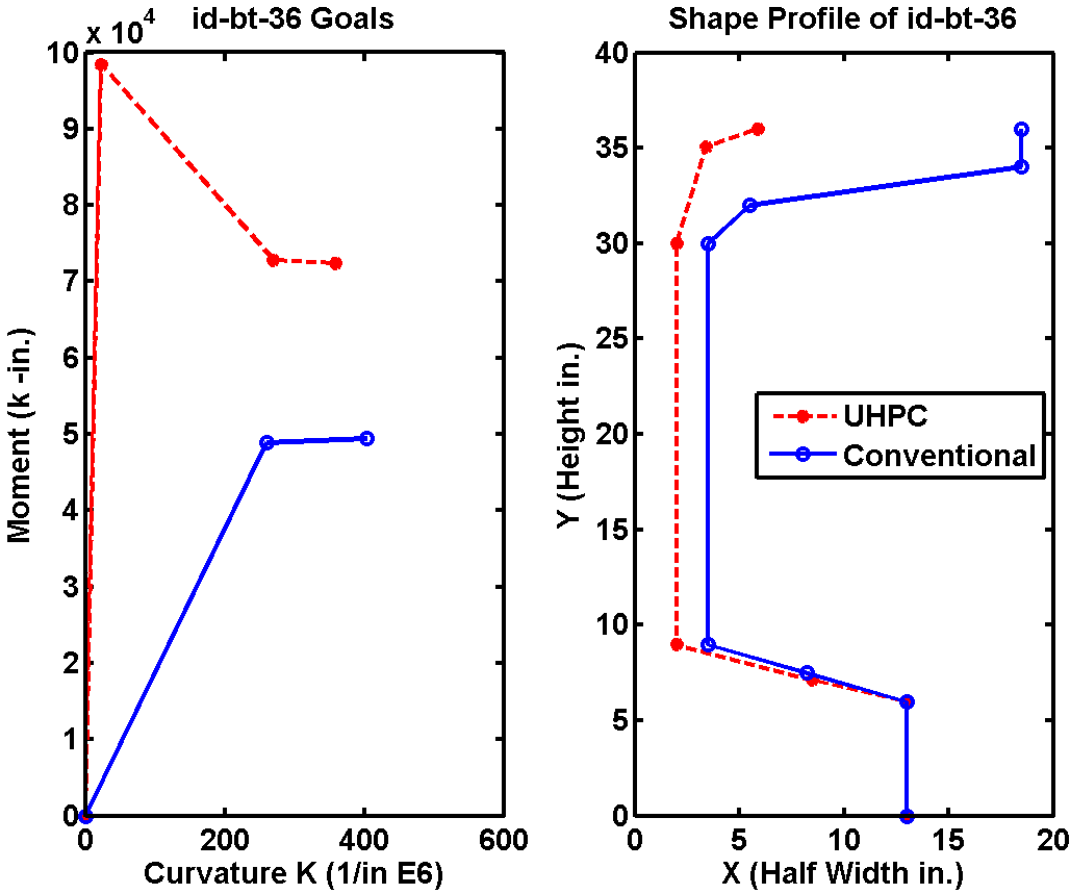

Figure 83. Graph. Idaho 36 in Bulb Tee Direct Replacement Optimization Results

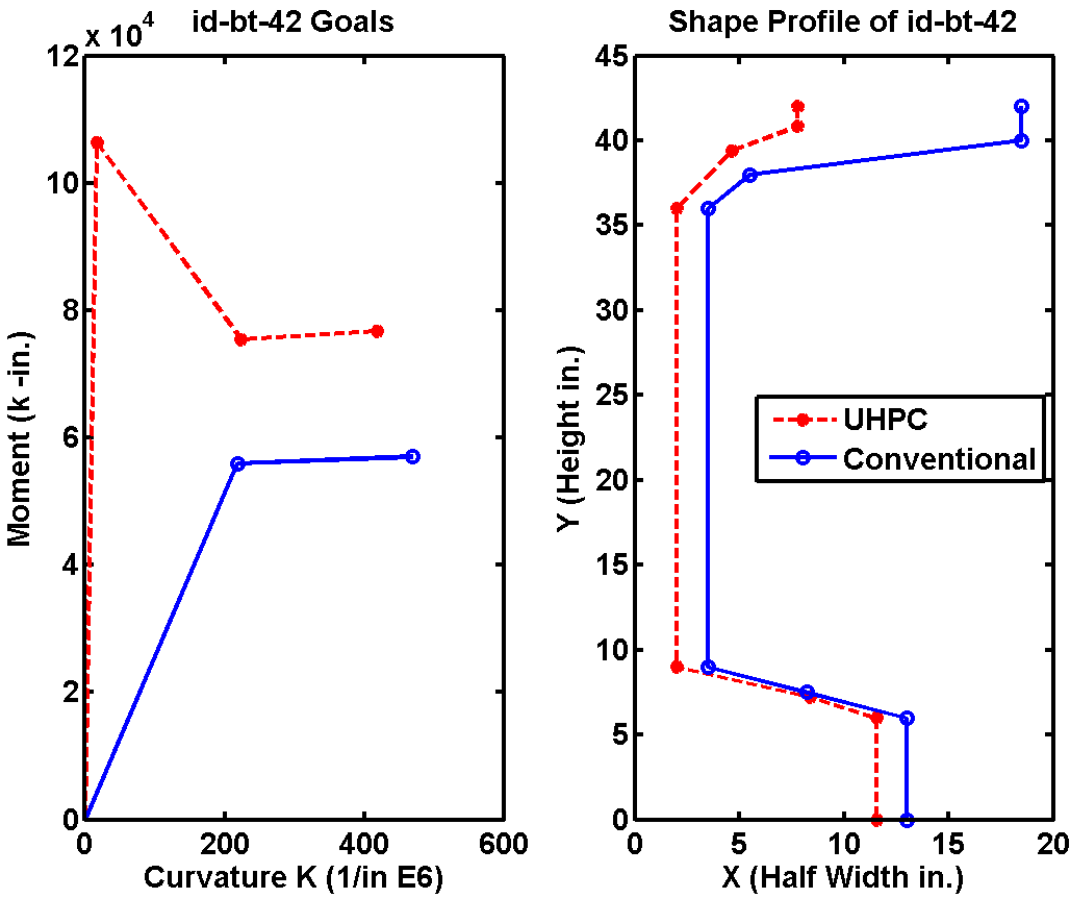

Figure 84. Graph. Idaho 42 in Bulb Tee Direct Replacement Optimization Results

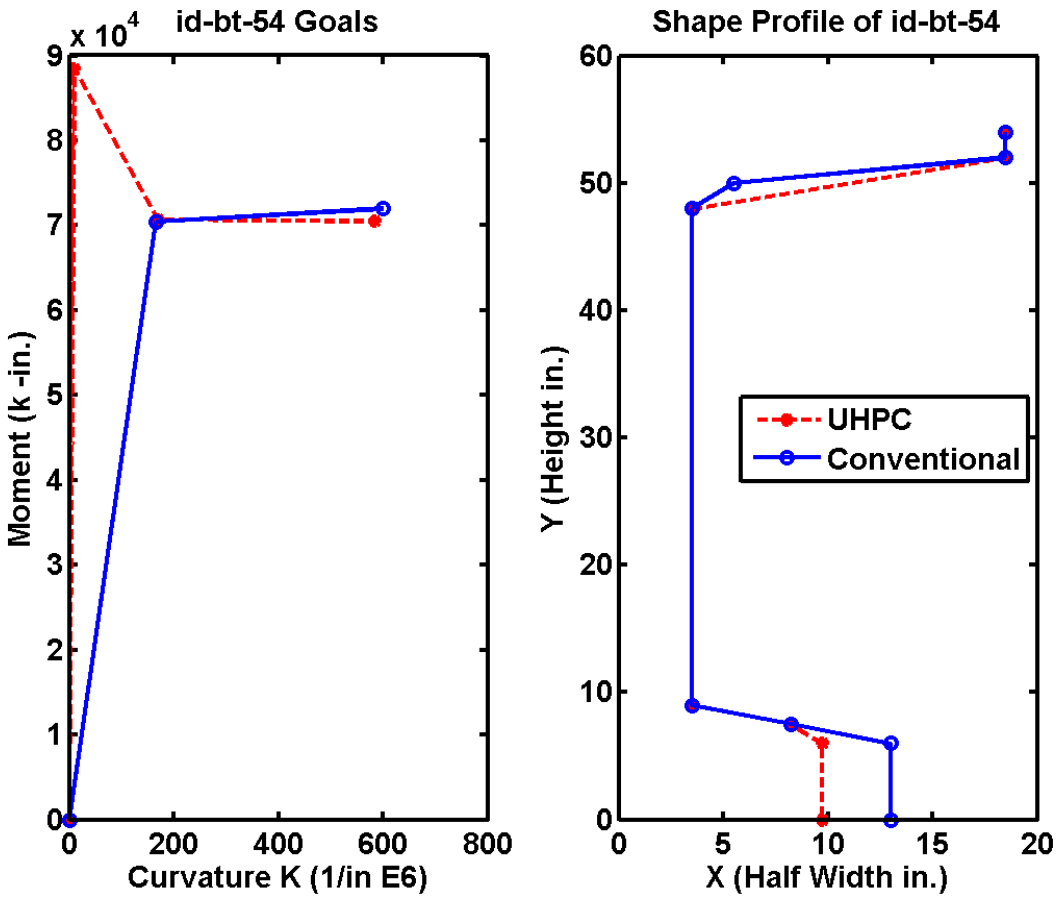

Figure 85. Graph. Idaho 54 in Bulb Tee Direct Replacement Optimization Results

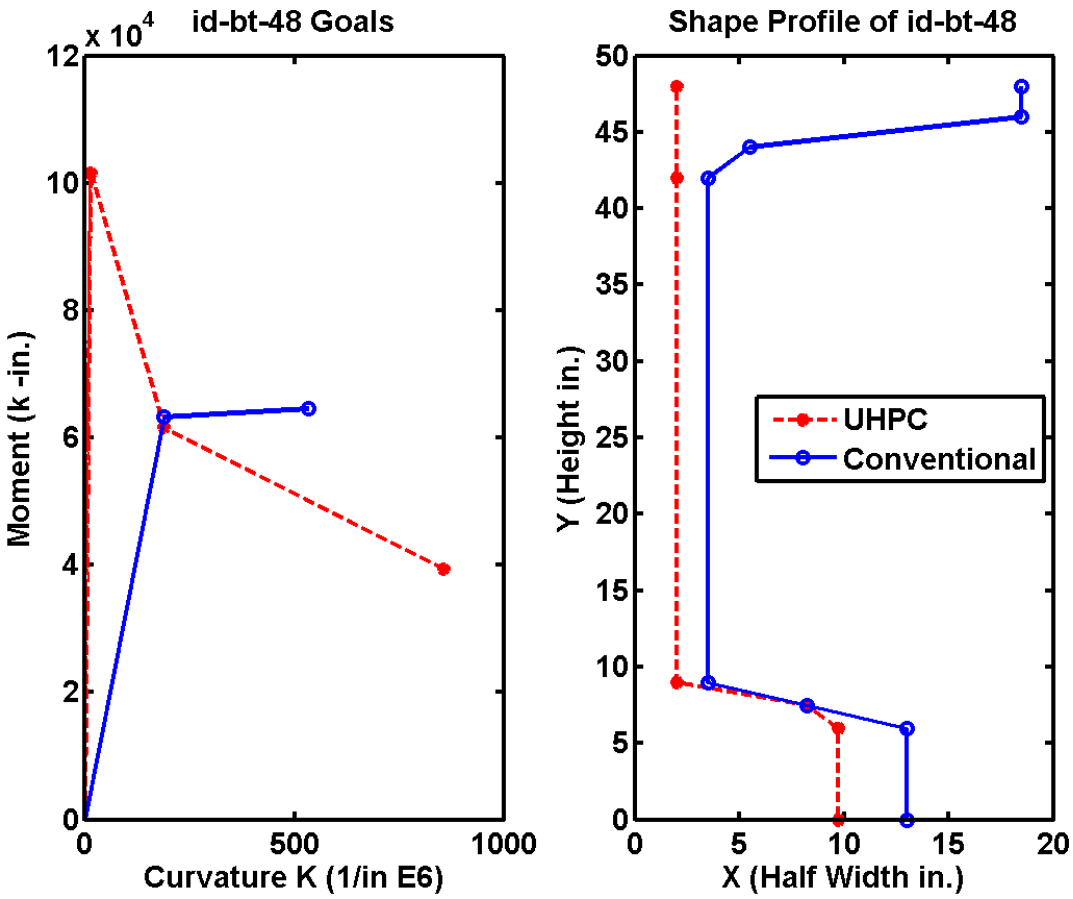

Figure 86. Graph. Idaho 48 in Bulb Tee Direct Replacement Optimization Results

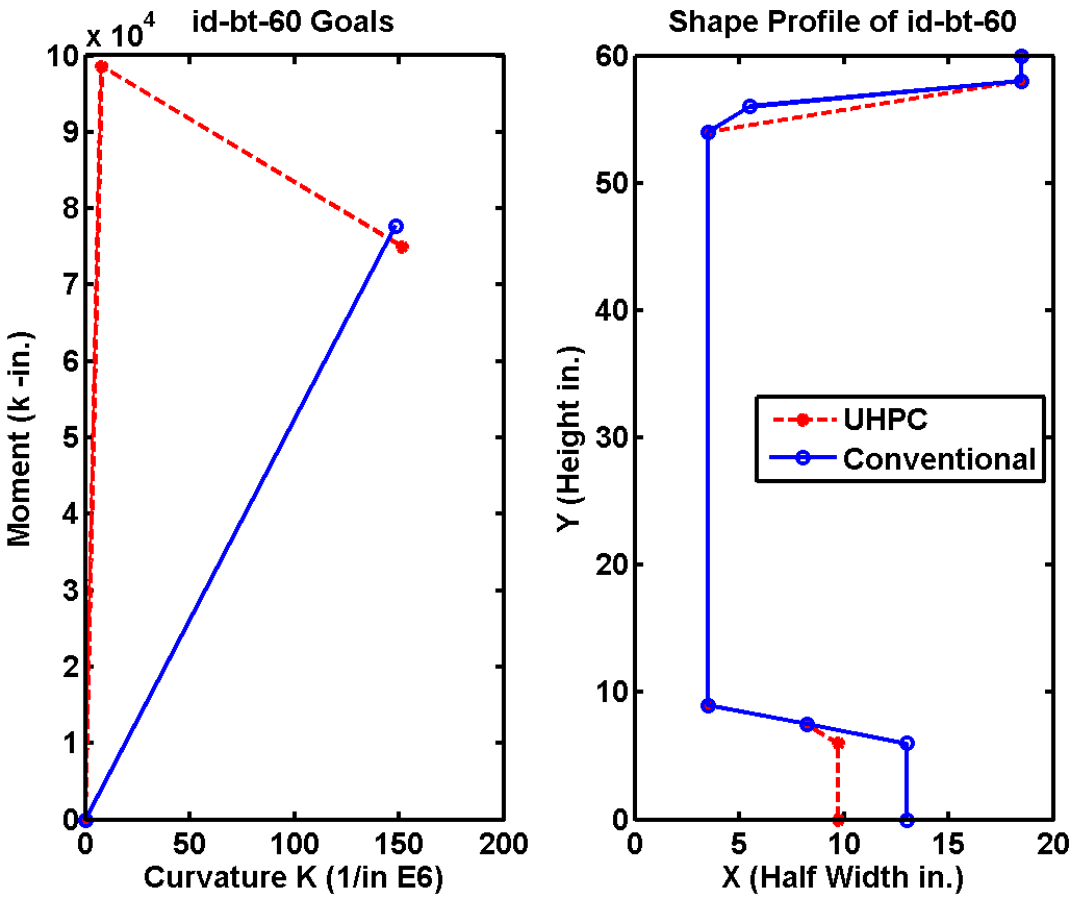

Figure 87. Graph. Idaho 60 in Bulb Tee Direct Replacement Optimization Results

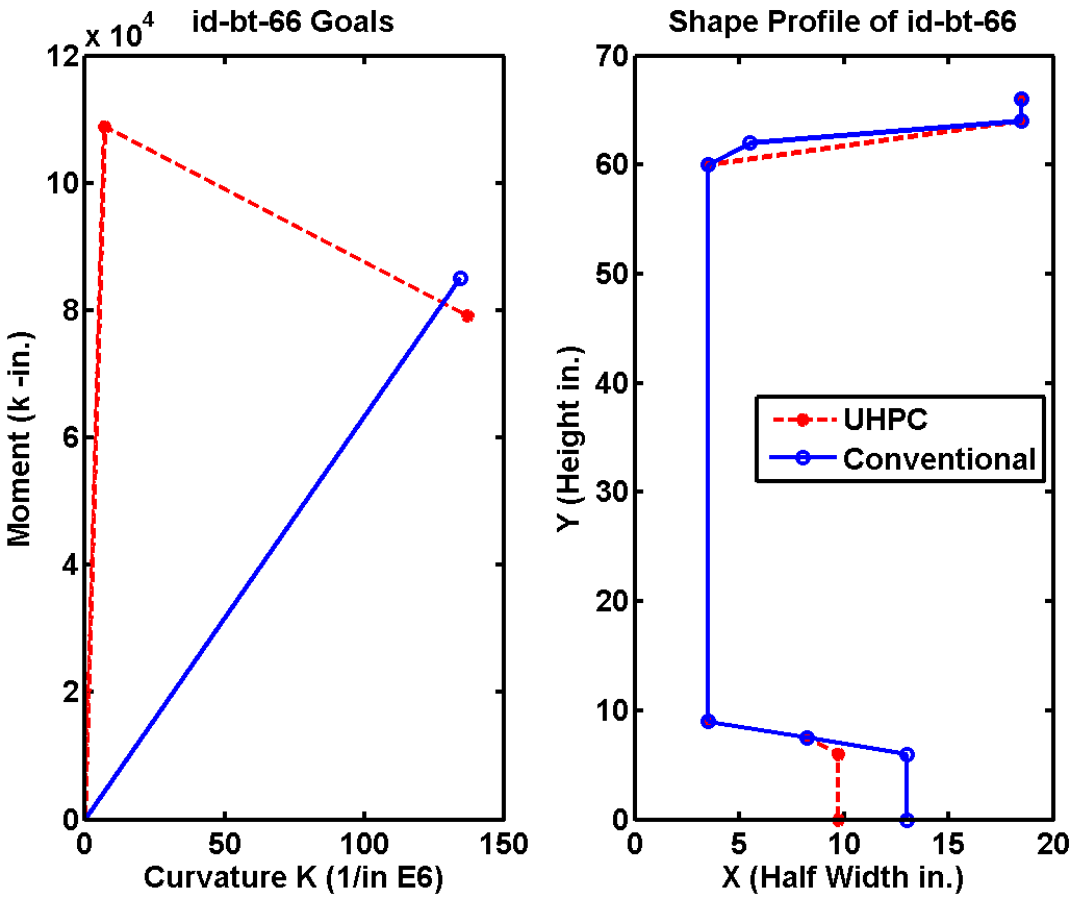

Figure 88. Graph. Idaho 66 in Bulb Tee Direct Replacement Optimization Results

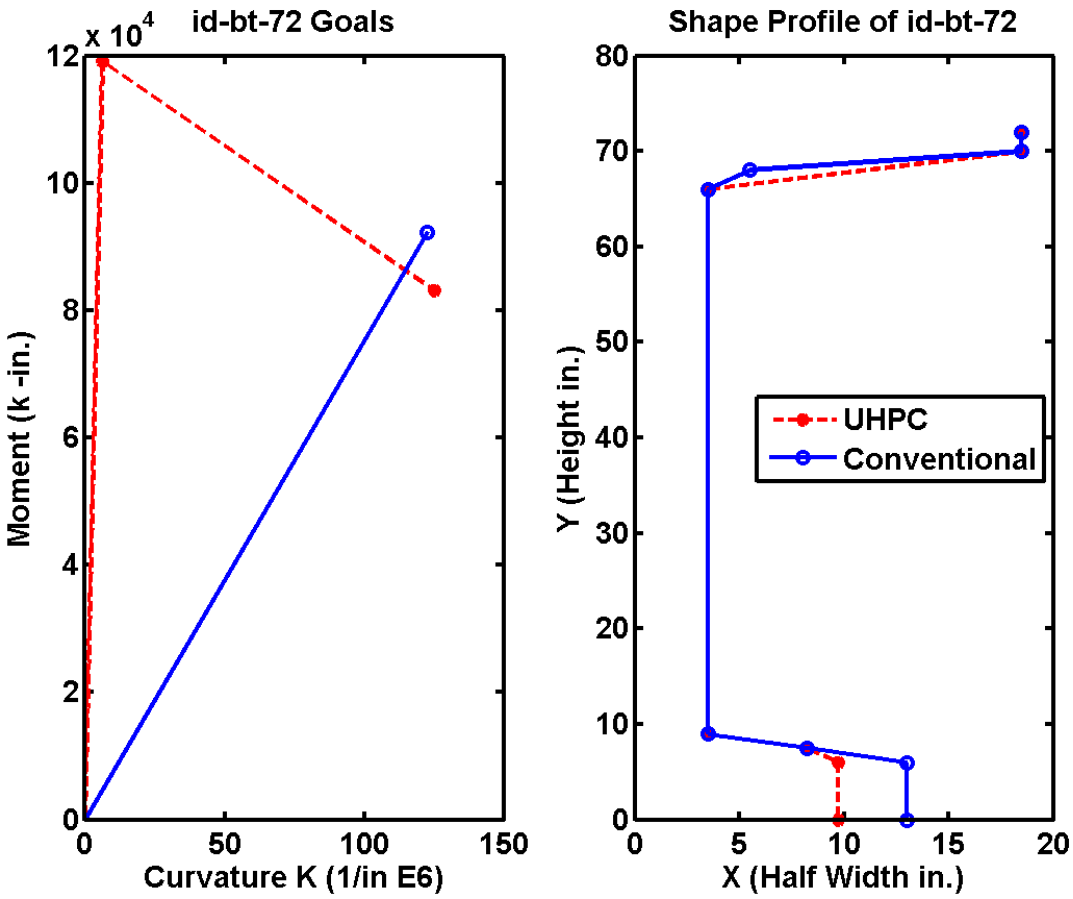

Figure 89. Graph. Idaho 72 in Bulb Tee Direct Replacement Optimization Results

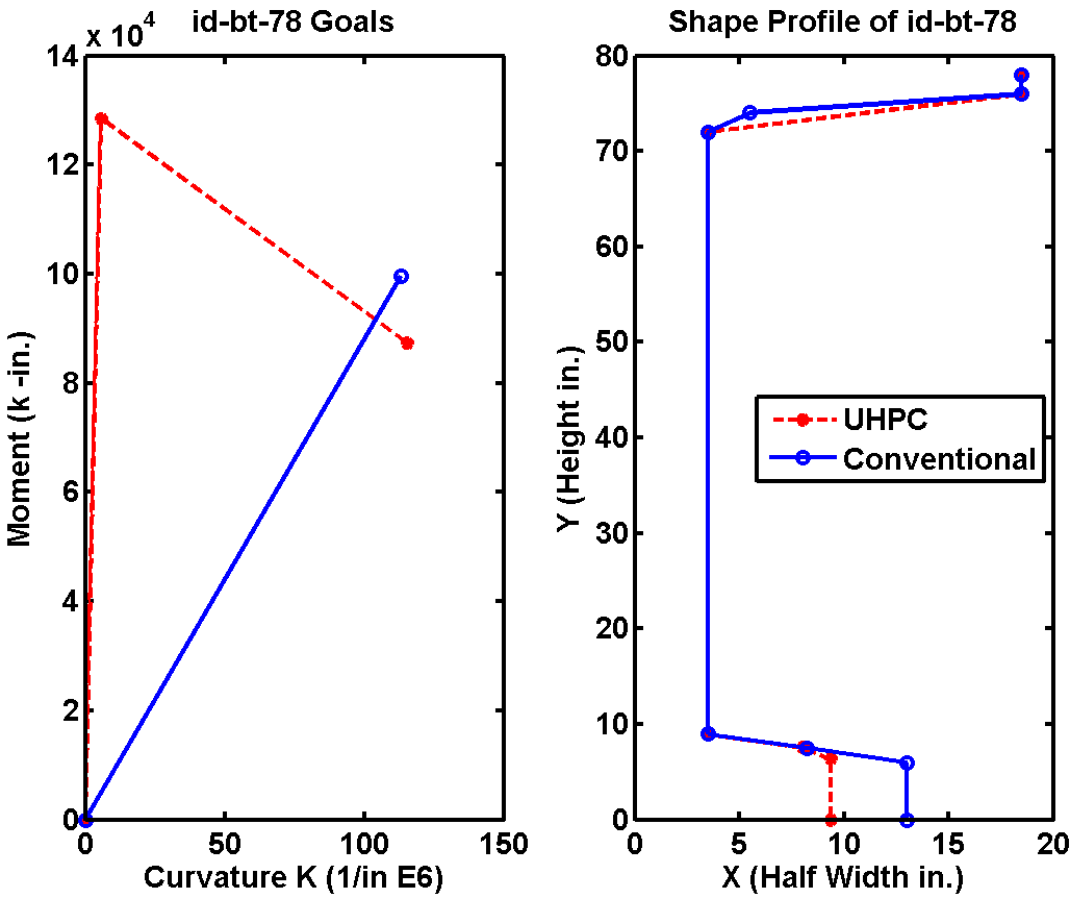

Figure 90. Graph. Idaho 78 in Bulb Tee Direct Replacement Optimization Results

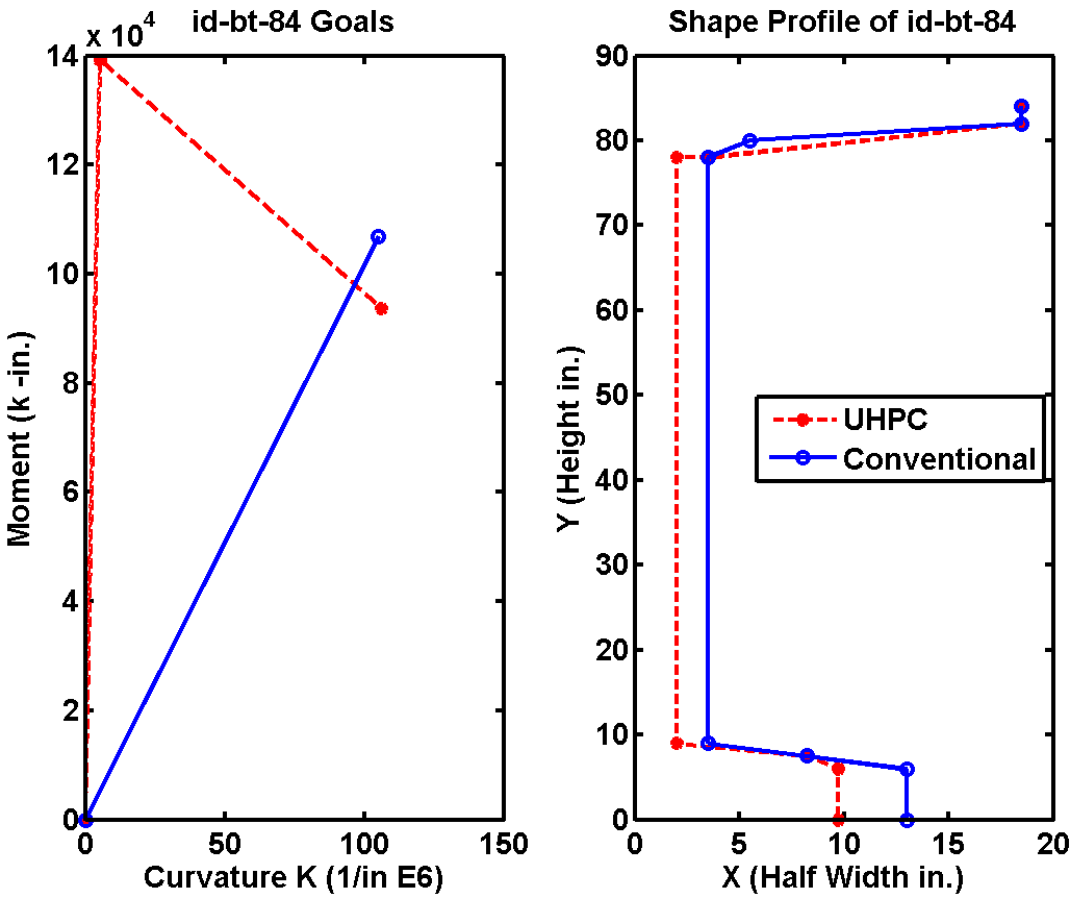

Figure 91. Graph. Idaho 84 in Bulb Tee Direct Replacement Optimization Results

Indiana Bulb Tee Girders

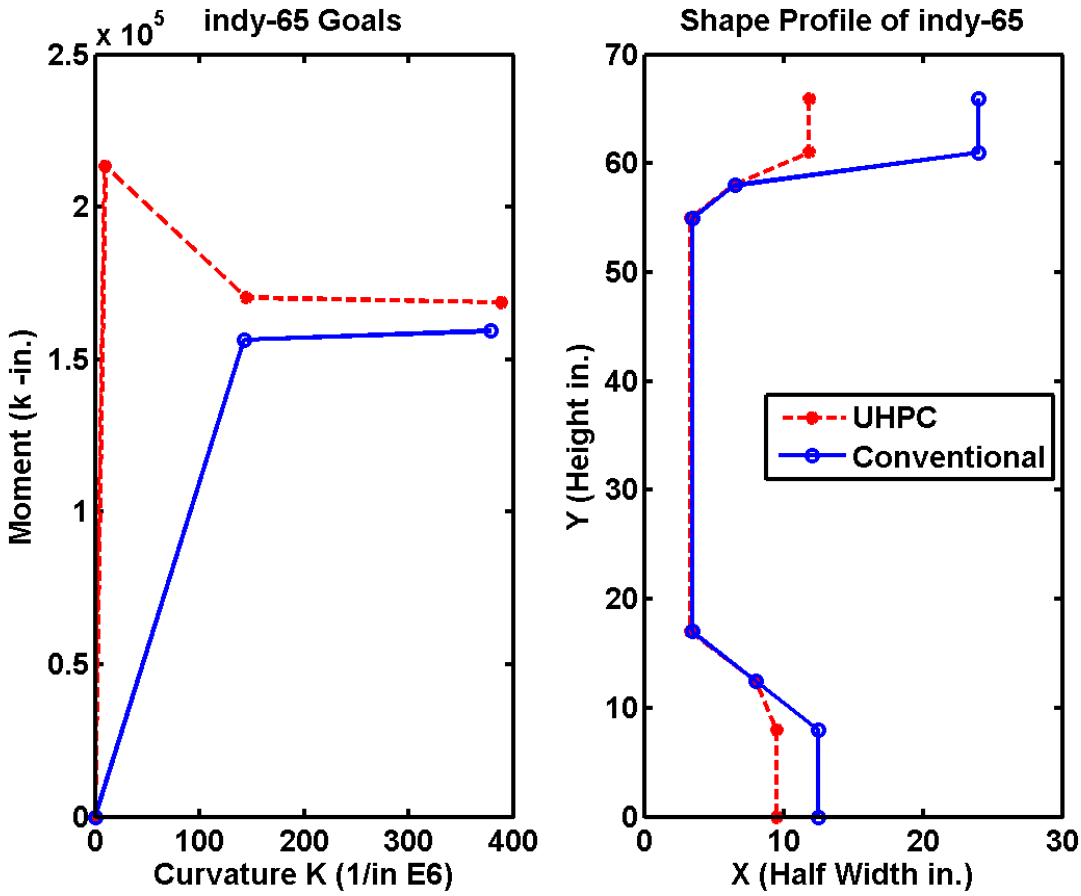

Figure 92. Graph. Indiana 65 in Bulb Tee Direct Replacement Optimization Results

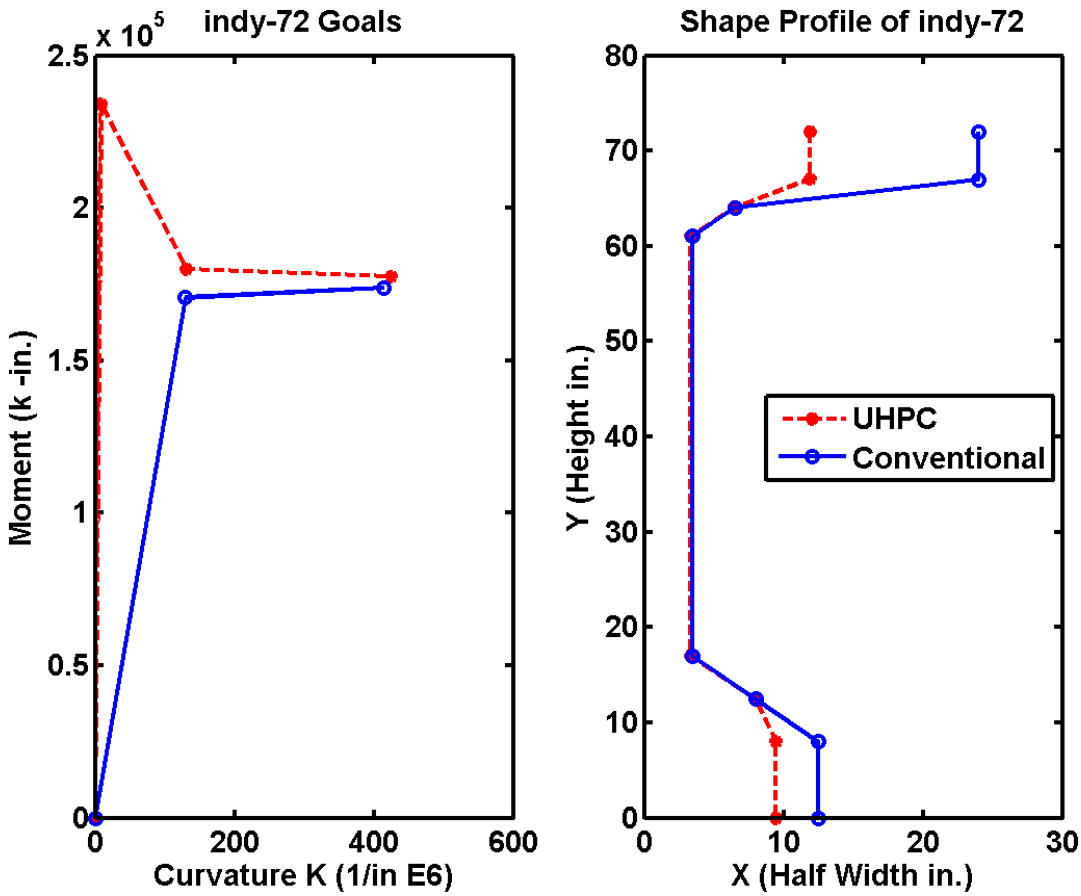

Figure 93. Graph. Indiana 72 in Bulb Tee Direct Replacement Optimization Results

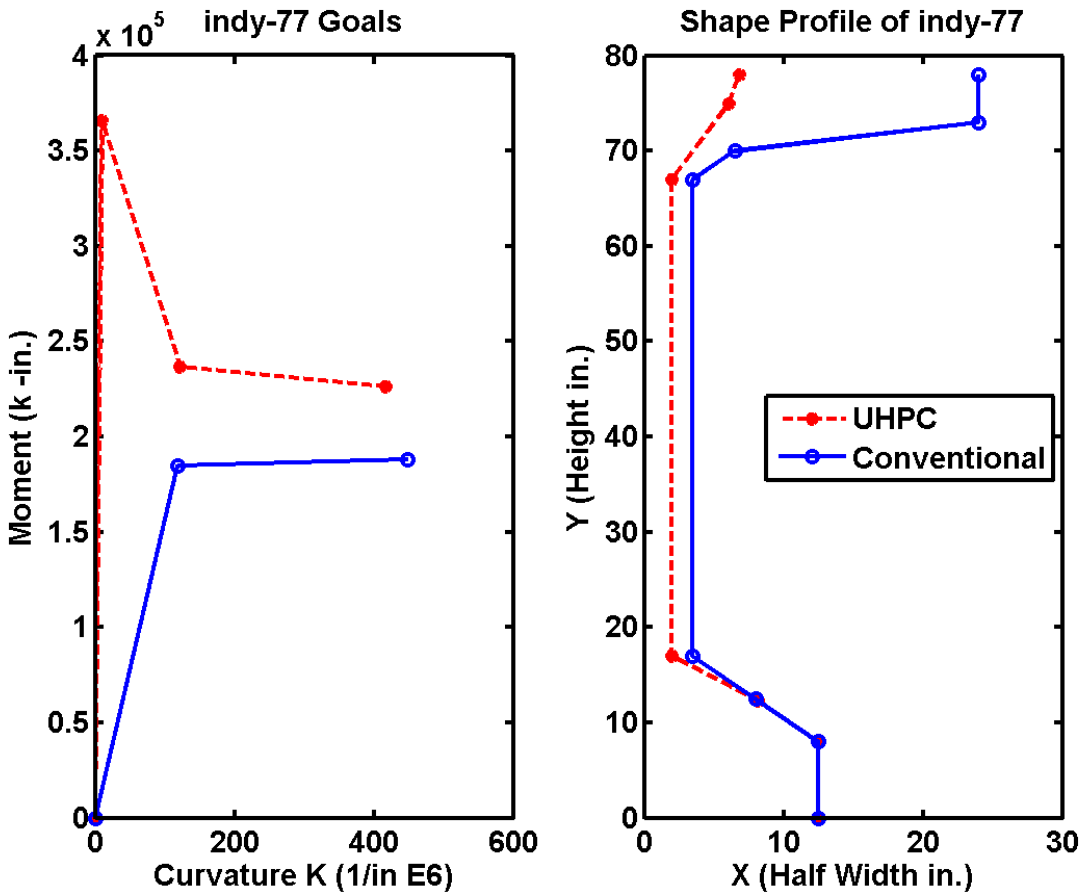

Figure 94. Graph. Indiana 77 in Bulb Tee Direct Replacement Optimization Results

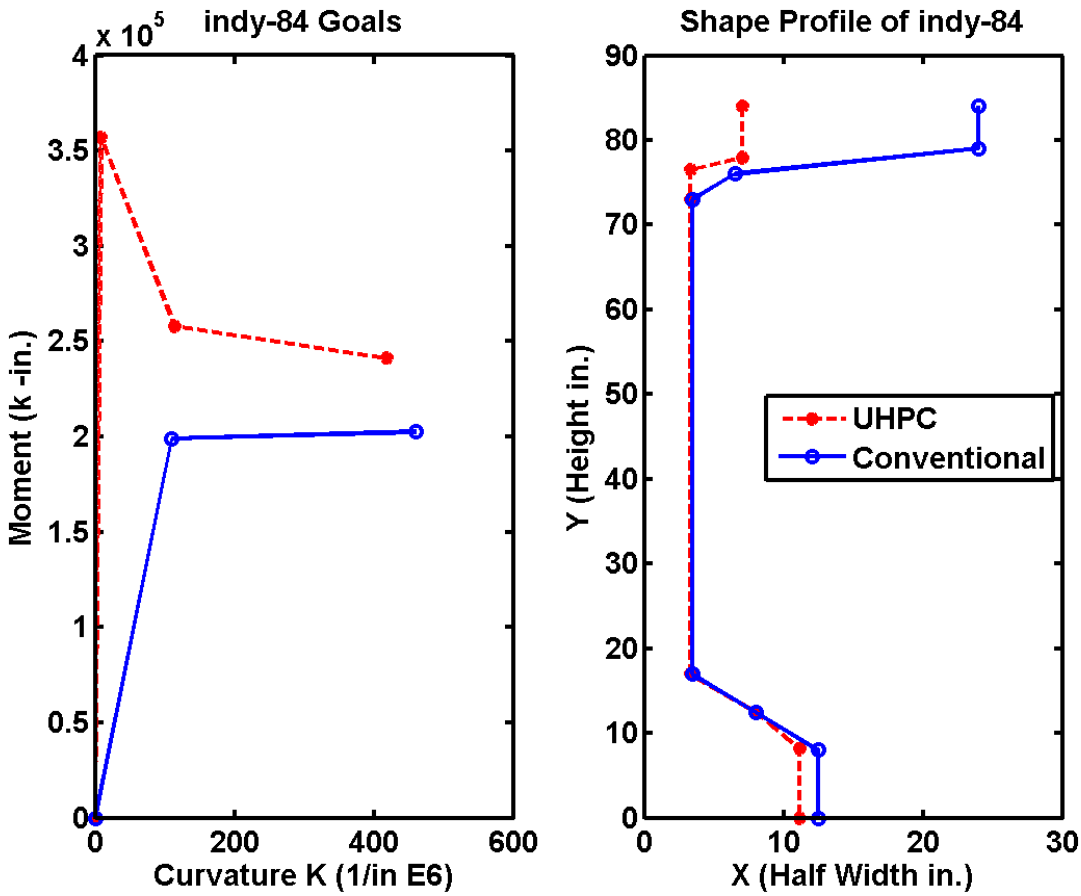

Figure 95. Graph. Indiana 84 in Bulb Tee Direct Replacement Optimization Results

New England Bulb Tee Girders

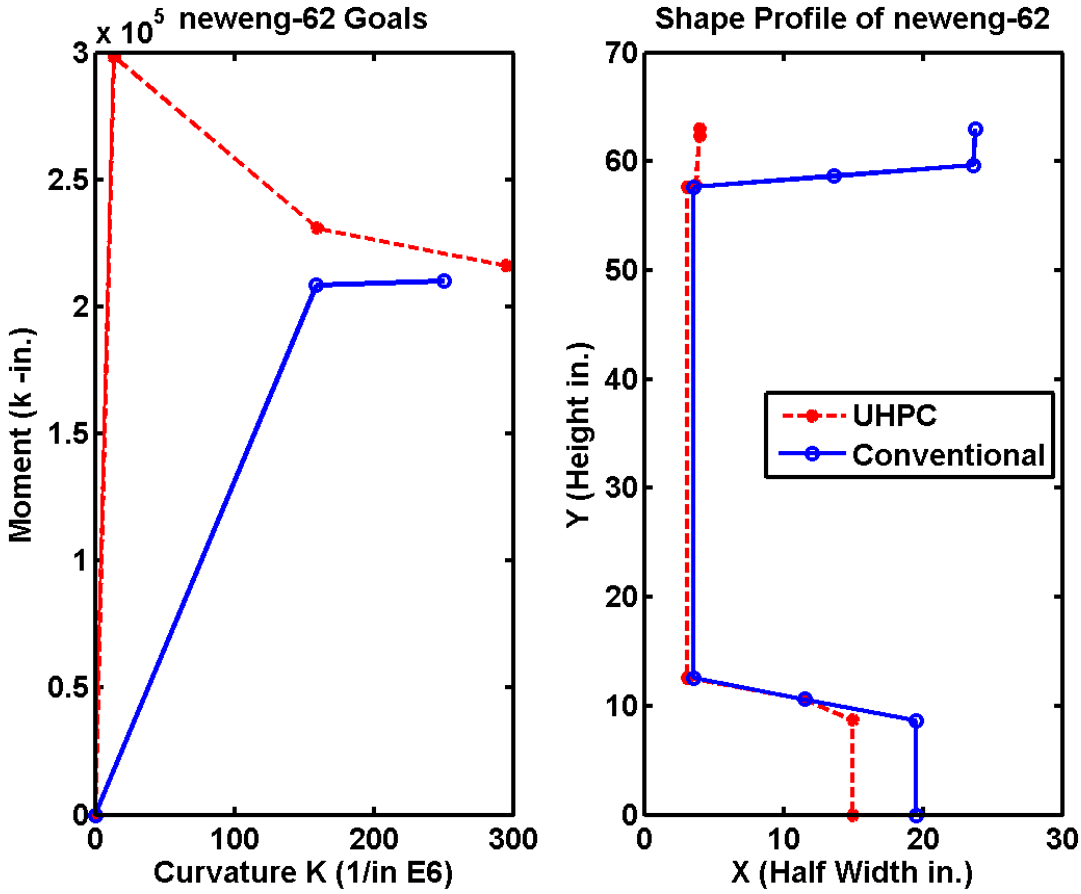

Figure 96. Graph. New England 62 in Bulb Tee Direct Replacement Optimization Results

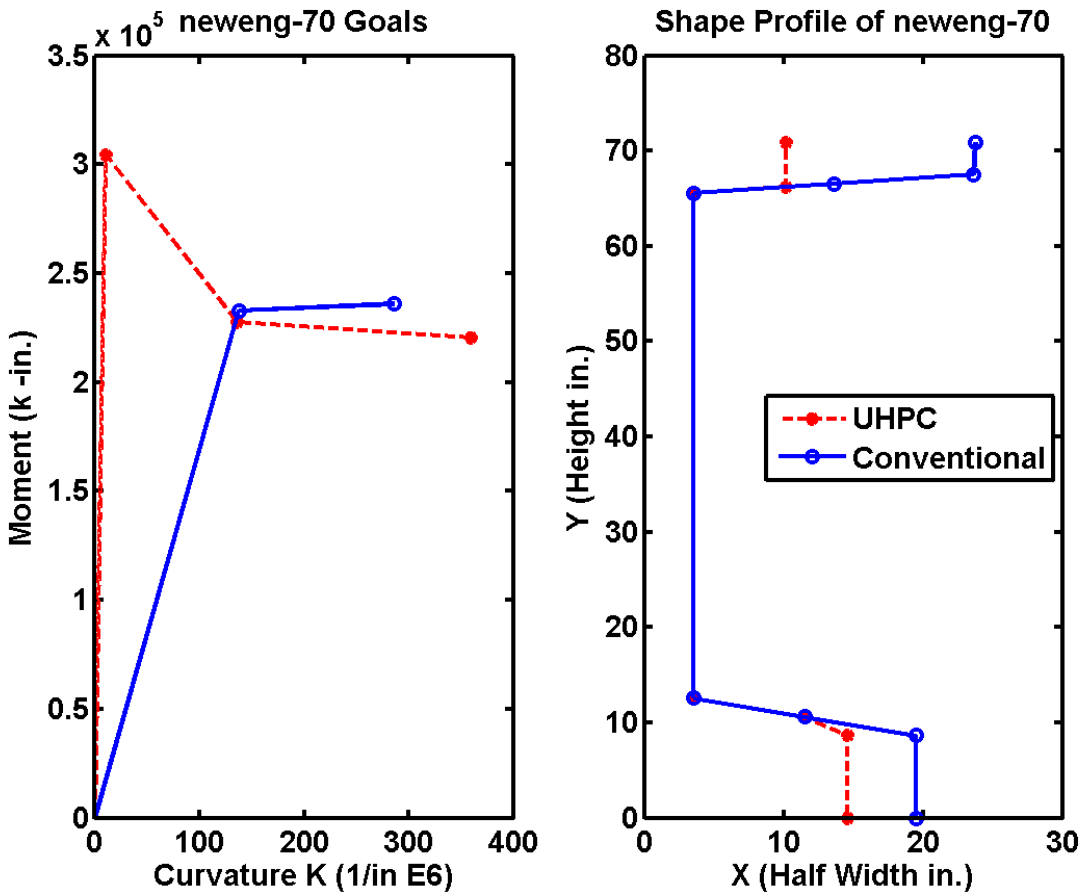

Figure 97. Graph. New England 70 in Bulb Tee Direct Replacement Optimization Results

Pennsylvania Bulb Tee Girders

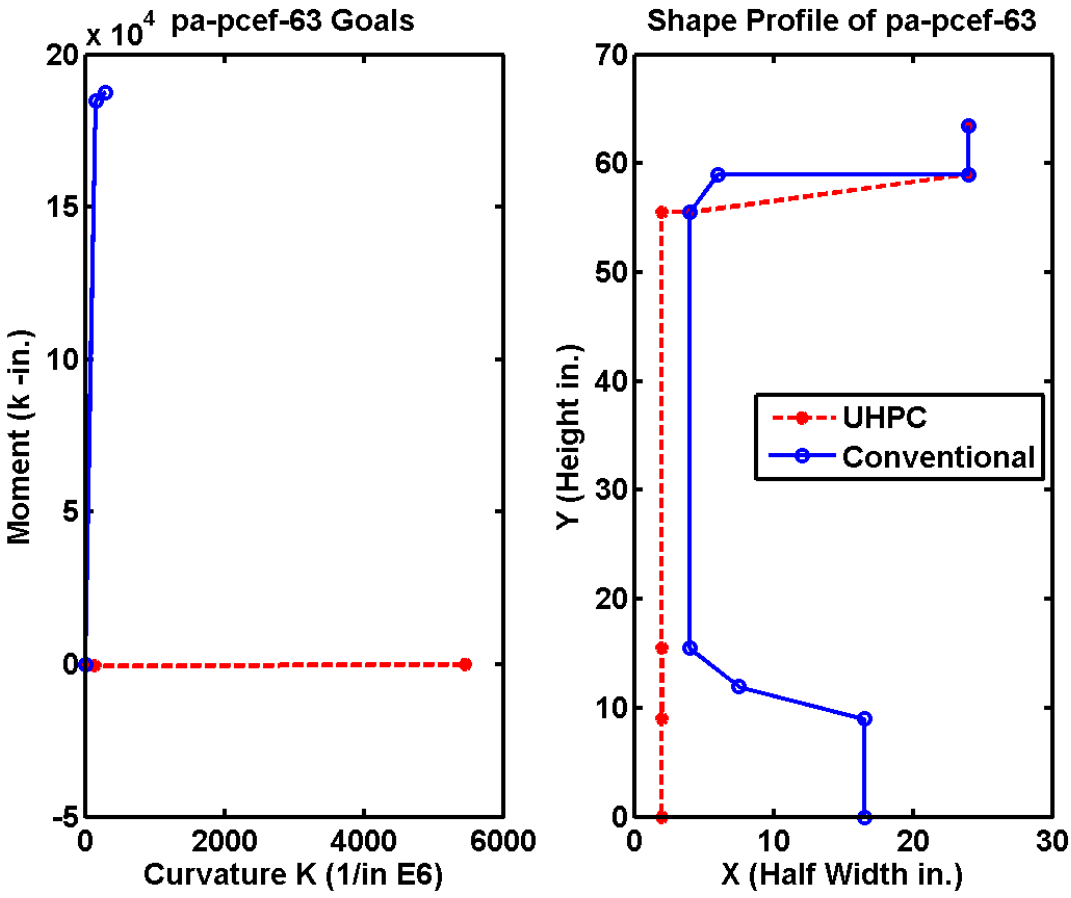

Figure 98. Graph. Pennsylvania 63 in Bulb Tee Direct Replacement Optimization Results

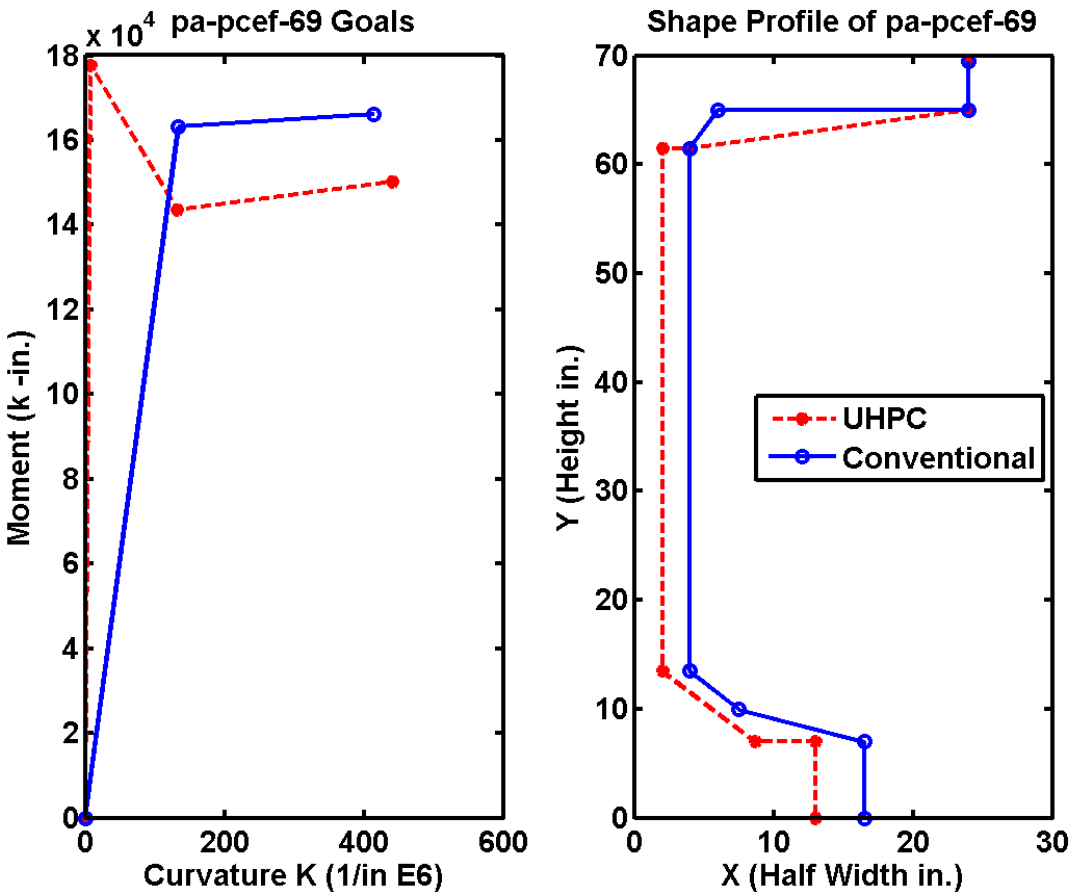

Figure 99. Graph. Pennsylvania 69 in Bulb Tee Direct Replacement Optimization Results

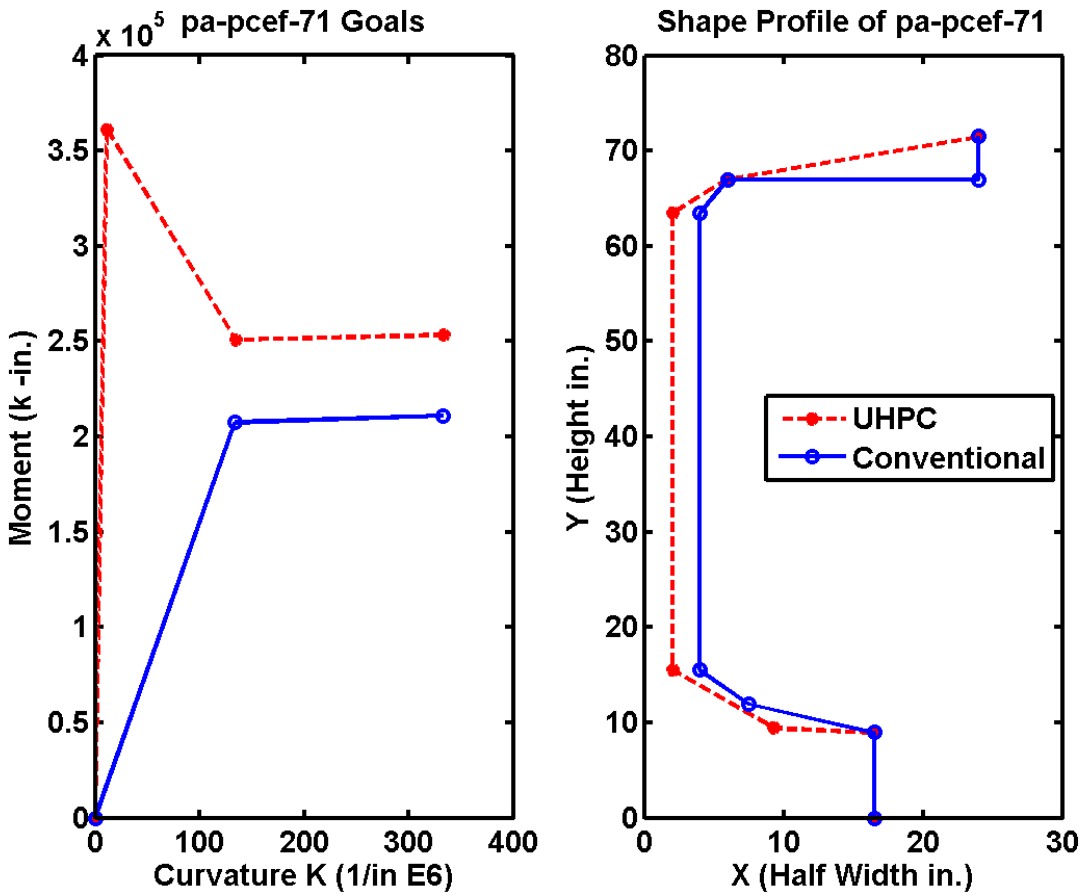

Figure 100. Graph. Pennsylvania 71 in Bulb Tee Direct Replacement Optimization Results

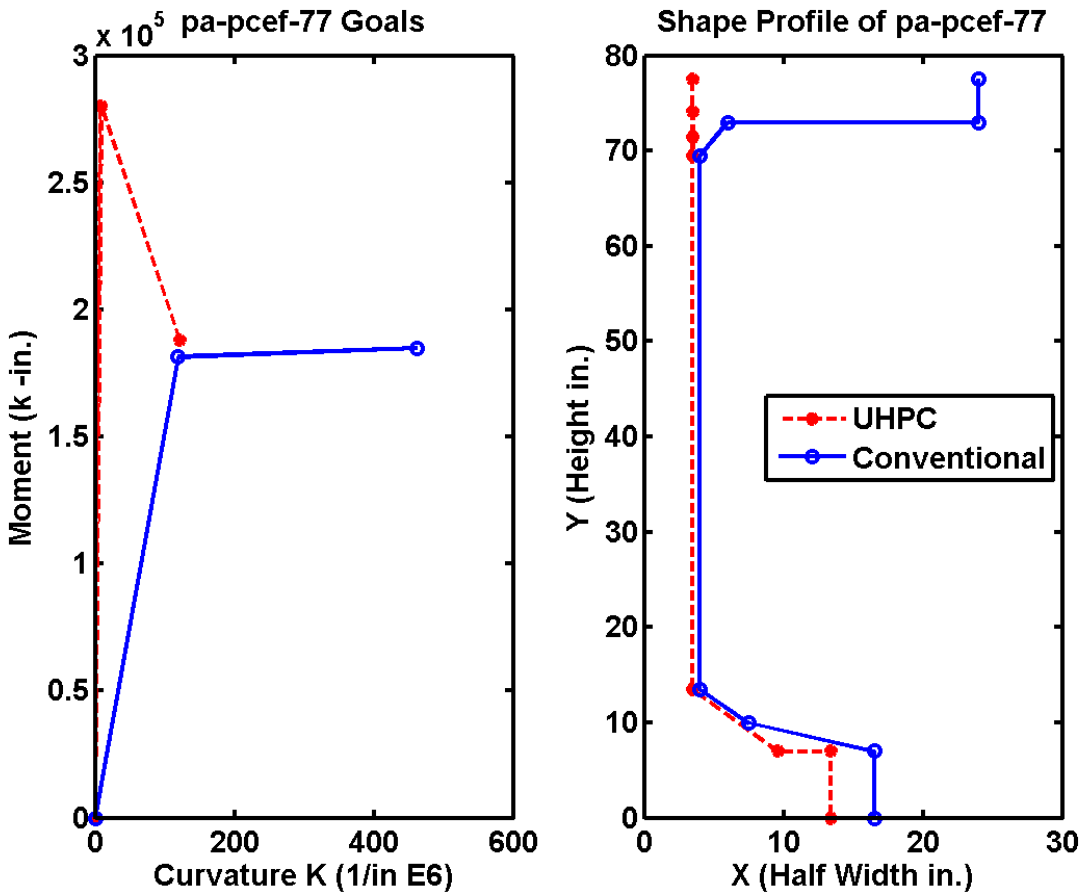

Figure 101. Graph. Pennsylvania 77 in Bulb Tee Direct Replacement Optimization Results

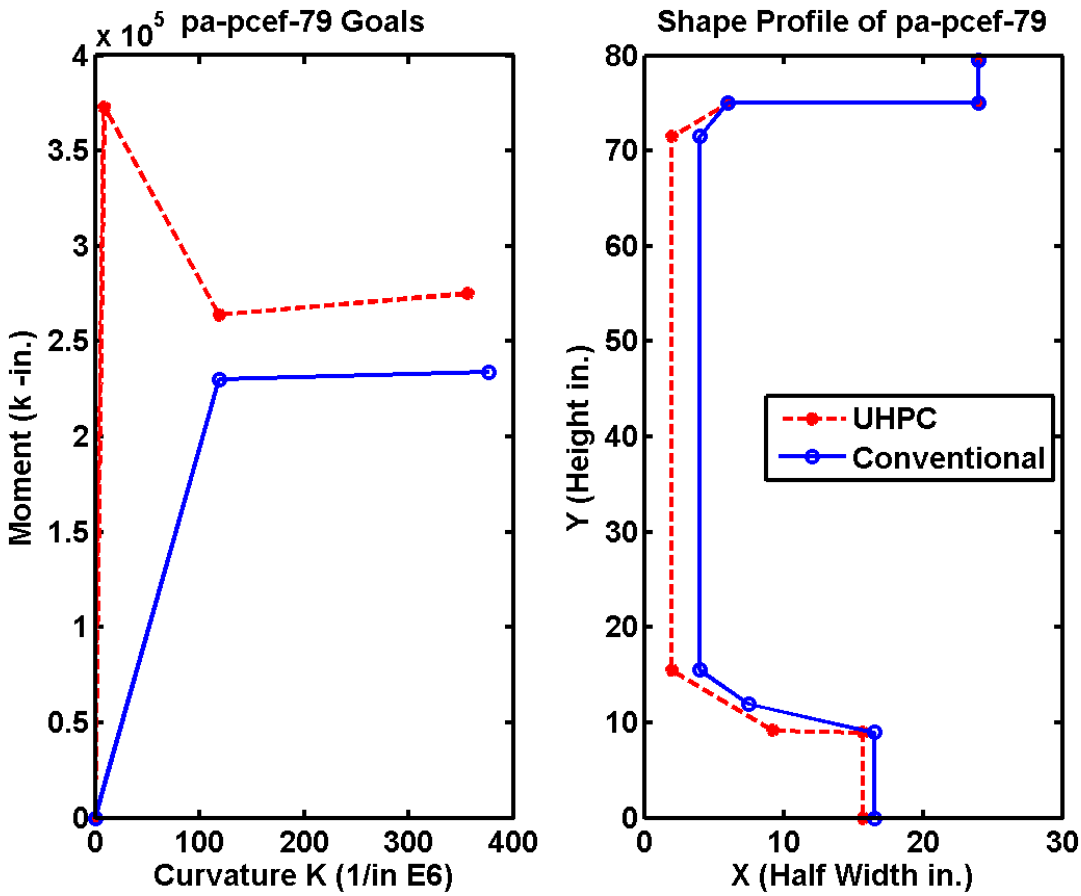

Figure 102. Graph. Pennsylvania 79 in Bulb Tee Direct Replacement Optimization Results

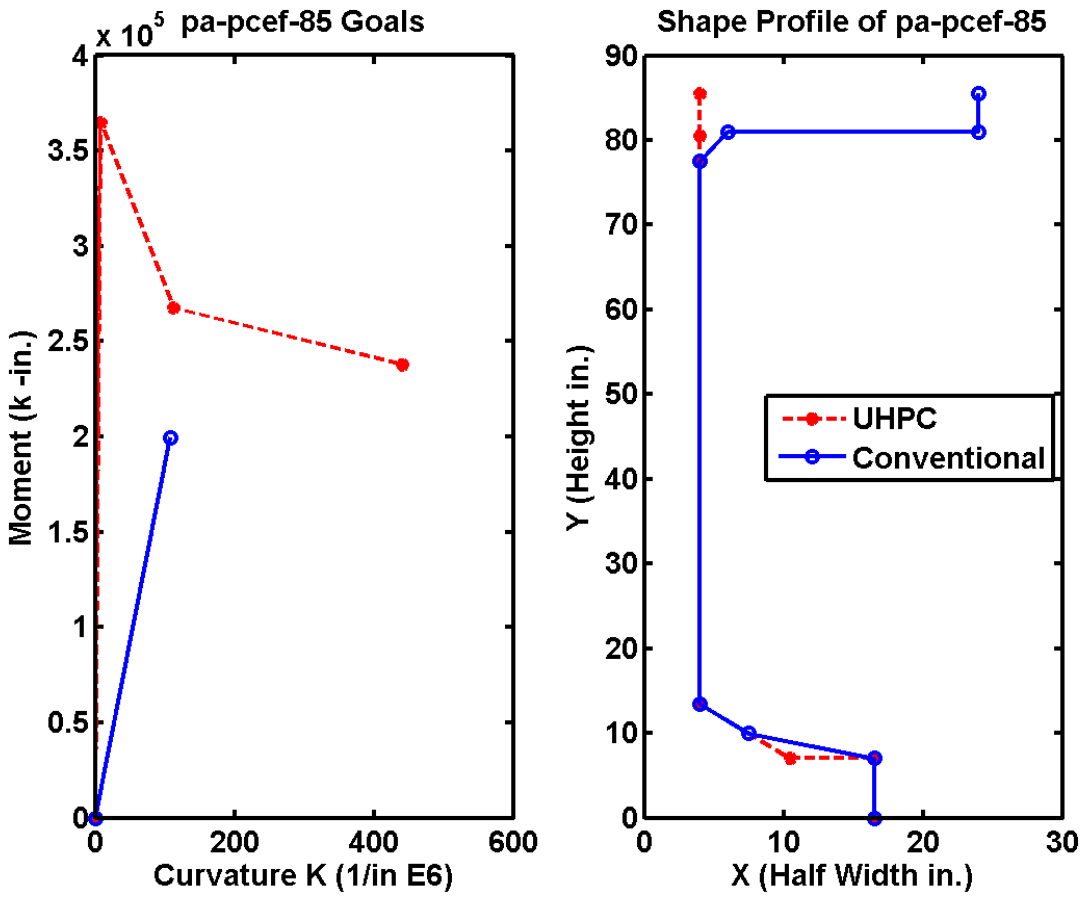

Figure 103. Graph. Pennsylvania 85 in Bulb Tee Direct Replacement Optimization Results

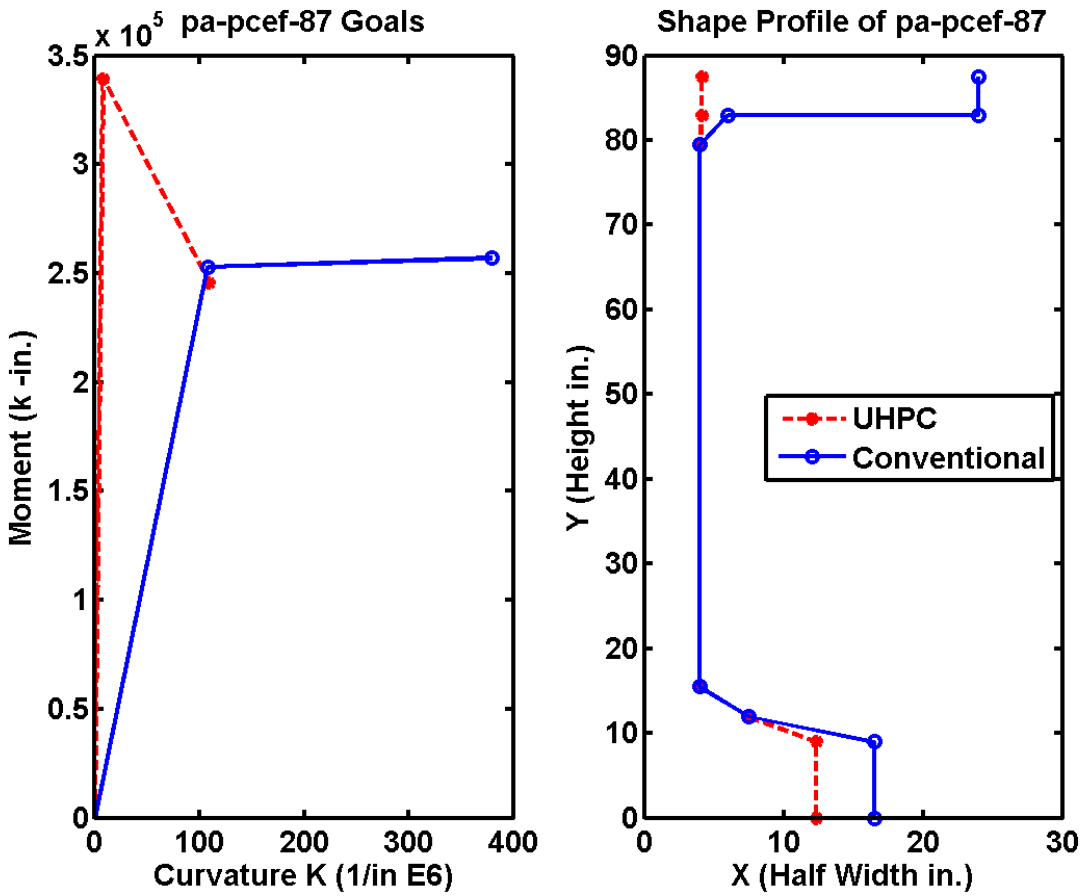

Figure 104. Graph. Pennsylvania 87 in Bulb Tee Direct Replacement Optimization Results

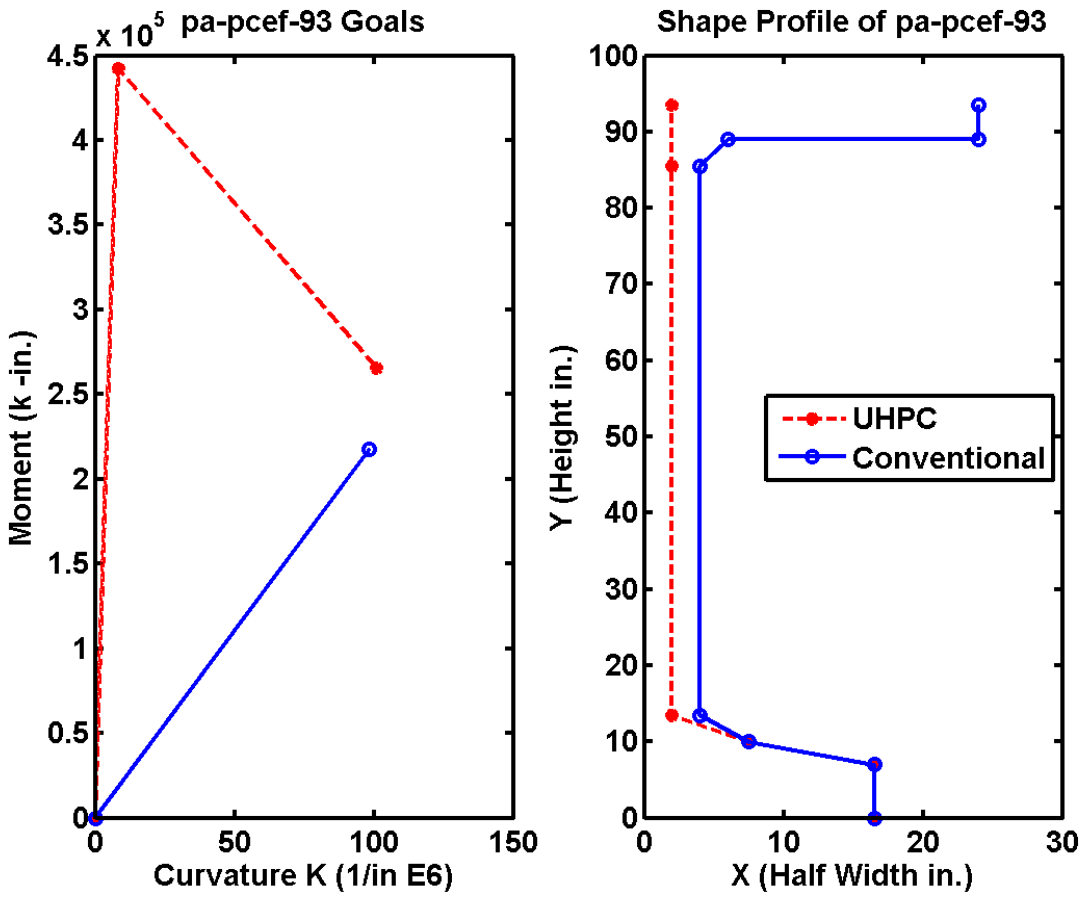

Figure 105. Graph. Pennsylvania 93 in Bulb Tee Direct Replacement Optimization Results

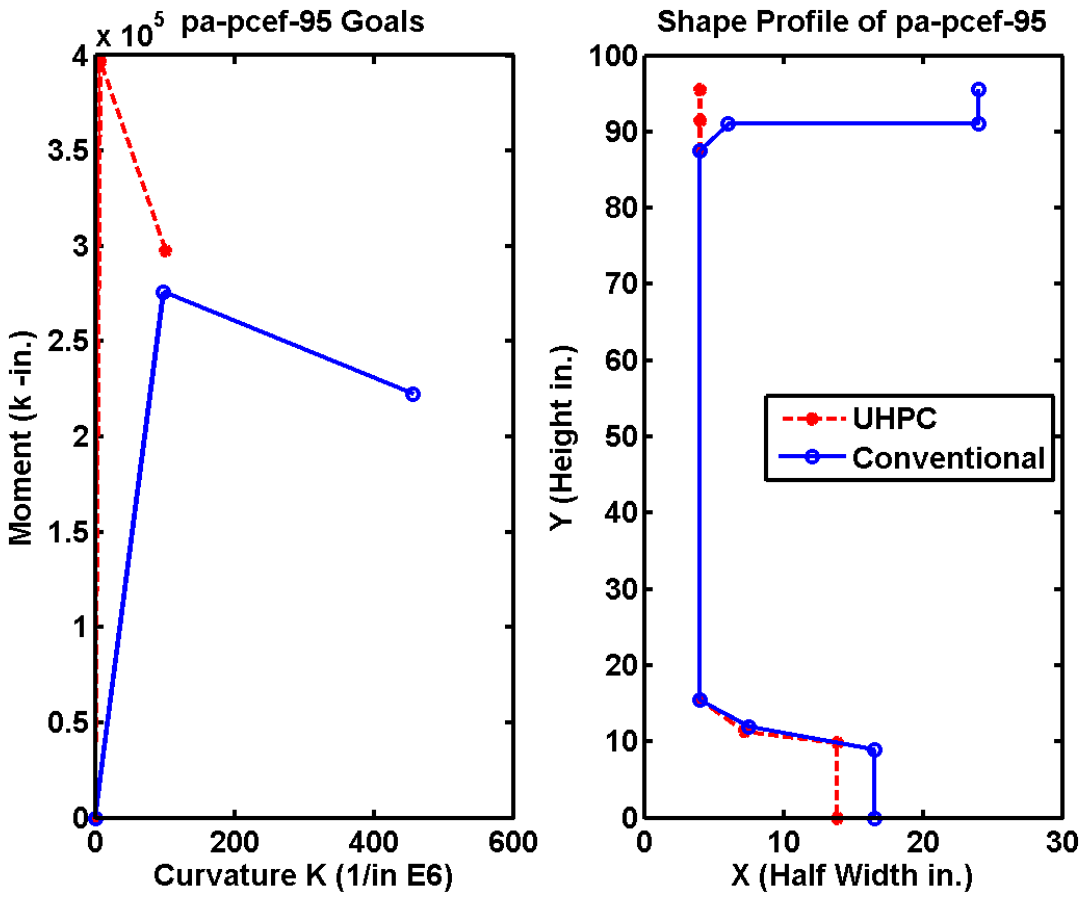

Figure 106. Graph. Pennsylvania 95 in Bulb Tee Direct Replacement Optimization Results

South Carolina Bulb Tee Girders

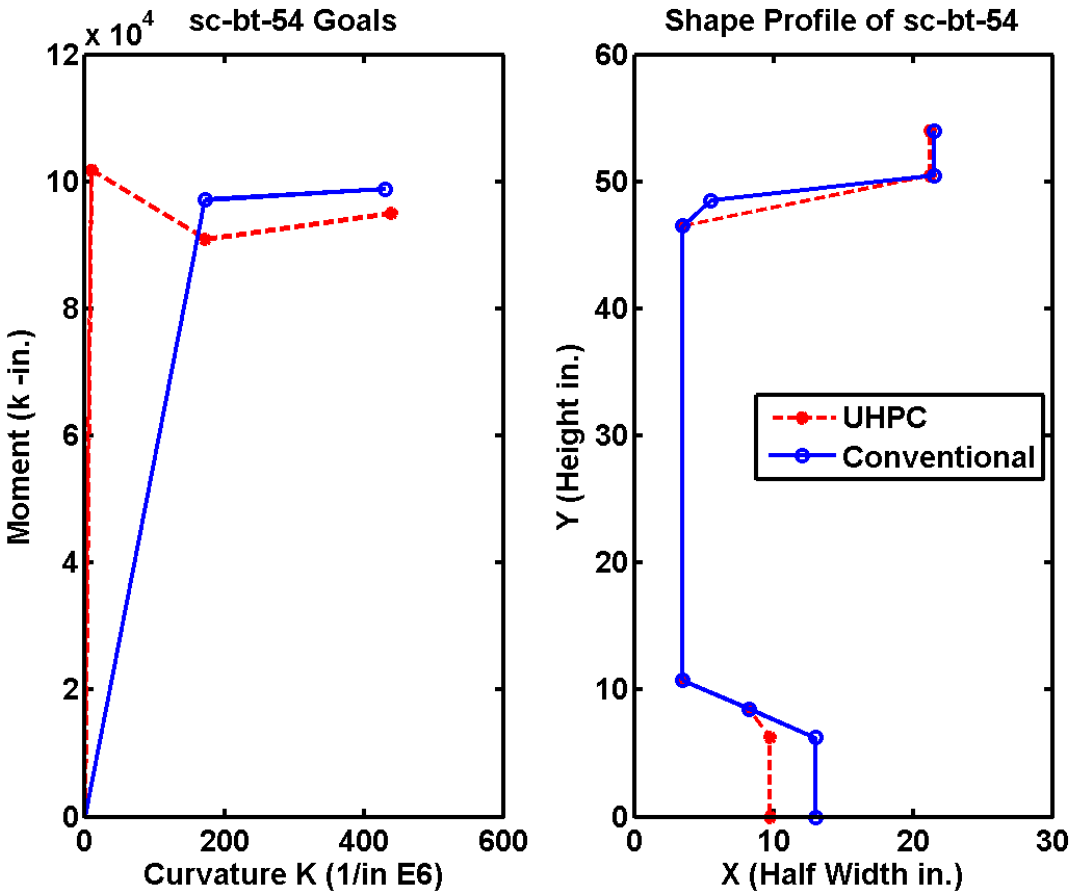

Figure 107. Graph. South Carolina 54 in Bulb Tee Direct Replacement Optimization Results

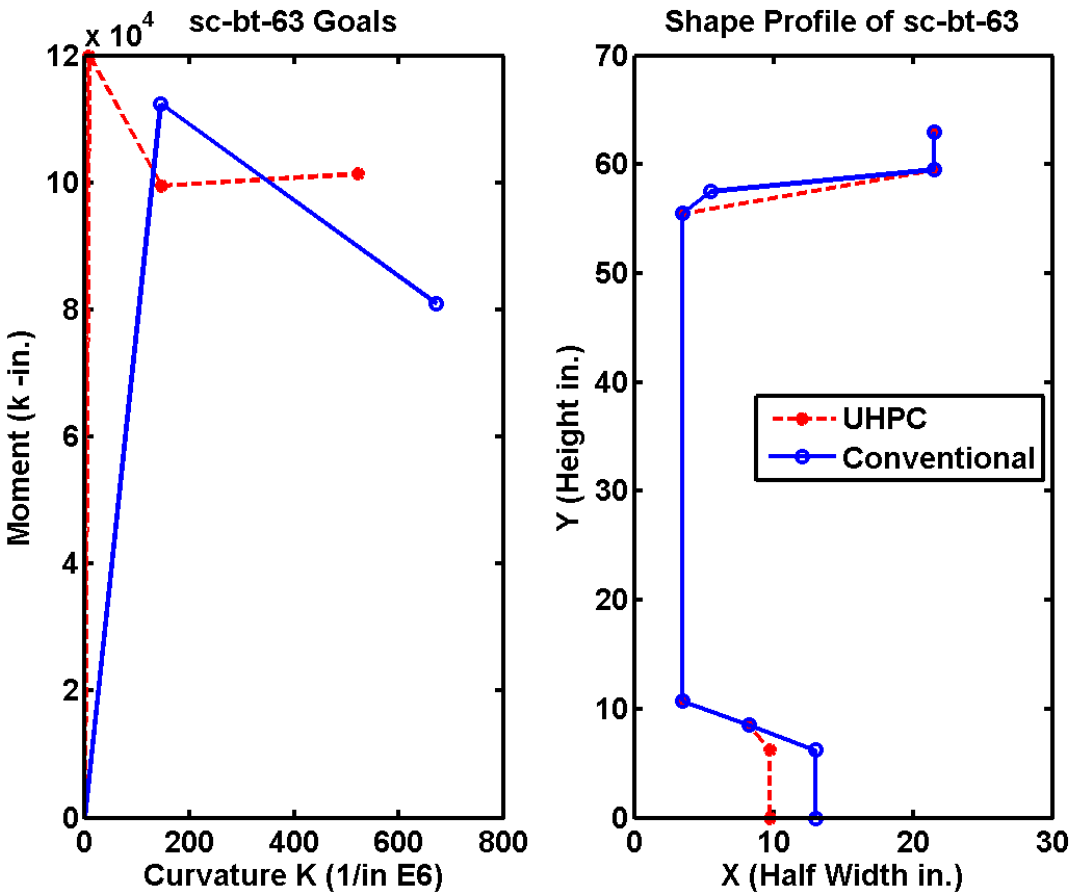

Figure 108. Graph. South Carolina 63 in Bulb Tee Direct Replacement Optimization Results

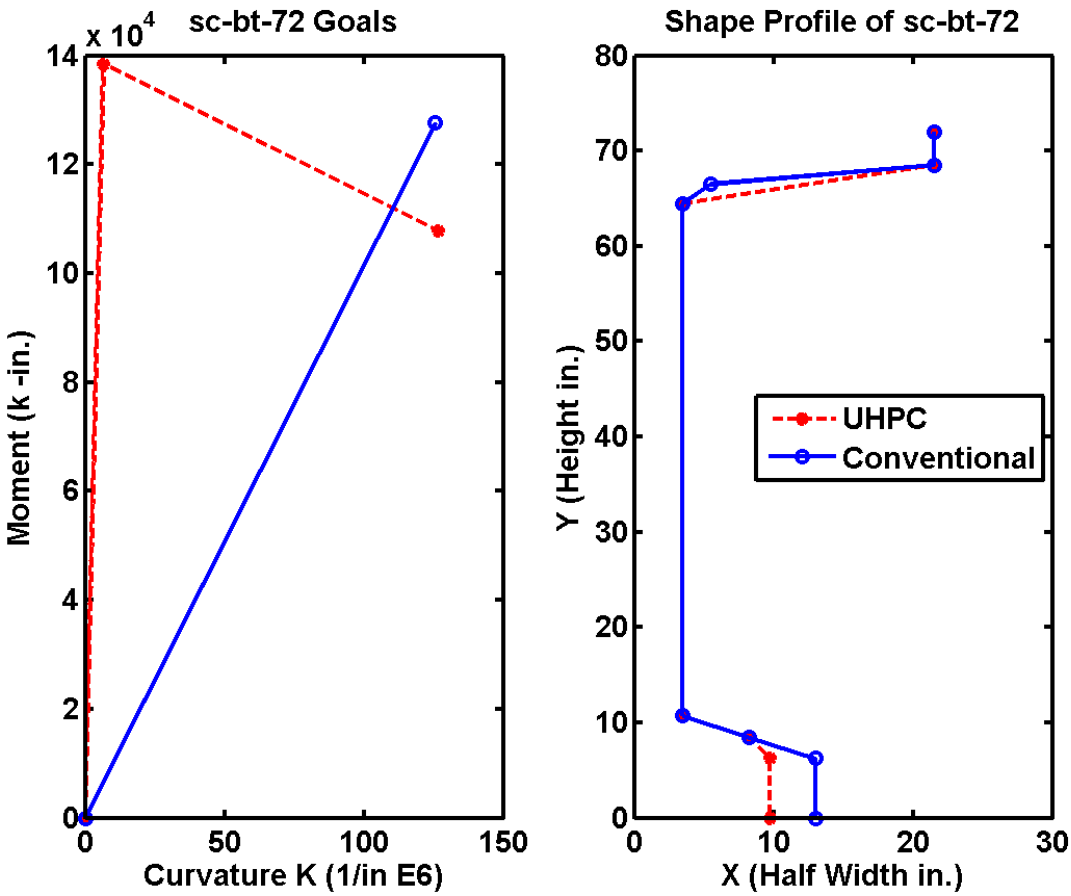

Figure 109. Graph. South Carolina 72 in Bulb Tee Direct Replacement Optimization Results

Virginia Bulb Tee Girders

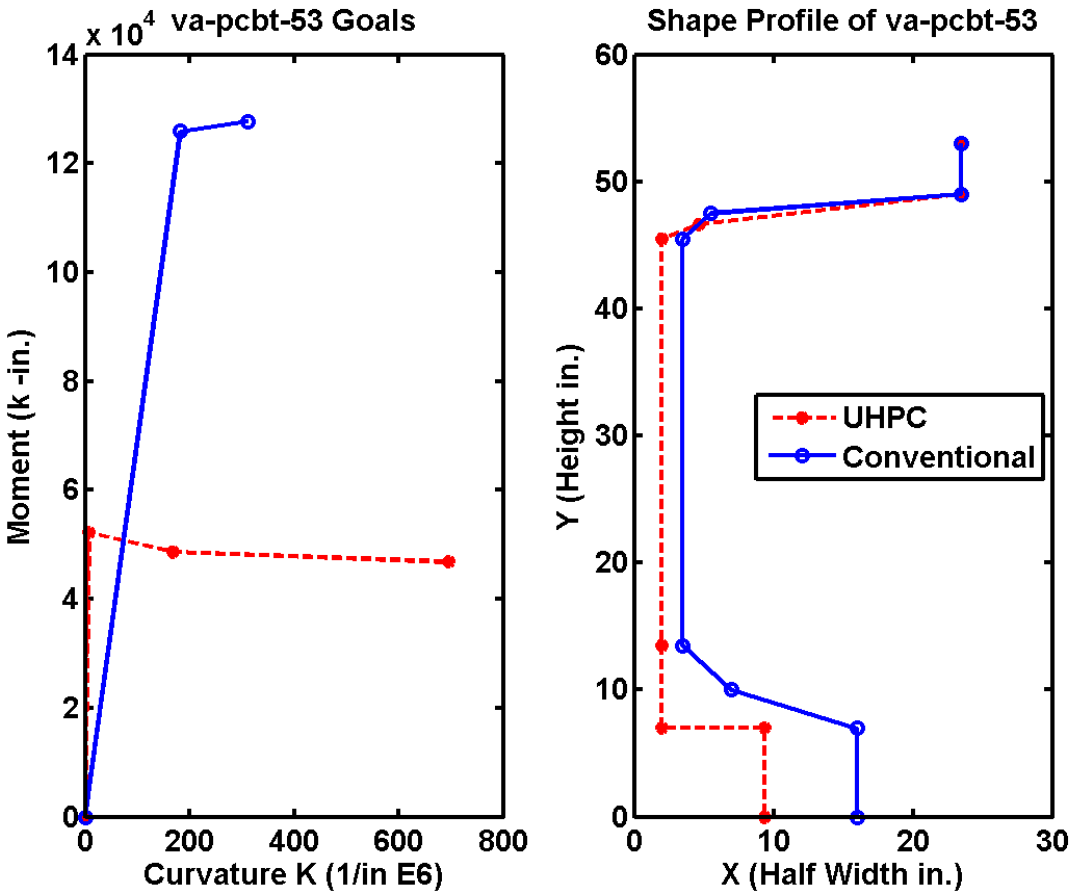

Figure 110. Graph. Virginia 53 in Bulb Tee Direct Replacement Optimization Results

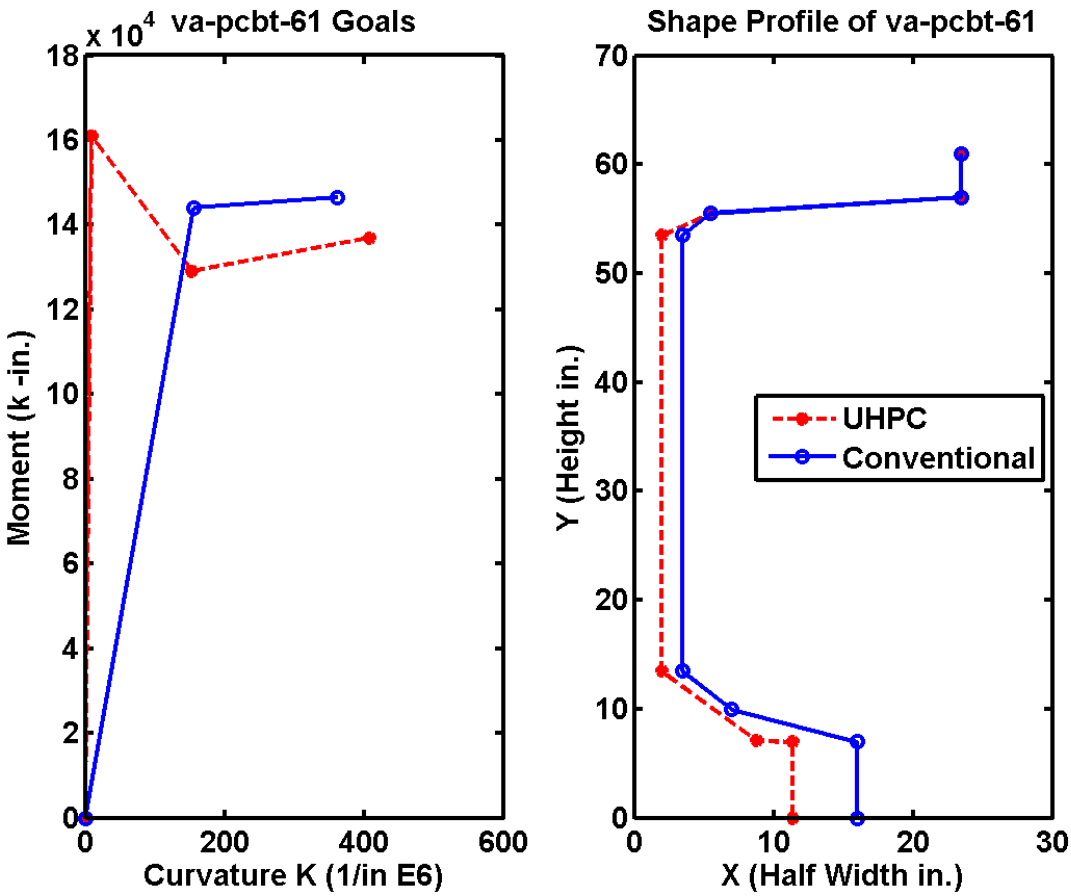

Figure 111. Graph. Virginia 61 in Bulb Tee Direct Replacement Optimization Results

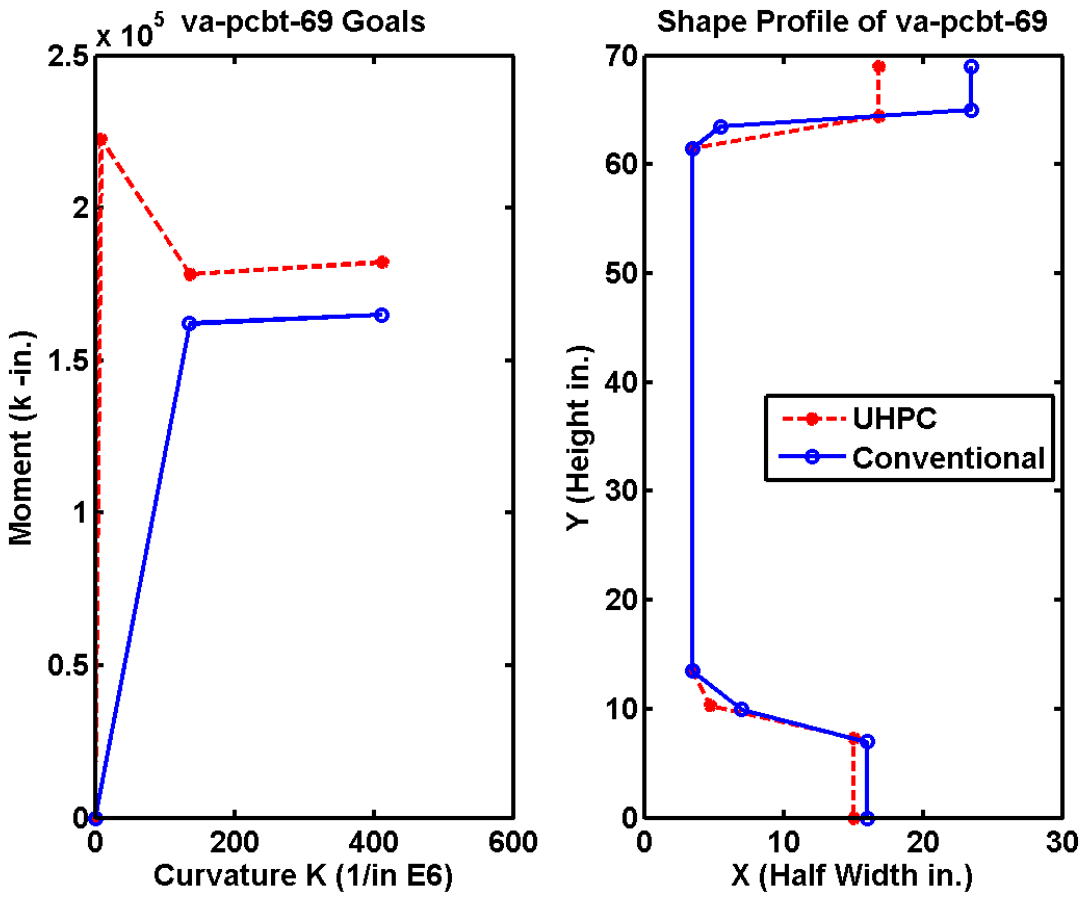

Figure 112. Graph. Virginia 69 in Bulb Tee Direct Replacement Optimization Results

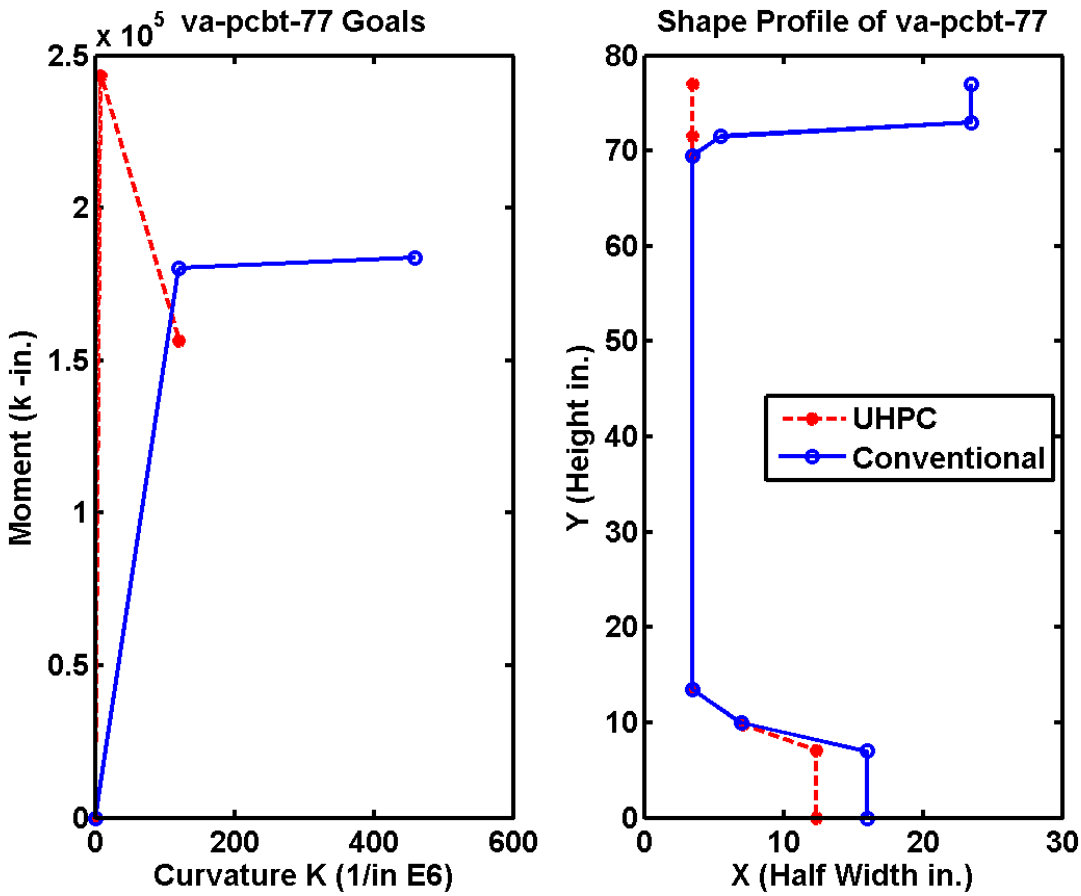

Figure 113. Graph. Virginia 77 in Bulb Tee Direct Replacement Optimization Results

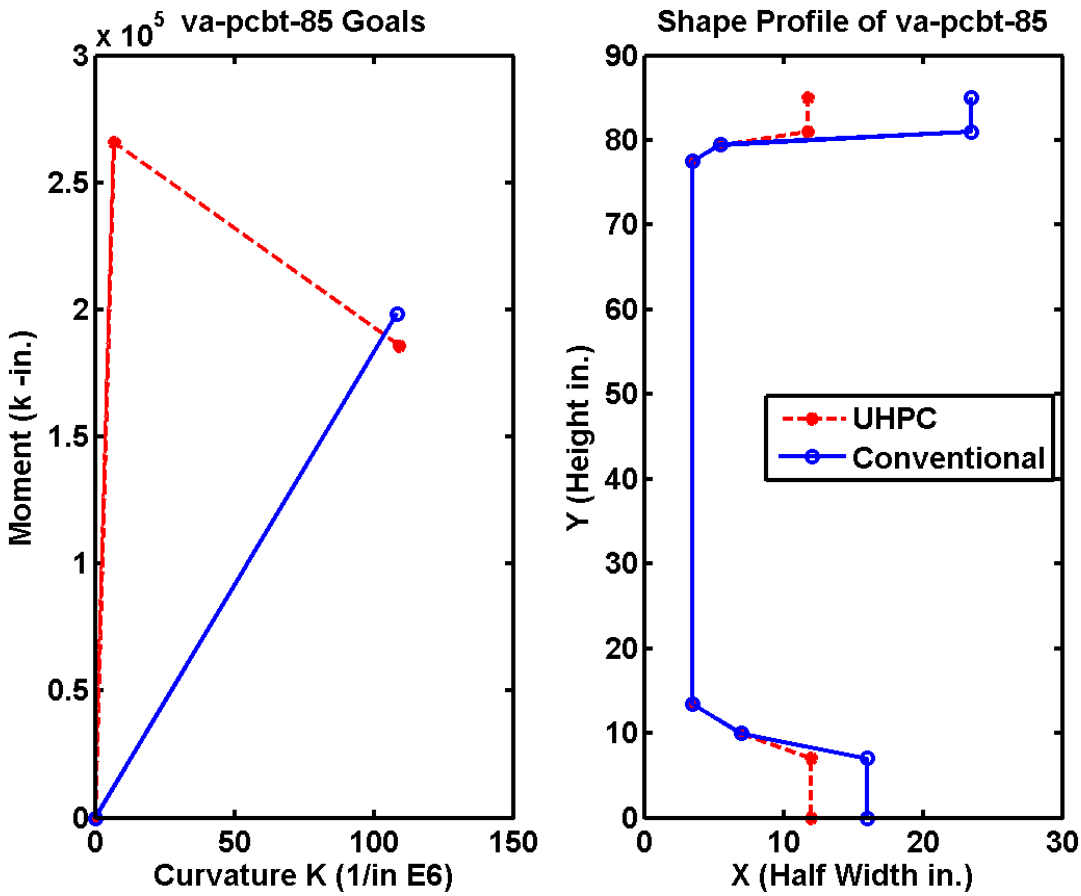

Figure 114. Graph. Virginia 85 in Bulb Tee Direct Replacement Optimization Results

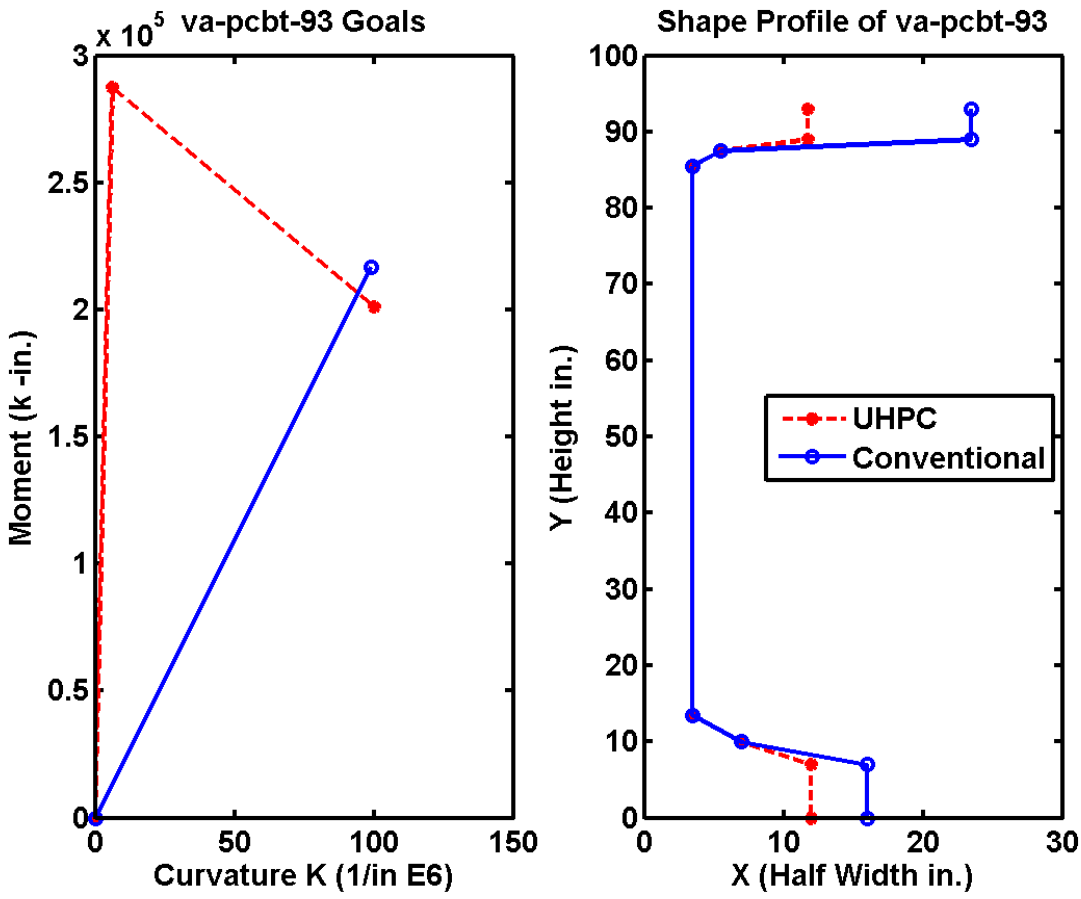

Figure 115. Graph. Virginia 93 in Bulb Tee Direct Replacement Optimization Results

Washington Bulb Tee Girders

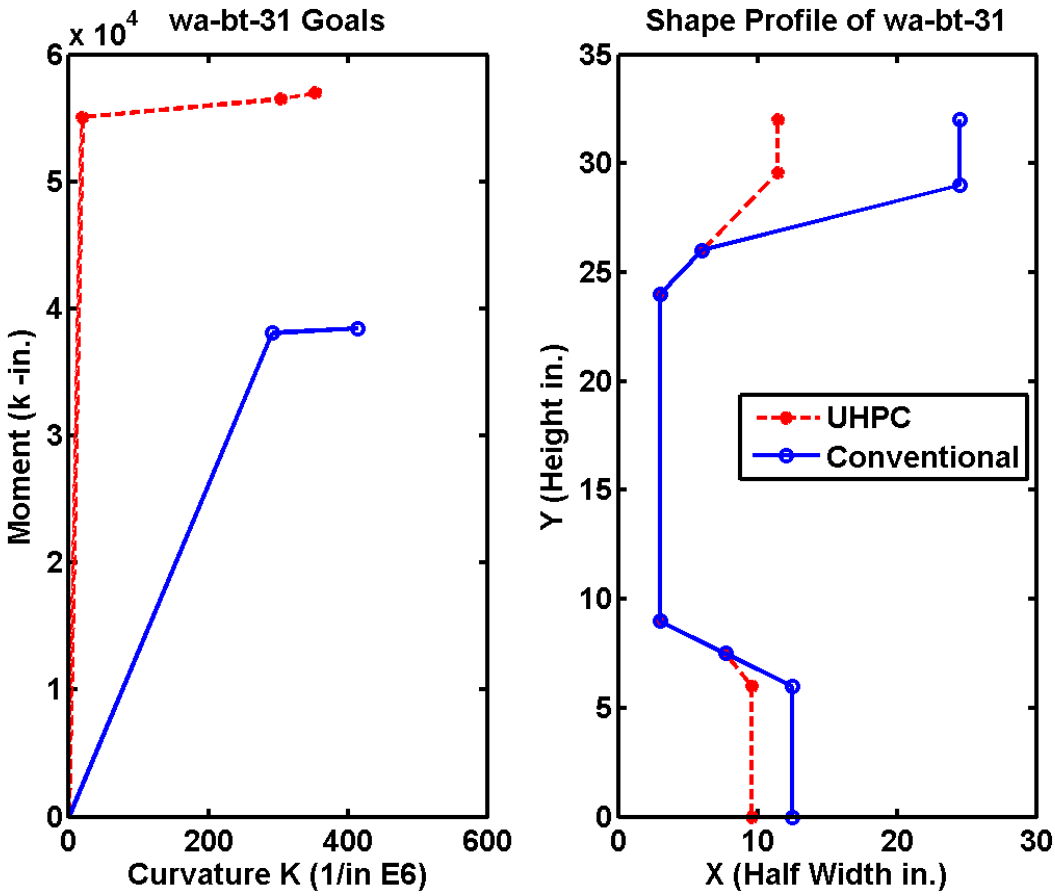

Figure 116. Graph. Washington 31 in Bulb Tee Direct Replacement Optimization Results

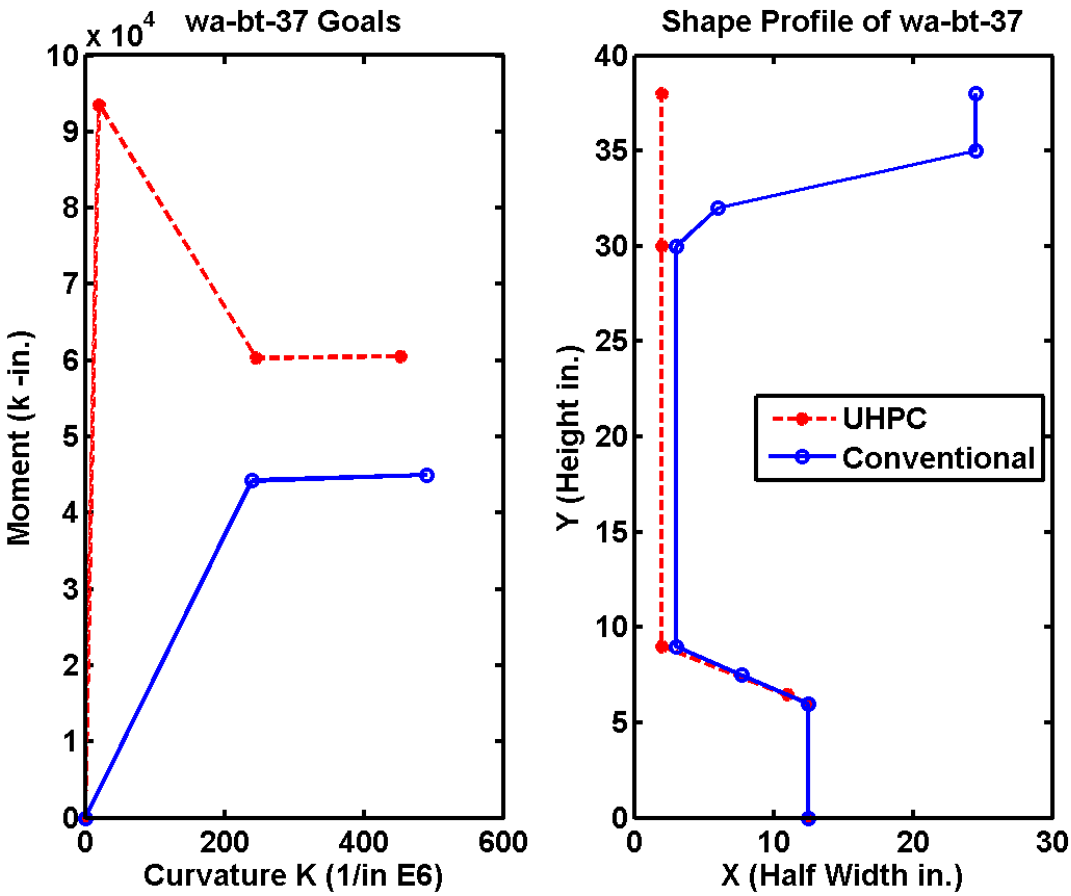

Figure 117. Graph. Washington 37 in Bulb Tee Direct Replacement Optimization Results

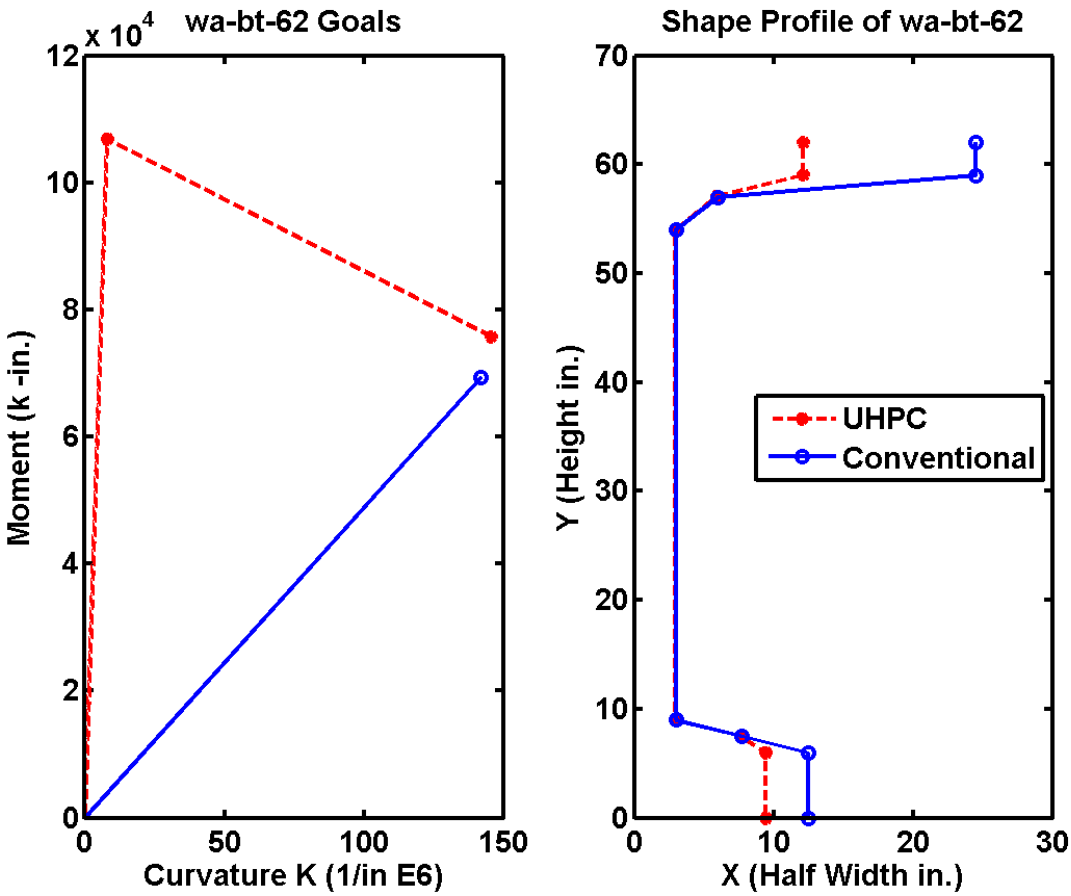

Figure 118. Graph. Washington 62 in Bulb Tee Direct Replacement Optimization Results

Washington Deck Girders

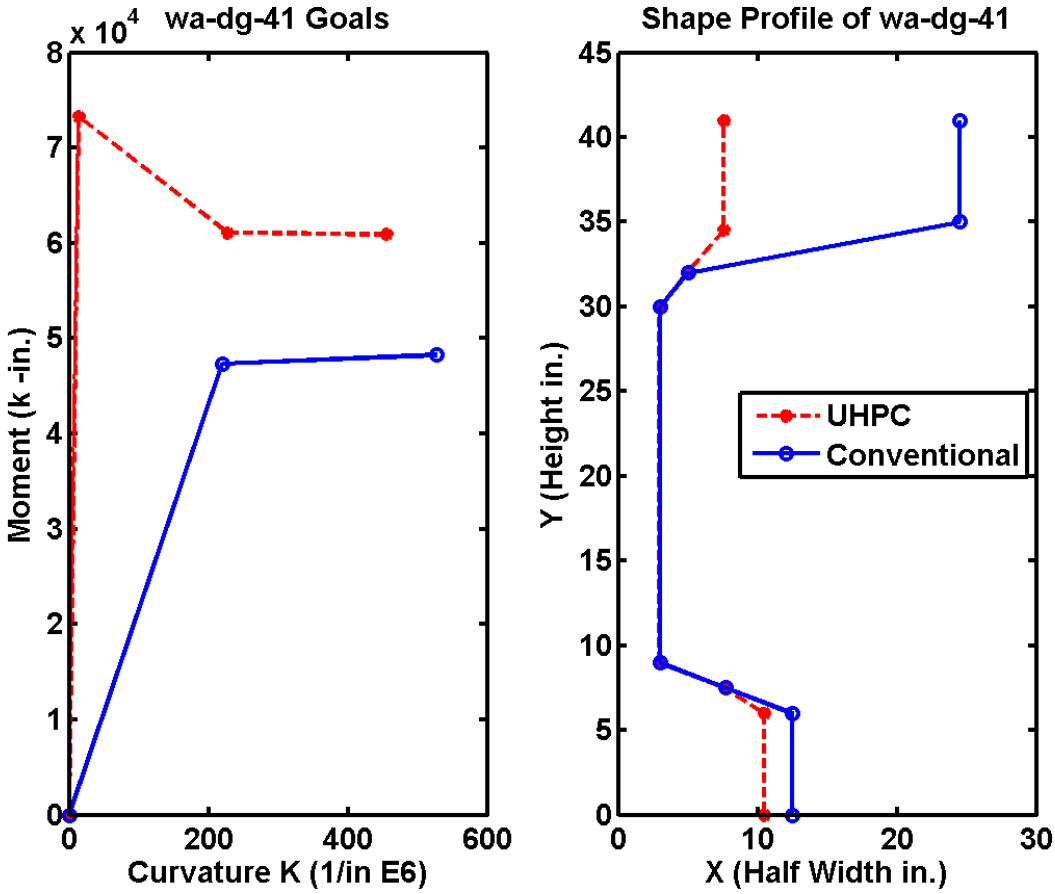

Figure 119. Graph. Washington 41 in Deck Girder Direct Replacement Optimization Results

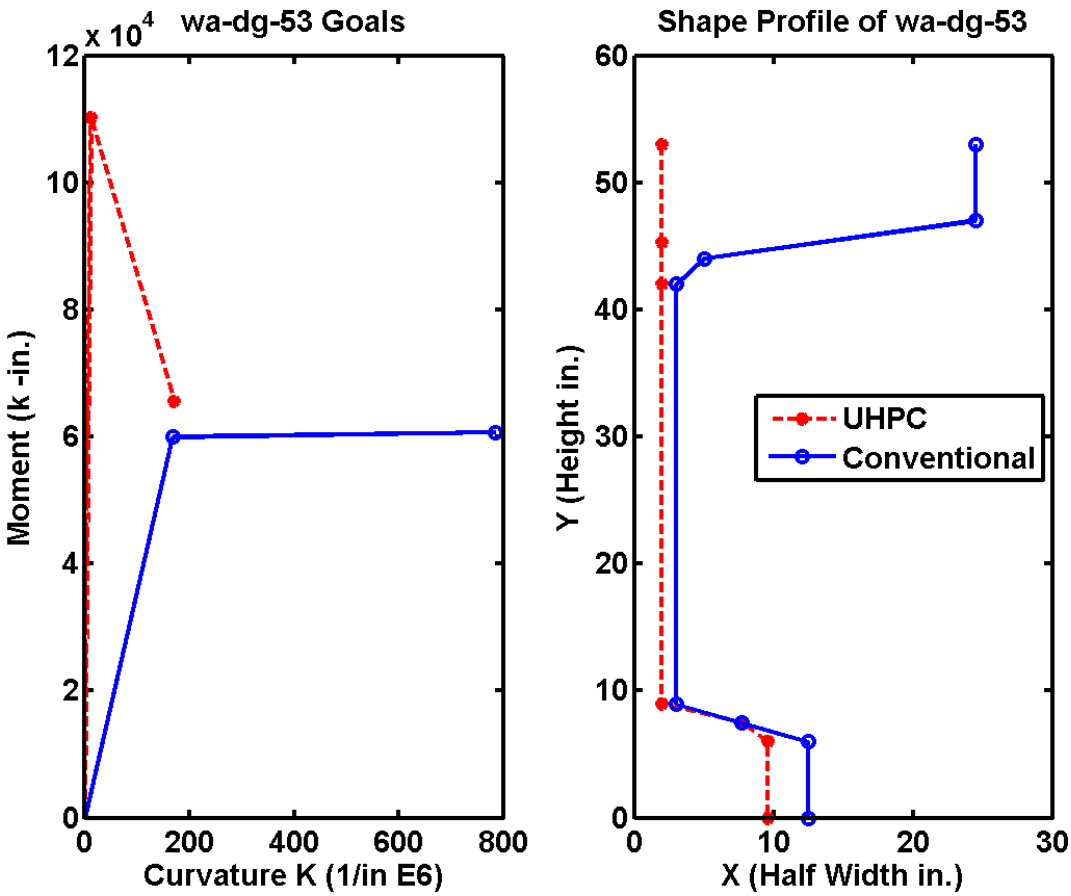

Figure 120. Graph. Washington 53 in Deck Girder Direct Replacement Optimization Results

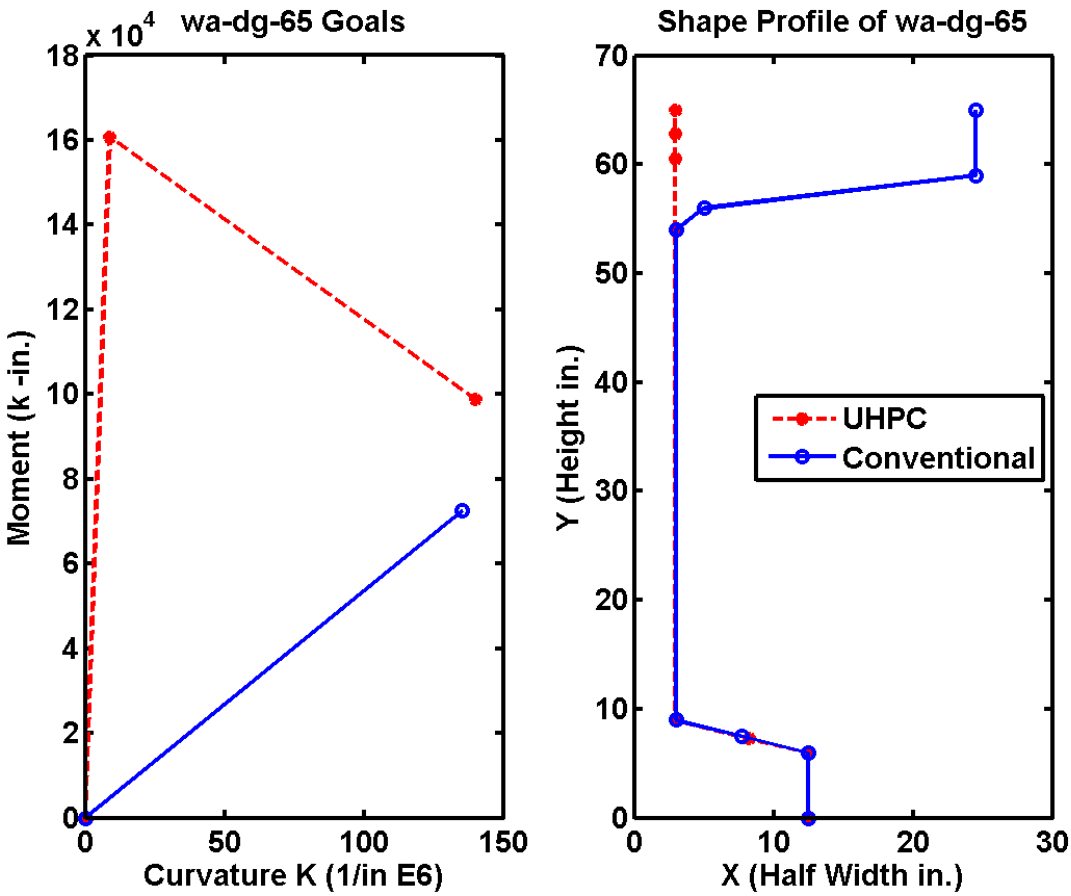

Figure 121. Graph. Washington 65 in Deck Girder Direct Replacement Optimization Results

Washington Wide Flange Girders

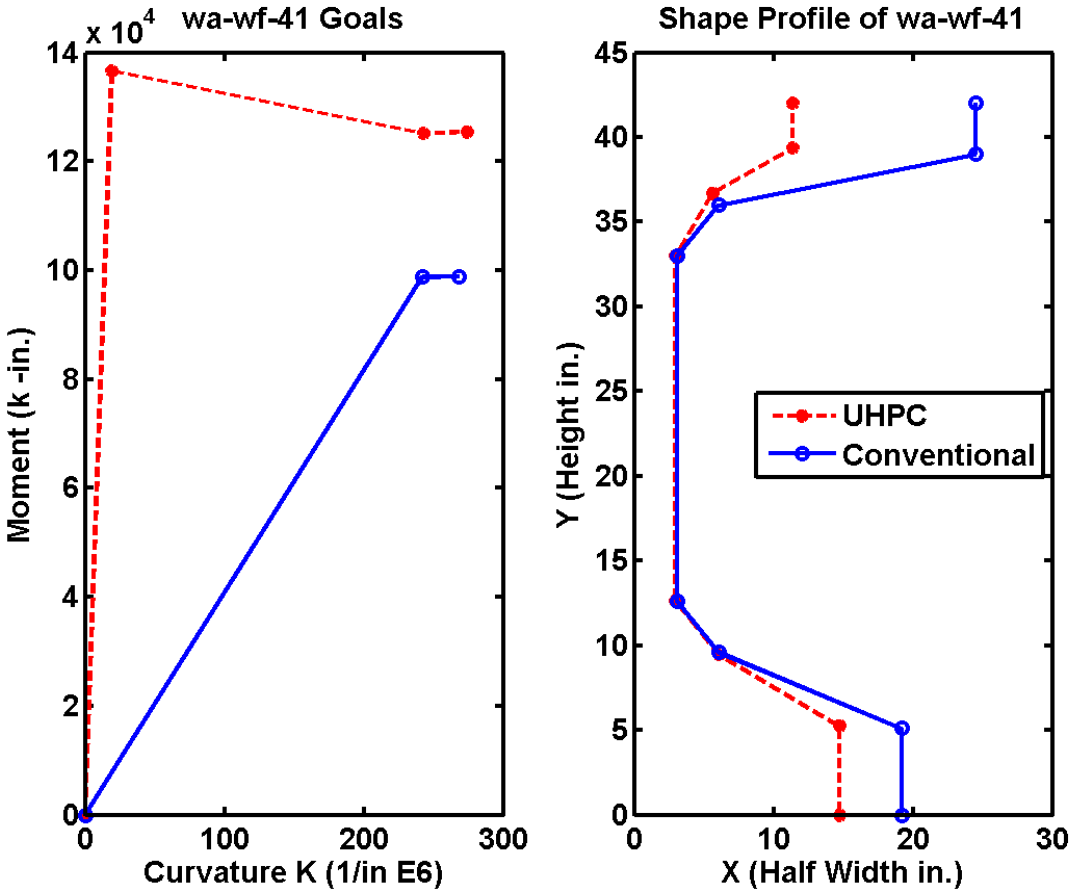

Figure 122. Graph. Washington 41 in Wide Flange Girder Direct Replacement Optimization Results

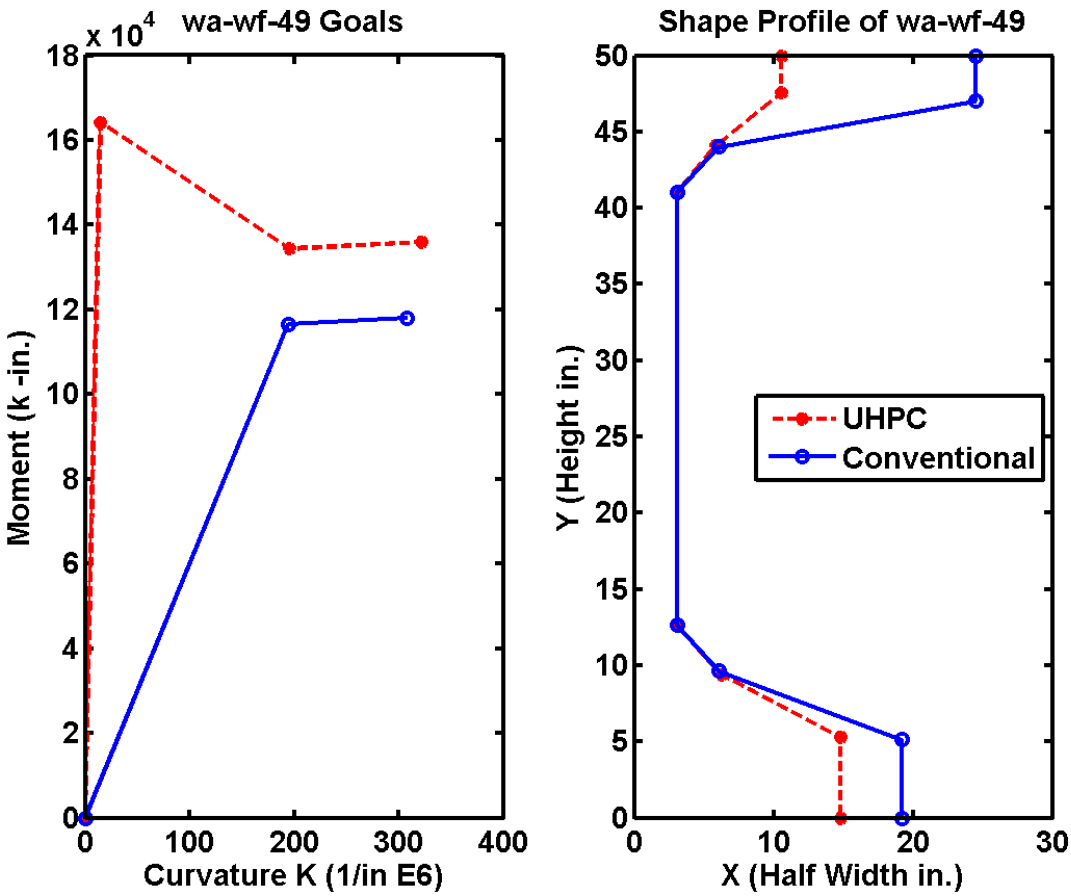

Figure 123. Graph. Washington 49 in Wide Flange Girder Direct Replacement Optimization Results

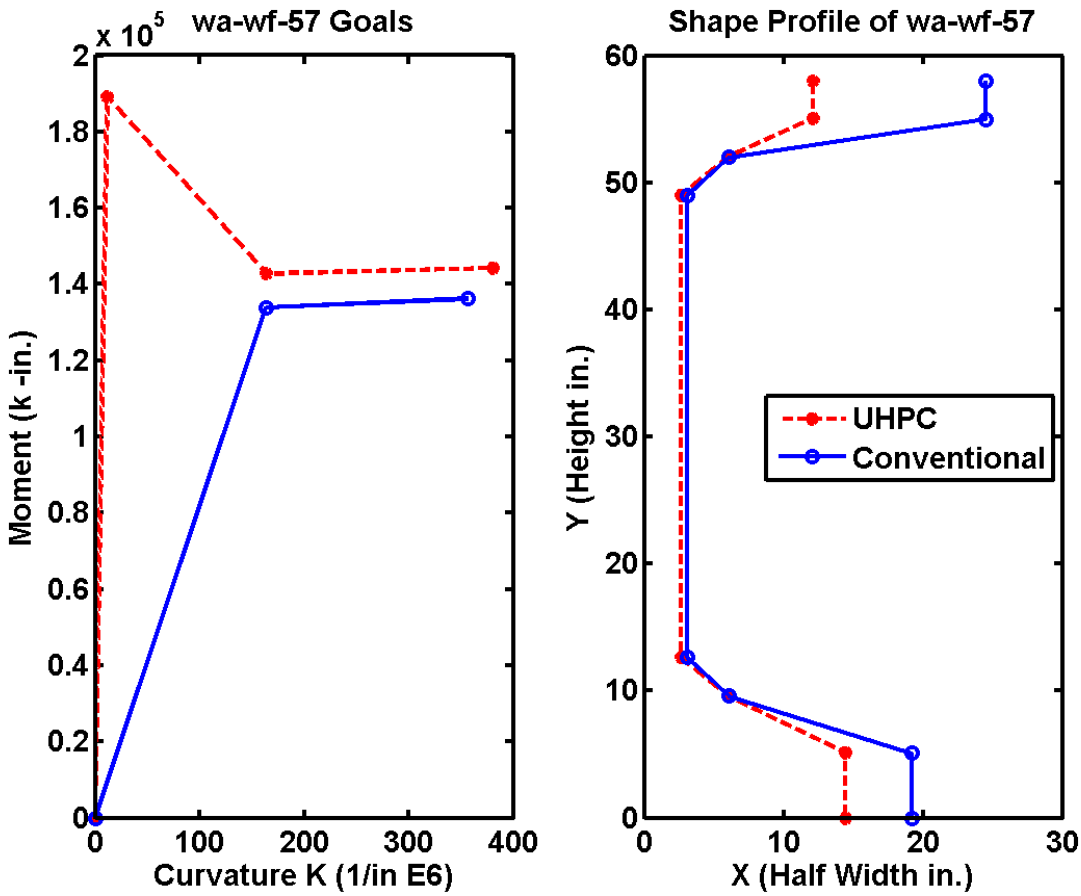

Figure 124. Graph. Washington 57 in Wide Flange Girder Direct Replacement Optimization Results

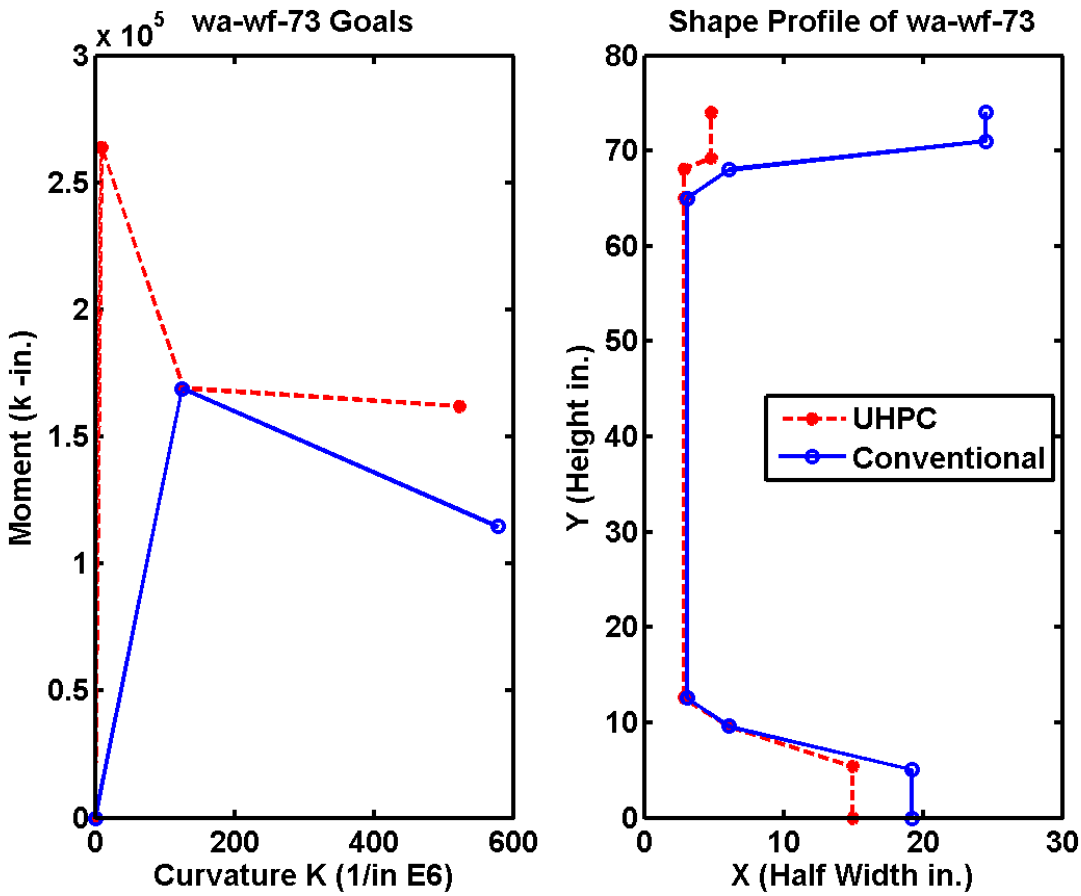

Figure 125. Graph. Washington 73 in Wide Flange Girder Direct Replacement Optimization Results

Appendix C: Full Bridge Optimization Results

Idaho Shapes

Table 28. Idaho Shape, 2 Lane Optimization Results

Conventional	50 FT	70 FT	90 FT	110 FT	130 FT
Cost without Penalty	10790	14079	27702	44784	0
Minimum Objective	11223	16007	31408	50441	0
Solution Depth	36.877	78.719	80.01	81.15	0
Solution Girders	8.5	5.5	7.5	6.5	0.0
Solution Steel Area	1.744	1.744	1.744	1.744	0.000
Active Constraint	0.043	0.193	0.371	0.566	0.000
Constraint Name	Strength	Strength	Strength	Strength	0

UHPC	50 FT	70 FT	90 FT	110 FT	130 FT
Cost without Penalty	10713	13622	17011	25469	0
Minimum Objective	11178	15285	19134	27359	0
Solution Depth	54	69	54	69	0
Solution Girders	5.5	4.0	4.0	6.5	0.0
Solution Steel Area	1.255	2.509	3.764	2.509	0.000
Active Constraint	0.047	0.166	0.212	0.189	0.000
Constraint Name	Mid Tr. Top	Mid Tr. Top	Strength	Strength	0

Cost Savings	5%	15%	46%	50%	0%
Objective Difference	1%	3%	39%	43%	0%
Constraint Difference	0.000	0.000	0.158	0.377	0.000

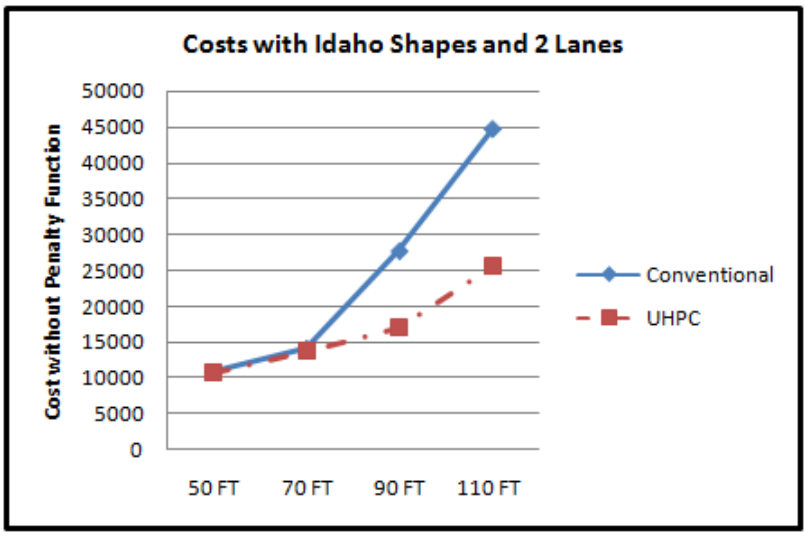

Figure 126. Graph. Idaho, 2 Lane Cost Comparison

Table 29. Idaho Shape 3, Lane Optimization Results

Conventional	50 FT	70 FT	90 FT	110 FT	130 FT
Cost without Penalty	11882	19481	34228	51013	0
Minimum Objective	12721	21726	38184	56438	0
Solution Depth	84	68.683	78.782	84	0
Solution Girders	7.6	9.5	10.5	10.5	0.0
Solution Steel Area	1.163	1.744	1.744	1.744	0.000
Active Constraint	0.084	0.224	0.396	0.543	0.000
Constraint Name	Strength	Strength	Strength	Strength	0

UHPC	50 FT	70 FT	90 FT	110 FT	130 FT
Cost without Penalty	13877	25159	32184	35020	0
Minimum Objective	14342	29249	36904	37218	0
Solution Depth	54	69	54	69	0
Solution Girders	8.5	4.0	4.0	9.5	0.0
Solution Steel Area	1.255	2.509	3.764	2.509	0.000
Active Constraint	0.047	0.409	0.472	0.220	0.000
Constraint Name	Mid Tr. Top	Strength	Strength	Strength	0

Cost Savings	-9%	-16%	16%	38%	0%
Objective Difference	-17%	-29%	6%	31%	0%
Constraint Difference	0.000	-0.185	-0.076	0.323	0.000

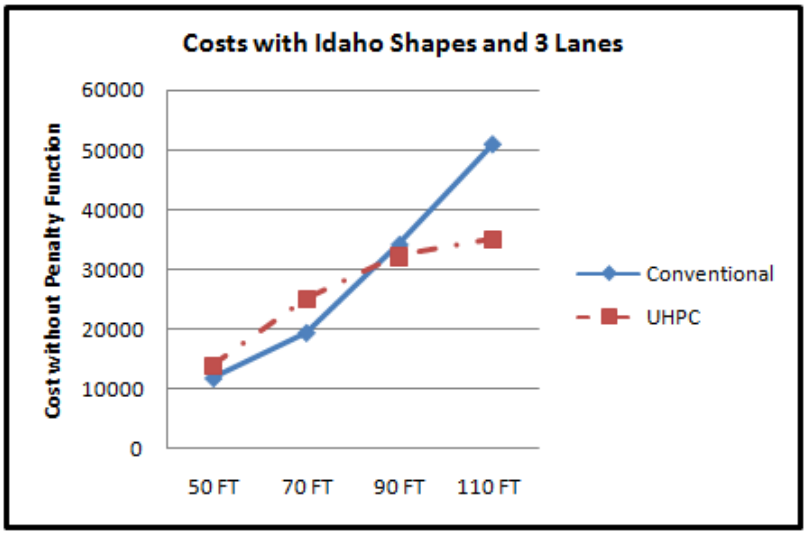

Figure 127. Graph. Idaho, 3 Lane Cost Comparison

Table 30. Idaho Shape, 4 Lane Optimization Results

Conventional	50 FT	70 FT	90 FT	110 FT	130 FT
Cost without Penalty	10785	21387	37050	55644	0
Minimum Objective	11221	23438	41365	61072	0
Solution Depth	84	84	80.665	84	0
Solution Girders	6.1	10.5	10.5	12.7	0.0
Solution Steel Area	1.744	1.744	1.744	1.744	0.000
Active Constraint	0.044	0.205	0.431	0.543	0.000
Constraint Name	Strength	Strength	Strength	Strength	0

UHPC	50 FT	70 FT	90 FT	110 FT	130 FT
Cost without Penalty	16086	25363	32888	32455	0
Minimum Objective	17938	29217	37406	34890	0
Solution Depth	54	69	54	69	0
Solution Girders	8.9	5.0	5.0	7.5	0.0
Solution Steel Area	1.255	2.509	3.764	3.764	0.000
Active Constraint	0.185	0.385	0.452	0.243	0.000
Constraint Name	Strength	Strength	Strength	Strength	0

Cost Savings	-43%	-8%	20%	47%	0%
Objective Difference	-49%	-19%	11%	42%	0%
Constraint Difference	-0.142	-0.180	-0.020	0.299	0.000

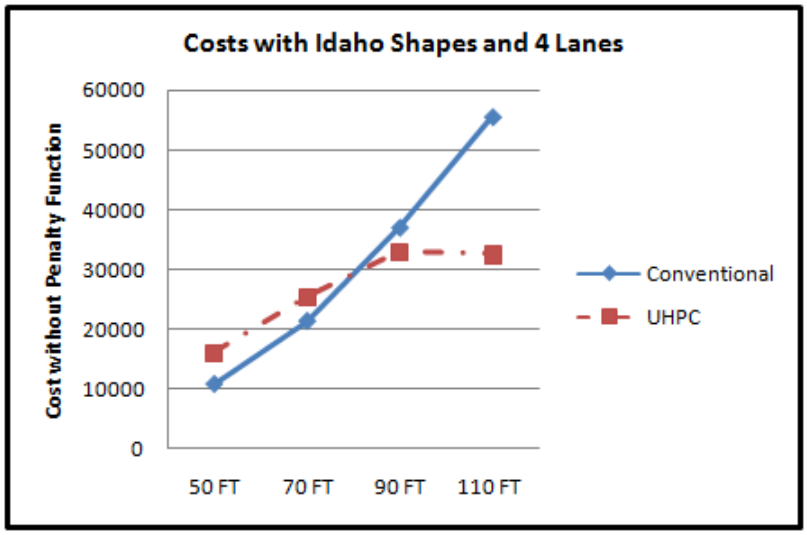

Figure 128. Graph. Idaho, 4 Lane Cost Comparison

Indiana Shapes

Table 31. Indiana Shape, 2 Lane Optimization Results

Conventional	50 FT	70 FT	90 FT	110 FT	130 FT
Cost without Penalty	10738	12401	22060	37305	46720
Minimum Objective	10835	12579	25327	42369	51659
Solution Depth	31.944	82.881	84.016	84.016	83.521
Solution Girders	5.5	4.0	4.0	4.0	6.5
Solution Steel Area	3.029	3.029	3.029	3.029	3.029
Active Constraint	0.010	0.018	0.327	0.506	0.494
Constraint Name	Strength	Strength	Strength	Strength	Strength

UHPC	50 FT	70 FT	90 FT	110 FT	130 FT
Cost without Penalty	10499	16310	16669	20550	25895
Minimum Objective	11417	17848	17577	20550	28077
Solution Depth	65.984	65.984	75	65.984	65.984
Solution Girders	4.0	5.5	4.0	4.0	4.0
Solution Steel Area	1.744	1.744	3.488	5.233	5.233
Active Constraint	0.092	0.154	0.091	-0.009	0.218
Constraint Name	Strength	Strength	Strength	Strength	Strength

Cost Savings	3%	-30%	34%	51%	50%
Objective Difference	2%	-32%	24%	45%	45%
Constraint Difference	-0.082	-0.136	0.236	0.516	0.276

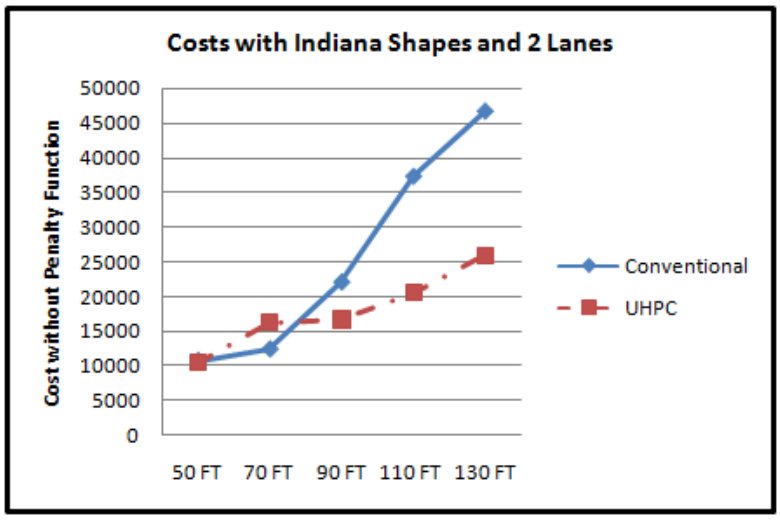

Figure 129. Graph. Indiana, 2 Lane Cost Comparison

Table 32. Indiana Shape, 3 Lane Optimization Results

Conventional	50 FT	70 FT	90 FT	110 FT	130 FT
Cost without Penalty	12014	16010	33075	38737	58402
Minimum Objective	12107	18427	37896	42722	63433
Solution Depth	38.233	84.016	84.016	84.016	84.016
Solution Girders	6.5	4.0	4.0	7.5	9.7
Solution Steel Area	3.029	3.029	3.029	3.029	3.029
Active Constraint	0.009	0.242	0.482	0.398	0.503
Constraint Name	Strength	Strength	Strength	Strength	Strength

UHPC	50 FT	70 FT	90 FT	110 FT	130 FT
Cost without Penalty	12544	18900	18726	29608	34462
Minimum Objective	13369	21621	20317	33159	35183
Solution Depth	65.984	75	65.984	65.984	65.984
Solution Girders	5.6	4.0	4.0	4.0	6.5
Solution Steel Area	1.744	3.488	5.233	5.233	5.233
Active Constraint	0.083	0.272	0.159	0.355	0.072
Constraint Name	Mid Tr. Top	Mid Tr. Top	Mid Tr. Top	Strength	Strength

Cost Savings	-4%	-3%	51%	31%	46%
Objective Difference	-4%	-18%	43%	24%	41%
Constraint Difference	0.000	0.000	0.000	0.043	0.431

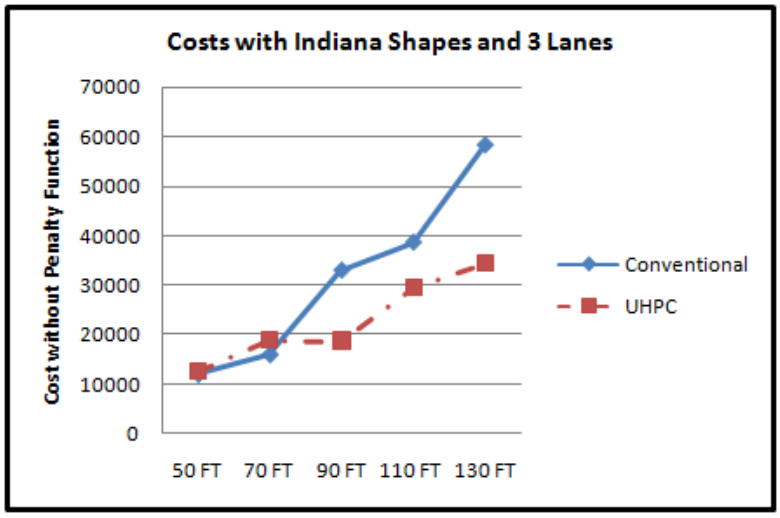

Figure 130. Graph. Indiana, 3 Lane Cost Comparison

Table 33. Indiana Shape, 4 Lane Optimization Results

Conventional	50 FT	70 FT	90 FT	110 FT	130 FT
Cost without Penalty	10918	16840	33875	42959	69272
Minimum Objective	11197	18968	38510	47518	74186
Solution Depth	59.221	84.016	84.016	82.838	84.016
Solution Girders	5.0	5.0	5.0	7.5	13.2
Solution Steel Area	3.029	3.029	3.029	3.029	3.029
Active Constraint	0.028	0.213	0.463	0.456	0.491
Constraint Name	Mid Tr. Top	Strength	Strength	Strength	Strength

UHPC	50 FT	70 FT	90 FT	110 FT	130 FT
Cost without Penalty	15277	21164	21882	32108	40371
Minimum Objective	16672	23885	23473	35429	42062
Solution Depth	65.984	75	65.984	65.984	65.984
Solution Girders	7.1	5.0	5.0	5.0	7.5
Solution Steel Area	1.744	3.488	5.233	5.233	5.233
Active Constraint	0.140	0.272	0.159	0.332	0.169
Constraint Name	Strength	Mid Tr. Top	Mid Tr. Top	Strength	Strength

Cost Savings	-36%	-12%	43%	32%	46%
Objective Difference	-40%	-26%	35%	25%	42%
Constraint Difference	0.000	0.000	0.000	0.124	0.322

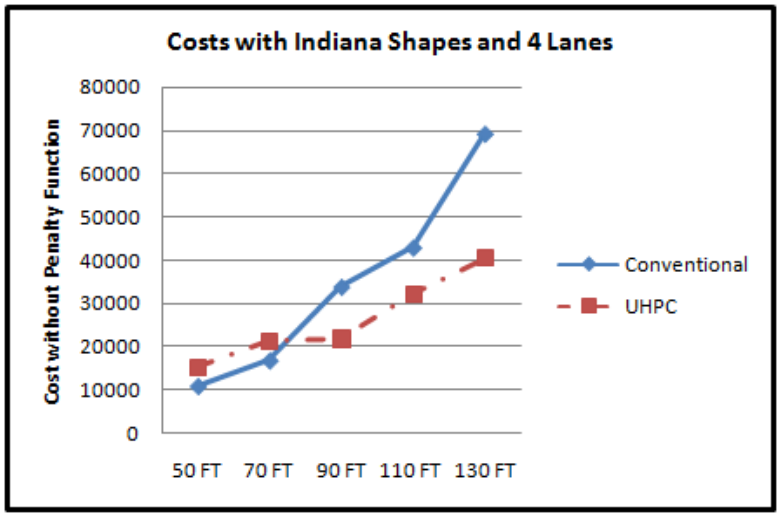

Figure 131. Graph. Indiana, 4 Lane Cost Comparison

New England Shapes

Table 34. New England Shape, 2 Lane Optimization Results

Conventional	50 FT	70 FT	90 FT	110 FT	130 FT
Cost without Penalty	9733	12298	18271	32176	40873
Minimum Objective	9733	12480	20672	36600	45423
Solution Depth	55.815	60.965	70.865	70.864	70.866
Solution Girders	4.0	4.0	4.0	4.0	5.6
Solution Steel Area	2.632	3.947	3.947	3.947	3.947
Active Constraint	-0.097	0.018	0.240	0.442	0.455
Constraint Name	Strength	Strength	Strength	Strength	Strength

UHPC	50 FT	70 FT	90 FT	110 FT	130 FT
Cost without Penalty	10751	14807	17638	28002	30937
Minimum Objective	11094	14911	18643	31113	34049
Solution Depth	55.118	62.992	62.992	55.118	55.118
Solution Girders	4.0	4.0	4.0	4.0	4.0
Solution Steel Area	1.897	3.794	3.794	5.692	5.692
Active Constraint	0.034	0.010	0.101	0.311	0.311
Constraint Name	Strength	Mid Tr. Top	Strength	End Tr. Top	End Tr. Top

Cost Savings	-10%	-20%	3%	13%	24%
Objective Difference	-14%	-19%	10%	15%	25%
Constraint Difference	-0.131	0.000	0.140	0.000	0.000

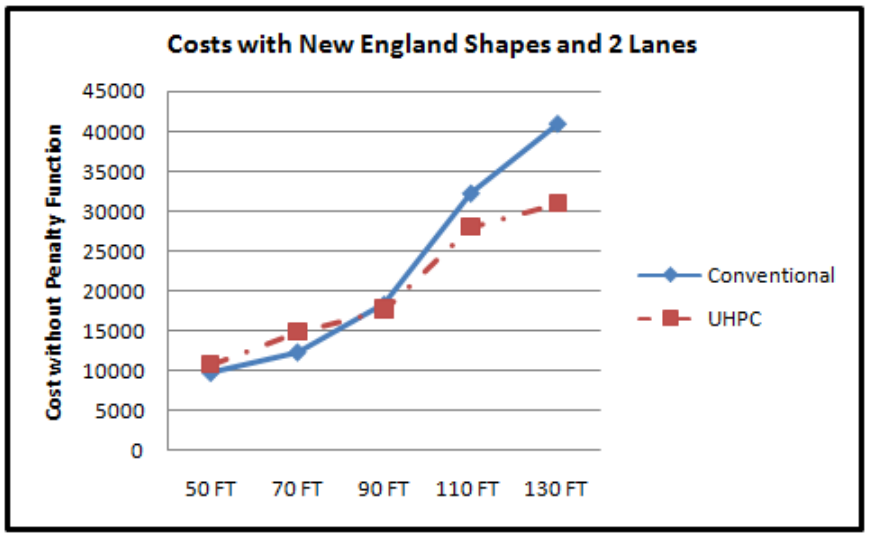

Figure 132. Graph. New England, 2 Lane Cost Comparison

Table 35. New England Shape, 3 Lane Optimization Results

Conventional	50 FT	70 FT	90 FT	110 FT	130 FT
Cost without Penalty	9941	13492	20679	34996	51153
Minimum Objective	10054	14973	22718	38330	55679
Solution Depth	68.668	70.864	70.858	68.799	70.863
Solution Girders	4.0	4.0	5.5	7.5	8.6
Solution Steel Area	2.632	3.947	3.947	3.947	3.947
Active Constraint	0.011	0.148	0.204	0.333	0.453
Constraint Name	Strength	Strength	Strength	Strength	Strength

UHPC	50 FT	70 FT	90 FT	110 FT	130 FT
Cost without Penalty	13035	15256	25070	32690	35839
Minimum Objective	13179	16534	28179	36582	39170
Solution Depth	55.118	62.992	55.118	55.118	62.992
Solution Girders	5.5	4.0	4.0	4.0	4.6
Solution Steel Area	1.897	3.794	5.692	5.692	5.692
Active Constraint	0.014	0.128	0.311	0.389	0.333
Constraint Name	Strength	Strength	End Tr. Top	Strength	Strength

Cost Savings	-31%	-13%	-21%	7%	30%
Objective Difference	-31%	-10%	-24%	5%	30%
Constraint Difference	-0.003	0.020	0.000	-0.056	0.120

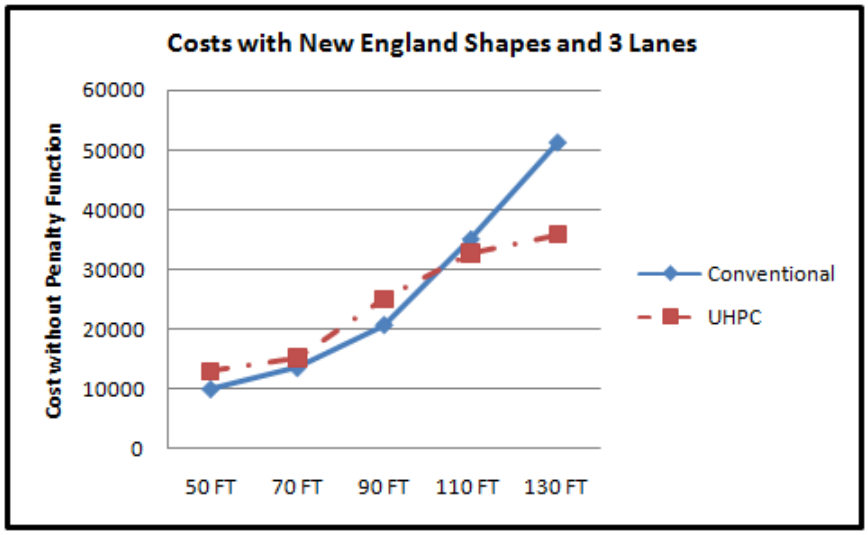

Figure 133. Graph. New England, 3 Lane Cost Comparison

Table 36. New England Shape, 4 Lane Optimization Results

Conventional	50 FT	70 FT	90 FT	110 FT	130 FT
Cost without Penalty	11071	14861	29100	39774	60933
Minimum Objective	11183	16014	33065	42906	65231
Solution Depth	65.642	70.865	70.864	68.828	70.753
Solution Girders	5.0	5.0	5.0	9.5	11.9
Solution Steel Area	2.632	3.947	3.947	3.947	3.947
Active Constraint	0.011	0.115	0.397	0.313	0.430
Constraint Name	Strength	Strength	Strength	Strength	Strength

UHPC	50 FT	70 FT	90 FT	110 FT	130 FT
Cost without Penalty	15134	17276	28408	35340	44724
Minimum Objective	15833	18213	31517	39015	48256
Solution Depth	55.118	62.992	55.118	55.118	62.992
Solution Girders	7.0	5.0	5.0	5.0	6.1
Solution Steel Area	1.897	3.794	5.692	5.692	5.692
Active Constraint	0.070	0.094	0.311	0.368	0.353
Constraint Name	Strength	Strength	End Tr. Top	Strength	Strength

Cost Savings	-37%	-16%	2%	11%	27%
Objective Difference	-42%	-14%	5%	9%	26%
Constraint Difference	-0.059	0.022	0.000	-0.054	0.077

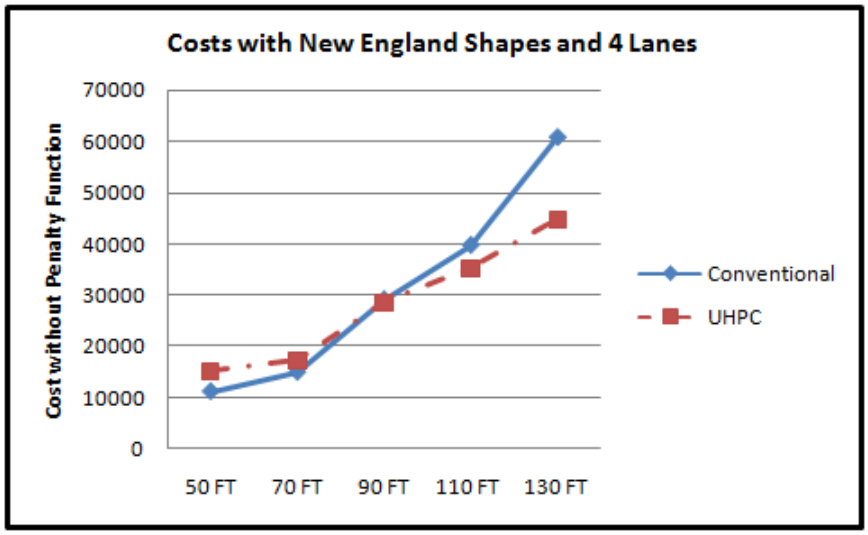

Figure 134. Graph. New England, 4 Lane Cost Comparison

Pennsylvania Shapes

Table 37. Pennsylvania Shape, 2 Lane Optimization Results

Conventional	50 FT	70 FT	90 FT	110 FT	130 FT
Cost without Penalty	9458	12834	18917	33244	41648
Minimum Objective	9458	12834	21430	37771	46262
Solution Depth	45.5	84.871	94	93.781	95.5
Solution Girders	4.0	4.0	4.0	4.0	5.5
Solution Steel Area	2.938	2.938	2.938	2.938	2.938
Active Constraint	-0.003	-0.007	0.251	0.453	0.461
Constraint Name	Strength	Strength	Strength	Strength	Strength

UHPC	50 FT	70 FT	90 FT	110 FT	130 FT
Cost without Penalty	10986	16783	18173	20953	27292
Minimum Objective	12130	18592	18173	21127	29684
Solution Depth	61.5	78.5	78.5	61.5	61.5
Solution Girders	4.0	4.0	4.0	4.0	4.0
Solution Steel Area	1.744	3.488	3.488	5.233	5.233
Active Constraint	0.114	0.181	-0.004	0.017	0.239
Constraint Name	Strength	Mid Tr. Top	Strength	Strength	Strength

Cost Savings	-16%	-31%	4%	37%	34%
Objective Difference	-28%	-45%	15%	44%	36%
Constraint Difference	-0.117	0.000	0.255	0.435	0.222

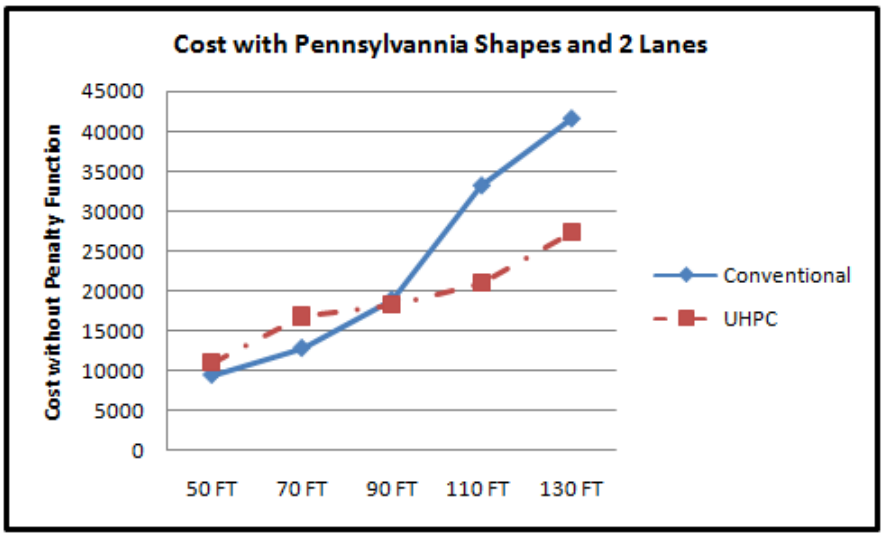

Figure 135. Graph. Pennsylvania, 2 Lane Cost Comparison

Table 38. Pennsylvania Shape, 3 Lane Optimization Results

Conventional	50 FT	70 FT	90 FT	110 FT	130 FT
Cost without Penalty	12272	13761	28450	35065	51100
Minimum Objective	13018	15293	32631	38782	55986
Solution Depth	30.562	94.031	94.78	95.042	95.031
Solution Girders	7.5	4.0	4.0	6.5	7.5
Solution Steel Area	2.938	2.938	2.938	2.938	2.938
Active Constraint	0.075	0.153	0.418	0.372	0.489
Constraint Name	Strength	Strength	Strength	Strength	Strength

UHPC	50 FT	70 FT	90 FT	110 FT	130 FT
Cost without Penalty	13063	16785	28450	31288	37842
Minimum Objective	14110	18594	32631	35019	41811
Solution Depth	61.5	78.5	94.78	61.5	78.5
Solution Girders	5.5	4.0	4.0	4.0	4.0
Solution Steel Area	1.744	3.488	2.938	5.233	5.233
Active Constraint	0.105	0.181	0.418	0.373	0.397
Constraint Name	Strength	Mid Tr. Top	Strength	Strength	Strength

Cost Savings	-6%	-22%	0%	11%	26%
Objective Difference	-8%	-22%	0%	10%	25%
Constraint Difference	-0.030	0.000	0.000	-0.001	0.092

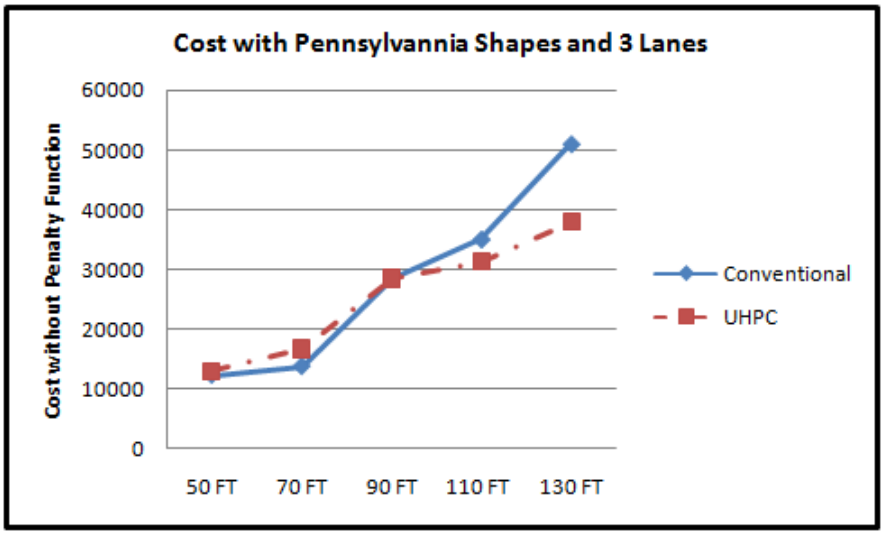

Figure 136. Graph. Pennsylvania, 3 Lane Cost Comparison

Table 39. Pennsylvania Shape, 4 Lane Optimization Results

Conventional	50 FT	70 FT	90 FT	110 FT	130 FT
Cost without Penalty	14185	21868	29722	39460	59152
Minimum Objective	14545	24040	33739	43807	63963
Solution Depth	30.682	45.952	94.01	94.237	95.5
Solution Girders	9.5	9.5	5.0	6.5	9.6
Solution Steel Area	2.938	2.938	2.938	2.938	2.938
Active Constraint	0.036	0.217	0.402	0.435	0.481
Constraint Name	Strength	Strength	Strength	Strength	Strength

UHPC	50 FT	70 FT	90 FT	110 FT	130 FT
Cost without Penalty	16080	19325	21780	33888	41723
Minimum Objective	16642	21134	23008	37397	45492
Solution Depth	61.5	78.5	61.5	61.5	78.5
Solution Girders	7.9	5.0	5.0	5.0	5.0
Solution Steel Area	1.744	3.488	5.233	5.233	5.233
Active Constraint	0.056	0.181	0.123	0.351	0.377
Constraint Name	Strength	Mid Tr. Top	Strength	Strength	Strength

Cost Savings	-13%	12%	27%	14%	29%
Objective Difference	-14%	12%	32%	15%	29%
Constraint Difference	-0.020	0.000	0.279	0.084	0.104

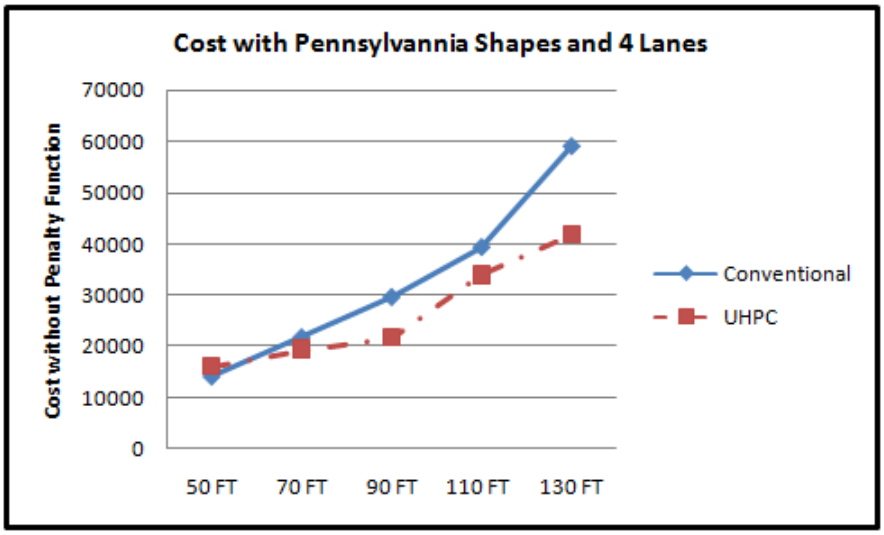

Figure 137. Graph. Pennsylvania, 4 Lane Cost Comparison

South Carolina Shapes

Table 40. South Carolina Shape, 2 Lane Optimization Results

Conventional	50 FT	70 FT	90 FT	110 FT	130 FT
Cost without Penalty	8807	12057	23179	17973	23294
Minimum Objective	9004	12057	26437	18735	25543
Solution Depth	55.965	52.805	72	72	72
Solution Girders	4.0	4.5	4.0	4.0	4.0
Solution Steel Area	2.246	3.961	6.426	6.426	6.426
Active Constraint	0.020	-0.054	0.326	0.076	0.225
Constraint Name	Mid Tr. Top	Strength	Mid Tr. Bot	End Tr. Top	Strength

UHPC	50 FT	70 FT	90 FT	110 FT	130 FT
Cost without Penalty	10315	12950	24183	31122	24101
Minimum Objective	11093	13434	25646	33461	24101
Solution Depth	63	63	67.5	63	67.5
Solution Girders	4.5	4.5	8.5	4.0	4.0
Solution Steel Area	1.377	2.314	1.683	14.076	7.196
Active Constraint	0.078	0.048	0.146	0.234	-0.046
Constraint Name	Strength	Strength	Strength	End Tr. Top	Stability

Cost Savings	-15%	-7%	9%	-66%	6%
Objective Difference	-17%	-7%	-4%	-73%	-3%
Constraint Difference	0.000	-0.103	0.000	-0.158	0.000

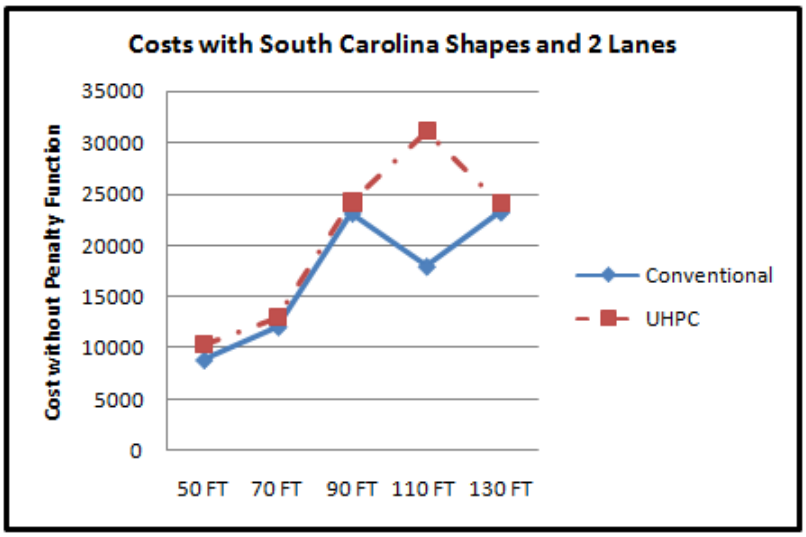

Figure 138. Graph. South Carolina, 2 Lane Cost Comparison

Table 41. South Carolina Shape, 3 Lane Optimization Results

Conventional	50 FT	70 FT	90 FT	110 FT	130 FT
Cost without Penalty	9152	12433	23179	21214	27927
Minimum Objective	9998	13803	26437	23533	29822
Solution Depth	63.422	72	72	72	72
Solution Girders	4.0	4.0	4.0	4.0	5.5
Solution Steel Area	2.497	3.958	6.426	6.426	6.426
Active Constraint	0.085	0.137	0.326	0.232	0.190
Constraint Name	Mid Tr. Top	Strength	Mid Tr. Bot	Strength	Strength

UHPC	50 FT	70 FT	90 FT	110 FT	130 FT
Cost without Penalty	12850	16853	26999	31122	29950
Minimum Objective	14461	17927	29337	33461	32768
Solution Depth	67.5	63	63	63	63
Solution Girders	5.5	6.5	4.0	4.0	4.0
Solution Steel Area	1.683	2.314	14.076	14.076	7.803
Active Constraint	0.161	0.107	0.234	0.234	0.282
Constraint Name	Mid Tr. Top	Strength	End Tr. Top	End Tr. Top	Strength

Cost Savings	-29%	-22%	-2%	-32%	0%
Objective Difference	-40%	-36%	-16%	-47%	-7%
Constraint Difference	-0.076	0.030	0.000	0.000	-0.092

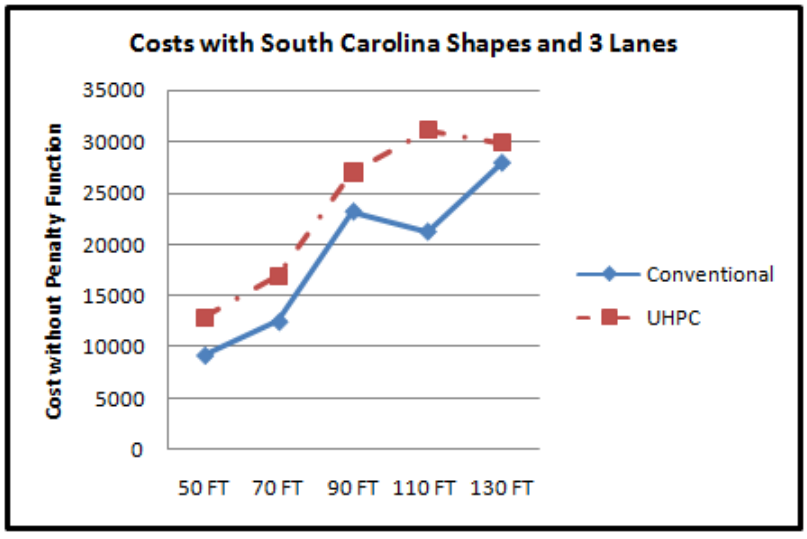

Figure 139. Graph. South Carolina, 3 Lane Cost Comparison

Table 42. South Carolina Shape, 4 Lane Optimization Results

Conventional	50 FT	70 FT	90 FT	110 FT	130 FT
Cost without Penalty	10138	17422	25845	23567	32515
Minimum Objective	10607	18068	29103	25621	34622
Solution Depth	71.85	45.203	72	72	71.249
Solution Girders	5.0	8.5	5.0	5.0	6.6
Solution Steel Area	2.151	3.954	6.426	6.426	6.426
Active Constraint	0.047	0.065	0.326	0.205	0.211
Constraint Name	Mid Tr. Top	Strength	Mid Tr. Bot	Strength	Strength

UHPC	50 FT	70 FT	90 FT	110 FT	130 FT
Cost without Penalty	16192	25190	31678	36830	33787
Minimum Objective	16706	27747	34016	39169	36358
Solution Depth	63	67.5	63	63	63
Solution Girders	9.5	9.5	5.0	5.0	5.0
Solution Steel Area	1.228	1.683	14.076	14.076	7.803
Active Constraint	0.051	0.256	0.234	0.234	0.257
Constraint Name	Strength	Strength	End Tr. Top	End Tr. Top	Strength

Cost Savings	-53%	-39%	-9%	-44%	2%
Objective Difference	-60%	-45%	-23%	-56%	-4%
Constraint Difference	0.000	-0.191	0.000	0.000	-0.046

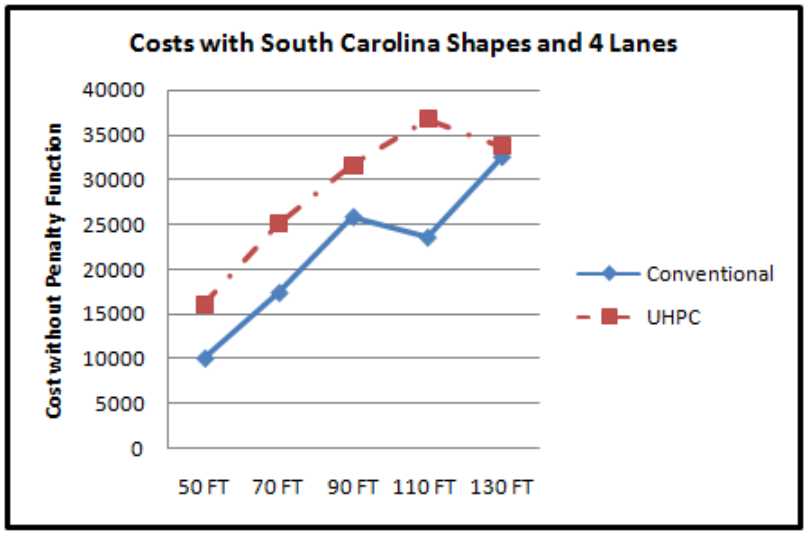

Figure 140. Graph. South Carolina, 4 Lane Cost Comparison

Virginia Shapes

Table 43. Virginia, 2 Lane Optimization Results

Conventional	50 FT	70 FT	90 FT	110 FT	130 FT
Cost without Penalty	10029	15779	18306	32357	40430
Minimum Objective	10466	16399	20804	36857	45048
Solution Depth	25.803	45.854	93	93	93
Solution Girders	5.5	7.5	4.0	4.0	5.5
Solution Steel Area	2.938	2.938	2.938	2.938	2.938
Active Constraint	0.044	0.062	0.250	0.450	0.462
Constraint Name	Strength	Strength	Strength	Strength	Strength

UHPC	50 FT	70 FT	90 FT	110 FT	130 FT
Cost without Penalty	10770	17252	17126	19966	26760
Minimum Objective	12050	19278	17276	20324	29288
Solution Depth	61	61	77	61	61
Solution Girders	4.0	5.5	4.0	4.0	4.0
Solution Steel Area	1.744	1.744	3.488	5.233	5.233
Active Constraint	0.128	0.203	0.015	0.036	0.253
Constraint Name	Strength	Strength	Strength	Strength	Strength

Cost Savings	-3%	-5%	18%	46%	41%
Objective Difference	-7%	-9%	6%	38%	34%
Constraint Difference	-0.084	-0.141	0.235	0.414	0.209

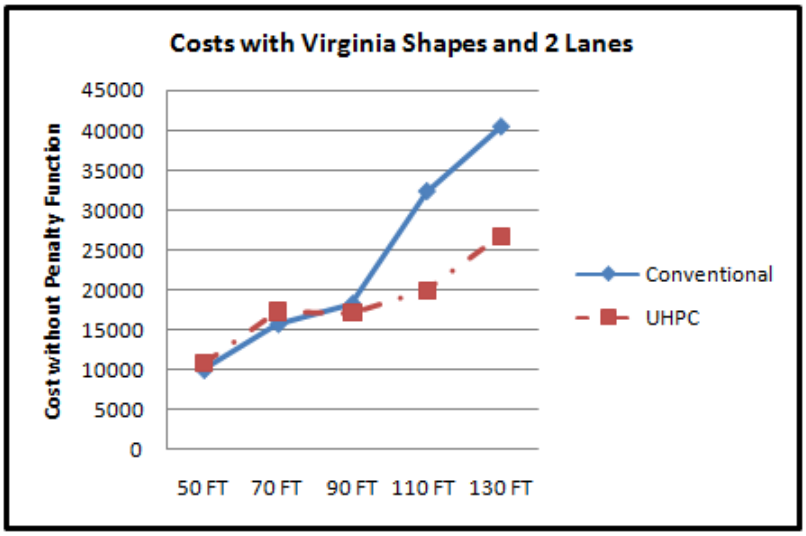

Figure 141. Graph. Virginia, 2 Lane Cost Comparison

Table 44. Virginia, 3 Lane Optimization Results

Conventional	50 FT	70 FT	90 FT	110 FT	130 FT
Cost without Penalty	12170	13385	28258	43827	49371
Minimum Objective	13002	14945	32492	49568	54247
Solution Depth	30.094	93	93	93	93
Solution Girders	7.5	4.0	4.0	4.0	7.5
Solution Steel Area	2.938	2.938	2.938	2.938	2.938
Active Constraint	0.083	0.156	0.423	0.574	0.488
Constraint Name	Strength	Strength	Strength	Strength	Strength

UHPC	50 FT	70 FT	90 FT	110 FT	130 FT
Cost without Penalty	12525	17743	18527	30789	36897
Minimum Objective	13632	20083	20159	34582	40920
Solution Depth	61	77	61	61	77
Solution Girders	5.5	4.0	4.0	4.0	4.0
Solution Steel Area	1.744	3.488	5.233	5.233	5.233
Active Constraint	0.111	0.234	0.163	0.379	0.402
Constraint Name	Strength	Mid Tr. Top	Strength	Strength	Strength

Cost Savings	4%	-19%	43%	38%	32%
Objective Difference	-3%	-33%	34%	30%	25%
Constraint Difference	-0.027	0.000	0.260	0.195	0.085

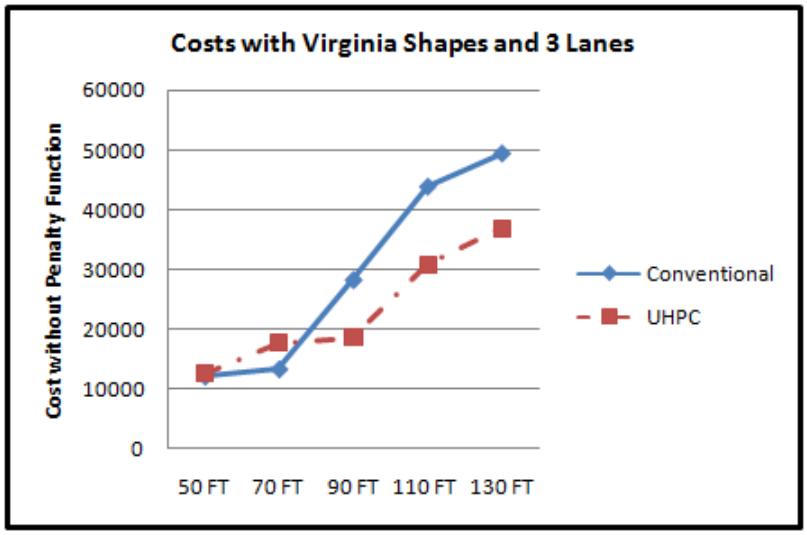

Figure 142. Graph. Virginia, 3 Lane Cost Comparison

Table 45. Virginia, 4 Lane Optimization Results

Conventional	50 FT	70 FT	90 FT	110 FT	130 FT
Cost without Penalty	13966	14644	29101	40127	56853
Minimum Objective	14446	15881	33128	43588	61665
Solution Depth	30.086	93	93	86.944	93
Solution Girders	9.5	5.0	5.0	9.5	9.9
Solution Steel Area	2.938	2.938	2.938	2.938	2.938
Active Constraint	0.048	0.124	0.403	0.346	0.481
Constraint Name	Strength	Strength	Strength	Strength	Strength

UHPC	50 FT	70 FT	90 FT	110 FT	130 FT
Cost without Penalty	15307	20104	20997	33138	40421
Minimum Objective	15879	22444	22315	36709	44244
Solution Depth	61	77	61	61	77
Solution Girders	7.9	5.0	5.0	5.0	5.0
Solution Steel Area	1.744	3.488	5.233	5.233	5.233
Active Constraint	0.057	0.234	0.132	0.357	0.382
Constraint Name	Strength	Mid Tr. Top	Strength	Strength	Strength

Cost Savings	-6%	-27%	37%	24%	34%
Objective Difference	-10%	-37%	28%	17%	29%
Constraint Difference	-0.009	0.000	0.271	-0.011	0.099

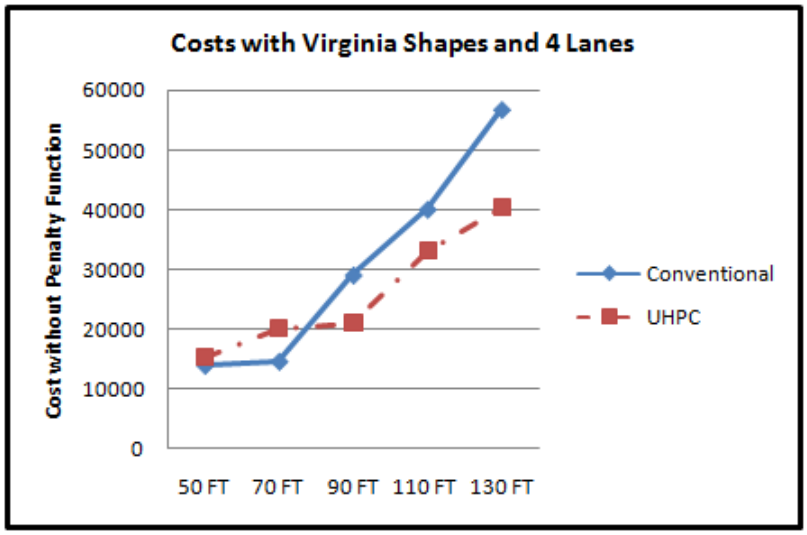

Figure 143. Graph. Virginia, 4 Lane Cost Comparison

Washington Shapes

Table 46. Washington, 2 Lane Optimization Results

Conventional	50 FT	70 FT	90 FT	110 FT	130 FT
Cost without Penalty	9254	11827	17299	30870	38649
Minimum Objective	9307	11961	19585	35211	43096
Solution Depth	44.011	80.293	94.5	94.5	94.5
Solution Girders	4.0	4.0	4.0	4.0	5.5
Solution Steel Area	2.846	2.846	2.846	2.846	2.846
Active Constraint	0.005	0.013	0.229	0.434	0.445
Constraint Name	Strength	Strength	Strength	Strength	Strength

UHPC	50 FT	70 FT	90 FT	110 FT	130 FT
Cost without Penalty	10738	14017	16395	21026	31783
Minimum Objective	10738	15144	17324	23057	34481
Solution Depth	58	76.25	58	58	76.25
Solution Girders	4.5	4.0	4.0	4.0	5.5
Solution Steel Area	1.622	3.244	4.865	4.865	3.244
Active Constraint	-0.065	0.113	0.093	0.203	0.270
Constraint Name	Strength	Mid Tr. Top	End Tr. Top	Strength	Strength

Cost Savings	-15%	-17%	16%	40%	26%
Objective Difference	-16%	-19%	5%	32%	18%
Constraint Difference	0.070	0.000	0.000	0.231	0.175

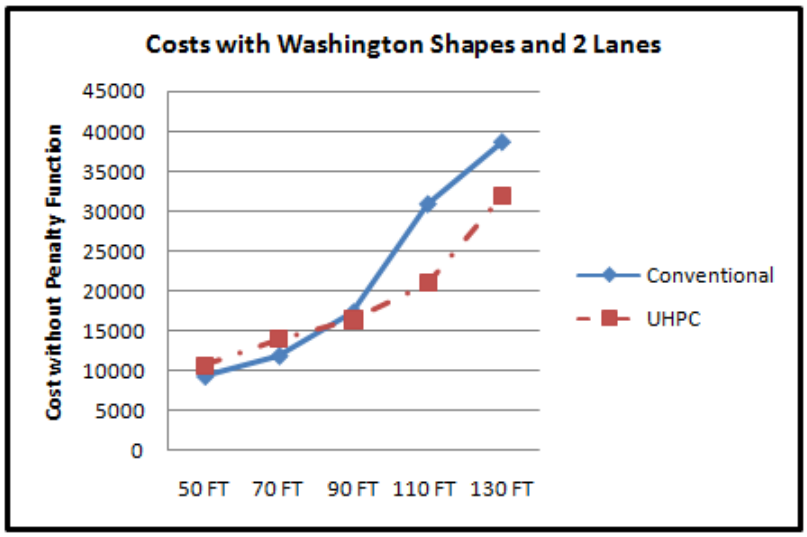

Figure 144. Graph. Washington, 2 Lane Cost Comparison

Table 47. Washington, 3 Lane Optimization Results

Conventional	50 FT	70 FT	90 FT	110 FT	130 FT
Cost without Penalty	9593	12805	26925	42383	47092
Minimum Objective	9666	14141	31005	48008	52144
Solution Depth	61.195	94.5	94.5	94.5	94.422
Solution Girders	4.0	4.0	4.0	4.0	6.5
Solution Steel Area	2.846	2.846	2.846	2.846	2.846
Active Constraint	0.007	0.134	0.408	0.563	0.505
Constraint Name	Strength	Strength	Strength	Strength	Strength

UHPC	50 FT	70 FT	90 FT	110 FT	130 FT
Cost without Penalty	13218	15176	21839	36409	43735
Minimum Objective	13218	16921	24711	41119	47196
Solution Depth	58	76.25	58	58	76.25
Solution Girders	6.5	4.0	4.0	4.0	7.5
Solution Steel Area	1.622	3.244	4.865	4.865	3.244
Active Constraint	-0.005	0.175	0.287	0.471	0.346
Constraint Name	Strength	Strength	Strength	Strength	Strength

Cost Savings	-37%	-7%	30%	24%	16%
Objective Difference	-38%	-19%	19%	14%	7%
Constraint Difference	0.012	-0.041	0.121	0.092	0.159

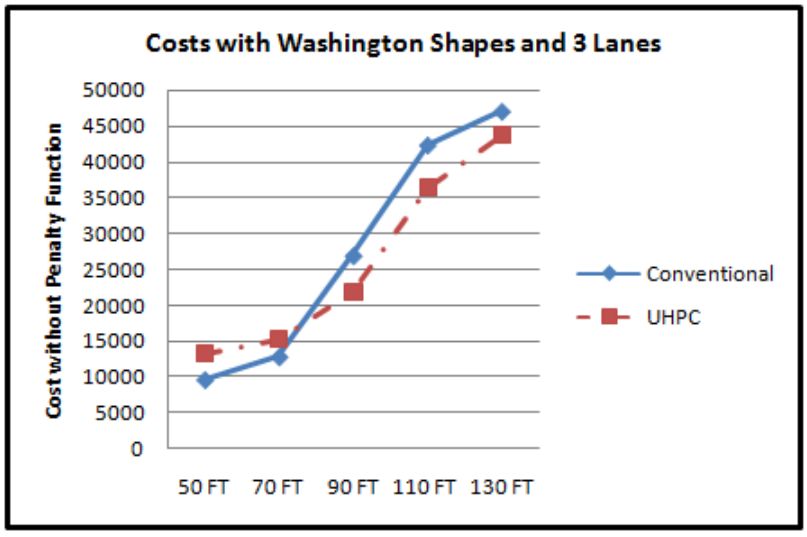

Figure 145. Graph. Washington, 3 Lane Cost Comparison

Table 48. Washington, 4 Lane Optimization Results

Conventional	50 FT	70 FT	90 FT	110 FT	130 FT
Cost without Penalty	10633	14158	27740	36283	47092
Minimum Objective	10720	15163	31606	39533	52144
Solution Depth	58.38	94.5	94.5	94.5	94.422
Solution Girders	5.0	5.0	5.0	8.5	6.5
Solution Steel Area	2.846	2.846	2.846	2.846	2.846
Active Constraint	0.009	0.100	0.387	0.325	0.505
Constraint Name	Strength	Strength	Strength	Strength	Strength

UHPC	50 FT	70 FT	90 FT	110 FT	130 FT
Cost without Penalty	14917	16649	23458	31305	43735
Minimum Objective	15655	18069	26061	33808	47196
Solution Depth	58	76.25	58	58	76.25
Solution Girders	8.0	5.0	5.0	6.5	7.5
Solution Steel Area	1.622	3.244	4.865	4.865	3.244
Active Constraint	0.074	0.142	0.260	0.250	0.346
Constraint Name	Strength	Strength	Strength	Strength	Strength

Cost Savings	-39%	-10%	26%	21%	16%
Objective Difference	-40%	-18%	15%	14%	7%
Constraint Difference	-0.065	-0.042	0.126	0.075	0.159

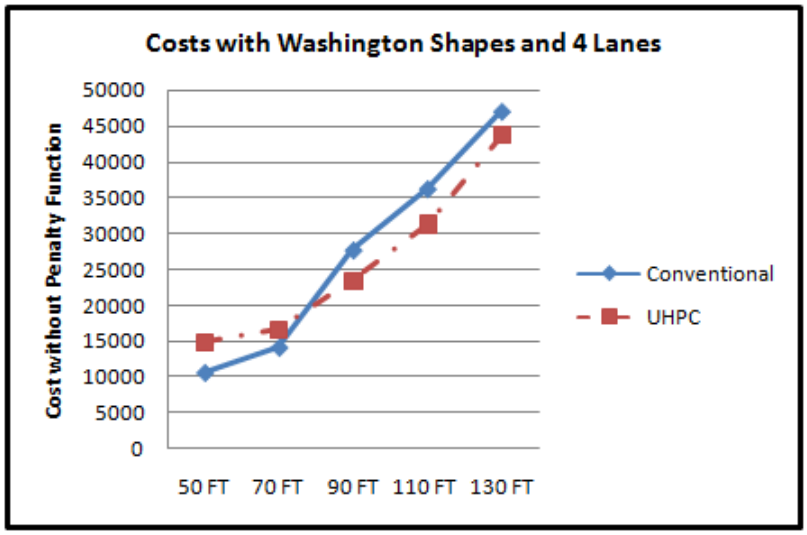

Figure 146. Graph. Washington, 4 Lane Cost Comparison

Appendix D: Design Summaries

Conventional Bridge Design Summary

Table 49. Conventional Bridge Design Summary

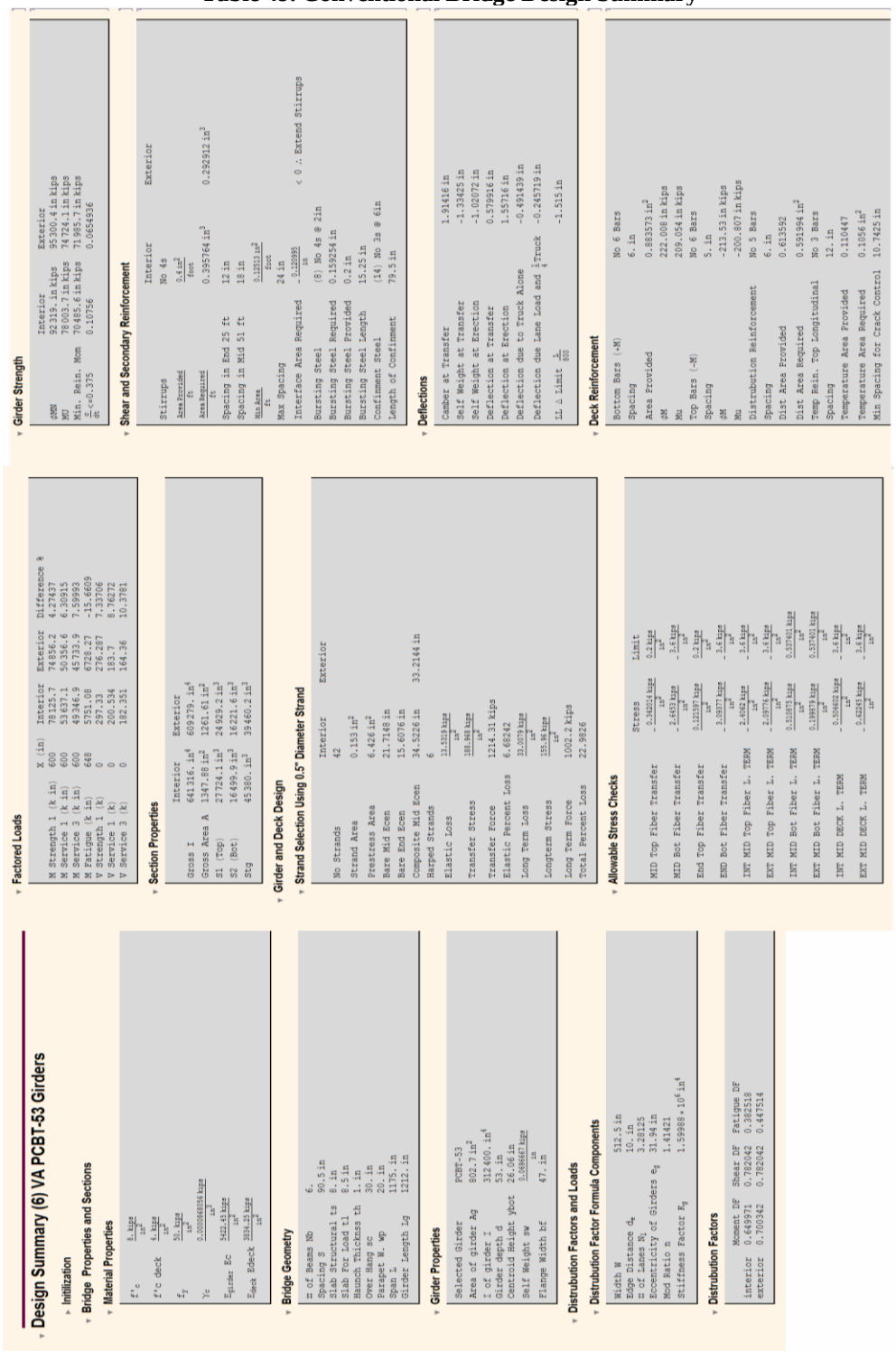

Design Summary (6) VA PCBT-53 Girders

Initialization

Bridge Properties and Sections

Material Properties

f'c	8. ksi
	8000. psi
f'c deck	4. ksi
	4000. psi
f_y	50. ksi
	50000. psi
Yc	0.0000868056 kcf
	0.15 pcf
Epsilon Ec	5422.45 ksi
	5422450. psi
Edeck Edeck	3834.25 ksi
	3834250. psi

Bridge Geometry

# of Beams Nb	6.
Spacing S	90.5 in
Slab Structural ts	8. in
Slab For Load ts	8.5 in
Haunch Across th	1. in
Over Hang Wc	30. in
Parapet W. wp	20. in
Span L	1175. in
Girder Length Lg	1212. in

Girder Properties

Selected Girder	PCBT-53
Area of girder Ag	802.7 in^2
I of girder I	312400. in^4
Girder depth d	53. in
Centroid Height ybot	26.06 in
Self Weight sw	0.05668 klf
	56.68 plf
Flange Width bf	47. in

Distrubution Factors and Loads

Distrubution Factor Formula Components

Width W	512.5 in
Edge Distance d_e	10. in
# of Lanes N_l	3.28125
Eccentricity of Girders e_g	31.94 in
Mod Ratio n	1.41421
Stiffness Factor K_g	$1.59988 * 10^6$ in^4

Distrubution Factors

	Moment DF	Shear DF	Fatigue DF
interior	0.649971	0.782042	0.382518
exterior	0.700342	0.782042	0.447514

Factored Loads

		X (in)	Interior	Exterior	Difference %
M Strength 1 (k in)		600	78125.7	74856.2	4.27437
M Service 1 (k in)		600	53637.1	50356.6	6.30915
M Service 3 (k in)		600	49346.9	45733.9	7.59993
M Fatigue (k in)		648	5751.08	6728.27	-15.6609
V Strength 1 (k)		0	297.33	276.287	7.33706
V Service 1 (k)		0	200.534	183.7	8.76272
V Service 3 (k)		0	182.351	164.36	10.3781

Section Properties

	Interior	Exterior
Gross I	641316. in^4	609279. in^4
Gross Area A	1347.88 in^2	1261.61 in^2
S1 (Top)	27724.1 in^3	24923.2 in^3
S2 (Bot)	16499.9 in^3	16221.6 in^3
Stg	45380. in^3	39460.2 in^3

Girder and Deck Design

Strand Selection Using 0.5" Diameter Strand

	Interior	Exterior
No Strands	42	
Strand Area	0.153 in^2	
Prestress Area	6.426 in^2	
Bare Mid Ecen	21.7149 in	
Bare End Ecen	15.6076 in	
Composite Mid Ecen	34.5226 in	33.2144 in
Harped Strands	6	
Elastic Loss	13.5319 ksi / in^2	
Transfer Stress	188.868 ksi / in^2	
Transfer Force	1214.31 kips	
Elastic Percent Loss	6.68242	
Long Term Loss	33.0078 ksi / in^2	
Longterm Stress	155.86 ksi / in^2	
Long Term Force	1002.2 kips	
Total Percent Loss	22.9826	

Allowable Stress Checks

	Stress	Limit
MID Top Fiber Transfer	-0.340214 ksi / in^2	0.2 ksi / in^2
	-0.2 ksi / in^2	
MID Bot Fiber Transfer	2.64653 ksi / in^2	3.6 ksi / in^2
End Top Fiber Transfer	0.121597 ksi / in^2	0.2 ksi / in^2
END Bot Fiber Transfer	1.03377 ksi / in^2	3.6 ksi / in^2
INT MID Top Fiber L. TERM	2.4562 ksi / in^2	3.6 ksi / in^2
EXT MID Top Fiber L. TERM	2.09776 ksi / in^2	3.6 ksi / in^2
INT MID Bot Fiber L. TERM	0.538873 ksi / in^2	0.637401 ksi / in^2
EXT MID Bot Fiber L. TERM	0.198973 ksi / in^2	0.637401 ksi / in^2
INT MID DECK L. TERM	0.504602 ksi / in^2	3.6 ksi / in^2
EXT MID DECK L. TERM	0.64245 ksi / in^2	3.6 ksi / in^2

Girder Strength

	Interior	Exterior
øMN	92319. in kips	95300.4 in kips
MRT	78003.7 in kips	74724.1 in kips
Min. Rein. Mcrn	70485.6 in kips	71985.7 in kips
$\frac{c}{de}$ <0.375	0.10756	0.0654936

Shear and Secondary Reinforcement

	Interior	Exterior
Stirrups	No 4s	
Area Provided / ft	0.4 in^2 / feet	
Area Required / ft	0.395764 in^3	0.292912 in^3
Spacing in End 25 ft	12 in	
Spacing in Mid 51 ft	18 in	
Min Area	0.12811 in^2 / feet	
Max Spacing	24 in	
Interface Area Required	-0.122665 kip / in	< 0 ∴ Extend Stirrups
Bursting Steel	(8) No 4s @ 2in	
Bursting Steel Required	0.159254 in	
Bursting Steel Provided	0.2 in	
Bursting Steel Length	15.25 in	
Confinement Steel	(14) No 3s @ 6in	
Length of Confinment	79.5 in	

Deflections

Camber at Transfer	1.91416 in
Self Weight at Transfer	-1.33425 in
Self Weight at Erection	-1.02072 in
Deflection at Transfer	0.579916 in
Deflection at Erection	1.55716 in
Deflection due to Truck Alone	-0.491439 in
Deflection due Lane Load and 1 truck	-0.245719 in
LL Δ Limit L/800	-1.515 in

Deck Reinforcement

Bottom Bars (-M)	No 6 Bars
Spacing	6. in
Area Provided	0.883573 in^2
øM	222.008 in Kips
Mu	209.054 in Kips
Top Bars (-M)	No 6 Bars
Spacing	5. in
øM	-213.53 in kips
Mu	-200.807 in kips
Distrubution Reinforcement	No 5 Bars
Spacing	6. in
Dist Area Provided	0.613592
Dist Area Required	0.591994 in^2
Temp Rein. Top Longitudinal	No 3 Bars
Spacing	12. in
Temperature Area Provided	0.1104477
Temperature Area Required	0.1056 in^2
Min Spacing for Crack Control	10.7425 in

UHPC Bridge Design Summary

Table 50. UHPC Bridge Design Summary

Works Cited

(AFGC), F. A. o. C. E. (2002). Interim Reccomendations for Ultra High Performance Fibre-Reinforced Concrete.

(JSCE), J. S. o. C. E., J. Niwa, et al. (2004). Outlines of JSCE Recommendations for Design and Construction of Ultra High-Strength Fiber-Reinforced Concrete.

Ahlborn, T. M., E. Steinberg, et al. (2003). Ultra-High Performance Concrete Study Tour 2002. International Symposium on High Performance Concrete, Orlando,Fl.

Al-Gahtani, A. S., S. S. Al-Saadoun, et al. (1995). "Design optimization of continuous partially prestressed concrete beams." Computers & Structures **55**(2): 365-370.

Barakat, S., K. Bani-Hani, et al. (2004). "Multi-objective reliability-based optimization of prestressed concrete beams." Structural Safety **26**(3): 311-342.

Barakat, S., N. Kallas, et al. (2003). "Single objective reliability-based optimization of prestressed concrete beams." Computers & Structures **81**(26-27): 2501-2512.

Behloul, M., O. Bayard, et al. (2006). Ductal (R) Prestressed Girders for a Traffic Bridge in Mayenne, France 7th International Conference on Short and Medium Span Bridges. Montreal,Canada.

Bierwagen, D. and N. McDonald (2005). Ultra High Performance Concrete Highway Bridge.

Blais, P. and M. Couture (1999). "Precast, Prestressed Pedestrian Bridge - Worlds First Reactive Powder Concrete Structure." PCI Journal.

Brouwer, G. (2001). Bridge to the Future. Civil Engineering. New York, ASCE Publications.

Burgoyne, C. J. and T. J. Stratford (2001). "Lateral instability of long-span prestressed concrete beams on flexible bearings." Structural Engineer **79**(6): 23-26.

Darwin, D., C. Dolan, et al. (2003). Design of Concrete Structures. New York, McGraw Hill Higher Education.

Erbatur, F., R. Al Zaid, et al. (1992). "Optimization and sensitivity of prestressed concrete beams." Computers and Structures **45**(5-6): 881-886.

Graybeal, B. A. (2005). Characterization of the Behavior of Ultra High Performance Concrete. Civil and Environmental Engineering. College Park, University of Maryland. **Doctor of Philosophy:** 360.

Graybeal, B. A. and J. L. Hartman (2005). Experimental Testing of UHPC Optimized Bridge Girders. PCI National Bridge Conference. Washington,D.C.

Hajar, Z., A. Simon, et al. (2003). Construction of the First Road Bridges Made of Ultra-High Performance Concrete. International Symposium on High Performance Concrete. Orlando, Fl.

Hassanain, M. A. and R. E. Loov (1999). "Design of Prestressed Bridges Using High Performance Concrete - An Optimization Approach." PCI Journal **44**(2).

Khaleel, M. A. and R. Y. Itani (1993). "Optimization of partially prestressed concrete girders under multiple strength and serviceability criteria." Computers and Structures **49**(3): 427-438.

Leps, M. and M. Sejnoha (2003). "New approach to optimization of reinforced concrete beams." Computers and Structures **81**(18-19): 1957-1966.

.

Lounis, Z. and M. Z. Cohn (1993). "Multiobjective Optimization of Prestressed Concrete Structures." Journal of Structural Engineering **119**(3): 794-808.

Lounis, Z., M. S. Mirza, et al. (1997). "Segmental and Conventional Precast Prestressed Concrete I-Bridge Girders." Journal of Bridge Engineering **2**(3): 73-82.

Nilson, A. (1987). Design of Prestressed Concrete. New York, Wiley.

Okuma, H., I. Iwasaki, et al. (2006). The First Highway Bridge Applying Ultra High Strength Fiber Reinforced Concrete in Japan. 7th International Conference on Short and Medium Span Bridges. Montreal,Canada.

Park, H., F.-J. Ulm, et al. (2003). Model-Based Optimization of Ultra high Performance Concrete Highway Bridge Girders. Cambridge, Massachusetts Institute of Technology 140.

Perry, V. H. and D. Zakariasen (2003). Overview of UHPC Technology, Materials, Properties, Marlets and Manufacturing. 2003 Concrete Bridge Conference. Orlando,Fl.

Rabbat, B. G. and H. G. Russell (1982). "Optimized Sections For Precast Prestressed Bridge Girders." PCI Journal **27**(4).

Rebentrost, M. and B. Cavill (2006). Australian Experience with Ductal: An Ultra High Performance Concrete. FIB 2nd International Congress, Naples,Italy.

Resplendino, J. and J. Petitjean (2003). Ultra-High-Performance Concrete: First Recommendations and Examples of Application International Symposium on High Performance Concrete. Orlando,Fl.

Sirca Jr, G. F. and H. Adeli (2005). "Cost optimization of prestressed concrete bridges." Journal of Structural Engineering **131**(3): 380-388.

Sritharan, S., B. J. Bristow, et al. (2003). Characterizing an Ultra High Performance Material For Bridge Applications under Extreme Loads. International Symposium on High Performance Concrete. Orlando,FL.

Steinberg, E. and T. M. Ahlborn (2005). Analysis of UHPC Bridge Girders. 2005 PCI National Bridge Conference. Palm Springs, CA.

Stratford, T. J. and C. J. Burgoyne (2000). "The toppling of hanging beams." International Journal of Solids and Structures **37**(26): 3569-3589.

Stratford, T. J., C. J. Burgoyne, et al. (1999). "Stability design of long precast concrete beams." Proceedings of the Institution of Civil Engineers, Structures and Buildings **134**(2): 159-168.